The role of RiPP proteins in plant pathogenic fungi

Rosie E. Ford

A dissertation submitted to the University of Bristol in accordance with the requirements for award of the degree of Doctor of Philosophy in the Faculty of Life Sciences.

School of Biological Sciences

September 2023

Word count: 55,380

Abstract

The ascomycete fungus, *Zymoseptoria tritici,* has risen in prevalence and significance in the past few decades, overtaking wheat pathogens such as *Stagonospora nodorum* for the title of most prevalent foliar wheat pathogen in the UK and Europe – as well as several other countries worldwide. Losses to the pathogen can be significant, as such, the fungus and its associated disease, Septoria tritici blotch, presents a huge threat to global wheat production and food security given the dietary importance of wheat grain. *Zymoseptoria tritici* infection of wheat includes a biotrophic-like latent phase and necrotrophic stage, however, the transition between the two is currently poorly understood, and assumed to involve fungal effectors which trigger the plant hypersensitive response. Equally, fungal ribosomally synthesised and post-translationally modified peptides (RiPPs) are under-researched, despite the RiPP victorin contributing to *Cochliobolus victoriae* virulence on Vb oat cultivars.

This thesis explores a fungal RiPP from *Z. tritici,* the biosynthetic pathway of which has been characterised bioinformatically with knockout strains produced for future experimental confirmation of the method predicted in this work. Bioinformatic investigation also proved informative regarding RiPP repeat variation between strains of the same species and in identifying novel RiPP producers entirely. Attempts were made to understand the function of the RiPP, to determine whether it was involved in pathogenicity, as with victorin, this however remains elusive. Although the *Zymoseptoria* RiPP does not have a clear role in virulence given that null mutants were fully virulent, results from this work demonstrated the impact of the environment on the wheat-*Zymoseptoria* interaction, demonstrating the multiple routes that can be explored to control *Z. tritici.*

Overall, this work has extended our understanding of *Zymoseptoria tritici* – by examining the environmental conditions conducive or inconducive to infection – and its RiPP, with this also contributing to our knowledge of fungal RiPPs more widely.

Acknowledgments

Firstly, I thank my supervisors Dr Andy Bailey and Professor Gary Foster. Without the support of Andy during my undergraduate study at the University of Bristol I would not have had the confidence to apply for a PhD position and would not be where I am today. Thank you for always encouraging me to step outside of my comfort zone, reminding me to appreciate my successes, and answering questions (in person and by email) at all hours of the day.

Secondly, I'd like to thank all members of Lab 321 – past and present. It was these past members, during a summer project undertaken in Lab 321, that showed me how welcoming a research environment can be and encouraged me to pursue academia further. In particular, I would like to thank Dr Kathryn Ford for supervising this summer project and teaching me many of the research skills I used throughout my PhD. Dr Ian Prosser and Dr Katherine Williams, both gave me indispensable support throughout my project, troubleshooting problems, teaching me new techniques, and reassuring me when things didn't go right, as they often don't. All members of Lab 321, you have made my PhD experience an enjoyable one, I will miss working with you all, discussing science – and general nonsense.

Thanks to the technical staff at the University of Bristol, in the Life Sciences Building and the Greenhouses, for making sure that I could focus on the science by taking care of everything else. But also, having discussions with me around experimental design, your insight was always appreciated.

To my funders, BBSRC (via SWBio DTP), I will forever be grateful for the opportunity you have given me, and for putting together a cohort of students many of whom I now call my friends.

To Lewis, thank you for letting me ramble on about science and fungi with you. Mostly, thank you for believing I was more than capable even when I did not, during my PhD but also at every stage before that.

And finally, to my parents and sister, thank you for supporting me in my endeavours as a PhD student and always. Without you all I would not have made it through my undergraduate studies let alone postgraduate. No words could ever express how grateful I am for everything you've all done to get me to this point.

COVID-19 statement

Numerous aspects of this work have been disrupted by COVID-19. The biggest and most obvious disruption being the government closure of laboratory facilities. Sudden periods of building closures were detrimental to several experiments but especially to plant experiments that were conducted over several months. Research efforts were further curtailed due to periods of enforced isolation or illness, which similarly to the building closures meant experiments and data were lost. This applied to plant experiments again but was also true for producing the Zttx cluster knockouts discussed in this work as putative transformants did not always survive these periods. Though much of the work curtailed or lost due to COVID was repeated, this ultimately resulted in delays and meant other experiments could not be completed – namely investigating additional abiotic factors to those discussed here and their impact on *Zymoseptoria tritici* infection. Plant experiments were also severely hindered by repeated bouts of powdery mildew in the wheat growing facilities.

During building closure periods, no wet laboratory experiments could be conducted and though efforts were made to minimise the impact of COVID on my research, by beginning a bioinformatic investigation of *Zymoseptoria tritici*, all other areas of my work were delayed. Even once university facilities were accessible again, lab access was still restricted as a working pattern had to be employed to ensure social distancing. This working pattern extended from the laboratory re-opening in summer 2020 to September 2021. The pattern in place involved alternating lab access: three days one week and two days the second week. This did not always allow enough time for experimental procedures to be carried out, restricting the work that could be done. Laboratory access was not only a problem within my own laboratory but also within others with much tighter restrictions. Specifically, chemistry samples were not permitted to be analysed until the easing of restrictions. As such, the first chemical sample was not analysed by LCMS until November 2021. Knockouts of several genes had been produced before we were aware of the challenges in isolating the peptide.

It was anticipated that within this work I would be able to characterise the peptide from fungal extracts, however, the delay in beginning this work has resulted in an inability to find the peptide within the timeframe. Only once we began analysing wildtype LCMS

chromatograms did it become apparent that the peptide was either not easily extractable or not produced in massive quantities. Though an overexpresser strain was then produced and work continued with this, had access to chemical analysis facilities been restored earlier, more progress with this fungal strain may have been made and the indications of chemical differences between the overexpresser and knockout strains may have been realised. Indeed, not identifying the mature peptide has impacted a larger element of this work, trying to characterise the RiPP biosynthetic pathway from knockouts, which is not possible until the former has been completed.

Author's declaration

I declare that the work in this dissertation was carried out in accordance with the requirements of the University's Regulations and Code of Practice for Research Degree Programmes and that it has not been submitted for any other academic award. Except where indicated by specific reference in the text, the work is the candidate's own work. Work done in collaboration with, or with the assistance of, others, is indicated as such. Any views expressed in the dissertation are those of the author.

SIGNED: ..... [redacted] ..... DATE: .....04/09/23.....

Table of contents

List of tables

List of figures

List of abbreviations

bp – base pairs

CCK – Cyclic cystine knot

CD+V8 – Czapek Dox + V8 juice

CD+YE – Czapek Dox + Yeast Extract

CDB – Czapek Dox broth

CLF – Cluster left flank

CRF – Cluster right flank

CWDEs – Cell wall degrading enzymes

DAD - Diode array detector

dH_2O – deionised water

DMI – Demethylation-inhibiting fungicides

dpi – Days post infection/days post inoculation

ELSD – Evaporative light scattering detector

GFP – Green fluorescence protein

ha - Hectares

HGT – Horizontal gene transfer

HH3 – Histone H3

kb – kilobases

LB – Lysogeny broth

LBA – Lysogeny broth agar

LCMS – Liquid chromatography–mass spectrometry

MS – Mass spectrometry

MTT – 3-(4,5-Dimethylthiazol-2-yl)-2,5-Diphenyltetrazolium Bromide

NCBI – National Centre for Biotechnology Information

NRPS – Non-ribosomal peptide synthetase

ORF – Open reading frame

PCD – Programmed cell death

PCR – Polymerase Chain reaction

PDA – Potato dextrose agar

PDB – Potato dextrose broth

PK – Proteinase K

PKS – Polyketide synthase

POP – Prolyl oligopeptidase

PRPS – Post Ribosomal Peptide Synthesis

QoI – Quinone outside inhibitor

RiPP – Ribosomally synthesised and post-translationally modified peptide

ROS – Reactive oxygen species

-RT – No reverse transcriptase

RT-qPCR – Quantitative reverse transcription polymerase chain reaction

S.E.M – Standard error of the mean

SDHIs – Succinate dehydrogenase inhibiting fungicides

STB – Septoria tritici blotch

TAE – Tris-acetate-EDTA

TE – Tris and EDTA

TSB – Tryptic Soy Broth

TTC – Tetrazolium chloride

WT – Wildtype

YPAD – Yeast extract-Peptone-Adenine-Dextrose

YSM – Yeast sucrose media

ZtGFP – *Z. tritici* codon-optimised GFP sequence

1 : Introduction

1.1 The importance of wheat

Scientists and non-scientists alike are acutely aware of the importance of wheat in human diets. Wheat grain is consumed in products including bread, noodles and beer; meanwhile, nutritionists recognise wheat as a dietary staple providing key vitamins, fibre and phytochemicals for human health (Shewry and Hey, 2015) as well as 20% of an individual's daily calories and proteins worldwide (Shiferaw et al., 2013). This is unsurprising since of all cereals, wheat is the most widely cultivated – globally 220 million ha wheat are planted annually (Shiferaw et al., 2013). Yet, wheat demand is still increasing, especially in developing countries (Shewry and Hey, 2015).

As a staple food resource, wheat production needs to match demand. However, the human population is growing, and predicted to reach 9.7 to 10.9 billion people by 2050 (Gu et al., 2021). Meanwhile, some estimates indicate that global cereal production is declining and supply is vulnerable (O'Hanlon et al., 2012). Indeed, in 2022 wheat yields in the UK increased from their 2021 level, but were still lower than past maxima (DEFRA, 2022) and so wheat production increases are not matching the growing population, putting food security at risk. Increased production is not always possible for several reasons: limited land availability to increase production (Grafton et al., 2015), or wheat fields already being at maximum productivity so further agrochemical inputs will not increase yield. Increasing yield by breeding specific beneficial traits into wheat plants may hold hope, as has proved successful in the past (Austin, 1999), but this is countered by public concern over how this breeding may alter the nutrient profile of the crop, rendering diets less healthy (Shewry et al., 2016). Whilst there is little to no scientific support for this, public opinion may make this option unviable. In addition, global temperature shifts due to climate change are predicted to reduce wheat production. Temperature increases between 1980-2008 are estimated to have reduced wheat production by 5.5% (Lobell et al., 2011). This sentiment is echoed by Nelson et al. (2010) whose simulations indicate that wheat yields obtained in the year 2000 will decline between 14.5 - 29% by 2080. Indeed, losses may become extreme as more recent estimates indicate that a 1°C global temperature increase may reduce global wheat production anywhere between 4.1 and 6.4%.

Aside from plant productivity, in nearly all crop producing systems a pest is present taking a cut of the total yield. Removing the pest would undoubtedly increase total food available to humans. Wheat is not exempt from being targeted by pests. In fact, losses of wheat to pests and pathogens can be extreme with estimates suggesting global yield losses of between 10.1 and 28.1% depending on the growing region (Savary et al., 2019). This is consistent with the 28.2% wheat production loss to pests and pathogens identified by Oerke (2005) in the 2001-2003 wheat growing period. Split down into its constituent parts, wheat losses in 2001-2003 totalled 7.7% to weeds, 7.9% to animal pests, 10.2% to pathogens and 2.4% to viruses (Oerke, 2005). The largest loss to wheat yield here comes from pathogens with one of the most globally devastating pathogens being the fungus *Zymoseptoria tritici*, the most prevalent foliar wheat pathogen in temperate regions (Figueroa et al., 2018) including the UK and Europe (CropMonitor, 2020, Jørgensen and Smedegaard-Petersen, 1999).

1.2 Taxonomy, identification and phylogenetics

Zymoseptoria tritici is the causal agent of Septoria tritici blotch (STB), also known as Septoria leaf blotch, as described by Desmazieres in 1842 (Ponomarenko et al., 2011). STB is identifiable as necrotic lesions containing fructifications on host leaves (Wittenberg et al., 2009)(Figure 1.1), targeting wheat species (Seifbarghi et al., 2009, Jing et al., 2008) with specialisation towards bread and durum wheat (*Triticum aestivum L.* and *T. turgidum ssp. durum L.*, respectively)(Kema and van Silfhout, 1997). The pathogen has occasionally been found on other grass species including rye (*Secale cereale L.*) (Sprague, 1950). Suffert et al. (2011) estimate that there may be as many as 26 host species for *Z. tritici*. However, the host range of the fungus remains contentious with others arguing that infection is limited to wheat and blocked after stomatal penetration for other species (Habig et al., 2020).

Figure 1.1 *Zymoseptoria tritici* infected wheat leaf showing symptoms of Septoria tritici blotch. A Riband wheat leaf, 21 days post introduction of *Zymoseptoria tritici* (strain IPO323), showing leaf necrosis with pycnidia formation within necrotic lesions.

Following the first description of *Z. tritici* as a disease (1842)(Ponomarenko et al., 2011) it was assigned the scientific name *Mycosphaerella graminicola.* However, after determination from sequence data that the *Mycosphaerella* genus was polyphyletic (Crous et al., 2007), the *Zymoseptoria* genus was proposed as part of a larger project attempting to subdivide the *Mycosphaerella* (Quaedvlieg et al., 2011)(Figure 1.2). *Zymoseptoria tritici* was named as the type species of the genus, *Mycosphaerella graminicola* now used to describe the teleomorph form of the fungus. The *Zymoseptoria* genus however still sits within the Mycosphaerellaceae family of fungi (Phylus: Ascomycete; Order: Dothideales; Class: Dothideomycete).

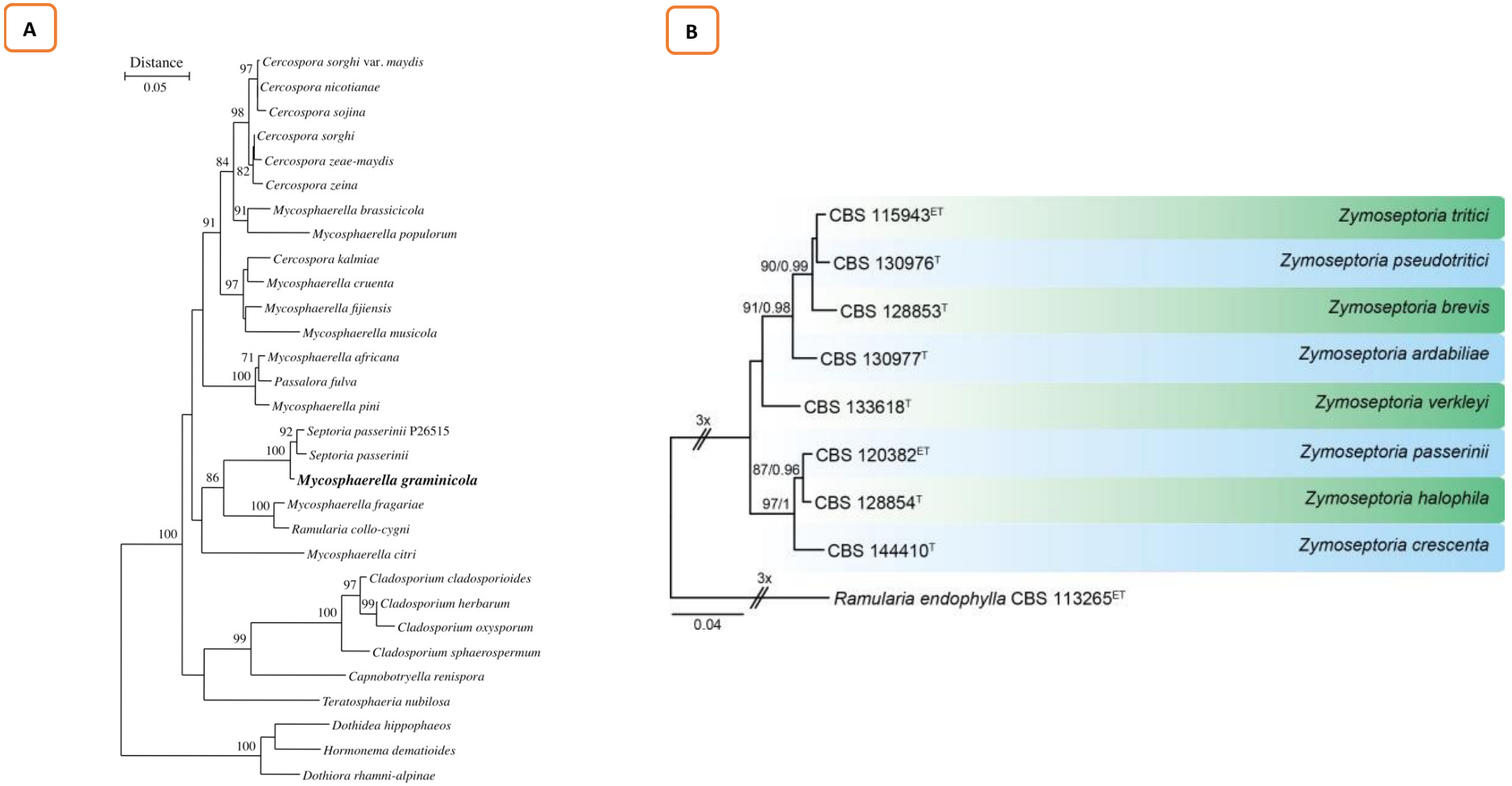

Figure 1.2 Phylogenetic arrangement of *Zymoseptoria tritici* pre- and post- reclassification of the fungus from *Mycosphaerella graminicola.*

A) Image from Ponomarenko et al. (2011) showing the phylogenetic relationships of *Mycosphaerella graminicola*. B) Phylogram from Chen et al. (2022) showing the phylogenetic relationships of *Zymoseptoria tritici*.

1.3 Septoria tritici blotch

Zymoseptoria tritici infection is biphasic including a latent and necrotrophic phase and involves the production of spores through both sexual and asexual reproduction.

1.3.1 Latent phase

Infection begins with the arrival of a *Z. tritici* spore onto the leaf of a wheat plant. From here, the spore germinates, extending its germ tube until it reaches a stomatal aperture through which it can enter the mesophyll tissue layer of the leaf (Jørgensen and Smedegaard-Petersen, 1999, Duncan and Howard, 2000). Entry to the leaf therefore does not involve specialised structures such as appressoria or haustoria but simply hyphal growth; though Duncan and Howard (2000) postulate that growth may be directed toward stomata by a thigmotropic signal. The whole process of plant leaf penetration from initial inoculation takes 24-48 hours (Cousin et al., 2006). The pathogen will also enter the leaf mesophyll through areas of leaf damage (Fones et al., 2017).

Once the pathogen has entered the plant leaf tissue the fungus resides within the intracellular space (Cousin et al., 2006). The colonised host plant remains asymptomatic for several days as the fungus grows slowly, attempting to avoid detection by means of the LysM effectors, of which there are three (Marshall et al., 2011). LysM effectors consist of Mg1LysM, Mg3LysM (Marshall et al., 2011) and Mgx1LysM (Tian et al., 2021) with all effectors binding chitin, protecting the fungal hyphae against plant hydrolytic enzymes, including chitinases (Marshall et al., 2011). LysM effectors also block the stimulation of chitin-mediated plant defence pathways, following recognition by the wheat CERK1 and CEBiP receptor proteins (Lee et al., 2014), through which reactive oxygen species are produced (Tian et al., 2021). Without the Mg3LysM effector, the progression of *Z. tritici* infection is hindered with this having knock-on effects on lesion development and asexual spore production (Marshall et al., 2011).

To further avoid detection, it has been proposed that the fungus uses its own energy resources during the latent phase in the form of nutrient stores within the fungal spore. Nutrients are presumably released by *β*-oxidation of fatty acids and lipids as genes for this metabolism are upregulated in the early stages of asymptomatic infection (1 to 4 days post infection)(Rudd et al., 2015). It should be noted though that Sanchez-Vallet et al. (2015) have equally described how plant cell wall degrading enzymes (CWDEs) may be at play in these

early stages of infection too since transcripts encoding these enzymes have been identified during the biotrophic-like phase of infection (Yang et al., 2013). However, given that widescale damage would risk a host response, the involvement of CWDEs in latent phase nutrient acquisition is questionable. Overall, we do not conclusively know how the pathogen gains nutrients during this latent phase. Yet, regardless of how nutrients are gained, the fungus remains largely successful in avoiding host defences during this time as symptoms of disease are minimal. Hence, the latent phase is often also referred to as the symptomless or asymptomatic phase.

1.3.2 Necrotrophic phase

Zymoseptoria tritici is often referred to as a hemibiotroph (Brennan et al., 2019), as defined by Luttrell (1974), and the nutrient reserves within the spore or the stealth nutrient acquisition from the plant cannot sustain the energetic demands of fungal sporulation. Therefore, the latent phase, which lasts ~8–10 days post infection (dpi)(Kema et al., 1996c), must come to an end and the fungus switches to the necrotrophic stage of its lifecycle with this typified by large changes in gene expression (Rudd et al., 2015, Keon et al., 2007) which notably is followed by host cell death. The coincidence of this shift in gene expression and cell death has resulted in the theory that *Z. tritici* itself is producing protein effectors that induce the plant's defences including the hypersensitive response (Hammond-Kosack and Rudd, 2008, Kema et al., 1996c) that causes cell death. The fungus converts the plant material into a form that is more readily accessible to it, the dead plant material needed by a necrotroph. It is upon release of these nutrients and energy to the pathogen that *Z. tritici* is then able to generate the biomass to support production of both sexual and asexual spores (Keon et al., 2007). Hence, it is within necrotic lesions that these spores are produced (Stewart et al., 2018, Stewart and McDonald, 2014), allowing the infection cycle to be renewed.

1.3.3 Spore production

Coinciding with the necrotrophic phase of the *Zymoseptoria tritici* life cycle is the production of spores via the sexual cycle (Palma-Guerrero et al., 2016). In the field, and under natural conditions, *Zymoseptoria tritici* regularly completes its sexually reproductive cycle (Zhan et al., 2003, Chen and McDonald, 1996), generating genomic diversity in the spores produced by meiosis (Wittenberg et al., 2009). The *Z. tritici* sexual cycle can be completed within five

weeks, thus the fungus can undergo several iterations of the cycle in one wheat growing season (Kema et al., 1996b). This is particularly pertinent when we consider that it is the spores produced by the sexual cycle, ascospores, which act as primary inoculum for infection (Kema et al., 1996b, Shaw and Royle, 1989)(Figure 1.3), allowing the initial introduction of the fungus to a plant (Sanderson and Hampton, 1978). This is to a large extent due to the large distances over which ascospores can spread (Sanderson, 1972) afforded by wind dispersal (Shaw and Royle, 1989). In addition, ascospores are capable of surviving for months following wheat harvest, with Sanderson and Hampton (1978) noting spore release from dead material and wheat stubble eight months post-harvest. This was a key adaptation to fungal survival when the wheat was solely spring-sown, however, modern farming employs winter wheat varieties meaning wheat crop is always present in a field – and available for *Z. tritici* to infect. As such, ascospores play a key role in the persistence of *Z. tritici*.

Meanwhile, asexual spores permit secondary infections, spreading the fungus only by several metres (Singh et al., 2021) to different leaves of the same plant or closely neighbouring plants with dispersal mediated by rain splash (Bannon and Cooke, 1998, Duncan and Howard, 2000, Stewart et al., 2018). Asexual spores therefore facilitate the rapid spread of *Z. tritici* between plants on a local level (Hunter et al., 1999b). Similar to their sexually produced counterpart, several asexual cycles can occur during the wheat growing season, generating further inoculum for spread of the disease, causing fieldwide epidemics (Stewart et al., 2018).

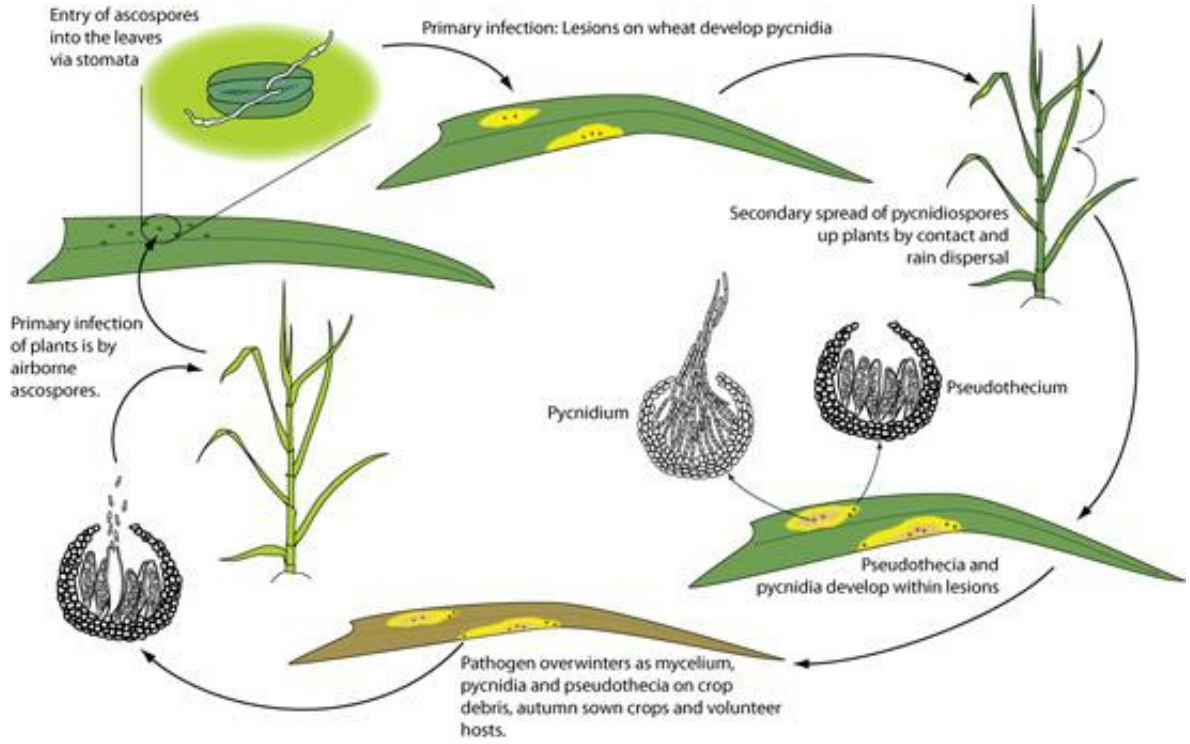

Figure 1.3 The infection cycle of *Zymoseptoria tritici* from Ponomarenko et al. (2011).

A schematic showing the different stages of *Z. tritici* infection of wheat including primary and secondary infection facilitated by the production of both sexual and asexual spore types.

1.4 Genetics of infection

Z. tritici infection of wheat, especially from a genetic perspective, is complex. There have been many *Z. tritici* Avr genes mapped in this interaction, and corresponding resistance genes in wheat, but none of these wheat genes give perfect control. Virulence, the severity of STB, is likely determined by many genes in combination to give quantitative virulence (Stewart et al., 2018). Not only this, but during the course of infection different groups of genes are up-regulated at varying stages of the infection process (Rudd et al., 2015, Palma-Guerrero et al., 2016). As such, the relative importance of a given gene in virulence is not only dependent upon its presence in the genome of a specific fungal strain but also the exact timing and strength of its expression. Of those virulence genes characterised, most are of large effect and certainly do not represent the entire range of genes responsible for *Z. tritici* infection, especially in light of transcriptional data. It must also be noted that any gene that impacts the overall fitness of the pathogen will also impact pathogen virulence.

Key virulence factors however, due to their substantial impact on the host plant, are more easily identifiable in research studies. The importance of the known *Z. tritici* virulence genes in infection can be significant, with deletion mutants preventing penetration and initial infection of host leaves (Cousin et al., 2006, Mehrabi et al., 2006b, Mehrabi et al., 2006a, Marshall et al., 2011, Mohammadi et al., 2020) or pycnidia production (Mehrabi and Kema, 2006, Mehrabi et al., 2009, Poppe et al., 2015, Habig et al., 2021). For other genes, the specific means by which virulence is reduced is not appreciated, however, knockouts still reduce overall pathogenicity of the fungus (Kramer et al., 2009). Furthermore, we must understand that the genes involved in pathogenicity are not simply those encoding virulence factors but also those regulating them. Several studies from Mirzadi Gohari et al. (2014), Mohammadi et al. (2017) and Habig et al. (2020) have demonstrated that loss of the transcription factors for effectors also reduces pathogenicity when deleted from the genome.

Greater numbers of effector genes with possible involvement in *Z. tritici* infection are continually coming to light (McDonald et al., 2016). However, information on genes encoding the effectors that trigger plant programmed cell death during the shift from the latent to necrotrophic phase of infection is still missing – although candidates ZtNIP1, ZtNIP2 (M'Barek et al., 2015) and MgNLP have been proposed (Motteram et al., 2009). ZtNIP1 and ZtNIP2 (M'Barek et al., 2015) show greatest promise due to their ability to trigger cell death in wheat plants (how this is induced is currently unknown (Kettles and Kanyuka, 2016)). For MgNLP, though capable of initiating programmed cell death (PCD) in non-host *Arabidopsis thaliana* the same is not seen for wheat, nor does gene deletion impact plant pathogenicity (Motteram et al., 2009).

1.5 Historic and current importance of *Z. tritici*

It is clear that *Z. tritici* is capable of infecting wheat and does so – the pathogen is one of the most prevalent foliar pathogens in Europe (Jørgensen and Smedegaard-Petersen, 1999). Though there are many known unknowns for *Z. tritici* infection of wheat, the significance of the pathogen is clear. Septoria tritici blotch instigates leaf cell death (chlorosis and necrosis) – presumably by protein effectors triggering the plant hypersensitive response (Hammond-Kosack and Rudd, 2008). Given that it is in leaf material that the photosynthesis necessary for the conversion of light energy to chemical energy takes place, *Z. tritici* infection results in

the reduction of the photosynthetic ability of the plant. As an extension to this, so too is the grain-filling potential of the wheat plant reduced (Orton et al., 2011, Lynch et al., 2016) as less energy can be channelled into grain growth. As such, STB severity is considered in terms of leaf damage or the proportion of the leaf showing signs of disease (Karisto et al., 2018). Though the impact of *Z. tritici* on an individual wheat plant can be significant, this does not guarantee consideration of the pathogen as one of importance. Indeed, an isolated infection need not warrant much concern, rather, the importance of *Z. tritici* comes from its prevalence which though abundant now has not historically always been the case.

1.5.1 Historic importance

As with many cereals, wild wheat progenitors originated in the fertile crescent where they were domesticated (Harlan and Zohary, 1966). So too did *Z. tritici* originate in the fertile crescent, most likely in modern day Israel (Banke et al., 2004, Banke and McDonald, 2005). As such, the history of *Z. tritici* and Septoria tritici blotch is a long one. The pathogen has co-evolved with its host – giving an explanation to the specificity of the pathogen towards wheat species (Stukenbrock et al., 2012). Despite the proposed origin of the pathogen in Israel, it has been determined that Europe is the origin for the global migration of the pathogen to the New World (Banke and McDonald, 2005). As such, it seems as though the pathogen has followed its host across continents as humans have migrated around the world, taking this crop (and unintentionally its pathogen) with them (Feurtey et al., 2023)(Figure 1.4).

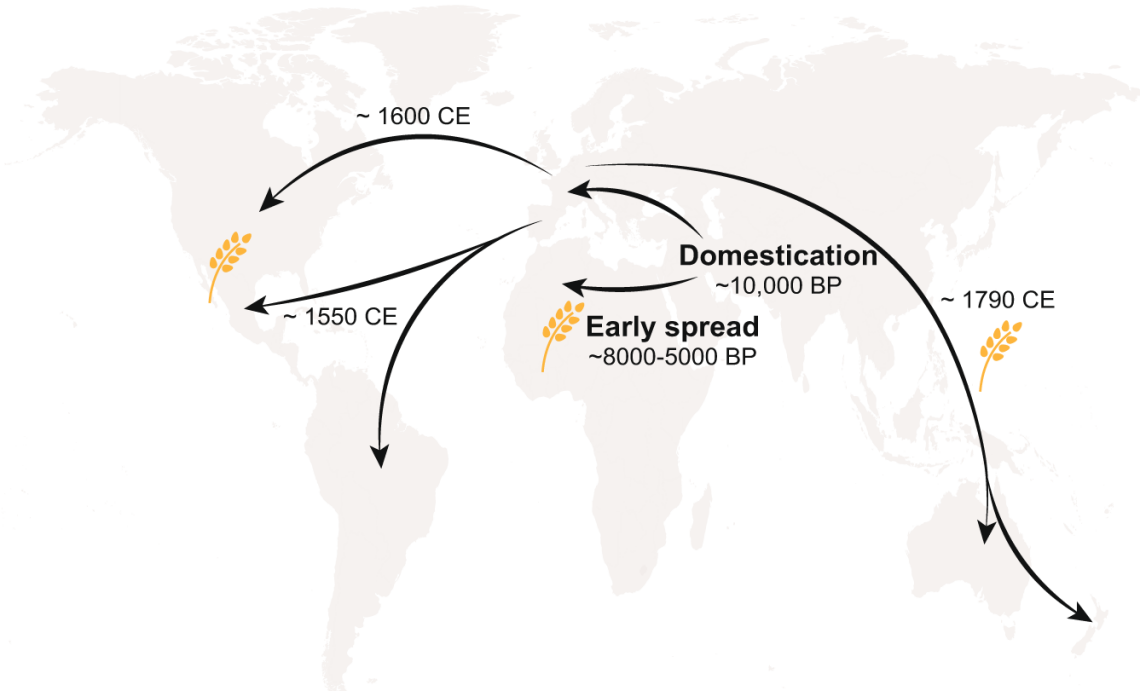

Figure 1.4 Schematic from Feurtey et al. (2023) showing the global spread of wheat.

The spread of wheat following domestication out of the fertile crescent and across the continents is demonstrated with the spread of the wheat pathogen *Zymoseptoria tritici* presumed to follow the movement of wheat (BP; before present, CE; common era).

Septoria tritici blotch has existed for many centuries but its importance in terms of yield loss has shifted through time. This has often been attributed to more recent human interventions, specifically the breeding and introduction of high-yielding dwarf wheat varieties selected where the pathogen was absent (Saari and Wilcoxson, 1974). It has therefore been argued that natural resistances to the fungus were unintentionally lost while other traits were gained (Torriani et al., 2015). Yet, this theory for the increased prominence of *Z. tritici* is contentious (Saari and Wilcoxson, 1974).

Nonetheless, *Z. tritici* has gained importance and significance rapidly in the past 50 years as it has overtaken *Stagonospora nodorum* (Jørgensen and Smedegaard-Petersen, 1999) to become the most prevalent wheat foliar pathogen in the UK and Europe (CropMonitor, 2020, Bearchell et al., 2005, Jørgensen and Smedegaard-Petersen, 1999). Reports in East Africa also suggest that *Zymoseptoria tritici* became more important as a pathogen than *S. nodorum* (Saari and Wilcoxson, 1974) here too over a similar time period. Until this point, *Z.*

tritici was regarded as a relatively trivial problem to wheat production, or perhaps, the pathogen was simply overlooked since *Stagonospora nodorum* was more apparent. This ignorance was to our detriment, but the pathogen's benefit, as control programmes have in the past been directed towards a different pest.

1.5.2 Present significance

Since the 1980s, *Z. tritici,* or more specifically STB, has maintained its mantle as the most damaging disease of wheat in Europe (Kettles and Kanyuka, 2016, O'Driscoll et al., 2014, Torriani et al., 2015) and one of the most damaging diseases of wheat worldwide (Allioui et al., 2016). Indeed, the pathogen can be devastating, and in extreme cases results in reduced wheat yields by 35-50% (Ponomarenko et al., 2011). The degree of severity of infection is likely dependent on the age and condition of the wheat plant, since plants infected at the seedling stage can see grain losses as high as 34.2% compared to uninfected control plots (Aydogdu, 2020). The importance of wheat yield loss has already been considered from the perspective of food security in section 1.1., however, dietary importance also links to economic importance. Studies conducted in England and Wales have demonstrated that past wheat yield losses of 2-3.25% resulted in financial losses of £34.5–35.5 million (Cook et al., 1991, Hardwick et al., 2001). In 2022 the value of UK wheat was £4,059 million (DEFRA, 2023) and so this same yield loss range now equates to monetary losses of ~£81.2-131.9 million. Given that epidemics of the pathogen can reduce yields much more significantly than 2-3.25%, and taking into account the significant expenditure on fungicide applications for control (Fones and Gurr, 2015), the impact of the pathogen on the economies of the countries within which it exists is clear. In addition to yield loss, STB infection also results in a reduction in grain quality (McKendry et al., 1995) which can render the grain unsuitable for use in baking. This undoubtedly reduces the value of infected crops. Economic implications are also felt on an individual level with wheat prices rising in years of poor yield, at times making this dietary staple inaccessible.

1.6 Control methods

Given the impact Septoria tritici blotch can have on wheat yield, and the subsequent implications of this, it is unsurprising that measures are frequently taken to limit this effect. Many different methods of control against *Z. tritici* exist, each varying in their benefit to crop protection as well as their difficulty of employment.

1.6.1 Mechanical control

Mechanical control of pathogens, physical measures to prevent the spread of a disease, is logical for *Z. tritici* control since the spread of disease across growing seasons is often attributed to infected crop debris permitting the release of spores once the new crop has been planted. Hence, removal of this material by burning or burying, before the new crop is planted would remove potential inoculum (Sanderson and Hampton, 1978). This is perhaps the simplest and cheapest form of intervention, but it is not necessarily the most effective. The practice relies on the absence of infected material, but given that ascospores can be dispersed over large areas (Sanderson, 1972), if this is the only control used in one field, it is easily overcome by stubble left in another. Not only this, but it requires near perfect control as a single infected leaf containing *Z. tritici* spores can act as primary inoculum, with repeated reproductive cycles throughout the crop growing season (both sexual and asexual) permitting fieldwide spread of the pathogen. As such, mechanical control is not a method that feasibly can be employed in isolation, but instead used in combination with another form of control against the fungus. The aim of mechanical control in this context is therefore to reduce the available inoculum in a field rather than eradicate it.

1.6.2 Biological control

A control method of increasing interest is that of biological control (biocontrol) – using living organisms, or biological products, to prevent pathogen infection. Preventing *Z. tritici* infection of wheat can be achieved by several means including the use of antifungal producing bacteria or even other fungi. Indeed, exploring the natural microbiome of *Z. tritici* infected wheat leaves lacking STB symptoms has enabled the identification of endophytic fungi *Penicillium olsonii ML37* and *Acremonium alternatum ML38* which in field trials saw significant reductions in disease symptoms compared to water controls (Latz et al., 2020).

Similar results have been identified for *Trichoderma* species with these not necessarily isolated from leaves or even from wheat at all (Perelló et al., 2008). Indeed, the beneficial impact of a biocontrol agent need not come from foliar application (as we would expect for a foliar pathogen) but can instead be provided by organisms in the rhizosphere. In a study by Stocco et al. (2016) identifying *Trichoderma harzianum* strains capable of limiting STB symptom severity upon wheat seed coating, 37 of the 240 strains examined reduced disease severity by greater than or equal to 50%. Equally, for bacteria as biocontrol, rhizobacteria

can limit STB. Recent work conducted by Samain et al. (2022) determined that mixtures of *Paenibacillus sp. B2* and *Arthrobacter spp. AA* applied to germinated wheat seeds effectively, and largely stably, provided protection against *Z. tritici.* Beyond this, bacteria are known to produce an array of chemicals, of which some can be categorised as biofungicides. Those known to show efficacy against *Z. tritici* include secretions by *Lactobacillus* (Lynch et al., 2016), as well as cyclic lipopeptides such as mycosubtilin M, surfactin S, and fengycin F from *Bacillus subtilis* (Mejri et al., 2018) and *Bacillus simplex* (Allioui et al., 2021).

Outside of direct application of biological products, how biocontrol from living organisms is effective against *Z. tritici* is not always clear. However, for *Paenibacillus sp. B2* and *Arthrobacter spp. AA*, wheat gene expression analysis during rhizobacteria-mediated resistance has determined that inoculation of these species onto wheat results in the upregulation of the plant's defence pathways (Samain et al., 2022), with similar suggestions having been put forward for endophyte-mediated control of cereal diseases more widely (O'Hanlon et al., 2012). Endophyte-mediated biocontrol has also been proposed as the result of endophyte-produced antifungals (Siegel and Latch, 1991). As such, in this instance, direct application of the organism itself facilitates delivery of the biological product (biofungicide).

Though biocontrol can be effective, it is important to note that it is not a 'one size fits all' solution. Biocontrol is far more complex than some other *Z. tritici* control methods since organisms are specialised to niches and their ability to survive is dependent on exact conditions both in terms of the host and environment (Latz et al., 2020, Hajieghrari et al., 2008, Perelló et al., 2008, Heick et al., 2017). As such, it may not always be possible to take an effective biocontrol agent from one place and introduce it to another. Simply adding a new species to a microbiome is not sufficient – especially when the microflora in a given environment can easily inhibit growth of the biocontrol species or metabolise any products it generates (Howell, 2003). This has led some scientists to suggest that biocontrol works best when using native strains (Stocco et al., 2016), screening these anew in each instance of planned application (Howell, 2003). In addition to this complexity, biocontrol may not be effective throughout the wheat growing season with Perelló et al. (2008) noting that efficacy of *Trichoderma* biocontrol was highest at early wheat developmental stages. As a result, and similarly to mechanical control, Perelló et al. (2008) doubts the capacity for biocontrol to be

used in isolation for the protection of wheat crops against *Z. tritici.* Furthermore, due to its complexity, for biocontrol there is a lack of education for users regarding the equipment required for application of the product on a large scale as well as how best to store such products.

1.6.3 Chemical control

As well as biological products with antifungal activity, synthetic chemicals capable of fulfilling the same purpose exist with these being the most commonly used method of control against *Z. tritici* (Fones and Gurr, 2015, Torriani et al., 2015). Fungicides are a huge business and in 2014 Europe, $1.7 billion was spent on fungicides for wheat – with 70% of this targeted at tackling Septoria tritici blotch (Torriani et al., 2015). Similar predictions have been made by Kettles and Kanyuka (2016), suggesting that ~€1 billion is spent annually on tackling the fungus. Costs indeed add up when as many as four fungicide sprays may be applied per growing season (Kildea et al., 2019).

Unsurprisingly, there is a long history of chemical control of *Z. tritici*, with the chemical control methods used changing to mirror shifts in agricultural practices as well as in the pathogen. Indeed, until the introduction of quinone outside inhibitor (QoI) based fungicides (strobilurins) in 1996, the pathogen was largely controlled by demethylation-inhibiting fungicides (DMIs) (Torriani et al., 2009) which had been in use since the 1970s (Fraaije et al., 2005b). QoIs were believed to be better able to control STB than their DMI predecessor (Torriani et al., 2009). However, this usurping was short-lived and resistance by the fungus to QoIs was identified in the UK in 2002 resulting from a single nucleotide polymorphism in the mitochondrial cytochrome b gene, replacing glycine for alanine at codon position 143 (G143A) when translated (Fraaije et al., 2005a, Gisi et al., 2002). The mutation has been shown to arise independently in several geographically and genetically distinct *Z. tritici* populations (Torriani et al., 2009).

As such, in many countries QoIs are only permitted to be used when mixed with other fungicides with a different mode of action (Table 1.1) – usually DMIs – so as to prevent selection for resistance (Fraaije et al., 2005b). In terms of the fungicides we use today, this has meant a reversion to the use of DMIs as the main fungicide employed against STB, as well as recently developed succinate dehydrogenase inhibiting fungicides (SDHIs) and multi-site inhibitors (Fraaije et al., 2012, Torriani et al., 2015).

Table 1.1 The modes of action of fungicides used to control STB.

Fungicide	Mode of action	Mechanism
Quinone outside inhibitor (QoI)	Mitochondrial respiration inhibition	Binds cytochrome b at the Q_o site inhibiting electron transfer to cytochrome c_1 and stopping ATP production (Bartlett et al., 2002).
Demethylation-inhibiting fungicides (DMIs)	Ergosterol synthesis inhibition	Binds a mixed-function oxygenase cytochrome p450 and inhibits binding to the lanosterol C14-methyl group, preventing C14-demethylation (Ziogas and Malandrakis, 2015, Gisi et al., 2000).
Succinate dehydrogenase inhibiting fungicides (SDHIs)	Mitochondrial respiration inhibition	Bind to the mitochondrial complex II ubiquinone-binding site preventing electron transfer to ubiquinone from succinate (Avenot and Michailides, 2010).
Multi-site inhibitors	Inhibit pathogen development before infection	Form a protective barrier on the plant surface, inactivating enzymes involved in pathogen metabolism in a non-specific manner (Gisi and Sierotzki, 2008).

At present, as there has been for the past half century, there is huge reliance on DMIs. Though these azole fungicides are still reasonably effective, this efficacy varies across Europe and is tightly interlinked with historic use of the fungicide. Countries with past intensive use of DMIs, including the UK and Ireland, show high mutation frequencies in CYP51 reducing sensitivity of the fungus to the chemical control (Jørgensen et al., 2017). Decreases in azole sensitivity are also noted across seasons (Jørgensen et al., 2020) and similarly to QoIs, resistance mutations to azole fungicides have been seen to independently arise in genetically distinct populations (McDonald et al., 2019).

In Northern Europe the most commonly used DMIs are prothioconazole and epoxiconazole (Wieczorek et al., 2015). This is largely due to maintained efficacy of these fungicides in the face of *Z. tritici* mutation. Indeed, *Z. tritici* mutations such as I381V which lead to reduced efficacy of certain azoles such as tebuconazole have no large impact on sensitivity to epoxiconazole (Fraaije et al., 2007). However, the efficacy of even these fungicides is now being impacted by *Z. tritici* mutation – particularly for these fungicides the S524T mutation

in the CYP51 gene impacts performance (Cools et al., 2011). Lack of resistance to this fungicide was unlikely since the chemical has a single target site (Cools and Fraaije, 2008) – and so mutation in just this one site would confer resistance.

For *Z. tritici* it is the diversity from sexually produced spores, and the frequency of sexual reproduction, that provides the variation required for adaptation against fungicides– or "evolutionary adaptability" (Linde et al., 2002, Chen and McDonald, 1996, Wittenberg et al., 2009). Though mutations for each fungicide have been noted, since each chemical has a different target, using combinations of fungicides can be beneficial. This is especially true for fungicides for which resistance mutations are at high risk of arising such as succinate dehydrogenase inhibiting fungicides (SDHIs)(Fraaije et al., 2012) – with these commonly combined with DMIs (Wieczorek et al., 2015, Fraaije et al., 2012). Integrated chemical control applications of DMIs alongside SDHIs and multi-site inhibitors not only slows resistance but can also provide the most effective control (Heick et al., 2017).

Importantly, control does not need to be absolute, eliminating the fungus entirely, but rather fungicides can help to reduce the levels of STB in a field below an economic threshold. Simply slowing the growth and reproduction of the fungus may be sufficient to achieve this.

1.6.4 Genetic Resistance/Wheat breeding

The second most common intervention against *Z. tritici* is breeding resistant cultivars – though it must be appreciated that complete resistance to the point of no pycnidia formation is rare and resistance is categorised instead by low symptom levels (Eyal, 1999). For STB, resistance to the fungus by wheat can be qualitative or quantitative (Brown et al., 2015). Qualitative resistance involves genes of large effect of which there are 21, including Stb6, while quantitative resistance is under the control of many genes of much smaller effect, arguably providing a much more durable form of resistance (Brown et al., 2015). Indeed, Stb6 receptor like kinase mediated detection and resistance to *Z. tritici* (Brading et al., 2002, Chartrain et al., 2005), based on detection of the fungal AvrStb6 effector protein (Zhong et al., 2017), is lost if the fungus or plant does not produce their respective protein. Not only this, but in Mg3LysM we can appreciate how host resistance is easily overcome by the fungus with this fungal effector binding chitin to prevent triggering the wheat defence response (Marshall et al., 2011).

As with fungicide resistance it is the capacity of the fungus to rapidly reassort beneficial alleles during sexual reproduction that affords it the ability to overcome wheat resistances with mutations in avirulence factors (*Z. tritici* effectors that the wheat plant is able to detect), or complete loss of these genes, preventing wheat detection and response to the pathogen. Therefore, introducing any one resistance gene into wheat is unlikely to provide stable and long-term control of *Z. tritici* (Goodwin, 2007). Instead, newer approaches to breeding for STB resistance are centred around the principle of "stacking" or "pyramiding" multiple resistance genes (Chartrain et al., 2004, Torriani et al., 2015). Work conducted by Yang et al. (2022) demonstrated that this method employed for multi-stage resistance genes improved resistance of wheat to STB anywhere between 10 and 37%.

However, perhaps one of the greatest problems facing wheat breeding as a means of STB control is that given the existence of other forms of control, most notably synthetic fungicides, Fraaije et al. (2012) have argued that breeding for resistance to the disease has not been a great priority. Instead, we often see selection of traits that encourage greater yield such as dwarfing, despite evidence that tolerance to STB and wheat dwarfing are often incompatible during breeding (Ziv et al., 1981) – selection for one trait often leads to loss of the other. Though, this can be overcome to some extent by breeding instead for semidwarf varieties (Dubin and Rajaram, 1996), the problem of perfect breeding for STB resistance and yield is not this simply solved as the negative association between the two traits remains (Torriani et al., 2015).

1.6.5 **Integrated management**

Given the pros and cons of each STB control method, integrated management of STB, employing multiple methods at once, may be the best course of action to take going forward. The added benefit, of course, that the fungus is unlikely to evolve resistance to several different types of control easily – requiring several mutations within the genome and the mutations to be beneficial at that. However, careful thought does need to be put into which methods are combined and the individual circumstances under which they are integrated. Indeed, knowing that biocontrol can exist in the form of beneficial fungi, employing fungicides impacts the wheat mycoflora (Müllenborn et al., 2007), and may remove the natural beneficial effects provided by wheat microbiome species. This makes integration of fungal biocontrol and fungicides difficult. Therefore, the use of resistant wheat

cultivars alongside fungicides perhaps offers the simplest form of integrated disease management. Often for any given crop there are several pathogens that need to be considered when selecting a suitable control method. Breeding of resistant cultivars is targeted to particular pests and therefore does not take into account these additional threats – this is potentially to blame for the rise in *Z. tritici* over *S. nodorum* as cultivars with resistance to the latter were selected over the former. The additional application of fungicides to STB 'resistant' cultivars is therefore needed to control multiple fungal pathogens. Despite the prevalence of STB over *S. nodorum*, this pathogen still exists as a pest of wheat.

1.7 *Z. tritici* secondary metabolism

In a review by Muria-Gonzalez et al. (2015) attention is drawn to recent investigations which have revealed the array of secondary metabolites produced by Dothideomycetes. However, in the same review, the lack of knowledge regarding *Z. tritici* secondary metabolites and toxins is highlighted (Muria-Gonzalez et al., 2015) – this is especially surprising given the recognition of *Z. tritici* as one of the "Top 10 fungal pathogens in molecular plant biology" (Dean et al., 2012). Not only this, but since Scharf et al. (2014) suggest that a single filamentous fungus may produce up to 100 secondary metabolites, *Z. tritici* may produce many compounds of interest with far-ranging biological functions. Other fungi within the Dothideomycete class produce secondary metabolites involved in plant pathogenicity as well as mycotoxins (reviewed by Muria-Gonzalez et al., 2015). Therefore, understanding the secondary metabolite profile of *Z. tritici* could shed light on how the pathogen causes STB or reveal alternative factors of ecological importance to the fungus.

By definition, secondary metabolites are compounds which are non-essential for growth. However, these metabolites can still be of importance to the fungus through roles in cellular processes (Brakhage, 2013) and ecologically (Spiteller, 2015, Keller, 2019, Scharf et al., 2014). Fungi employ several mechanisms for secondary metabolite production, these can involve specialist enzymes of non-ribosomal peptide synthetases or polyketide synthases (Scharf et al., 2014), equally secondary metabolites can be produced ribosomally through a process called post-ribosomal peptide synthesis (PRPS)(Figure 1.5).

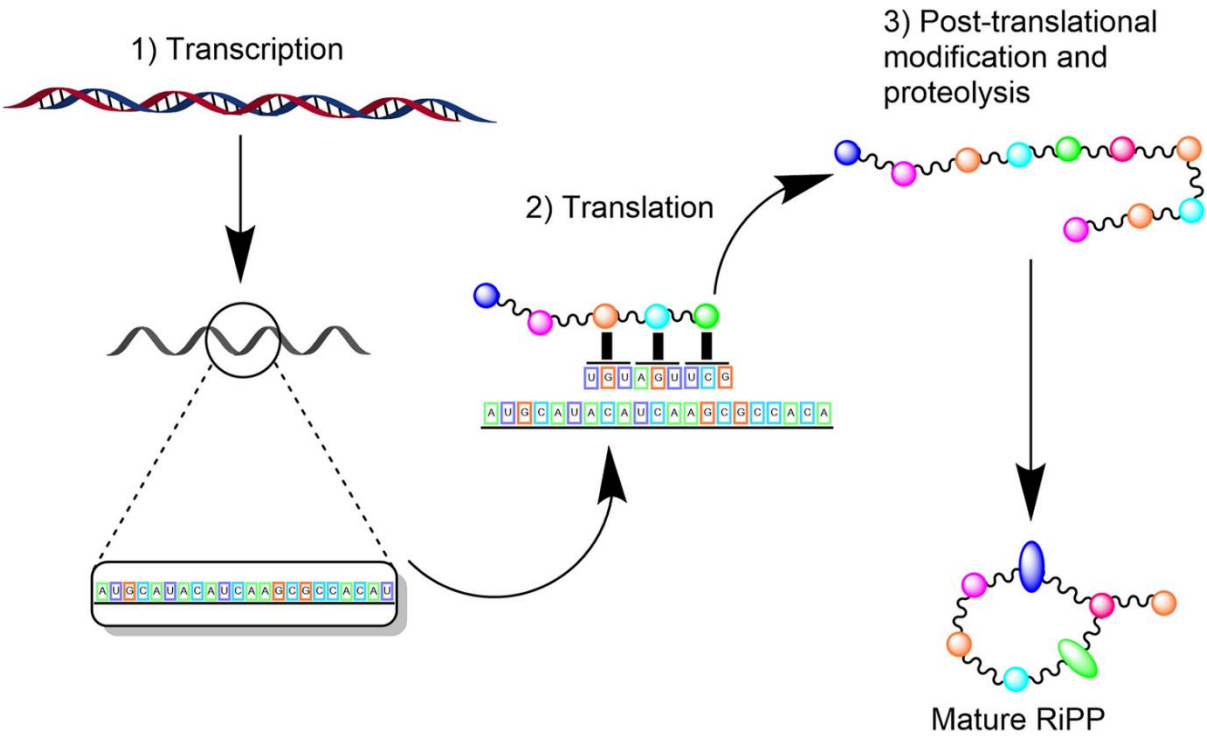

Figure 1.5 Schematic from Ford et al. (2022) illustrating the process of RiPP production by post-ribosomal peptide synthesis.

1.8 Post ribosomal peptide synthesis

The term PRPS was first proposed by Arnison et al. (2013) as a means of describing secondary metabolite synthesis through conventional peptide production, followed by peptide maturation (reviewed in Ford et al., 2022). It is this method of biosynthesis that generates compounds known as Ribosomally synthesised and Post-translationally modified Peptides (RiPPs). PRPS begins with the transcription and translation of a precursor gene which encodes a precursor peptide with a leader and core sequence, as well as either an N-terminal signal sequence or C-terminal recognition sequence (Vogt and Kunzler, 2019)(Figure 1.6). Post-translational modifications are then applied to the large peptide and the core of the RiPP is excised from the larger molecule by proteolysis to give the mature RiPP. In fungi, the tailoring enzymes through which post-translational modifications are conferred exist in biosynthetic gene clusters contiguous to the precursor gene within the fungal genome as is common for fungal secondary metabolites from filamentous fungi (Almeida et al., 2019, Keller, 2019).

Figure 1.6 Schematic of general RiPP precursor peptide arrangement based on Arnison et al. (2013).

All RiPP precursor peptides contain a leader peptide to direct post-translational modifications (Arnison et al., 2013) to the core peptide region which is subsequently excised to give the final mature peptide. Dashed boxes illustrate sequences that are not common to all RiPPs. Eukaryotic RiPPs tend to have an N-terminal signal peptide, while the C-terminal recognition sequence has been indicated in cyclisation (Arnison et al., 2013).

1.9 Ribosomally synthesised and post-translationally modified peptides (RiPPs)

The name RiPPs, as with PRPS, is one designated by Arnison et al. (2013) and is defined as any peptide synthesised by PRPS but with the caveat that the peptide is no larger than 10kDa in size. RiPPs are found in all kingdoms of life, and in fact, bacterial RiPPs have received far more interest than those produced by fungi and are largely well-documented (Ortega and van der Donk, 2016). The functions of RiPP peptides of bacterial, plant, animal, and fungal origin are discussed in detail in Chapter 4.

Unlike the bacterial and animal RiPPs which have been understood and exploited for several years, the first fungal RiPP, called amatoxin, was described in 2007 (Hallen et al., 2007). Additional fungal RiPPs have since been recognised – giving three fungal RiPP families: amatoxins/phallotoxins, dikaritins, and borosins. RiPP literature often makes reference to an epichloëcyclin family (Vogt and Kunzler, 2019, Johnson et al., 2015), however, recent work has reclassified peptides from this family into the dikaritin class (Kessler and Chooi, 2021). The unique features of fungal RiPP synthesis for each family are described fully in Chapter 3.

1.9.1 Amatoxin/Phallotoxins

Although amatoxins have been known of for a long time (famously these toxins result in the lethality of the death cap fungus), it was only in 2007 when they were shown to be fungal RiPPs, alongside the related phallotoxins (Hallen et al., 2007). Amatoxins are arguably more widespread since phallotoxins are largely produced by *Amanita* species (Hallen et al., 2002), however exceptions do exist (Luo et al., 2009). Amatoxins are generated by four different

Basidiomycete genera; the *Amanita*, *Galerina*, *Lepiota* and *Conocybe* (restricted to *C. filaris* for this genus (Diaz, 2018))(Enjalbert et al., 2004, Drott et al., 2023, Luo et al., 2012). In 2002 at least 35 amatoxin producing species were documented (Enjalbert et al., 2002); by 2018 only a further three species had been added to this list (Diaz, 2018). However, there are likely many more amatoxin producing fungi that have not yet been recognised.

Of the amatoxins, which include: α-amanitin, β-amanitin, γ-amanitin, ε-amanitin, amanin, amanullin, amanullinic acid, amaninamide, and proamanullin; α-amanitin is the most highly researched and understood. α-amanitin exerts its toxicity by inhibiting eukaryotic RNA polymerase II (Stirpe and Fiume, 1967, Novello et al., 1970, Rudd and Luse, 1996). The peptide binds to the polymerase and in doing so changes the conformational state of the enzyme, reducing the elongation rate of the polymerase as well as interfering with incorporation and translocation of the DNA template (Brueckner and Cramer, 2008, Kaplan et al., 2008). This in turn prevents mRNA synthesis and as mRNA levels become depleted, protein synthesis is reduced. The disruption caused by the toxin ultimately results in the death of affected cells by apoptosis (Wong and Ng, 2006). Phallotoxins do not interact with RNA polymerase, instead these RiPPs tightly bind to F-actin and prevent conversion to G-actin (Wieland, 1977). Through interfering with the cytoskeleton (Garcia et al., 2015), cell membranes become weakened, leading to cell necrosis (Fantozzi et al., 1986).

1.9.2 Borosins

The borosin RiPPs represent the newest addition to the fungal RiPP family having been discovered and described in 2017 (Van Der Velden et al., 2017), 10 years after the first fungal RiPP (Hallen et al., 2007). Despite this, due to extensive analysis of select borosin peptides prior to their classification as RiPPs, originally assumed to be produced by non-ribosomal peptide synthetases, the functions of some borosin metabolites are understood (Mayer et al., 1997, Vanyolos et al., 2016). For many fungal metabolites the biosynthetic pathways behind their creation are unknown, hence a lag between the identification of peptide structure and/or function and its biosynthetic pathway is not uncommon.

Borosins, as a RiPP family, was formed following analysis of the omphalotin peptides from the fungus *Omphalotus olearius* (Mayer et al., 1997, Van Der Velden et al., 2017). The toxin was identified as part of a larger search for a means of control against the plant parasitic *Meloidogyne incognita* nematode (Mayer et al., 1997). Analysis showed the toxin to be

effective and selective – targeting *Meloidogyne incognita* specifically (Sterner et al., 1997). However, the mode of action of the peptide is still to be determined (Mayer et al., 1999a). Borosins are synthesised in a unique way whereby the N-terminal region of the RiPP precursor itself has catalytic activity homologous to a SAM-dependent methyltransferase (van der Velden, 2017). This unique domain embedded in the precursor has led to the identification of 50 putative borosin gene clusters (Quijano et al., 2019). Characterised peptides are continually being re-evaluated and so the RiPP family can also grow by this means. For example, gymnopeptides, which show anti-proliferative effects on human cancer cells (Vanyolos et al., 2016) are now known to belong to the borosin RiPP class (Quijano et al., 2019). The anti-proliferative effect of gymnopeptides lies largely in the cytotoxic activity of the metabolite, inhibiting cell growth (Vanyolos et al., 2016).

1.9.3 Dikaritins

Dikaritins, named by Ding et al. (2016), are a family of RiPPs produced by species belonging to the subkingdom Dikarya which includes the Ascomycota and Basidiomycota. This RiPP class is unique as each precursor gene encodes multiple repeats of the core peptide sequence. After translation, the precursor peptide is processed by peptidases that release each core peptide. These RiPPs are commonly referred to as multicore RiPPs (Rubin and Ding, 2020). To date, several dikaritin RiPPs have been identified, including ustiloxin (from *Ustilaginoidea virens* (Tsukui et al., 2015) and *Aspergillus flavus* (Umemura et al., 2013, Umemura et al., 2014)), phomopsin (from *Phomopsis leptostromiformis* (Ding et al., 2016)), asperipin-2a (from *Aspergillus flavus* (Nagano et al., 2016)), epichloëcyclins (from *Epichl*oë *sp.* endophytic fungi (Johnson et al., 2015)) and victorin (from *Cochliobolus victoriae* (Kessler et al., 2020)). Of these dikaritins, the most well-understood are those which were investigated prior to their designation as RiPPs – these are ustiloxin, phomopsin and victorin.

Ustiloxin and phomopsin both are mammalian toxic (Peterson et al., 1987, Koiso et al., 1992, Koiso et al., 1994, Battilani et al., 2011) and in each instance this effect is exerted by inhibiting microtubule assembly following binding, preventing the spindle formation required in mitosis (Iwasaki, 1992, Koiso et al., 1992, Koiso et al., 1994, Battilani et al., 2011). A shared antimitotic function is what initially led to comparisons being drawn between phomopsin and ustiloxin. Victorin, however, is selectively phytotoxic, inducing cell death by instigating a signal transduction cascade for apoptosis in susceptible host cultivars (Navarre

and Wolpert, 1999). Asperipin-2a represents the only known example to date of asperipins, discovered computationally by identification of ustiloxin homologues (Nagano et al., 2016). The biochemistry of this peptide is known however, to our knowledge no function has yet been assigned to the RiPP.

The epichloëcyclins, which have recently been reclassified as dikaritins, are produced by *Epichloë* endophytes which are able to form associations with plants ranging from parasitic to mutualistic (Johnson et al., 2015). In fact, it was *Epichloë* fungi that were identified as the first endophyte capable of use in biocontrol against a fungal pathogen (Latch, 1993). The range of existing epichloëcyclins (epichloëcyclin A-F) are generated by means of small differences in the core sequence repeated within the precursor gene, known as *GigA* (Green et al., 2020). Once translated, these variations within the repeat sub-units produce modified peptides. Epichloëcyclin metabolites are synthesised in abundance while the *Epichloë* fungus is associated with the host plant, secreting these peptides into the plant apoplast and as a result causing a shift in the metabolome here (Johnson et al., 2015, Green et al., 2020). The exact functions of the epichloëcyclins remain unknown, though increased expression of *GigA* by *Epichloë* fungi during endophytic associations compared to *in vitro* culture (A. Koulman, G. Lane, unpublished data; Johnson et al., 2015) has led to the proposal that the epichloëcyclin peptides could be involved in symbiosis in some form (Johnson et al., 2015, Vogt and Kunzler, 2019).

Preliminary work done in the Bailey/Foster laboratory identified that the *Z. tritici* genome contains a biosynthetic gene cluster with similarity to the known dikaritin RiPPs. Given the range of ecological functions performed by dikaritin RiPPs, including involvement in pathogenicity, it is possible that the putative *Z. tritici* RiPP effects disease.

1.10 Objectives of the thesis

- Determine if the novel *Zymoseptoria tritici* RiPP is involved in the biology of this important plant pathogen.
- Piece together the biosynthetic mechanism behind the production of the RiPP and see how this compares to those mechanisms documented for other dikaritin RiPP producers.
- Use our current knowledge of the *Zymoseptoria tritici* RiPP to computationally identify novel putative fungal RiPPs.
- Better understand the interaction between abiotic factors and *Z. tritici* infection.

2 : Materials and Methods

Within this chapter, the experimental procedures utilised in the investigations outlined in Chapters 3 to 6 are described. Components of media used throughout this section were supplied by Formedium unless otherwise specified; equally, chemicals were supplied by Fisher Scientific, and Merck/Sigma Aldrich. Deionised water was used throughout.

2.1 Strains and storage

2.1.1 *Zymoseptoria tritici* isolates

Unless otherwise specified, the IPO323 strain of *Zymoseptoria tritici* was used in all experimental analyses. This is the most commonly used experimental isolate as its genome has been fully sequenced (Goodwin et al., 2011) and is publicly available on the National Centre for Biotechnology Information (NCBI). Geographically diverse isolates of *Z. tritici* (from outside of the United Kingdom) were supplied by Professor Bruce McDonald (Table 2.1). The UK collected strains were isolated throughout the 1990s; St93 in 1993 (Lovell et al., 2004) and 1995 for St11, St16 (both isolated by S. J. Kendall from Long Ashton Research Station) and L951 (Hunter et al., 1999a). Additionally, a transformant *Z. tritici* IPO323 containing the codon optimised green fluorescence protein (GFP) gene was acquired from Professor Gero Steinberg (Kilaru et al., 2015).

Table 2.1 Countries of origin of all *Zymoseptoria tritici* isolates used in this work (Badet et al., 2020).

Fungal isolate	Country of Origin
St11	United Kingdom
St16	United Kingdom
St93	United Kingdom
L951	United Kingdom
IPO323	Netherlands
1A5	Switzerland
3D7	Switzerland
ISY921	Israel
StAus01	Australia
StOreg	Oregon, USA
TN26	Tunisia

2.1.2 *Saccharomyces cerevisiae*

For experiments involving *Saccharomyces cerevisiae,* the yeast strain BY4742 (Y10000) was employed. This is a deletion strain derived from S288C with the *MATα; his3Δ1; leu2Δ0; lys2Δ0; ura3Δ0* genotype (Baker Brachmann et al., 1998).

2.1.3 Bacteria

2.1.3.1 Escherichia coli

Different *Escherichia coli* strains were employed depending on their intended purpose – mainly for transformations. *E. coli* Top10 was used to produce electro-competent cells for transformations while DH5α was employed in the production of chemically competent cells and for bioassays. Neither possess natural antibiotic resistances making them ideal strains into which vectors containing antibiotic resistant genes may be introduced.

2.1.3.2 Agrobacterium tumefaciens

The LBA1126 strain of *Agrobacterium tumefaciens* (Bundock and Hooykaas, 1996) was utilised in this work, the strain is resistant to rifampicin, carbenicillin and spectinomycin. However, this strain is kanamycin sensitive allowing for selection of plasmids containing a kanamycin resistance gene.

2.1.3.3 Bacillus subtilis

The gram-positive Bacterium *Bacillus subtilis* strain ATCC 6633 was employed in plate-based bioassays testing for antibiotic activity.

2.1.4 Culture maintenance

All media for culture maintenance were prepared with deionised water (dH_2O) in Duran bottles – these were autoclaved prior to use at 121°C for 15 minutes (Table 2.2).

Table 2.2 Media used for general culture maintenance.

Media names and any abbreviations are indicated alongside their methods of preparation (indicated for a litre of media). The use of each medium is noted with reference to the organism it maintains.

Media	Preparation	Use
Yeast sucrose media (YSM)	• 10g Sucrose • 10g Yeast extract powder	Liquid medium for filamentous growth of *Z. tritici.*
CD+YE	• 33.4g Thermo Scientific™Oxoid™ Czapek Dox Liquid Medium • 10g Yeast extract powder	Medium for *Z. tritici* growth conducive to peptide production.
Potato dextrose agar (PDA)	• 41g Potato dextrose agar	General medium for *Z. tritici* growth.
Potato dextrose broth (PDB)	• 24g Potato dextrose broth	General medium for *Z. tritici* growth.
CDV8 agar	• 33.4g Thermo Scientific™ Oxoid™ Czapek Dox Liquid Medium • 3g Calcium carbonate • 200ml V8 juice - Campbell's • 20g Agar	General medium for *Z. tritici* growth.
Yeast extract-Peptone-Adenine-Dextrose (YPAD) agar	• 70g YPAD agar	Solid medium for yeast growth.
Yeast extract-Peptone-Adenine-Dextrose (YPAD) broth	• 50g YPAD broth	Liquid medium for yeast growth.
Lysogeny broth (LB)	• 20g LB-Broth Lennox powder	Liquid medium for bacterial growth.
Lysogeny broth agar (LBA)	• 35g LB-Agar Lennox powder	Solid medium for bacterial growth.
CD+V8 liquid media	• 33.4g Thermo Scientific™ Oxoid™ Czapek Dox Liquid Medium • 3g Calcium carbonate • 200ml V8 juice - Campbell's (centrifuged before use)	Liquid medium for *Z. tritici* growth.
Tryptic Soy Broth (TSB)	• 30g/L Tryptic Soy Broth	Liquid medium for *Bacillus subtilis* growth.

2.1.4.1 Bacterial maintenance conditions

E. coli strains were maintained on LBA or in LB broth. Strains were cultured from frozen glycerol stocks by dispensing 20µl of thawed culture onto an LBA plate (supplemented with appropriate antibiotics where needed) with an inoculating loop. Freshly cultured *E. coli* cells were then grown at 37°C overnight (~16 hours). Single colonies from such plates were picked using an autoclaved toothpick and inoculated into an autoclaved universal tube containing 5ml LB broth, again supplemented with appropriate antibiotics, for maintenance of *E. coli* plasmids in liquid culture. Liquid cultures were incubated at 37°C, 200RPM overnight (~16 hours). Kanamycin or ampicillin selection was used for transformed *E. coli* – kanamycin for pCAMBIA0380-YA transformed cells and ampicillin for pJET transformed cells.

Agrobacterium tumefaciens cultures were also inoculated onto LBA plates, as above, but grown at 28°C for two days. A single colony of *Agrobacterium tumefaciens* was then inoculated into LB broth (28°C, 200RPM for 48 hours). When growing untransformed *A. tumefaciens* LBA1126 rifampicin, carbenicillin and spectinomycin antibiotics were added to the media (for both liquid and solid cultures). For growth of pCAMBIA0380-YA transformed *A. tumefaciens*, kanamycin was additionally supplemented into LB media.

Similarly, *Bacillus subtilis* was maintained on LBA from a frozen glycerol stock. Stocks were thawed and 20µl inoculate was streaked onto agar plates using a loop or toothpick. This was grown at 28°C for 24 hours. A single colony was picked and inoculated in TSB and incubated at 28°C (200RPM) for 24-48 hours.

2.1.4.2 Fungal maintenance conditions

Yeast was maintained on YPAD agar from frozen glycerol stocks. While stocks were still frozen, a small amount of culture (~20µl) was picked using a sterile pipette tip and spread onto YPAD agar plates. These were then incubated at 28°C for three days. A single yeast colony was then inoculated in 10ml YPAD broth and grown at 28°C for ~12 hours (200RPM).

*Z. tritici s*trains in long-term storage were cultured by thawing the glycerol stock, and a sterile inoculating loop was used to streak mycelia onto solid media (CDV8 or PDA). This was grown at 20°C for five days. For growth in liquid media, after these five days, an inoculating loop was used to transfer a small clump of mycelia into 50-100ml liquid media (PDB or YSM) within 250 ml flasks.

2.1.5 Long term strain storage

For long term storage, bacterial and fungal strains were grown as described in section 2.1.4. up to the point of liquid culture maintenance. In all instances 500µl of culture were then mixed with 500µl 30% glycerol (Fisher) and mixed by pipetting in 2ml cryotubes (Starstedt). These were then flash-frozen in liquid nitrogen before storage at -70°C.

2.1.6 Antibiotics

With the exception of rifampicin, all antibiotics were prepared with sterile dH_2O and filter-sterilised through a 0.22µm Millipore filter (Starstedt) into autoclaved microcentrifuge tubes. The stock concentrations in which antibiotics were produced and the working concentrations at which the antibiotics were used are outlined in Table 2.3.

Table 2.3 Antibiotic stock solutions and working concentrations.

Antibiotic stocks were produced and added to media to achieve the final working concentration.

Antibiotic	**Eluate**	**Stock concentration**	**Working concentration**	**Storage temperature**
Kanamycin	Water	50mg/ml	50µg/ml	-20°C
Ampicillin	Water	100mg/ml	100µg/ml	-20°C
Rifampicin	Methanol	20mg/ml	50µg/ml	-20°C
Carbenicillin	Water	75mg/ml	75µg/ml	-20°C
Spectinomycin	Water	50mg/ml	250µg/ml	-20°C
Hygromycin	Water	50mg/ml	100µg/ml	4°C
Timentin	Water	200mg/ml	200µg/ml	-20°C

2.2 Molecular methods

2.2.1 Nucleic acid extractions

2.2.1.1 E. coli plasmid extraction

E. coli plasmid DNA was extracted from 5ml overnight *E. coli* liquid cultures, grown from single colonies. DNA was extracted using the Macherey-Nagel™ Nucleospin™ Plasmid Kit or the Zymo Research ZymoPURE Plasmid Miniprep Kit. Plasmid extraction was completed in accordance with the manufacturers protocol in both instances. Plasmids rescued from *E. coli*

were run on a 1% agarose gel to check the success of the extraction, then stored at -20°C in sterile dH_2O.

2.2.1.2 Yeast plasmid extraction

Yeast plasmid DNA was rescued from yeast colonies grown on SM-URA agar (Table 2.7) plates for three days following recombination. A toothpick was used to pick colonies and transfer them to Eppendorf tubes. Yeast plasmid extraction then followed the Zymoprep Yeast Plasmid Miniprep II (ZymoResearch) Kit manufacturer's instructions for "Protocol for use with colonies or patches" but modified following isopropanol precipitation of DNA whereby a 70% ethanol wash step was additionally performed adding 400µl EtOH. The sample was centrifuged at 11,000x g for one minute and the supernatant removed. The pellet was airdried before being resuspended in sterile dH_2O.

2.2.1.3 Zymoseptoria DNA extraction

Two methods were employed for extracting *Zymoseptoria tritici* DNA. In both instances DNA was extracted from five-day old CDV8 plate cultures grown at 20°C. The first method used protocol II from the YeaStar Genomic DNA Kit™ (Zymo Research) with minor modifications, opting for a 60-minute incubation time at step two and a ten-minute centrifugation at step four (rather than the two minutes indicated). These DNA extracts were used in PCR reactions where products were intended to be employed in yeast recombination for plasmid construction or cloned into pJET for sequencing. Otherwise, for largescale DNA extractions, such as those for use in diagnostic PCR of putative transformants, the DNA extraction method outlined by Liu et al. (2000) was employed – stocks are listed in Table 2.4.

Briefly, *Zymoseptoria tritici* was harvested from a CDV8 plate with a sterile toothpick and dispersed in 500µl lysis buffer within an Eppendorf tube. This was incubated for 10 minutes at room temperature before 150µl of potassium acetate was added. The Eppendorf was then vortexed before centrifuging at 10,000x g for one minute. The supernatant was transferred to a new microfuge tube and centrifuged as before. The supernatant was again transferred to a new tube. An equal volume of isopropanol was mixed with the supernatant by inversion, this was then centrifuged at 10,000x g for two minutes. The supernatant was discarded, and the remaining DNA pellet was washed with 300µl 70% EtOH. This was once again centrifuged at 10,000x g for one minute. The supernatant was aspirated, and the DNA

pellet left to dry at room temperature. The pellet was then dissolved with an appropriate volume of TE (10mM Tris-HCl; 1mM EDTA).

Table 2.4 DNA extraction buffers from Liu et al. (2000).

Buffers alongside their method of preparation are noted.

Buffer	Preparation
Lysis buffer (200ml)	• 400mM Tris-HCl pH 8.0 • 60mM EDTA pH 8.0 • 150mM NaCl • 1% SDS
Potassium acetate pH 4.8 (100ml)	• 60 ml 5M potassium acetate • 11.5ml glacial acetic acid

2.2.1.4 Zymoseptoria RNA extraction

Several methods of RNA extraction from *Z. tritici* were trialled, including the Zymo Research YeaStar RNA Kit and the Qiagen RNeasy® Plant Mini Kit. Greatest success was achieved from RNA extractions using freeze dried material. Liquid cultures were usually freeze-dried nine-days post media inoculation based on transcriptomics data from Rudd et al. (2015) indicating that *in planta*, this was when expression of the peptide precursor gene was greatest. This was true of all samples except those collected for analysis of gene expression over several time points. Once ready for harvesting, cultures were decanted into 50ml falcon tubes and centrifuged at 10,000x g for five minutes. The supernatant was discarded, and this step repeated as needed for cultures with a volume greater than 50ml. The pellet was then washed with 35ml sterile Milli-Q water and again centrifuged at 10,000x g for five minutes. The water was poured off and the remaining pellet was flash frozen in liquid nitrogen and stored at -70°C overnight. The pellet was freeze-dried for five days then material was ground to a fine powder using a sterile mortar and pestle. 50mg of ground mycelia was used in a phenol chloroform extraction using buffers outlined in Table 2.5. 8ml of 1:1 v/v RNA extraction buffer:phenol was added to the ground mycelia in a 15ml falcon tube and vortexed for 30 seconds. 4ml 24:1 chloroform:IAA was added and the mixture again vortexed for 30 seconds. This was then centrifuged at 10,000x g for 10 minutes. The aqueous phase was transferred to a clean 15ml falcon tube and the phenol chloroform extraction was

repeated, this time using an equal volume of 25:24:1 phenol:chloroform:IAA, and centrifuged as before. 1.5ml of the aqueous phase was transferred to a clean 15ml falcon tube and an equal volume of ice cold 100% ethanol added. This was kept on ice.

Table 2.5 Extraction buffers used to isolate *Z. tritici* RNA.

Buffers alongside their method of preparation are noted.

Buffer	Preparation
RNA extraction buffer (200ml)	• 0.1M Tris pH8.0 • 0.1M LiCl • 10mM EDTA • 1% SDS Made up to 200ml with sterile Milli-Q water.
24:1 Chloroform: IAA (100ml)	• 96ml chloroform • 4ml isoamyl alcohol
25:24:1 phenol:chloroform:IAA (100ml)	• 50ml phenol - Fisher • 48ml chloroform • 2ml isoamyl alcohol

1ml of the mixture was then transferred to a Zymo-Spin™ IIICG Column (YeaStar™ RNA kit), centrifuged at 10,000x g for one minute and the flowthrough discarded – this was repeated until all of the ethanol mixture had been loaded onto the column. The column was washed with 100µl RNA wash buffer (YeaStar™ RNA kit) and centrifuged at 10,000x g for 30 seconds, discarding the flowthrough.

5µl of DNase I (Thermofisher) was mixed with 75µl Monarch® DNase I Reaction Buffer (Monarch® Total RNA Miniprep Enzyme Pack) per reaction and the total 80µl added to each Zymo-Spin™ IIICG Column. This was left at room temperature for 15 minutes then 100µl RNA wash buffer (YeaStar™ RNA kit) was added. The column was centrifuged at 10,000x g for 30 seconds, discarding the flowthrough. The column was washed again with 200µl RNA wash buffer (YeaStar™ RNA kit) and dried by centrifugation for one minute at 10,000x g before it was transferred to an RNase-Free Eppendorf tube. 60µl RNase-Free water was added and this was centrifuged at 10,000x g for 30 seconds to elute the RNA. RNA was immediately checked for degradation and concentration by nanophotometer (Implen Geneflow) and gel

electrophoresis. If of sufficient quality and quantity cDNA synthesis was carried out and the remaining RNA stored at -70°C.

2.2.1.5 RNA extraction from Triticum aestivum

Riband wheat leaves were cut from the plant and placed in 15ml falcon tubes before being flash-frozen in liquid nitrogen and stored at -70°C for at least 24 hours. 75mg material was transferred to a microfuge tube and ground with a micro-pestle. Care was taken to ensure the sample did not thaw. The Qiagen RNeasy® Plant Mini Kit, with the manufacturer's instructions, was used to extract total RNA. This extraction method was modified after step five to include an on-column DNase treatment adding 5µl of DNase I (Thermofisher) mixed with 75µl Monarch® DNase I Reaction Buffer (Monarch® Total RNA Miniprep Enzyme Pack) to each column. RNA quality was assessed as in section 2.2.1.4.

2.2.2 Nucleic acid manipulation

2.2.2.1 Agarose gel electrophoresis

To visualise DNA or RNA samples gel electrophoresis was performed. In all instances, agarose gels were made with 1xTris-acetate-EDTA (TAE) buffer (diluted from 50x TAE; Formedium) and 0.002% Midori Green Advance DNA stain (Geneflow Limited). 1% agarose gels were used throughout this work unless stated otherwise. Gels were generated by microwaving 1xTAE buffer and Midori Green mixture with genetic analysis grade agarose powder (Fisher) until melted. Once cooled, they were poured onto gel trays with appropriate combs and allowed to set. Solidified gels were transferred to a gel tank and submerged in 1xTAE buffer. DNA agarose gels were run at 120V for 30-45 minutes while RNA gels were run at 80V for 40 minutes (Bio-Rad PowerPac Basic). Agarose gels were placed upon a Bio-Rad Gel Doc™ EZ UV sample tray and nucleic acids were visualised with the Gel Doc EZ System, using the 1kb plus (NEB) 2-log ladder as a size reference (Figure 2.1).

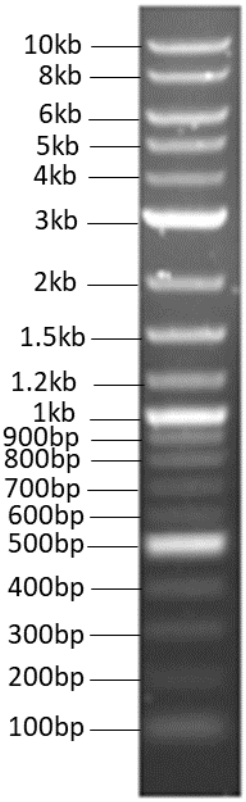

Figure 2.1 1kb plus (NEB) 2-log ladder.

The fragment length that corresponds to each band of the 1kb plus (NEB) 2-log ladder is noted on a 1% agarose gel.

2.2.2.2 Primers

All primers used within this work were sourced from Integrated DNA Technologies. These were each supplied at a concentration of 100mM and diluted to 10mM in sterile dH_2O for general PCRs on DNA or 600nM for amplifying cDNA. All primer stocks and dilutions were stored at -20°C. Primers were designed using Benchling [Biology Software] (2023).

2.2.2.3 Polymerase Chain reaction (PCR)

For amplification of DNA PCR was undertaken. For diagnostic PCR, simply determining the presence or absence of a particular target when identifying transformants (primers for this purpose are listed in Table 9.1), DreamTaq polymerase was used. 2x DreamTaq DNA polymerase mastermix was produced as follows: 1000µl 10x buffer (Thermo Scientific™), 200µl 10mM dNTPs (Thermo Scientific™), 3750µl Milli-Q water, 50µl DreamTaq DNA

Polymerase (5 U/µl)(Thermo Scientific™). In individual 20µl PCR reactions 10µl of 2x DreamTaq mastermix was used alongside 7µl sterile dH_2O, 1µl 10mM forward primer, 1µl 10mM reverse primer, and 1µl DNA template. Reactions were completed in a BioRad T100 Thermal Cycler using the following programme: One cycle at 95°C for 3 minutes, 30 cycles of 95°C for 30 seconds, Tm-5 for 30 seconds, 72°C for 1 minute/kb, finishing with one cycle of 72°C for 10 minutes.

Where amplified fragments were intended to be used in yeast recombination for knockout, overexpresser or GFP construct formation (primers are listed in Table 9.2), or to be cloned into pJET for sequencing, the proofreading PhusionTaq was employed. To produce 2x PhusionTaq mastermix 2000µl 5x Phusion green buffer, 200µl 10mM dNTPs, 2750µl sterile Milli-Q water, 50µl Phusion DNA Polymerase (2 U/µL) (Thermo Scientific™) were mixed. As with DreamTaq, 2x PhusionTaq mastermix was used in 20µl reaction volumes using the same reaction component quantities and thermocycler however a modified programme was employed: one cycle of 98°C for 30 seconds, 30 cycles of 98°C for 10 seconds, Tm-5 for 30 seconds, 72°C for 30 seconds/kb, finishing with one cycle at 72°C for 10 minutes.

2.2.2.4 Agarose gel DNA purification

Where gel purification of bands was necessary, the Macherey-Nagel™ NucleoSpin™ Gel and PCR Clean-up Kit was employed. Bands were cut out from agarose gels and weighed in 1.5ml Eppendorf tubes. The manufacturer's instructions were followed.

2.2.2.5 Colony PCR

Following *E. coli* transformation, single colonies growing on selection plates were picked with sterile toothpicks and DNA extracted by placing cells in 25µl TE+PK – consisting of 1xTE buffer with 50µg/ml proteinase K. The samples underwent a 55°C incubation for 15 minutes followed by a second incubation at 80°C for 15 minutes after which they were briefly centrifuged and 2.5µl of the supernatant then used in DreamTaq PCR.

2.2.2.6 cDNA synthesis

For qPCR analysis, RNA underwent cDNA synthesis using either the RevertAid H Minus First Strand cDNA Synthesis Kit (ThermoFisher) or the UltraScript™ cDNA Synthesis Kit (PCR Biosystems) – following the manufacturer's instructions in each instance. For each sample a no reverse transcriptase (-RT) control was set up. Successful cDNA synthesis was assessed by

using a 1/50 dilution of cDNA in a DreamTaq PCR reaction using qPCR reference gene primers. This also allowed the determination of any gDNA contamination of the -RT controls.

2.2.2.7 qPCR

qPCR was carried out for investigations outlined in Chapters 3, 4, and 6. qPCR primers are listed in Table 9.3 and Table 9.4. For qPCR of *Z. tritici* genes novel primers were designed with the exception of the HH3 reference gene (Tiley, 2016); for wheat, qPCR primers from Paolacci et al. (2009), Deihimi et al. (2013) and Baloglu et al. (2012) were used. qPCR used PowerUp™ SYBR™ Green Master Mix (applied biosystems) in 20µl reaction volumes consisting of 10µl SYBR mastermix, 5µl cDNA (diluted 1/50) and 5µl forward and reverse primer pre-mix. Following reaction set-up, plates were sealed with adhesive PCR plate seals. A CFX Connect Real-Time PCR Detection System was used with the following programme: 50°C for 2 minutes, 95°C for 2 minutes, 40 cycles of: 95°C for 15 seconds, 60°C for 1 minute. Following this, a melt curve analysis was completed, heating samples to 95°C for 15 seconds, then 65 to 95°C over the course of 0.5 seconds. Relative gene expression of fungal genes was determined using 'Cq reference gene – Cq gene of interest'.

Relative expression of wheat genes was determined using the $2^{-\Delta\Delta CT}$ method (Livak and Schmittgen, 2001) used in other wheat RT-qPCR studies (Deihimi et al., 2013). Genes of interest were normalised against the Ta54227 reference gene (encoding a cell division control protein) identified in Paolacci et al. (2009). Expression changes are relative to control samples.

2.2.2.8 Restriction digests

Within this work restriction digestions of plasmid DNA were undertaken for two main purposes. The first, to linearise circular plasmids for use in homologous yeast recombination. The second, as a diagnostic tool for determining whether constructed plasmids had been assembled correctly. Different mastermixes were set up depending on the intended use of the digested product.

For general diagnostic digests small reaction volumes of 20µl were employed, consisting of: 1µl each restriction enzyme, 3µl plasmid DNA, 2µl 10x FastDigest Green Buffer (Thermo Scientific) and sterile dH_2O to 20µl. To ensure plasmids were linearised for yeast homologous recombination they were 'double digested' using two enzymes with cut sites lying close to the desired insert site within the plasmid. These reactions were completed in 55µl volumes

using 1µl of each restriction enzyme, 10µl plasmid DNA, 20µl 10x FastDigest Green Buffer (Thermo Scientific) and 23µl sterile dH_2O. In all instances digests were incubated at 37°C for a minimum of one hour before being viewed by gel electrophoresis. Double digested plasmids were stored at -20°C.

2.2.2.9 Cloning

Where products amplified by PCR were required to be sequenced, using the CloneJET PCR Cloning Kit (Thermo Scientific) they were ligated into the pJET1.2 vector, following the manufacturer's instructions for the blunt-end cloning procedure (since PCR products for sequencing were amplified with PhusionTaq). The PCR product and pJET1.2 ligation was transformed into chemically competent DH5α *E. coli* and transformed colonies picked from LBA plates (supplemented with ampicillin) for analysis by colony PCR. Successfully transformed colonies were grown overnight in 5ml LB broth (supplemented with ampicillin) and this culture used in a plasmid DNA extraction. These plasmids were checked by diagnostic PCR or restriction digestion before the concentration of plasmid DNA was assessed by nanophotometer and the plasmid sent for sequencing using the pJET1.2F and pJET1.2R primers (Table 9.5).

2.2.3 Bacterial transformation

2.2.3.1 Preparation of electrocompetent E. coli

A single Top10 *E. coli* colony, from an LB agar plate, was inoculated into 50ml LB broth in a 250ml flask and incubated at 37°C overnight. One litre of LB broth (pre-warmed to 37°C) was inoculated with 25ml of the overnight culture in a 2-litre baffled flask and returned to 37°C (150RPM). This was allowed to grow until the OD_{600} measured 0.5-0.6. The culture was then cooled in an ice-water bath for 15-30 minutes before it was decanted into pre-cooled 500ml centrifuge bottles. The cells were centrifuged at 5,000x g for 10 minutes (4°C), the supernatant removed, and the cell pellet resuspended in 500ml ice-cold dH_2O. The centrifugation was repeated, a second water wash of the cells completed, and the culture again centrifuged. The supernatant was discarded, and the pellet resuspended in 250ml ice-cold 10% glycerol. This underwent centrifugation as before, and the pellet was again resuspended in 10ml ice-cold 10% glycerol. Cells were then transferred to 50ml falcon tubes, centrifuged, and the supernatant removed by pipetting. Cells were resuspended in 1ml ice-cold 10% glycerol by swirling. The OD_{600} of a 1:100 dilution of the cells was checked by spectrophotometry and the cell suspension diluted to $2x10^{10}$ to $3x10^{10}$ cells/ml with ice-cold

10% glycerol. 50µl aliquots of cell suspension were transferred to sterile Eppendorf tubes and frozen in liquid nitrogen before being stored at -70°C.

2.2.3.2 Electroporation of E. coli

Tubes of 50µl aliquoted electrocompetent cells were thawed on ice, and 2µl plasmid DNA added to the competent cells. The entire tube volume was then transferred to an ice-cold sterilised 1mm electroporation cuvette (Scientific Laboratory Supplies). The mixture was electroporated using a Bio-Rad GenePulser set to 2.5 kV (pulsed for 5ms). 1ml LB broth was immediately added to the cuvette before its contents was transferred to a sterile 1.5ml Eppendorf tube. This was incubated at 37°C 200RPM for one hour before plating 20µl and 200µl aliquots onto LBA supplemented with appropriate antibiotic selection. Plates were incubated overnight at 37°C and PCR performed on resultant colonies. After use, cuvettes were sterilised in 10% bleach for 10 minutes before being washed thrice with sterile dH_2O. These were then UV sterilised in a UVP CL-1000 ultraviolet crosslinker and stored filled with 70% ethanol – which was removed in a laminar flow hood and the cuvette dried before its next use.

2.2.3.3 Preparation of chemically competent E. coli

The method of chemically competent *E. coli* cell preparation was derived from Inoue et al. (1990). The media and buffers used in this protocol are described in Table 2.6. Briefly, a single colony of DH5α *E. coli* was inoculated in 10ml LB broth and incubated at 37°C overnight (200RPM). 2.5ml of the overnight culture was then added to 250ml SOB in a one litre flask. This was incubated at 19°C 200RPM until the OD_{600} measured 0.5-0.6 at which point the culture was cooled in an ice-water bath for 10 minutes. The culture then underwent centrifugation at 2,500x g for 10 minutes (4°C). The supernatant was removed, and the cell pellet resuspended in 80ml ice-cold transformation buffer, incubating the mixture on ice for 10 minutes before centrifuging as before. After removing the supernatant, cells were resuspended in 20ml ice-cold transformation buffer (including 1.4ml DMSO). 50µl aliquots were decanted to sterile Eppendorf tubes and flash-frozen in liquid nitrogen before storing at -70°C.

Table 2.6 Media and solutions used in the preparation of chemically competent *E. coli* cells.

SOB was autoclaved prior to use while transformation buffer was filter sterilised with a 0.22µm Millipore filter.

Media/ solution	Preparation
SOB	• 2% Bacto tryptone • 0.5% yeast extract powder • 10mM NaCl • 2.5mM KCl • 10mM $MgCl_2$ • 10mM $MgSO_4$
Transformation buffer	• 0.01M PIPES • 0.015M $CaCl_2$ • 0.25M KCl Buffer was pH adjusted to pH 6.7 with KOH before adding 0.055M $MnCl_24H_2O$.

2.2.3.4 Heat shock transformation of E. coli

Chemically competent cells were thawed on ice. 2µl plasmid DNA or ligation mixture (for pJET cloned plasmids) was added to the thawed cells and the mixture placed on ice for 30 minutes. The cells then underwent a heat-shock at 42°C for 30 seconds before being returned to the ice for five minutes. 950µl LB broth was added to the tube and the sample incubated at 37°C 200RPM for an hour before plating 20µl and 200µl onto LBA containing antibiotic selection. These were incubated at 37°C overnight before colonies were selected for analysis by PCR.

2.2.3.5 Preparation of electrocompetent Agrobacterium tumefaciens

To prepare electrocompetent *A. tumefaciens*, following two days of growth on LBA (supplemented with antibiotics) from glycerol stock, a single colony of LBA1126 *A. tumefaciens* was inoculated into 5ml LB broth (supplemented with antibiotics) in a sterile universal vial. This was incubated at 28°C 200RPM for 48 hours. 500µl of culture was used to inoculate 50ml LB in a 250ml flask, incubating this secondary culture at 28°C 200RPM overnight – or until the OD_{600} measured ~0.5. At this point the culture was transferred to a 50ml falcon tube and centrifuged at 4,000x g for 10 minutes at 4°C. The supernatant was removed, and the cell pellet resuspended in 50ml ice-cold 10% glycerol. This was then centrifuged as before, again removing the supernatant, and resuspending the pellet in 25ml ice-cold 10% glycerol. The cells were pelleted again, the supernatant removed, and the cells

resuspended in 2ml 10% glycerol. Once more the cells were pelleted and the supernatant removed, resuspending the cells in 1ml 10% glycerol. This was then aliquoted in 50µl volumes into sterile 1.5ml Eppendorf tubes and the cells flash-frozen in liquid nitrogen before storing the competent cells at -70°C.

2.2.3.6 Electroporation of A. tumefaciens

Eppendorf tubes containing competent *A. tumefaciens* cells were thawed on ice before adding 2µl plasmid DNA. The entire Eppendorf tube contents was transferred to an ice-cold 1mm electroporation cuvette and this electroporated at 400 ohms, 2.5 kV with a Bio-Rad GenePulser. 900µl LB broth was immediately added and the electroporation cuvette contents transferred to a new sterile Eppendorf tube. The cells were then incubated at 28°C (200RPM) for three hours before 20µl and 200µl aliquots were transferred to LB plates supplemented with rifampicin, spectinomycin and kanamycin. Cells were grown at 28°C for two days. Electroporation cuvettes were cleaned as described in section 2.2.3.2.

2.2.4 Fungal transformations

2.2.4.1 Preparation of competent yeast cells

Homologous recombination by yeast followed the protocols outlined in Gietz and Woods (2002), and Gietz and Schiestl (2007). Solutions used in yeast transformation are laid out in Table 2.7.

Table 2.7 Media and solutions used in homologous recombination of yeast.

All solutions and media were autoclaved following preparation with the exception of ss-DNA.

Solutions	Preparation
Lithium acetate (LiAc) 1M	10.2g of LiAc dihydrate dissolved in 100ml dH_2O.
Lithium acetate (LiAc) 0.1M	10ml of the 1M LiAc diluted in 100ml dH_2O.
PEG 3350 50%	50g PEG 3350 dissolved in 100ml dH_2O.
Single-stranded carrier DNA (2mg ml^{-1})(ssDNA)	100mg high molecular weight herring sperm DNA dissolved in 50ml sterile water overnight. This was dispensed into microcentrifuge tubes and DNA was denatured by incubating the tube at 95°C for 5 minutes then immediately chilling the DNA on ice. ss-DNA was stored at -20°C.
SM-URA (400ml)	• 1.7g Yeast Nitrogen Base (without amino acids) • 5g ammonium sulphate – VWR • 20g Glucose – Acros • 770mg yeast dropout mix (-ura3) • 15g agar

For preparation of yeast cells for homologous recombination, 10ml YPAD broth decanted into a sterile universal tube was inoculated with a single colony of yeast using a sterile pipette tip. The starter culture was incubated at 28°C (200RPM) overnight then transferred to a sterile conical flask containing 40ml YPAD broth and incubated at 28°C (200RPM) for a further four hours. The culture was then divided equally into two 50ml falcon tubes and centrifuged at room temperature for five minutes at 3,000x g to pellet the yeast cells. The supernatant was poured off and the pellet resuspended in 25ml sterile dH_2O by vortexing. The centrifugation was repeated, again pouring off the supernatant but now resuspending each pellet in 1ml 0.1M LiAC before transferring to 1.5ml microcentrifuge tubes. These cells were then pelleted at 4,000x g for 60 seconds and the supernatant removed. The pellet was finally resuspended in 400µl 0.1M LiAc. At this stage, cells were stored on ice if they were to be used on the same day, if not, cells were stored at 4°C and used up to one-week post-production.

2.2.4.2 Transformation/homologous recombination of competent yeast

For the transformation of competent yeast cells, 50µl aliquots of competent cells were transferred to sterile Eppendorf tubes. These were then centrifuged at 2,000x g for one

minute and the supernatant discarded. On ice the following were added to the tube sequentially: 240µl 50% PEG 3350, 36µl 1M LiAc, 50µl boiled ss-DNA. Finally, 5µl each DNA fragment and vector for transformation were added using sterile dH_2O to make the final volume up to 34µl. The cells were resuspended by vortexing and incubated at 30°C for 30 minutes, then 42°C for 30 minutes. Following incubation, cells were centrifuged at 4,000x g for one minute, and the supernatant was discarded. Cells were resuspended in 1ml sterile dH_2O and 20µl and 200µl aliquots spread onto selection plates to be grown at 28°C for three days.

2.2.4.3 Agrobacterium-mediated transformation of Zymoseptoria tritici

The method for transforming *Zymoseptoria tritici* was an *Agrobacterium*-mediated procedure based on the protocol outlined by Zwiers and De Waard (2001). Media and solutions are laid out in Table 2.8. Prior to transformation, an LB plate, supplemented with 50µg/ml kanamycin was inoculated with transformed *A. tumefaciens* cells containing the desired plasmid for transformation (with the kanamycin resistance gene in this plasmid) by streaking and incubated at 28 °C for three days. A sterile pipette tip was then used to pick a single colony of *A. tumefaciens* and this was inoculated into 40ml LB broth in a 250ml flask to which 50µg/ml kanamycin was added in order to maintain the resistance-containing plasmid. This liquid culture was incubated at 28°C (200RPM) for ~20 hours.

Table 2.8 Media and solutions used in *Agrobacterium tumefaciens* mediated transformations of *Zymoseptoria tritici*.

The methods of preparation of solutions are described. Stock A and B were made to 400ml volumes as well as solid media. The remaining solutions and stocks were made to 200ml volumes with sterile dH_2O and autoclaved prior to their use.

Media/solution	Preparation
Stock A	• 34.84g/l Potassium phosphate dibasic (K_2HPO_4 ($3H_2O$)) • 27.22g/l Potassium dihydrogen phosphate (KH_2PO_4) • 2.93g/l Sodium chloride (NaCl).

Stock B	• 9.86g/l Magnesium sulphate heptahydrate ($MgSO_4.7H_2O$) • 10.58g/l Ammonium sulphate – ($(NH_4)_2SO_4$).
Calcium chloride dihydrate ($CaCl_22H_2O$)	10.3g/l Calcium chloride dihydrate.
D-glucose	180.16g/l D-glucose
MES	213.25g/l (pH adjusted to pH5.3 with 5M KOH).
Iron(II) sulphate heptahydrate ($FeSO_4.7H_2O$)	2.5g/l Iron(II) sulphate heptahydrate ($FeSO_4.7H_2O$)
Agrobacterium Induction Media (AIM)	50ml/l Stock A 50ml/l Stock B 10ml/l $CaCl_22H_2O$ 1ml/l $FeSO_47H_2O$ 10ml/l D-glucose 40ml/l MES 10ml/l 50% glycerol.
Agrobacterium Induction Media (AIM) agar	As for Agrobacterium Induction media but with 1.5% agar added prior to autoclaving to solidify the media. Media was supplemented with 20µg/ml acetosyringone post-autoclaving.
Acetosyringone	20mg in 500µl DMSO. This was made fresh on the day of use and was not autoclaved or sterilised.
Aspergillus minimal media (AMM)	• 70mM $NaNO_3$ • 7mM KCl • 2mM $MgSO_4$ • 11mM KH_2PO_4 • 1% (w/v) D-glucose • 1ml/l 1000x trace element solution
1000x trace element solution	• 76mM $ZnSO_47H_2O$ • 178mM H_3BO_3 • 25mM $MnCl_24H_2O$ • 18mM $FeSO_47H_2O$ • 6.7mM $CoCl_26H_2O$ • 6.5mM $CuSO_45H_2O$ • 890µM $(NH_4)_6Mo_7O_{24}4H_2O$ • 130mM Na_4 Ethylenediaminetetraacetic acid (EDTA) The solution was boiled and then pH adjusted to pH6.7 with KOH.

Following this incubation period, the OD_{600} was measured. The amount of culture required to dilute the OD_{600} to 0.15 in 10ml AIM (supplemented with 50µg/ml kanamycin and 1µl/ml freshly prepared 200µM acetosyringone) was calculated using the equation:

$$\frac{0 \cdot 15\ (final\ OD) \times 10\ (final\ volume)}{OD_{600}}$$

The calculated volume of culture was centrifuged at 16,000x g for two minutes, the supernatant was discarded, and the cells resuspended in 1ml AIM (with the kanamycin and acetosyringone additions described above) and this then transferred to a sterile universal containing the remaining 9ml AIM. The culture was then incubated at 28°C (200RPM) until the OD_{600} measured 0.25-0.3. While the *Agrobacterium* culture was incubating, *Zymoseptoria tritici* mycelia were scraped from a five-day old CDV8 plate with an inoculating loop and transferred to 1ml AIM in an Eppendorf tube. The concentration of the solution was measured using a haemocytometer and adjusted to $4x10^6$ spores/ml with AIM.

Once the OD_{600} reached the desired range, 100µl *Agrobacterium* and 100µl $4x10^6$ spores/ml *Zymoseptoria tritici* were added to a sterile Eppendorf tube along with 1µl acetosyringone. This was incubated at room temperature for five minutes before plating 20µl, 50µl and 100µl aliquots onto freshly prepared AIM agar plates overlaid with sterile cellophane discs (one disc per plate; 80mm diameter 325P cellulose; A.A. Packaging Limited). *Zymoseptoria tritici* without the addition of *Agrobacterium tumefaciens* was used as both a negative and positive control. Plates were left at room temperature in the dark for two days before the cellophane discs were transferred to AMM plates to which 100 µg/ml timentin was added, to kill off the *Agrobacterium*, alongside 100µg/ml Hygromycin B. Positive control plates lacked any antibiotics. The AMM plates were then returned to darkness (room temperature) and checked periodically for colonies growing on the cellophane.

Transformed colonies tended to appear no earlier than two weeks post-transformation. These colonies were picked from the cellophane using sterile toothpicks and transferred to PDA plates supplemented with timentin and hygromycin in the same concentrations as previously noted. Putative transformants were cultured alongside untransformed and selection susceptible wildtype *Z. tritici* for comparison. If the colony successfully grew on

PDA selection, it was once again sub-cultured onto fresh PDA selective plates before it was sub-cultured onto CDV8 plates free from antibiotics. DNA was extracted from mycelia grown on CDV8 plates and successful transformation was determined by diagnostic PCR before mycelia from these plates were used to inoculate 50ml YSM cultures (in 250ml flasks) for production of glycerol stocks for long-term strain storage.

2.3 Microscopy

All microscopy was performed using a Leica DMLB microscope. Microscopy was required for determining concentrations of fungal mycelia in solutions and morphology of transformants. To visualise fluorescence of GFP transformed fungal strains a 450-490nm excitation filter, 515nm emission filter, and 510nm dichroic filter were employed.

2.4 Plate-based antibiotic bioassay

Assays to determine the potential antibiotic activity of the *Z. tritici* RiPP were completed using the media and solutions outlined in Table 2.9.

Table 2.9 Media and solutions used in plate-based antibiotic bioassays.

Media were made to one litre with dH_2O and autoclaved prior to use. Stains were prepared and filter sterilised by passing the solution through a 0.22µm Millipore filter.

Media/solution	**Preparation**
Tryptic Soy Agar-b (TSAb)	• 30g/l Tryptic Soy broth • 20g/l agar
Tryptic Soy Agar-g (TSAg)	• 30g/l Tryptic Soy broth • 5g/l agar • 10g/l glucose
4% TTC solution	• 400mg TTC (Tetrazolium chloride) dissolved in 10ml dH_2O. Stored at 4°C.
MTT (3-(4,5-Dimethylthiazol-2-yl)-2,5-Diphenyltetrazolium Bromide)	• 10mg/ml MTT in water. Stored at -20°C.

2.4.1 Preparation of test organisms

Zymoseptoria tritici strain IPO323 as well as the *ZttxA* knockout strain (ZttxA-Δ2) and the OxR T4 overexpresser strain were grown on CDV8 agar for five days. Where solid media grown fungi were to be tested, plugs of *Zymoseptoria* mycelia from these plates were cut using a cork borer with an internal diameter of 7mm and transferred to the center of TSAb plates.

Fungi were allowed to grow for a further five days at 20°C. Where liquid media grown *Z. tritici* were to be tested, mycelia from five-day old CDV8 plates was inoculated in 50ml CD+YE broth and grown for a further five days.

Y10000 yeast, DH5α *E. coli*, and *Bacillus subtilis*, were all grown overnight in liquid culture using LB media for *E. coli*, TSB for *Bacillus subtilis*, and YPAD broth for yeast. All microorganisms were grown in their respective optimal conditions, outlined in section 2.1.4. These cultures were grown until their OD_{600} measured 1 or adjusted to this value using the equation in 2.2.4.3.

2.4.2 Bioassay set-up

5ml of TSAg containing 5µl *E. coli*, *Bacillus subtilis*, or *Saccharomyces cerevisiae* culture and 37.5µl 4% TTC (for bacteria) or MTT (for yeast) was pipetted onto TSAb plates. For TSAb plates which had a mycelial plug pre-transferred care was taken to ensure the TSAg overlay came in contact with, but did not flood, the plugs. For assays of liquid media grown *Z. tritici,* as well as *Z. tritici* extracts, a 7mm cork-borer was used to excise agar from TSAg overlaid TSAb plates and 40µl liquid media added. These plates were then allowed to grow at the appropriate temperature for the organism within the TSAg overlay and checked daily for the presence of clearing zones.

2.5 In planta assays

In planta assays, were completed in the University of Bristol greenhouses (Old Park Hill; 51.456310, -2.599110) or in growth cabinets (Snijders Labs Micro clima-series™ Economic Lux chamber; Snijders Labs Micro clima-series™ High Specs Plant Growth Chamber) with 16-hour day lengths (24°C; 112µmol/m^2/s^{-1}; 50% humidity for High Specs Plant Growth Chamber) and eight hours darkness (20°C, 50% humidity). Riband wheat plants were used in all *in planta* experiments unless otherwise specified. Wheat plants were grown in 20.5cmx15cmx5cm trays in Levington F2-S seed compost.

2.5.1 Inoculum preparation

Inoculum for plant assays was prepared by scraping *Zymoseptoria tritici* mycelia from CDV8 plates into volumes of 0.5% Tween 80 using an inoculating loop. In all instances *Zymoseptoria tritici* strains were inoculated onto wheat plants in 0.5% tween solutions at a concentration of $4x10^6$ sporidia/ml. The volume of inoculum applied, and application method, was dependent on the nature of the experiment; either by painting of leaves with

cotton buds dipped in inoculum (four strokes per leaf) or spraying inoculum onto leaves with a sprayer head. In all instances, the second true leaf was scored for symptoms of disease. Following application of the inoculum wheat plants were sealed in transparent autoclave bags, to create a 100% humidity environment, for 48 hours.

2.5.2 Disease assessment

2.5.2.1 Visual disease assessment

To assess the progression of *Zymoseptoria tritici* infection on inoculated wheat leaves a disease symptom scale was produced (Figure 2.2). Infected leaves were photographed and scored according to the scale at designated time points following inoculation.

Figure 2.2 *S*cale used to assess symptoms of *Zymoseptoria tritici* infection on wheat.

The scale was produced based on symptoms of infection on the Riband cultivar of wheat. The scale ranged from 0 (no symptoms) to 4 (senesced leaf displaying pycnidia). Intermediate disease levels were described as follows (1 – small chlorotic leaf lesions with no pycnidia; 2 – large chlorotic lesions with pycnidia; 3 – chlorotic leaf lesions cover the majority of the leaf area, but some living plant tissue remains).

2.5.2.2 Quantitative method of disease assessment.

When assessing symptoms of *Z. tritici* infection after a specified period, a quantitative approach was applied following the protocols of Stewart and McDonald (2014), Stewart et al. (2016), and Karisto et al. (2018). Briefly, Ubuntu linux code (Stewart et al., 2016) was used to generate documents containing QR codes which were associated with treatments. These were then printed and leaves excised and affixed to the pages using opaque white tape (Figure 2.3). Leaves were pressed with a 5kg weight for 24-48 hours then scanned at 1200dpi using an HP ScanJet G2170 scanner. Images were then processed in Image J 1.53k using the macro updated from Stewart et al. (2016) by Karisto et al. (2018). The parameters used in

analysis are outlined in Table 2.10. For each application of the macro, several images were selected for calibration and symptoms were manually assessed.

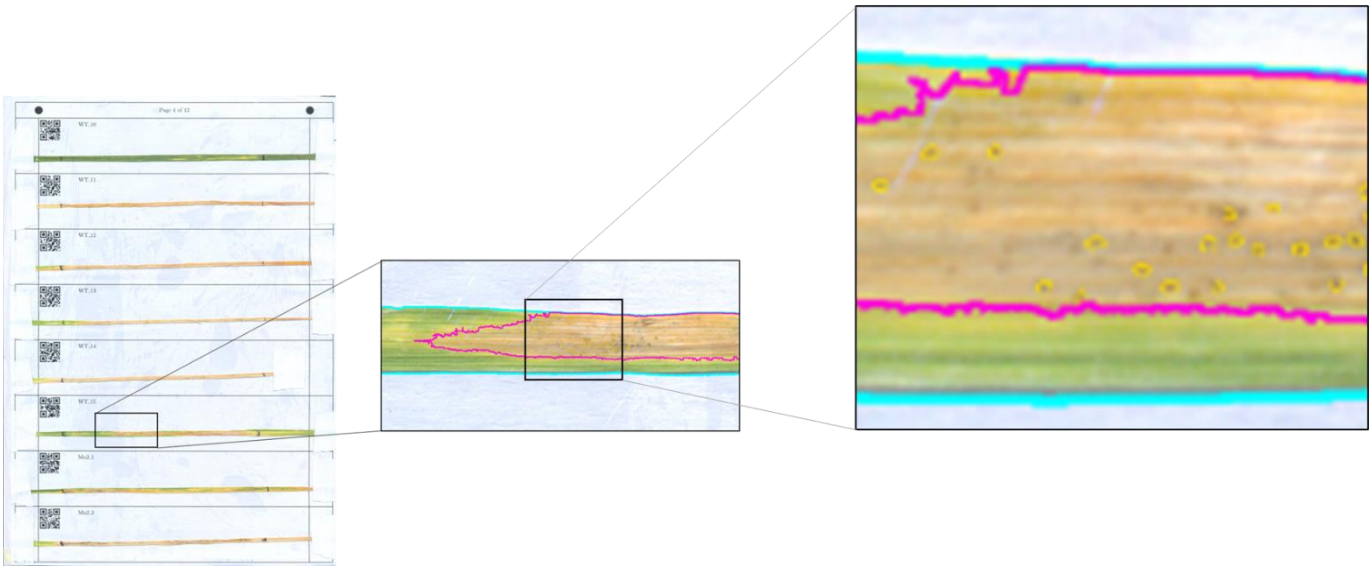

Figure 2.3. Example ImageJ processed wheat leaves.

Infected leaves taped to the QR code printed sheet (left). The overlay applied by the ImageJ macro to the leaf (middle and right). Leaf area is highlighted with a blue line, chlorosis area is highlighted with pink, while pycnidia are highlighted in yellow.

Table 2.10 ImageJ macro settings used in quantitative assessment of disease.

Setting	Set
Min0	202
Max0	255
Min1	114
Max1	255
Min2	47
Max2	161
colmode	2
Pass_Stop_H	1
Pass_Stop_S	1
Pass_Stop_B	1
maximaNoise	18
leafAreaUpper	239
leafAreaLower	0
pycnidiaLesionSize	5
lesionSize	5
red_weight_pycn	0.75
green_weight_pycn	0.25
blue_weight_pycn	0
sigmaGauss	0.25
pycnidiaSize	0.001-0.022
pycnidiaCircularity	0.75-1.0
pycnidiaPerLesion	No

2.5.3 Wind treatment assay

Wheat plants, after three weeks of growth in a Snijders Labs Micro clima-series™ Economic Lux chamber, were subjected to a wind treatment provided by a Sealey Fan (16" 3-speed Desk/floor Fan 230V; Model No.SFF16). Wheat trays were placed 10cm from the fan (Figure 2.4). Three different fan settings translated to the following wind speeds: 2.23m/s (1),

2.63m/s (2), 3.15m/s (3). A single wind speed was applied in each experiment for six hours a day for a week. The wheat plants were then sprayed with 20ml inoculum per tray. No wind controls were also sprayed with inoculum. Equally, a 0.5% tween spray (20ml) was applied to both wind and untreated plants as a further control to determine whether factors outside of wind or *Zymoseptoria tritici* application impacted plant health. Three-weeks post-inoculation wheat leaves (the second true leaf) were excised, and symptoms of infection were assessed.

Figure 2.4 The wind experiment set-up within the growth cabinet.

Wind treated plants were separated from non-wind treated plants by a clear plastic sheet. The position of the fan, whether this was on the top or the bottom shelf, was varied within experiments to ensure external factors were not contributing to any supposed impacts of wind on *Zymoseptoria tritici* infection of wheat.

2.5.3.1 Chlorophyll content measurement

The method and equation used is derived from Leigh et al. (2006), Porra et al. (1989), and Lichtenthaler and Buschmann (2001). Five 5mm discs per wheat leaf were cut with a leaf borer from the second true leaf of wheat plants, using the leaf area which would usually be inoculated by spore-painting. Leaf discs were frozen and ground in a pestle and mortar along with 5ml 80% acetone. The solution was transferred to a sterile falcon tube which was vortexed, and the contents poured into two microcentrifuge tubes. These were centrifuged at 10,000x g for one minute. The supernatant was transferred to a spectrophotometer cuvette and measured at 750nm, 663nm and 646nm. Total chlorophyll content was determined using the equation:

$$Chlsa + b = 19.54^{(646-750)} + 8.29^{(663-750)}$$

2.5.3.2 Leaf architecture measurements

To appreciate differences in leaf architecture between wind and non-treated plants, leaf height and leaf weight were measured. Measurements were completed on four-week-old plants following three weeks of growth and one week of treatment (wind or untreated). Wheat plant height measurements were taken from the tip of the second true leaf of each plant to the soil. For weight measurements, whole plants were cut and randomly assigned to one of five groups. Five plants were assigned to each group and these leaves dried at 50°C for one month before final dry weight was measured.

2.5.4 pH treatment assay

Riband wheat seeds were grown in perlite. Trays were watered with dH_2O until seedling emergence at which point, they were watered with pH adjusted Letcombe solution (Table 2.11). pH ranges of 5.5, 7 and 8.5 (adjusted with 2M HCl or 3M NaOH) were used alongside unadjusted Letcombe which provided a pH 6.58 treatment. Plants were watered twice a week. At three-weeks old wheat plants were sprayed with 20ml wildtype *Zymoseptoria tritici* inoculum adjusted to $4x10^6$ spores/ml in 0.5% tween or 20ml 0.5% tween control. After three weeks wheat leaves were examined.

Table 2.11 Letcombe nutrient stock solutions for growth of Riband wheat in an inorganic substrate.

Stock solutions were made in one litre quantities and stored at 4°C in darkness. Letcombe solution consisted of 1ml each stock (2ml for KNO_3) made up to one litre with dH_2O.

Ingredient	**Stock**
KNO_3	1.25M
$Ca(NO_3)_24H_2O$	0.75M
$NaNO_3$	1M
$MgSO_47H_2O$	0.5M
$MgCl_26H_2O$	0.5M
KH_2PO_4	0.5M
FeEDTA	0.0125M
$Cu(NO_3)_23H_2O$	160µM
H_3BO_3	9.2mM
$MnCl_24H_2O$	3.6mM
$(NH_4)_6Mo_7O_{24}4H_2O$	16µM
KCl	5mM
$ZnCl_2$	770µM

2.5.5 Salt treatment assay

Three-week-old Riband wheat plants were watered with one litre salt solution of either: 0g/l, 0.5g/l, 2.5g/l 5g/l NaCl – 5g/l NaCl provided an effective salt treatment in Poustini and Siosemardeh (2004). Plants were watered in trays to prevent run-off and maintain the salt concentration. After one week of salt treatment, wheat plants were inoculated with wildtype *Zymoseptoria tritici,* or 0.5% tween as a control. Three weeks post-inoculation, wheat leaves were assessed for symptoms of disease.

2.6 Animal feeding assay

2.6.1 Animal rearing conditions

Third instar *Schistocerca gregaria* (desert locusts) were kept in non-crowded conditions with a photoperiod of 12-hours light (33.6 µmol/m^2/s^{-1}) and 12-hours dark (50% humidity; 24°C).

Prior to experimentation, locusts were fed bran, and water-soaked cotton wool was provided as a source of water.

2.6.2 Feeding experiment

To assess the antifeedant activity of the *Zymoseptoria tritici* RiPP, wheat plants were infected with either wildtype, ZttxA-Δ2 or OxR-T4 *Z. tritici* strains after three weeks of growth. Infection was allowed to progress for five weeks at which time infected material was excised. At this stage, signs of infection were clear as pycnidia were present on inoculated leaves. Only leaves displaying pycnidia were used in the feeding experiment after being dried at 50°C for one month, negating the need for a water loss control as used in Dillen et al. (2014). A seed tray was cut down to consist of 16 cells. Five cells per *Z. tritici* strain were filled with 150mg dried wheat leaf material. The final cell was filled with water-soaked cotton wool (Figure 2.5). The seed tray was placed in an insect rearing cage (BUGDORM-1) and 10 locusts introduced. Animals were permitted to feed for five days then the plant material was weighed, and leaf consumption of each treatment type was calculated.

Figure 2.5 Feeding experiment set-up for analysis of locust preference for material containing or lacking the *ZttxA* RiPP.

2.7 Light and fungicide assay

Wildtype *Z. tritici* mycelia were disrupted in water and the solution of the concentration adjusted to $1x10^3$, $1x10^4$, $1x10^5$, $1x10^6$, and $1x10^7$ spores/ml. 3µl dots of the solution were

pipetted onto PDA plates supplemented with various low level hygromycin concentrations including 0µg/ml, 0.0125µg/ml, 0.125µg/ml, 1.25µg/ml and 12.5µg/ml. Plates were either grown in constant light (31.3 µmol/m^2/s^{-1}) or constant darkness (plates were wrapped in foil) at 20°C for one week. Images of the plates were taken and processed in ImageJ using the Analyze Particles function following thresholding to determine fungal growth. Images were first converted to 8-bit grayscale and made binary (Figure 2.6). Statistical analysis was conducted on the $1x10^6$ concentration.

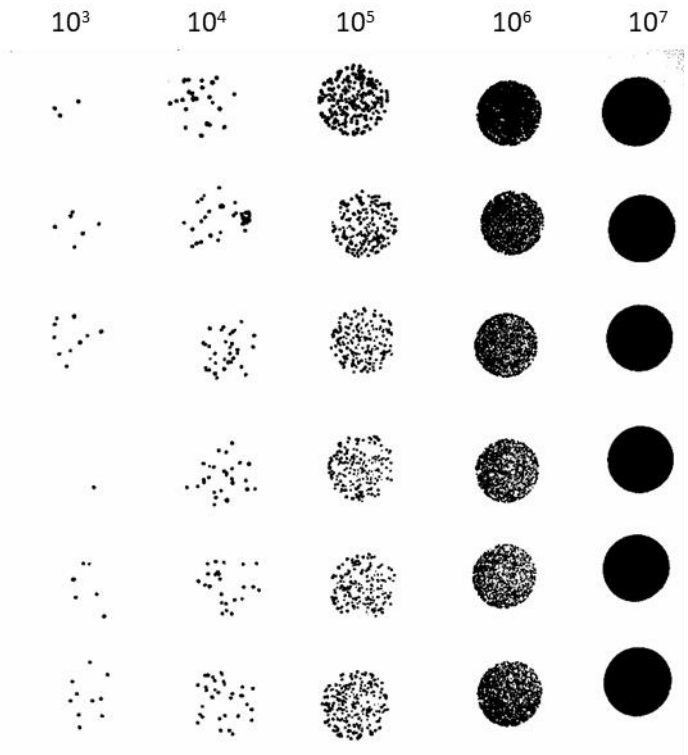

Figure 2.6 Example ImageJ processed image.

2.8 RiPP extraction

Peptides were extracted from cultures of either wildtype, ZttxA-Δ2 or OxR T4 fungal strains. Initial extractions were conducted on wildtype strains prior to production of the OxR T4 strain. All wildtype or OxR T4 extractions were completed alongside extractions of the ZttxA-Δ2 strain so that comparisons between the two extracts could be made. All peptide extracts were diluted to 10mg/ml and analysed using a Waters Acquity LCMS system using a Phenomenex Kinetex C_{18} column (2.6µ, 4.6x100 mm, 100 Å) into which 10µl sample was

injected. Detection was performed using a Waters 2998 diode array, a Waters SQD-2 mass detector (detecting in ES+ and ES− modes), and a Waters 2424 evaporative light scattering detector (ELSD). All solvents used were analytical grade and included water containing 0.05% formic acid as mobile phase A, and acetonitrile containing 0.05% formic acid as mobile phase B. Unless otherwise stated a gradient of 5% B to 95% B over 20 minutes was used – with a 0.25ml/min flow rate. Peaks in the wildtype or overexpresser strain DAD chromatograms where they were absent in the knockout strain were analysed.

2.8.1 Amberlite column extraction

XAD-2 amberlite column-based extractions followed the methods outlined by Lanigan et al. (1979), Ding et al. (2016), Sogahata et al. (2021), and Li et al. (1992). The amberlite column was prepared as follows. Amberlite XAD-2 resin was washed with 100ml autoclaved Milli-Q water which was then poured off through miracloth. Resin was then washed with potassium phosphate buffer (50mM pH 5.7; K_2HPO_4 6.4g/l, KH_2PO_4 1.8g/l) in a one litre Schott bottle, this was left at 4°C overnight before the buffer was poured off through miracloth. Columns were set up in 50ml syringes plugged with glass wool.

50ml starter cultures of each *Z. tritici* strain were set up in 250ml flasks. After five days the starter culture was used to inoculate 20 250ml CD+YE flasks each containing 100ml CD+YE. These cultures were grown at 20°C for nine days before they were pooled, adjusted to pH 8.5-9 with 2M NaOH, and stored at 4°C overnight. These were then adjusted to pH 7.3-7.5 with 2M HCl (Lanigan et al., 1979). Samples were centrifuged at 12,000x g for 10 minutes at 4°C and the supernatant poured through miracloth into one litre Schott bottles containing the processed amberlite. This was then mixed at room temperature for one hour (150RPM). This mixture was poured into the column and the amberlite resin plugged with glass wool before it was washed with water (60ml). The column was eluted in 90ml methanol in three 30ml fractions. Elutions were dried down and weighed to give 10mg/ml extract concentrations diluted in methanol. Extracts were run on LCMS using the standard programme as well as an isocratic elution programme of 80% A and 20% B for 25 minutes, followed by 95% B for 3 minutes. A 10µl injection volume and 0.25ml/min flow rate was used.

2.8.2 Ethyl acetate extraction

Ethyl acetate extractions followed a standard procedure described in Banks et al. (2020) for isolation of sesquiterpene metabolites. Extractions again used 20 nine-day old 100ml CD+YE cultures as the extraction material. Cultures were filtered with miracloth and the supernatant pooled, adjusted to pH3 with 2M HCl, and an equal volume of ethyl acetate added. This was mixed at room temperature for one hour. Using a separating funnel, the aqueous and organic phases were separated. The organic phase was evaporated using a rotary evaporator (90RPM, 35°C). The extract was then dissolved in methanol at 10mg/ml.

2.8.2.1 Plate-based peptide extraction

The plate-based peptide extraction method used in this work was from Hassani et al. (2021b) using five freeze-dried YMS plates (0.4% yeast extract, 0.4% malt extract, 0.4% sucrose, 2% agar) as the material for the extraction. Solid cultures were grown at 20°C for seven days from mycelia disturbed in water spread over an entire plate with an inoculation cell spreader. Freeze-dried cultures were ground and 400ml ethyl acetate added. This was mixed for one hour. Ethyl acetate extracts were washed with water (200ml) and separated in a separating funnel twice before the organic phase was collected and dried using a rotary evaporator. Extracts were dissolved in methanol to a concentration of 10mg/ml.

2.8.3 Acetone/methanol extraction

Twenty CD+YE cultures were pooled and filtered with miracloth. The filtered mycelia were gathered and freeze dried for a week. This material was then ground with a mortar and pestle. 600ml acetone was then added and this mixed for one hour. The mixture was then filtered through miracloth and the collected liquid centrifuged at 8,000x g for five minutes. The supernatant was then filtered through whatman 2M filter paper using a buchner funnel attached to a vacuum pump. The acetone was removed using a rotary evaporator (90RPM, 35°C) and the residue dissolved at 10mg/ml in methanol.

2.8.4 Acetone/ethyl acetate extraction

An extraction method for use in ustiloxin extraction was also trialled (Yoshimi et al., 2016). Nine-day old CD+V8 cultures were used from which 10ml culture were mixed with an equal volume of acetone. This was left at room temperature for one hour before the mycelia were filtered off with miracloth. The collected filtrate was mixed with an equal volume of ethyl acetate at room temperature for one hour. In a universal tube the mixture was centrifuged at 1,500x g for 10 minutes. The water layer was run directly on LCMS; the ethyl acetate layer

was transferred to a new tube and dried before extracts were dissolved in methanol to a concentration of 10mg/ml.

2.9 Bioinformatics and statistics

2.9.1 Bioinformatics

Sequences were analysed largely in Benchling. For more in-depth sequence analysis BioEdit was utilised. Sequences were either attained from NCBI or from sequencing data received from Source Bioscience. Homologous proteins to those in the *Zttx* gene cluster were identified by protein BLAST searches against the NCBI database as well as Cblaster (Gilchrist et al., 2021). Clinker (Gilchrist and Chooi, 2021) was used to align homologous proteins in putative RiPP biosynthetic gene clusters.

2.9.2 Statistics

Statistical analyses were all performed in R Studio version (2022.07.1+554).

2.10 Image processing

All images were taken using either a digital camera (Nixon D3300) or an iPhone. Images have not been altered aside from minimal corrections to brightness and contrast for clarity.

3 : Investigating the *Zymoseptoria tritici* putative RiPP biosynthetic cluster - the genes involved, their regulation, and peptide production.

One of the most intriguing aspects of the wheat-*Zymoseptoria* interaction is the switch from latent phase to necrotrophic growth. Various possibilities have been suggested to explain this, with prominent suggestions being the production of toxic small secondary metabolites, or secreted effector proteins (Hammond-Kosack and Rudd, 2008, Kema et al., 1996c), but with very limited experimental evidence to support either theory.

Others in my lab have performed extensive investigations into the possibility of small metabolites. Mohd Khalid (2011) extracted and analysed small metabolites generated under a range of growth conditions but only managed to identify MG1 and MG2, both of which are prenylated para benzoic acid derivatives, neither of which would be regarded as typical secondary metabolites and neither of which showed phytotoxicity. Mohd Khalid et al. (2015) catalogued the possible secondary metabolite gene clusters, highlighting 10 possible polyketide synthase (PKS) clusters (and 1 PKS-nonribosomal peptide synthetase hybrid) but could not identify the likely compounds. Koay (2010) and Ali (2015) generated. *Z. tritici* lines transformed with Promoter:GFP constructs for all these genes but only saw expression of PKS3. Disruption of this PKS, whilst eliminating melanisation, had no impact on virulence (Derbyshire et al., 2018). To further compound this, the loss of virulence of the PPTase knockout that eliminated function of all PKS and non-ribosomal peptide synthetases (NRPSs) could be ascribed to loss of lysine biosynthesis (Derbyshire et al., 2018) rather than other toxic secondary metabolites, possibly further exacerbated by the concomitant loss of siderophores (Ali, 2015) impacting on iron acquisition.

Secreted proteins were assessed by other groups, most notably Kettles et al. (2017), Kettles et al. (2018), and Welch et al. (2022), and whilst transient expression in *Nicotiana benthamiana* proved a successful route for analysis, the function of the effectors in *Z. tritici*

pathogenicity is unknown or unessential. These studies seemed to exhaust the possible classes of trigger for the switch to necrotrophy, however the recent emergence of the RiPP class of metabolites suggested these might also be worthy of investigation.

3.1 Introduction

Fungal RiPP classes are united by shared methods of production that are specialised beyond the basic foundations of post-ribosomal peptide synthesis (PRPS). The basic PRPS mechanism of traditional peptide synthesis (produced by transcription and translation of the precursor gene) is unchanged across fungal RiPP classes, it is the processing of the precursor peptide (mechanism of peptide maturation) that varies. As fungal RiPP biosynthetic genes are known to form a cluster of contiguous genes within the producer's genome, bioinformatic investigation of gene clusters of novel RiPPs can shed light on the likely classification of these peptides as the presence or absence of genes encoding modifying enzymes, which typify RiPP biosynthesis of a specific class, can be recognised. For many fungal RiPP classes, the exact steps in RiPP biosynthesis that occur following peptide translation are hard to decipher purely from sequence data and require lab experiments. Furthermore, the function of modifying enzymes encoded by genes within RiPP biosynthetic clusters are often still unknown, or the order of application of modifications uncertain. The level of detail in which RiPP biosynthesis is understood varies between RiPP classes, with three fungal RiPP classes currently recognised: amatoxin/phallotoxins, borosins and dikaritins.

3.1.1 Amatoxin/phallotoxin RiPPs

Peptides belonging to this RiPP class are bicyclic with varying amino acid chain lengths depending on their designation; amatoxin peptides are octapeptides, while phallotoxins are heptapeptides (Wong and Ng, 2006). The amatoxin/phallotoxin precursor peptides also belong to the MSDIN peptide family, characterised by the conserved MSDIN N-terminal amino acid sequence of the peptide as well as proline amino acids flanking a hypervariable region (Walton et al., 2010). It is at these proline residues that a prolyl oligopeptidase (POP) acts, cleaving the precursor peptide at the N-terminus (Luo et al., 2009), and catalysing macrocylization of the RiPP at the C-terminal proline residue by transpeptidation/transamidation (Luo et al., 2014a, Czekster et al., 2017). Aside from core peptide liberation and cyclisation, amatoxin/phallotoxin RiPPs also undergo hydroxylation,

tryptophan-cysteine cross-linking (tryptathionine formation), and for phallotoxins exclusively, a singular amino acid epimerization (Walton et al., 2010). Hydroxylation modifications vary between amatoxin/phallotoxins in regard to the amino acid residue to which they are applied and the number of modifications (Walton, 2018). Much is still to be learnt about this method of RiPP biosynthesis with many of the genes, and resulting enzymes, responsible for these post-translational modifications currently unknown.

3.1.2 Borosin RiPPs

Borosin RiPPs are largely understood in the context of their founding member omphalotin A from *Omphalotus olearius*, a wood-inhabiting basidiomycete fungus (Mayer et al., 1997). Omphalotin A is a highly modified dodecapeptide (Mayer et al., 1999b) – with nine amino acids showing methylation modifications (Sterner et al., 1997). Other omphalotin variants show differing post-translational modifications (Liermann et al., 2009). Like the amatoxin/phallotoxins, the core RiPP amino acids are cleaved from the precursor gene by a POP protease, with this protein again responsible for cyclisation of the RiPP (Ramm et al., 2017). However, uniquely, the borosin precursor peptide is fused to one of its modifying enzymes – with the N-terminal region of the precursor peptide displaying homology to S-adenosylmethionine (SAM)-dependent methyltransferases (Ramm et al., 2017, Van Der Velden et al., 2017). This protein fusion of precursor and modifying enzyme is what typifies the borosin group.

3.1.3 Dikairitin RiPPs

The dikaritin RiPP name derives from the subkingdom Dikarya, since producers of these RiPPs belong to either the Ascomycota or Basidiomycota (Ding et al., 2016). Unlike the amatoxin/phallotoxin and borosin RiPPs which are retained within fungal cells (Mayer et al., 1997, Luo et al., 2010), dikaritin precursor peptides are processed within the golgi apparatus (Yoshimi et al., 2016) and typically secreted. Whilst other RiPP classes employ POP enzymes for core peptide proteolysis from the precursor, dikaritin RiPPs lack these flanking proline residues. Instead, flanking the core peptide subunits are KR (Lysine-Arginine) amino acids, known recognition sites for Kex2 endoproteases (Julius et al., 1984) which are active within the golgi (Redding et al., 1991). Known dikaritin RiPP precursors all contain multiple copies of the core peptide subunit, each liberated by Kex2 endoproteases, further categorising RiPPs in this family as multicore RiPPs (Rubin and Ding, 2020). Multicore RiPPs are unique to

the dikaritin fungal RiPP family but exist in other RiPP classes from different Kingdoms of life (Rubin and Ding, 2020). Like other fungal RiPPs, the dikaritins are cyclic peptides most commonly cyclised at tyrosine-isoleucine or phenylalanine-tyrosine amino acid residues (Vogt and Kunzler, 2019) with DUF3328 encoding genes playing a vital role in this cyclisation – gene knockouts are unable to produce a mature RiPP (Nagano et al., 2016, Sogahata et al., 2021).

To date, due to the relatively recent discovery of fungal RiPPs more widely, few dikaritin RiPPs have been confirmed and explored in any real detail. Dikaritin RiPPs include: phomopsin a hexapeptide from *Phomopsis leptostromiformis*, ustiloxin tetrapeptides from *Ustilaginoidea virens* and *Aspergillus flavus* (two ustiloxin RiPPs are produced by *U. virens* while *A. flavus* produces only one of these RiPPs (Koiso et al., 1992, Umemura et al., 2014)); and asperipin-2a. Rather less is known about asperipin-2a compared to phomopsin and ustiloxin largely due to its identification from genome mining prior to chemical isolation and functional analysis (Nagano et al., 2016). In opposition to this, since both phomopsin and ustiloxin have roles in animal toxicity, which can be detectable from field concentrations, isolation and investigation of these peptides occurred prior to their classification as RiPPs. For phomopsin, the activity of the peptide was identifiable in the form of lupinosis with this RiPP peptide, a toxin, being the causal agent (Gardiner, 1975, Allen et al., 1979). As with many well-characterised RiPPs that have subsequently been identified as belonging to this class of peptides – phomopsin was initially believed to be the product of NRPSs. As such, an understanding of the mechanism of dikaritin biosynthesis has been lacking compared to functional exploration.

3.1.4 Dikaritin RiPP biosynthetic gene clusters

As more dikaritin RiPPs are discovered, the shared method of RiPP production for this class is further elucidated. Typical dikaritin biosynthetic gene clusters include the precursor gene (xA) which encodes the RiPP precursor peptide with this gene and others in the cluster under the regulation of a transcription factor (xR). Cyclisation, for phomopsin and ustiloxin peptides, occurs on tyrosine and isoleucine residues of the core peptide sequence (Ding et al., 2016, Nagano et al., 2016) and is achieved by tyrosinase enzymes (xQ)(Ding et al., 2016, Umemura et al., 2014) and specific DUF3328 proteins (xY1/Yb) encoded within the cluster (Sogahata et al., 2021, Ye et al., 2016, Nagano et al., 2016).

Methylation modifications of dikaritin RiPPs are applied by S-adenosylmethionine dependent methyltransferases (xM) on specific amine backbone groups of the core peptide (Ding et al., 2016), as seen in the borosins but without the protein fusion in the dikaritin class. Dikaritin RiPP clusters tend to contain several DUF3328 encoding genes (Figure 3.1A) with the implications of these on RiPP biochemistry considered in Sogahata et al. (2021). Of course, dikaritin RiPPs though united by name, must differ so as to generate different peptides. These differences exist in the form of modified core amino acid sequences (Figure 3.1B) as well as variations in post-translational modifications. For example, a RiPP does not need to be methylated to be classed as a RiPP, neither do modifications typical of one RiPP need to be shared by all dikaritins. Notably, though both ustiloxin and phomopsin are dikaritins, the latter has a chlorination modification (Sogahata et al., 2021) while the former does not (Figure 3.1C). Variation in dikaritin biosynthesis exists and understanding the biosynthetic origin of one peptide does not guarantee an understanding for all dikaritins. Only by analysing RiPP biosynthesis of newly identified dikaritins can it be determined which genes are indispensable for production of this family of peptides, and which genes apply additional accessory modifications.

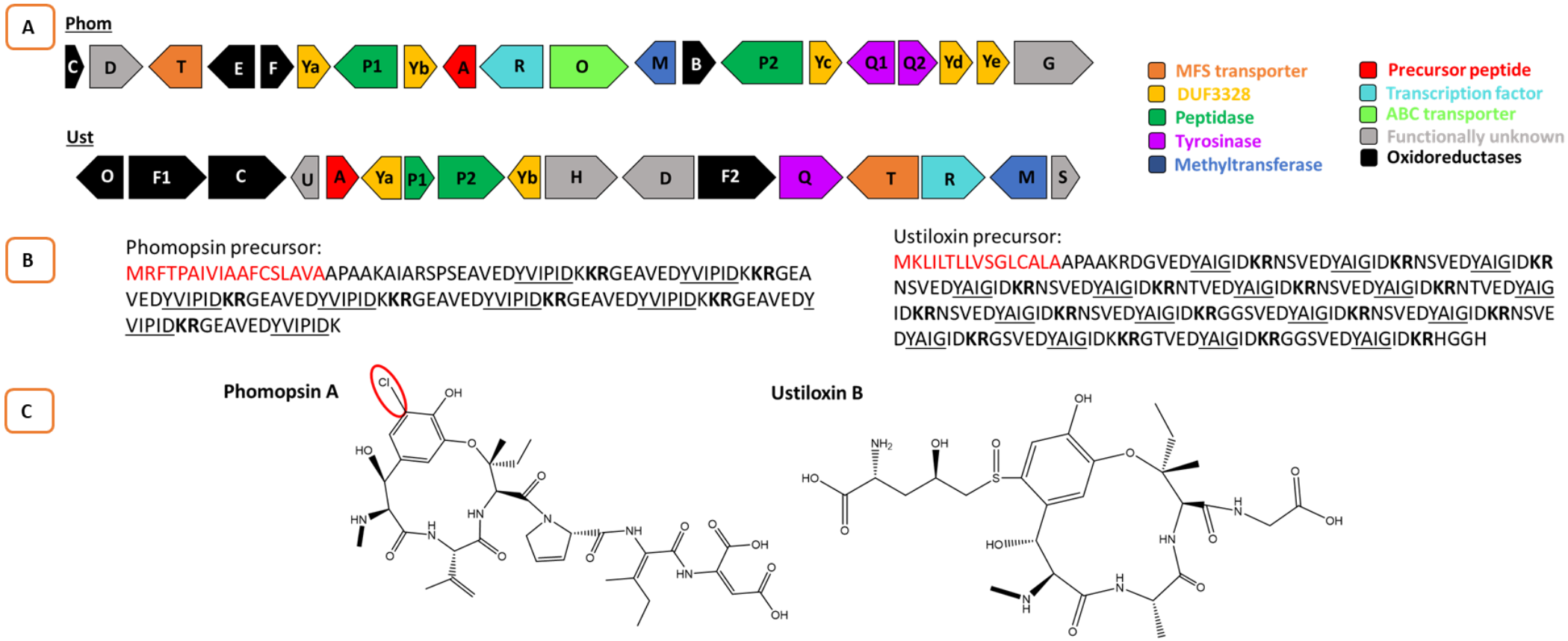

Figure 3.1. A comparison of the phomopsin A and ustiloxin B dikaritin RiPPs.

A) Dikaritin gene clusters are compared, and homologous genes colour coded. Gene product functions are indicated by the displayed key (right). B) Derived from Vogt and Kunzler (2019). Amino acid sequence comparison of precursor peptides of ustiloxin B (from *Aspergillus flavus*; XP_002381318) and phomopsin A (AMR44282). Signal peptides are coloured red. Kex2 endoprotease recognition sites are in bold and core peptide sequences are underlined. C) The chemical structures of the phomopsin A and ustiloxin B RiPPs – red circling highlights the chlorination modification of phomopsin A.

3.1.5 The *Zymoseptoria tritici* RiPP

Our current understanding of dikaritin production has allowed novel putative RiPPs to be identified by BLAST searches for dikaritin biosynthetic genes followed by genome analysis to determine if these genes form a cluster. It is from such work carried out by Ding et al. (2016) that a putative RiPP cluster within the genome of *Z. tritici* was identified. Previous work by Child and Bailey (unpublished) began investigating this cluster and knockout strains of the precursor gene were produced by replacing the gene with the hygromycin resistance cassette, yielding: ZttxA-Δ1, ZttxA-Δ2, ZttxA-Δ3 (the function of the peptide is assessed using these strains in Chapter 4). This chapter looks to explore the putative *Z. tritici* biosynthetic gene cluster in more detail, and continue the work of Child and Bailey (unpublished) by producing additional biosynthetic cluster gene knockouts, extracting the mature RiPP and the intermediates produced by the knockout strains.

3.2 Aims

- To explore the *Z. tritici* putative RiPP biosynthetic gene cluster and compare the *Z. tritici* cluster to other known RiPP-producing clusters.
- To create *Z. tritici* transformants deficient in *Z. tritici* RiPP biosynthetic cluster genes.
- To create *Z. tritici* transformants that overexpress the *Z. tritici* RiPP biosynthetic cluster genes.
- To purify the *Z. tritici* RiPP and gene knockout intermediates from the overexpresser and knockout strains produced in this work.
- To determine the mechanism of *Z. tritici* RiPP biosynthesis.
- To visualise production of the *Z. tritici* RiPP with GFP fused to the precursor peptide.

3.3 Results

3.3.1 Analysis of the *Zymoseptoria tritici* RiPP genomic region

The *Zymoseptoria tritici* putative RiPP biosynthetic cluster genes (Zttx cluster) were first identified by Child and Bailey (unpublished) and assumed functions assigned to the genes within the cluster. This work repeated and confirmed such analysis by carrying out BLASTx searches on these cluster genes (Altschul et al., 1990)(conducted October 2019). The most homologous protein was noted, and the function of this protein assigned as the predicted function of the gene product.

Twelve genes belong to the Zttx cluster (Table 3.1), this includes several genes present in both the phomopsin and ustiloxin gene clusters (Figure 3.2A). Notably, the *Z. tritici* precursor core sequence differs from phomopsins YVIPID by only one amino acid to give YVIPVD (Figure 3.2B). Further comparison to phomopsin, reveals the Zttx cluster to lack the Ye DUF3328 encoding gene and the Q1 gene within the phomopsin gene cluster. Genes that immediately flank the *Z. tritici* cluster (left of *ZttxP1* and right of *ZttxA*) are located on chromosome four at locations of 1,677,000-1,678,580 and 1,707,820-1,708,511, respectively. These genes have locus tags of MYCGRDRAFT_71209 (left flank) and MYCGRDRAFT_58104 (right flank) and are designated as cluster left flank (CLF) and cluster right flank (CRF) in this work.

Table 3.1. Predicted functions of the proteins produced by Zttx cluster genes.

Zttx cluster genes were BLAST searched using the BLASTx functionality. Homologous proteins were identified, assigning the function of the protein with greatest homology to the RiPP gene product. Zttx genes are assigned a name according to convention for dikaritin genes (Umemura et al., 2014). The genomic locus of each Zttx cluster gene within the IPO323 genome is noted along with its MYCGDRAFT identifier. All genes but *ZttxR* have been annotated for this assembly and as such it has not been assigned an identifier. The location of the *ZttxR* gene on chromosome 4 is however noted.

Gene	**Locus identifier**	**Location on chromosome 4**	**Putative protein function**
ZttxP	MYCGRDRAFT_92612	1,681,686 - 1,683,950	Peptidase S41 family protein
ZttxY1	MYCGRDRAFT_28978	1,684,438 - 1,685,014	DUF3328 oxidase
ZttxY2	MYCGRDRAFT_85740	1,686,972 - 1,687,360	DUF3328 oxidase
ZttxQ	MYCGRDRAFT_39869	1,688,171 - 1,689,246	Tyrosinase
ZttxY3	MYCGRDRAFT_92614	1,689,340 - 1,690,777	DUF3328 oxidase
ZttxY4	MYCGRDRAFT_40021	1,691,332 - 1,691,995	DUF3328 oxidase
ZttxAP2/S28	MYCGRDRAFT_40103	1,692,026 - 1,693,749	S28 serine carboxypeptidase
ZttxT	MYCGRDRAFT_40824	1,694,042 - 1,695,664	Major facilitator superfamily transporter
ZttxM	MYCGRDRAFT_17135	1,696,670 - 1,697,425	S-Adenosyl methionine (SAM) dependent methyltransferase
ZttxO	MYCGRDRAFT_71215	1,697,477 - 1,702,334	ATP binding cassette (ABC) transporter
ZttxR	N/A	1,703,305 – 1,705,489	C6 Zinc-finger protein
ZttxA	MYCGRDRAFT_71216	1,706,050 - 1,706,713	Precursor peptide

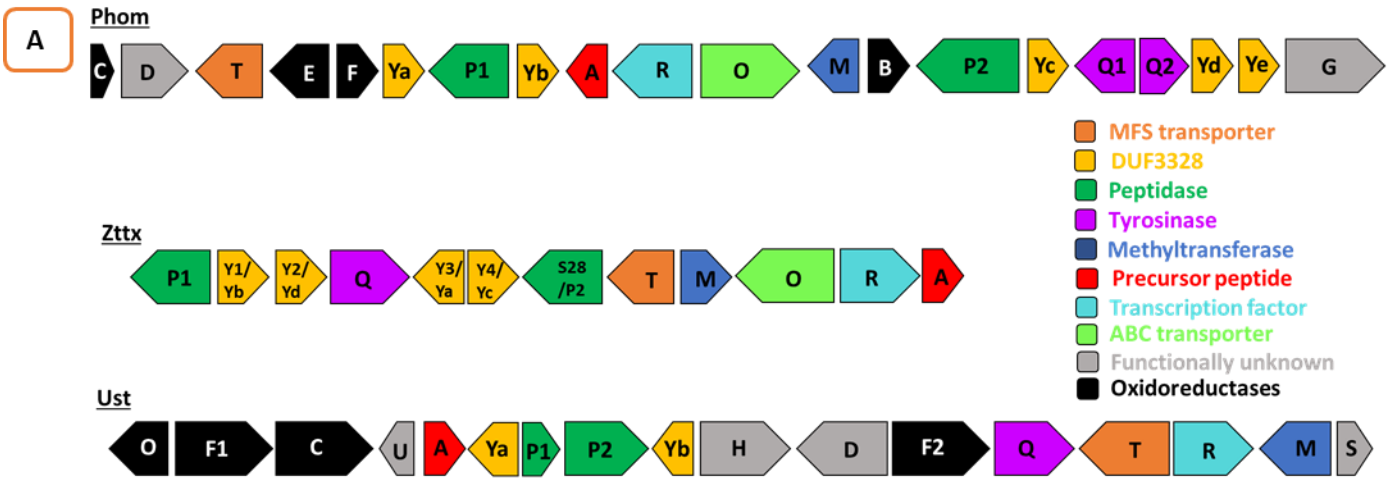

B

Z. tritici RiPP precursor:

MHTSSATWALFALSCTGALSAPIFNGPPLPALAPRHEAVTAVEDYLDKT**KR**AEAVEDYVI
PVDKT**KR**AEAVEDYVIPVDKT**KR**AEAVEDYVIPVDKT**KR**AEAVEDYVIPVDKT**KR**AEAVE
DYVIPVDKT**KR**AEAVEDYVIPVDKT**KR**AEAVEDYVIPVDKT**KR**AEAVEDYVIPVDKT**KR**A
EAVEDYVIPVDKT**KR**A

Figure 3.2 Schematic comparison of the phomopsin, ustiloxin and *Zttx* gene clusters.

A) The gene cluster comparison in Figure 3.1A of phomopsin A (Phom), ustiloxin B (Ust) is extended to include the Zttx cluster (Zttx) – orientations of the Table 3.1. genes are shown here. Colours again are used to represent genes with homology. Functions of the gene products are listed in the key to the right of the image. B) The amino acid sequence of the *Z. tritici* RiPP precursor peptide sequence. The signal peptide of the precursor is predicted by SignalP-5.0 (Almagro Armenteros et al., 2019) and coloured red. Kex2 endoprotease recognition sites are in bold and core peptide sequences underlined.

The expression levels of several Zttx cluster genes (except *ZttxR*, *ZttxT* and *ZttxO*) *in planta* relative to in Czapek Dox broth (CDB) medium at various time points were determined by RNAseq in Rudd et al. (2015)(Figure 3.3). Relative expression was determined as expression *in planta* divided by expression in culture.

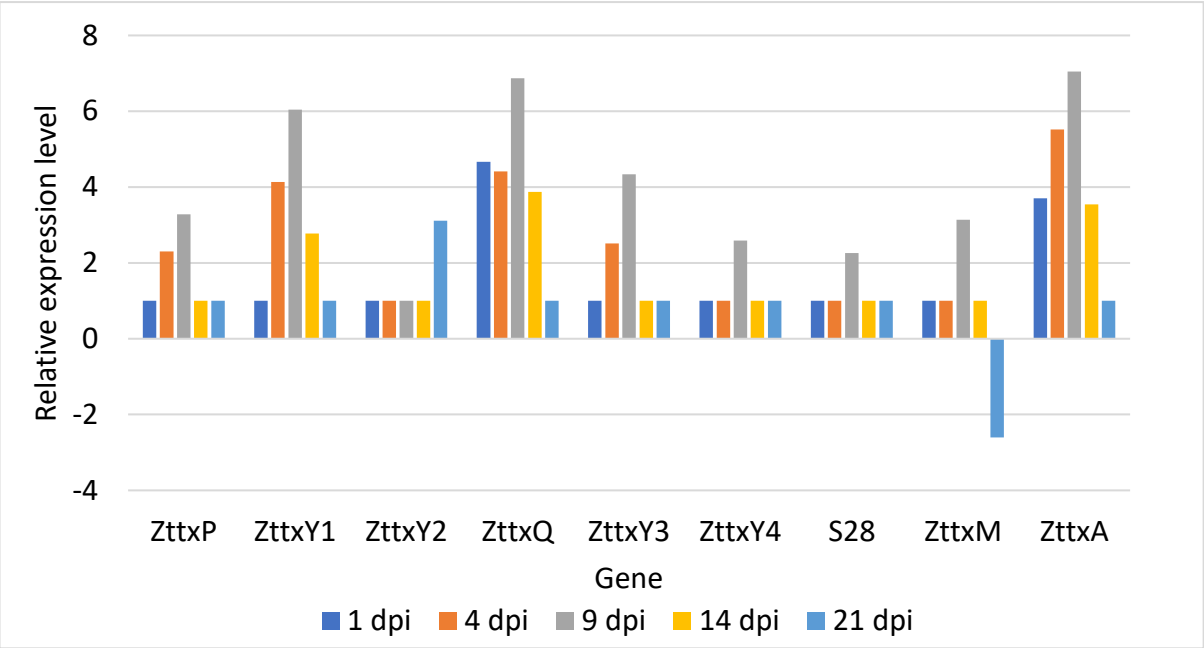

Figure 3.3 Relative expression of the Zttx cluster genes *in planta* compared to in media.

Expression levels of the Zttx cluster genes are shown at several timepoints during wheat infection (data from Rudd et al., 2015).

3.3.2 RiPP cluster gene knockout production

The functions assigned to the *Z. tritici* gene products by BLAST searches are speculative, and despite homology to the annotated proteins, the actual action of the gene product in *Z. tritici* RiPP biosynthesis may differ to that predicted. As such, alongside bioinformatic investigation, gene knockouts of the Zttx cluster genes should also be generated and the impact of this on RiPP chemistry assessed. This is the same process as that proved highly informative for both ustiloxin and phomopsin (Ding et al., 2016, Sogahata et al., 2021). Therefore, this was embarked on for the *Zymoseptoria tritici* RiPP gene cluster, seeking to individually knockout each gene from the cluster, resulting in several strains deficient in just one RiPP modifying enzyme. This was designed and built using yeast-based recombination followed by transformation of the construct into *Z. tritici* by an *Agrobacterium*-mediated method (Zwiers and De Waard, 2001).

Regions of the genome around 1500bp upstream and downstream from the gene targeted for knockout were selected and amplified by PCR. These PCRs employed primers that had 30bp extensions to overlap with either the pCAM0380YA plasmid or the hygromycin resistance cassette. Due to the nature of these extensions, when these left flank and right

flank amplified regions were mixed with EcoR1/Sal1 digested pCAM0380YA plasmid alongside the hygromycin resistance cassette in a yeast recombination these fragments were united to form a knockout construct (Figure 3.4).

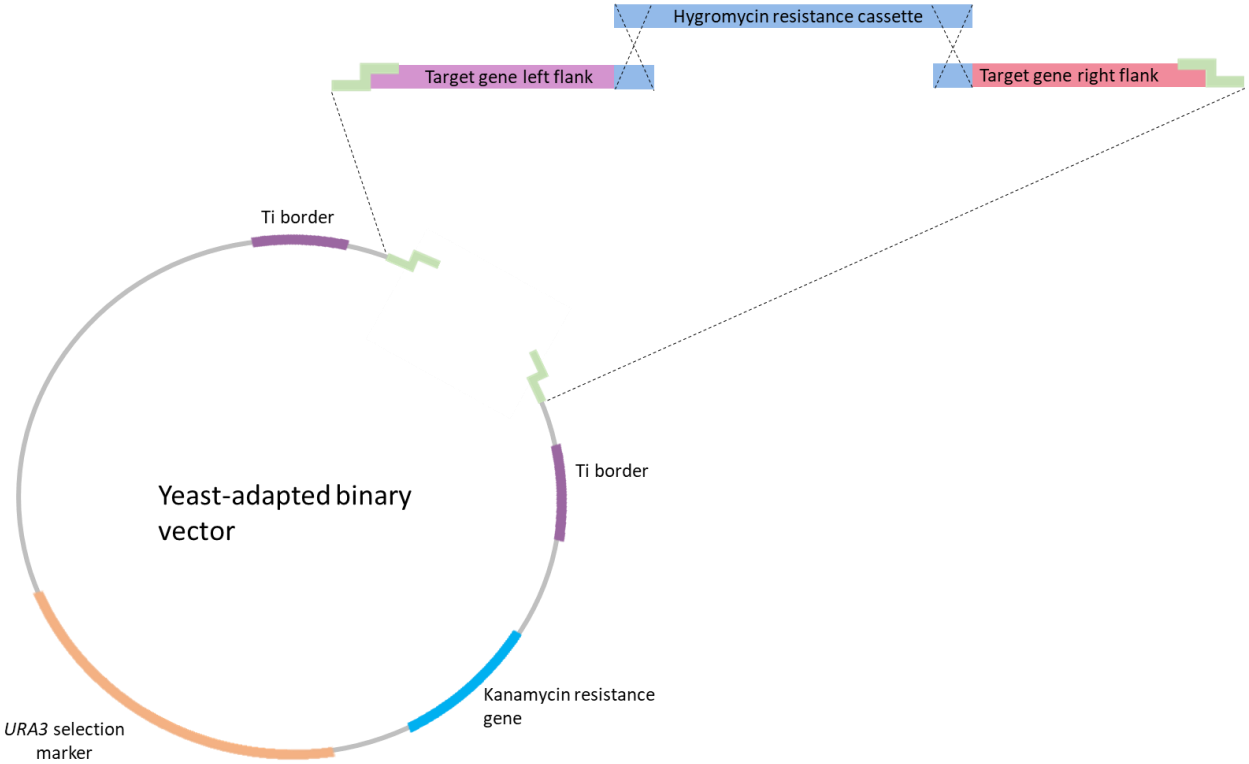

Figure 3.4 Schematic of the production of pCAMBIA0380YA knockout constructs of Zttx cluster genes.

Once extracted from yeast and transformed sequentially into *E. coli* then *Agrobacterium tumefaciens,* the construct was ready for use in *Z. tritici* knockout production. Following two rounds of subculturing putative transformants under hygromycin selection (Figure 3.5), the hygromycin resistance cassette was assumed to have successfully been transformed into the fungal genome. Mycelia were then used in DNA extractions (Liu et al., 2000) and the resultant DNA employed in diagnostic PCR whereby the success of the knockout targeting was determined.

Figure 3.5 Zttx gene knockout transformants growing on a hygromycin selection plate.

Putative *ZttxY4* knockout strains inoculated onto PDA plates supplemented with 100 µg/ml hygromycin for selection of strains containing the hygromycin resistance cassette. The wildtype (WT) IPO323 strain is used as a comparison, showing no growth compared to the transformant strains.

Three PCR reactions per suspected knockout strain were set up (Figure 3.6; primers are listed in Table 9.1). (**1**) The first amplified from the 5' (left flank) region of the deleted gene into the gene of interest, using this amplification to determine if the gene had been deleted. The second and third reactions (**2**) amplified from before the 5' region of the target gene into the hygromycin resistance cassette and (**3**) from the hygromycin resistance cassette into the 3' region beyond the flanking region. These reactions confirmed that the transformation construct had inserted into the *Z. tritici* genome as intended (Figure 3.7). In each instance, the wildtype IPO323 strain was used in PCR reactions as both a positive (for reaction 1) and negative control (for reactions 2 and 3).

This process was completed successfully for genes: *P*, *S28*, *Q*, *O*, *M*, *T*, *Y2*, *Y3*, *Y4*. The efficiencies of the transformations are noted in Table 3.2. Knockout of the *Y1* gene was attempted but yeast recombination efforts were unsuccessful – the knockout construct could not be produced.

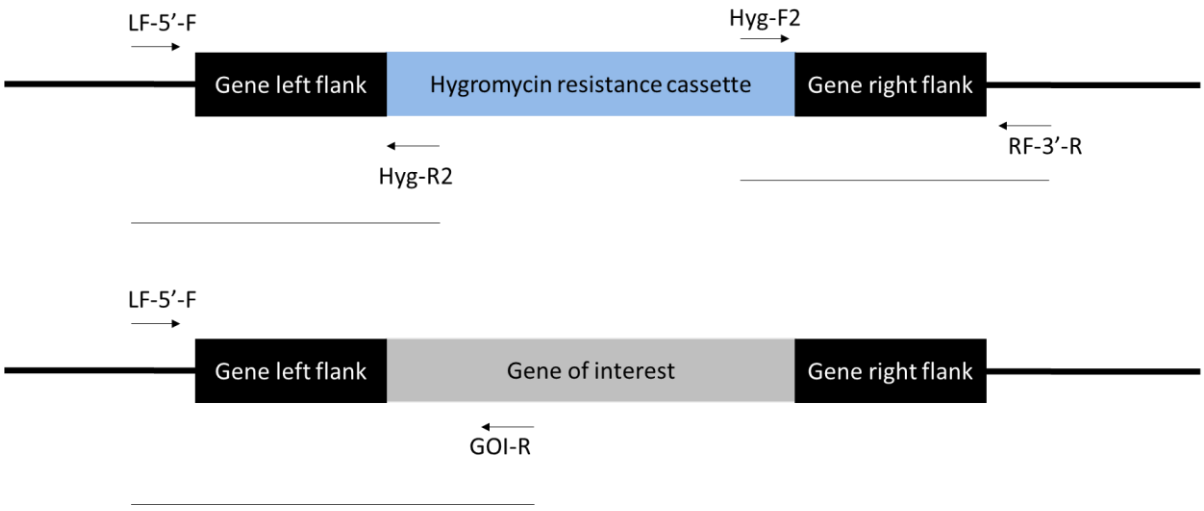

Figure 3.6 Schematic showing the general method employed in diagnostic PCR of putative *Z. tritici* RiPP biosynthetic gene knockouts.

Left flank and right flank primers amplified regions outside of those used in knockout plasmid construction – these are designated in black.

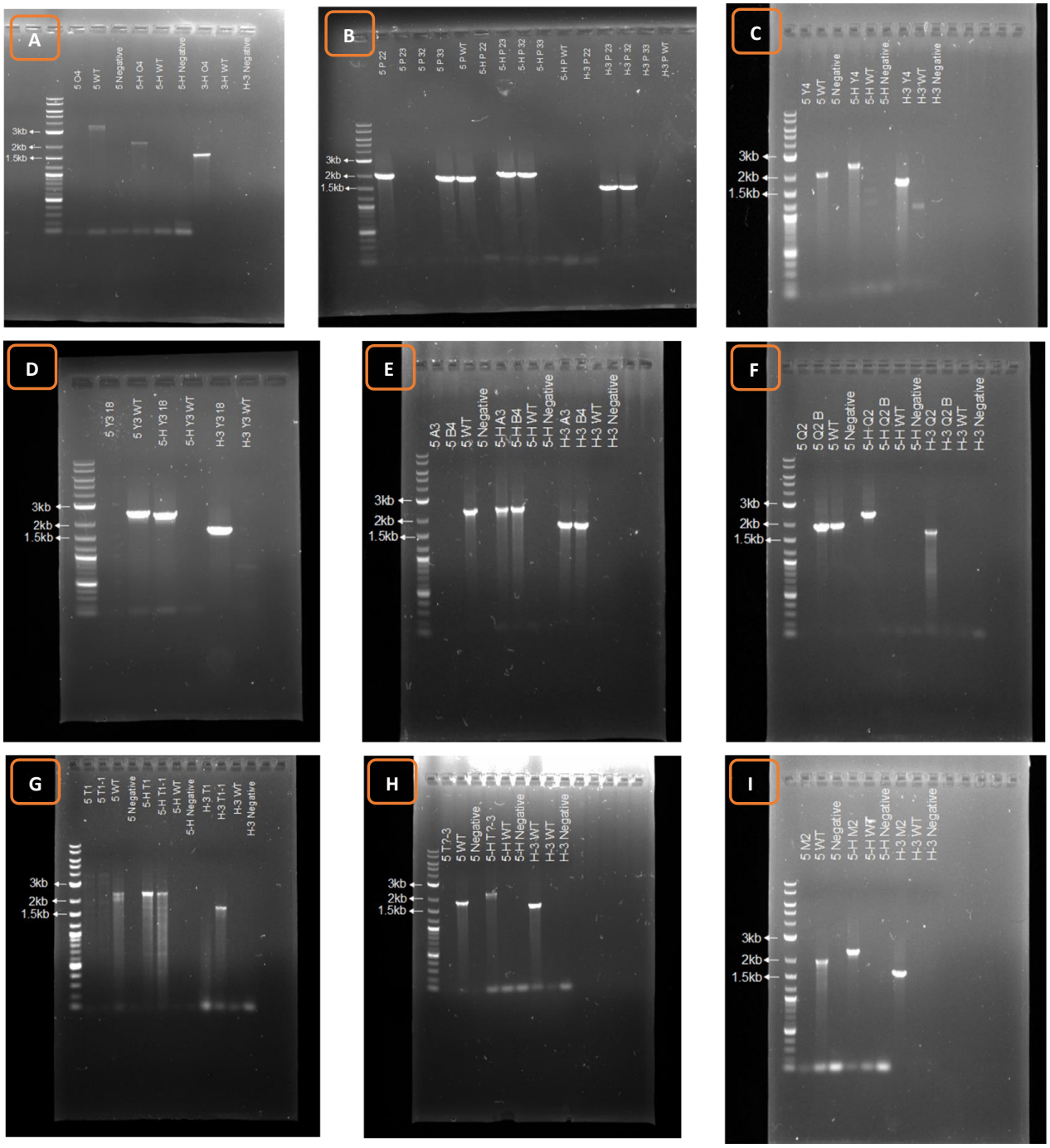

Figure 3.7 Gel electrophoresis images confirming knockout of Zttx cluster genes by diagnostic PCR.

Diagnostic PCR with the Figure 3.6. scheme was completed for all knockout strains produced of the Zttx cluster genes: *O* (A), *P* (B), *Y4* (C), *Y3* (D), *S28* (E), *Q* (F), *T* (G), *Y2* (H) and *M* (I). Additional water controls (Negative) were also employed for some genes. The LF-5-F/GOI-R primed reaction determining gene deletion (amplifying from the 5' region into the gene of interest) is designated as 5 – followed by the transformant/strain name e.g., O4, or WT (for wildtype). The LF-5'-F/HygR2 and Hyg-F2/RF-3'-R reactions are designated as 5-H (amplifying from the 5' region to hygromycin) and H-3 (amplifying from hygromycin to the 3' region), respectively – again followed by the strain name.

Table 3.2 The efficiencies of Zttx knockout transformations and the targeting efficiency of gene deletion.

The total number of transformants (fungal strains capable of growing on hygromycin selection) is stated alongside the number of these determined to be knockouts by diagnostic PCR for each gene. Targeting efficiency is given as the percentage of transformants that were confirmed knockouts.

Gene	Transformants	Knockouts	Targeting efficiency (%)
ZttxP	20	2	10
ZttxY2	4	1	25
ZttxQ	7	1	14.29
ZttxY3	7	1	14.29
ZttxY4	11	4	36.36
S28	8	2	25
ZttxT	11	3	27.27
ZttxM	11	1	9
ZttxO	4	1	25

3.3.3 Phenotypic observations of Zttx gene knockouts.

To determine whether deletion of Zttx cluster genes had any obvious impacts on fungal phenotype, knockout strains including the *ZttxA* gene knockout produced by Child and Bailey (unpublished) were grown both in liquid and on solid media. Spore suspensions at a concentration of $1x10^6$ (in sterile dH_2O) were produced for each fungal strain. Liquid cultures (50ml PDB) were inoculated with 500µl of this spore suspension while solid media (PDA) were inoculated with 3µl droplets of the suspension. Growth phenotype in liquid was visually assessed after six days at 20°C (200RPM for liquid cultures), however, there were no readily apparent difference in amount or growth form (Figure 3.8). Agar plates were observed over a 14-day course, but there were no differences in growth, colony morphology or pigmentation (Figure 3.9). As such, gene knockouts of the Zttx cluster genes do not seem to have a noticeable impact on the *Z. tritici* IPO323 strain.

Figure 3.8 Phenotypic observations of the Zttx gene cluster knockouts in liquid media compared to the wildtype IPO323 *Z. tritici* strain.

Fungal strains were each grown for six days in PDB. Each strain is pictured next to the wildtype (WT; on the left) for comparison. Knockout strains are of genes A) *ZttxA* B) *ZttxQ* C) *ZttxY3* D) *ZttxY2* E) *ZttxP* F) *ZttxT* G) *S28* H) *ZttxO* I) *ZttxM* J) *ZttxY4.*

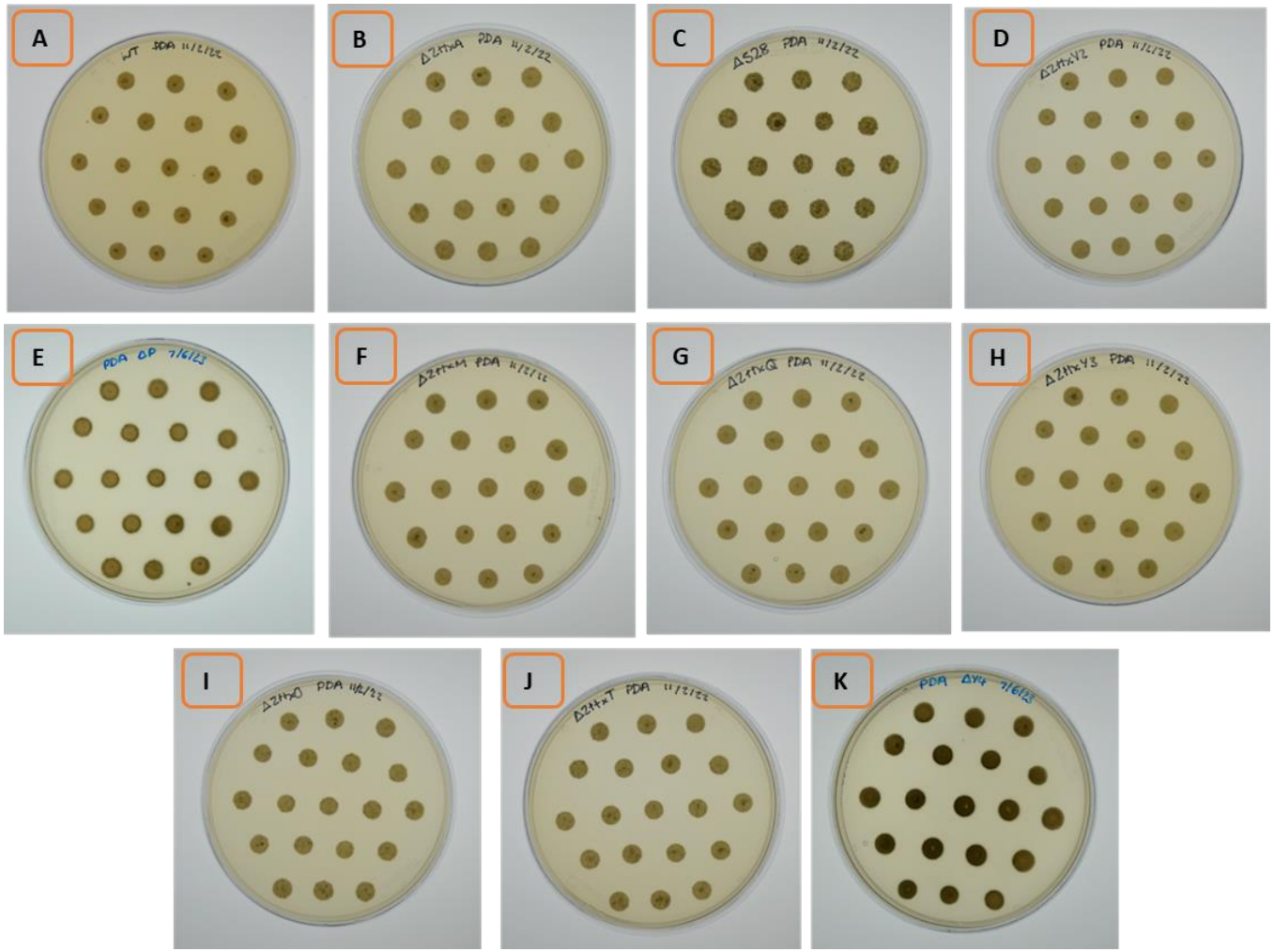

Figure 3.9 Phenotypic observations of the Zttx gene cluster knockouts on solid media.

Fungal strains were pictured after six days of growth on PDA. Knockout strains are of genes B) *ZttxA* C) *S28* D) *ZttxY2* E) *ZttxP* F) *ZttxM* G) *ZttxQ* H) *ZttxY3* I) *ZttxO* J) *ZttxT* K) *ZttxY4*. The wildtype IPO323 strain is also pictured (A) for comparison.

3.3.4 *ZttxR* overexpresser production

A knockout strain of the *ZttxR* gene was not produced in this work, instead an overexpresser of this gene was generated. Vector construction involved yeast recombination of fragments into pCAMBIA0380YA as before, but the site of construct insertion was not directed in the *Z. tritici* genome. For *ZttxR* overexpression, the *ZttxR* coding region (alongside its terminator region) was amplified from wildtype IPO323 DNA by PCR with overlaps of the Histone H3 (HH3) promoter region (left flank overlap) and the hygromycin resistance cassette (right flank overlap) designed into the primers (Figure 3.10). The HH3 promoter region was amplified from WT IPO323 genomic DNA, selecting this region to drive constitutive expression (with a left flank overlap to the pCAMBIA0380YA plasmid), and the hygromycin resistance cassette fragment was amplified with primers generating an overlap with the pCAMBIA0380YA on the right flank.

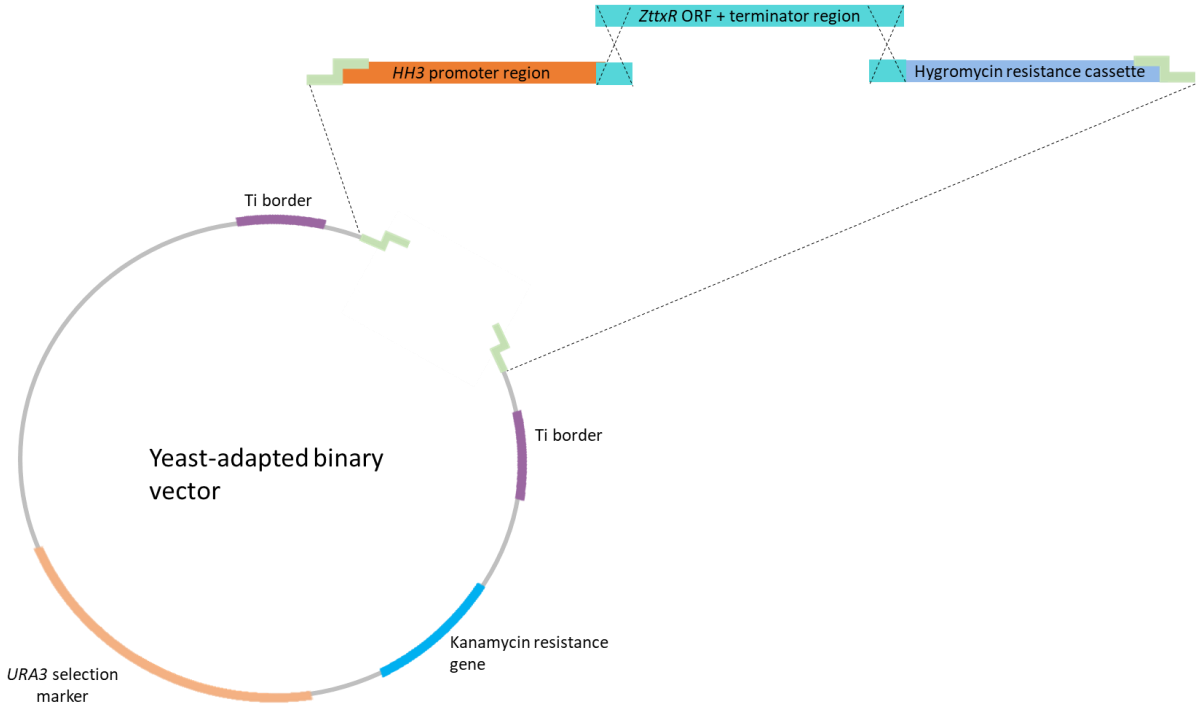

Figure 3.10 Schematic diagram of *ZttxR* overexpresser construct production.

The *ZttxR* overexpresser transformation construct was designed using the pCAMBIA0380YA backbone in a similar way to the knockout plasmids. Overlaps between fragments introduced by PCR primers were employed to assemble the construct in the desired order and encourage recombination into the pCAMBIA0380YA backbone. The HH3 promoter region, of a constitutively expressed gene, was selected to promote expression of the *ZttxR* transcription factor. Hygromycin resistance was included in the vector as a marker for selection.

The overexpression vector was transformed into wildtype IPO323 *Z. tritici* using an *Agrobacterium*-based method. DNA was extracted from transformants (Liu et al., 2000) and subject to diagnostic PCR (with the primer pairs outlined in Figure 3.11A) to confirm the overexpresser construct to be intact and present in the *Z. tritici* genome. Two of the three inserted DNA fragments are native to the wildtype IPO323 form of the fungus; hence, primers were designed to amplify across unique junctions.

Diagnostic PCR identified three overexpresser strains in this work: OxR T4, OxR T7 and OxR T8 (Figure 3.11B, C, D). The wildtype IPO323 strain was also used as a template in reactions with these primers to confirm that these amplicons were not from genes already within the wildtype strain, but rather the novel construct. Absence of amplicons in wildtype reactions confirmed that this amplification was not of the native DNA. Diagnostic PCR confirms insertion of the overexpression construct into the fungal genome but does not inform us regarding the impact of this genomic modification on expression of the *ZttxR* gene.

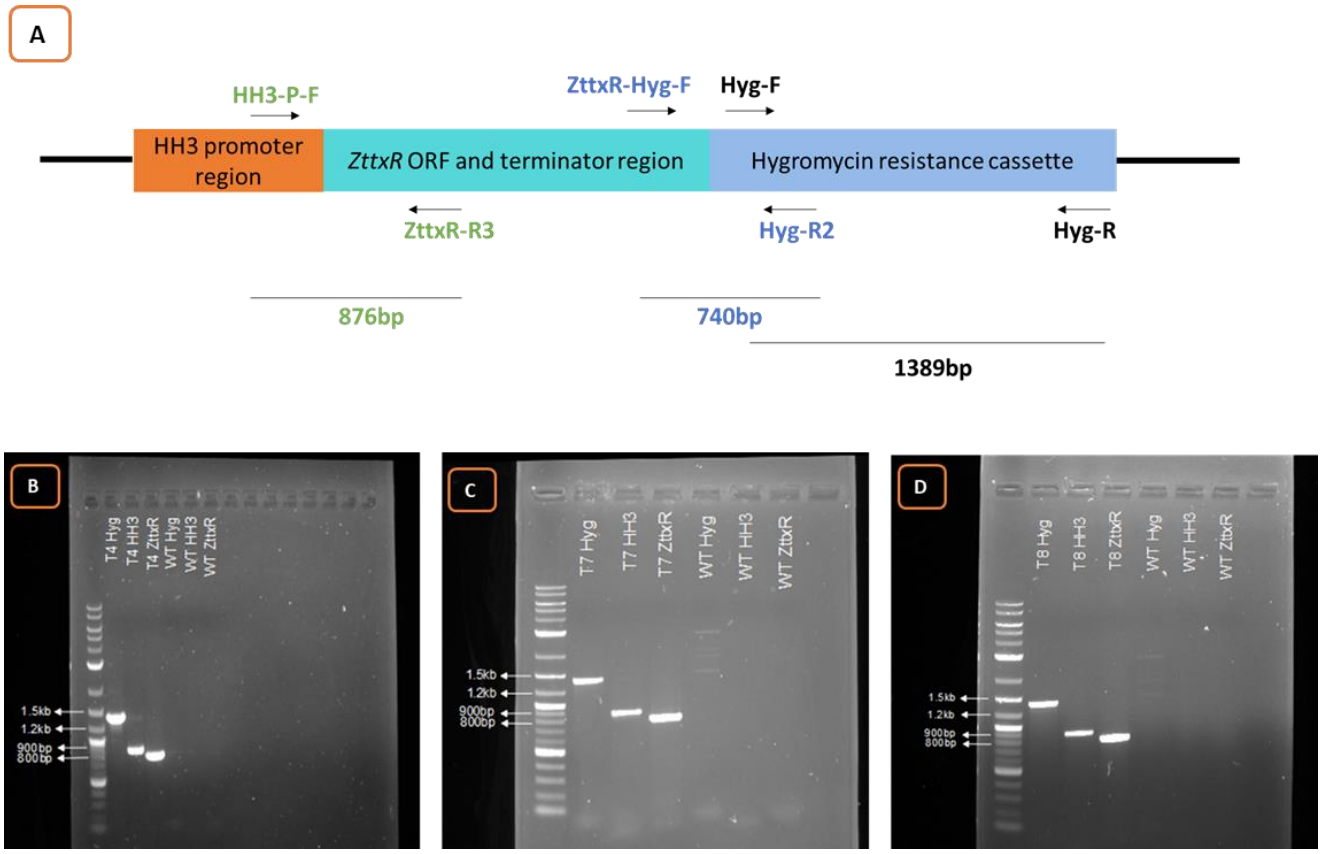

Figure 3.11 Diagnostic PCR to confirm presence of HH3:ZttxR in the "overexpresser" transformants.

A) Schematic demonstrating the diagnostic PCR completed to confirm *ZttxR* overexpresser transformation. Primer names are written in bold, and pairs are indicated by shared colours. Arrows designate the binding sites of the primers with solid black lines linking primer pairs – amplicon sizes are noted. Putative overexpresser transformant DNA was amplified with Hyg-F/Hyg-R primers, amplifying the hygromycin resistance cassette (Hyg); HH3-P-F/ZttxR-R3, amplifying from the *HH3* promoter region into the *ZttxR* fragment (HH3); and ZttxR-Hyg-F/Hyg-R2, amplifying from the *ZttxR* fragment into the hygromycin resistance cassette (ZttxR). Diagnostic PCR products were gel electrophoresed and the result confirming production of overexpresser strains: (B) T4 OxR (C) T7 OxR (D) T8 OxR, shown.

3.3.5 Impact of *ZttxR* overexpression on *Z. tritici* phenotype

As with the knockout strains of *Zymoseptoria tritici*, the overexpresser strain OxR T4 (the first overexpresser strain produced) was grown from a $1x10^6$ spores/ml inoculum, adding 500µl of this to 50ml PDB for liquid culture assessment and 3µl drops to PDA plates for solid culture assessment (Figure 3.12). The phenotype of the cultures was visually monitored after six days at 20°C (200RPM for liquid cultures).

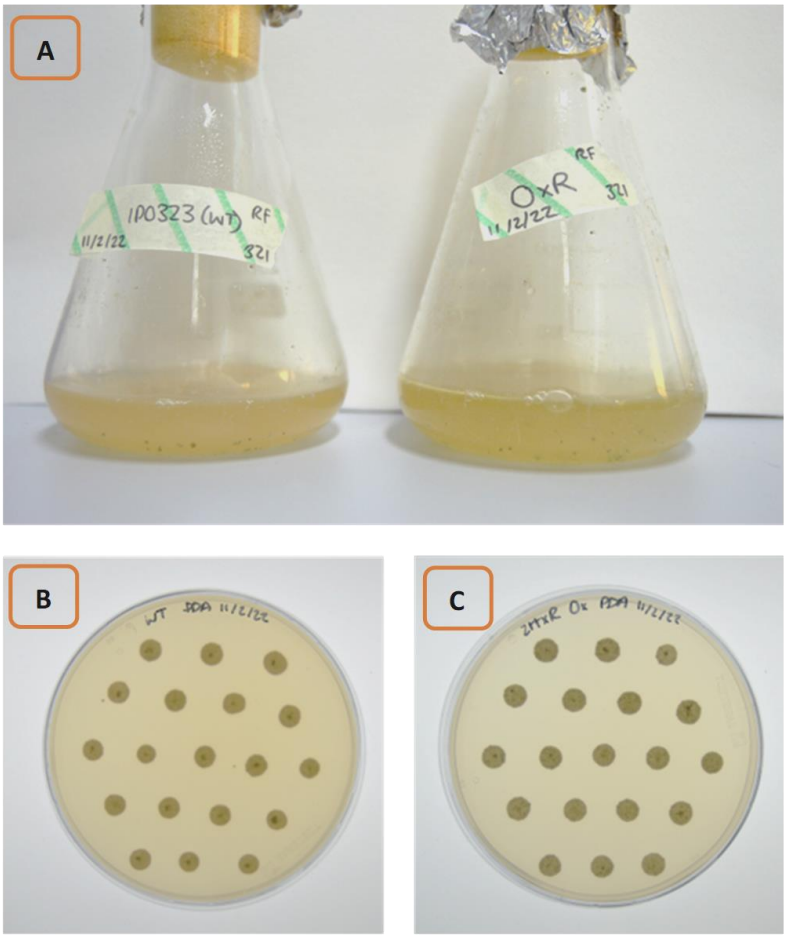

Figure 3.12 Phenotypic observations of *Z. tritici* IPO323 wildtype and the transformant OxR T4.

A) The growth phenotype of *Z. tritici* wildtype IPO323 (left) and OxR T4 (right) strains in PDB after six days. The growth phenotype on solid media (PDA at six days post inoculation) for B – IPO323 and C – OxR T4.

The phenotypes of the two fungal strains were similar regardless of whether the fungi were grown in liquid or on solid media. Overexpression of the *ZttxR* transcription factor did not appear to influence the phenotype of the fungus. To determine whether the growth rate of

the fungal strains was impacted by *ZttxR* overexpression, rather than the final phenotype, 100ml PDB cultures were set up, inoculating each with sporidia from a five-day-old CDV8 plate. After nine days of growth (selected as several Zttx genes showed highest expression levels at this point *in planta* (Figure 3.3)(Rudd et al., 2015)) at 20°C (200RPM) cultures were harvested by centrifugation at 9,000x g. Harvested cells were washed with sterile dH_2O and centrifuged as before. Pellets were frozen then freeze dried and weighed to give a measure of fungal biomass (Figure 3.13).

Figure 3.13 Biomass of *Z. tritici* strains following *Agrobacterium*-mediated transformation.

Fungal culture biomass after nine days of growth in 100ml PDB for wildtype (WT), a *ZttxA* deletion strain (ZttxA-Δ2) and a *ZttxR* overexpresser strain (OxR T4). Error bars are +/- standard error of the mean (S.E.M), N=3.

Slight differences in fungal biomass can be noted with the wildtype having the greatest biomass and OxR T4 the lowest biomass of the three strains examined. The difference in biomass between strains, however, was shown to be non-significant in a Kruskal-Wallis test. *ZttxR* gene overexpression did not significantly alter fungal growth from the wildtype level, nor did *ZttxA* deletion.

3.3.6 Determining the impact of *ZttxR* overexpression on Zttx cluster gene expression

Based on what is known of other dikaritin RiPP gene clusters, the *ZttxR* gene (presumed to encode a C6 transcription factor) is predicted to regulate gene expression of the Zttx cluster, including the *ZttxA* precursor gene. By looking at gene expression of the *ZttxA* gene in both wildtype and the *ZttxR* overexpresser strains this identifies whether the *ZttxR* gene product is a transcription activator or repressor as its influence on a key Zttx cluster gene is assessed.

qPCR was performed on cDNA from nine-day old CD+YE cultures, again selected based on transcriptomic data from Rudd et al. (2015), using the ZttxA-F/ZttxA-R primer pair to determine the impact of *ZttxR* overexpression on *ZttxA* gene expression. HH3 reference gene primers FWD_HH3/RVS_HH3 produced by Tiley (2016) were also used (primer sequences are listed in Table 9.3). *ZttxR* overexpresser strains showed ~390% greater transcript levels of the *ZttxA* gene compared to the wildtype *Z. tritici* strain (Figure 3.14). However, no significant difference in *ZttxA* gene expression was identified between any of the strains in a Kruskal-Wallis test ($p=0.09$). Whilst not significant at the $p<0.05$ level, with a greater sample size statistical significance may then be seen. The OxR T4 strain was arbitrarily selected for further analysis looking at whether different media impacted *ZttxA* production as well as whether expression of *ZttxA* varied over a set time course.

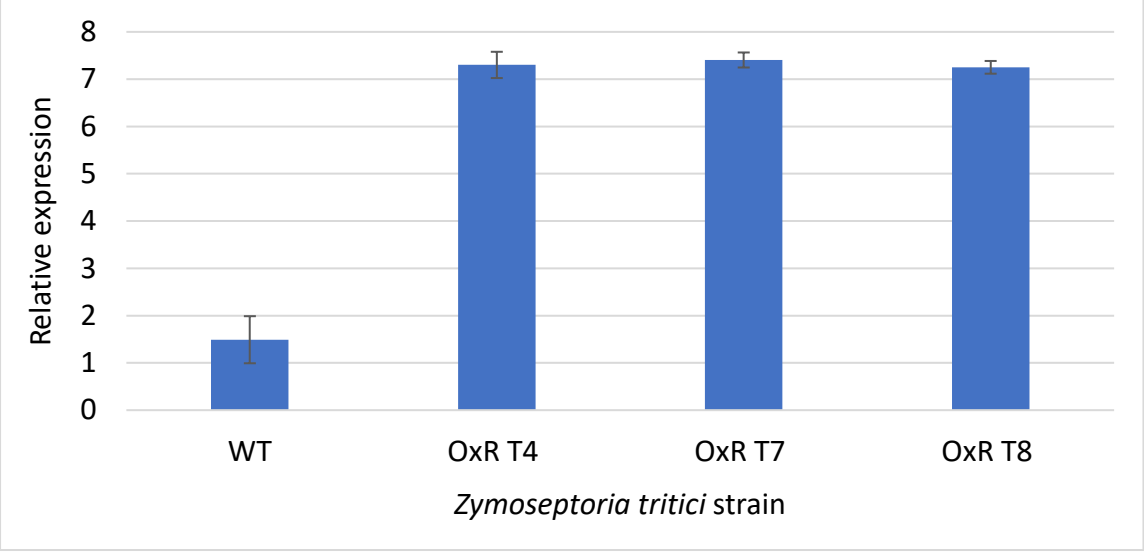

Figure 3.14 Expression of the *Zymoseptoria tritici ZttxA* gene in wildtype IPO323 and *ZttxR* overexpresser strains of the fungus.

Gene expression of the *ZttxA* was determined by RT-qPCR using the primers ZttxA-F/ZttxA-R. Values are of *ZttxA* gene expression relative to *HH3* expression for each strain. Error bars are +/- standard error of the means (N=3).

The IPO323 and OxR T4 strains were grown in V8 liquid media for nine days and RNA extracted as before. *ZttxA* gene expression was assessed with the ZttxA-F/ZttxA-R primers. The increased expression of the *ZttxA* gene compared to the wildtype strain was consistent across media types (Figure 3.15). Expression of the *ZttxA* gene in wildtype IPO323 *Z. tritici* was reduced when grown in V8 media (~244% greater *ZttxA* expression in CD+YE) making the upregulation of gene expression in the OxR T4 strain in this media type more pronounced (~380% greater expression of the overexpresser strain compared to the WT vs. 329% increase for CD+YE). Indeed, Kruskal Wallis testing identified a significant difference in gene expression between groups ($p<0.05$). A Dunn post-hoc test with Benjamini-Hochberg correction determined expression of the *ZttxA* gene to be significantly greater in the OxR T4 strain grown in CD+YE compared to the wildtype strain grown in CD+V8 ($p<0.05$).

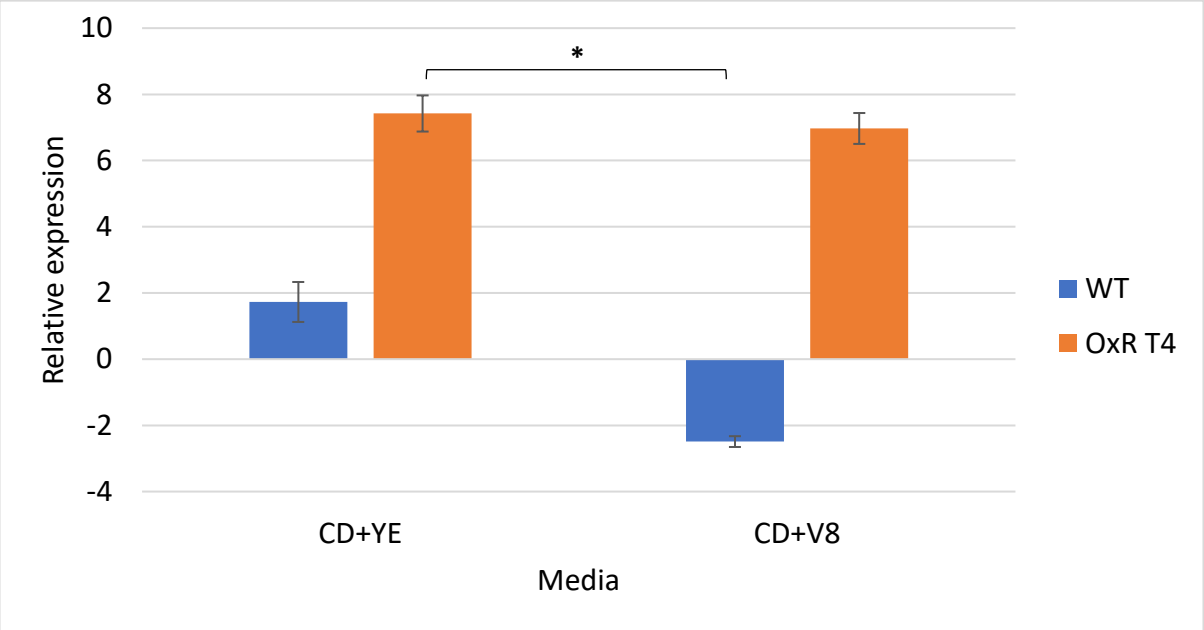

Figure 3.15 Comparison of *ZttxA* expression in CD+YE and CD+V8 media by qPCR.

Wildtype IP0323 and OxR T4 strains of *Z. tritici* were grown in 100ml media, either CD+YE or CD+V8 at 20°C 200PRM for nine days. Gene expression of *ZttxA* was determined using the primers ZttxA-F/ZttxA-R. Data for each media are grouped (left; CD+YE and right; CD+V8). Colour is used to separate the strains (wildtype; blue and OxR T4; orange). Values are *ZttxA* gene expression relative to the expression of *HH3* for each strain. Error bars are +/- standard error of the means (N=3). Horizontal lines with an asterisk are used to specify conditions under which *ZttxA* gene expression significantly differs at the $p<0.05$ level.

Transcript levels of the *ZttxA* gene were greatest in the CD+YE media configuration for the wildtype strain of the fungus, and so whether transcript levels of *ZttxA* varied over time was examined in 100ml CD+YE cultures. These cultures were set up as before but processed for RNA extraction at varying time points of 4-, 7-, 9-, 14- and 21-days post inoculation of the media. This was completed for both the wildtype IPO323 and OxR T4 strains of the fungus. *ZttxA* gene expression was assessed with the ZttxA-F/ZttxA-R primers as before (Figure 3.16). In the wildtype strain of the fungus, natural variation in expression of the *ZttxA* gene was seen within the time course with greatest relative expression of the gene at 7- and 9-days post inoculation. The trend of increased gene expression of *ZttxA* in the OxR T4 strain is consistent across all timepoints, however the difference varies with increases from the wildtype of ~616%, ~389%, ~239%, ~604% and ~1396% from day 4, 7, 9, 14 and 21, respectively.

A Kruskal-Wallis test determined that groups significantly differed in their expression of *ZttxA* ($p<0.05$). Dunn post-hoc testing with Benjamini Hochberg correction however determined that no WT or OxR T4 samples significantly differed in their *ZttxA* expression at the same time point (though day four comparisons gave a p-value of 0.09), nor were there significant differences within strains in *ZttxA* transcript levels over time.

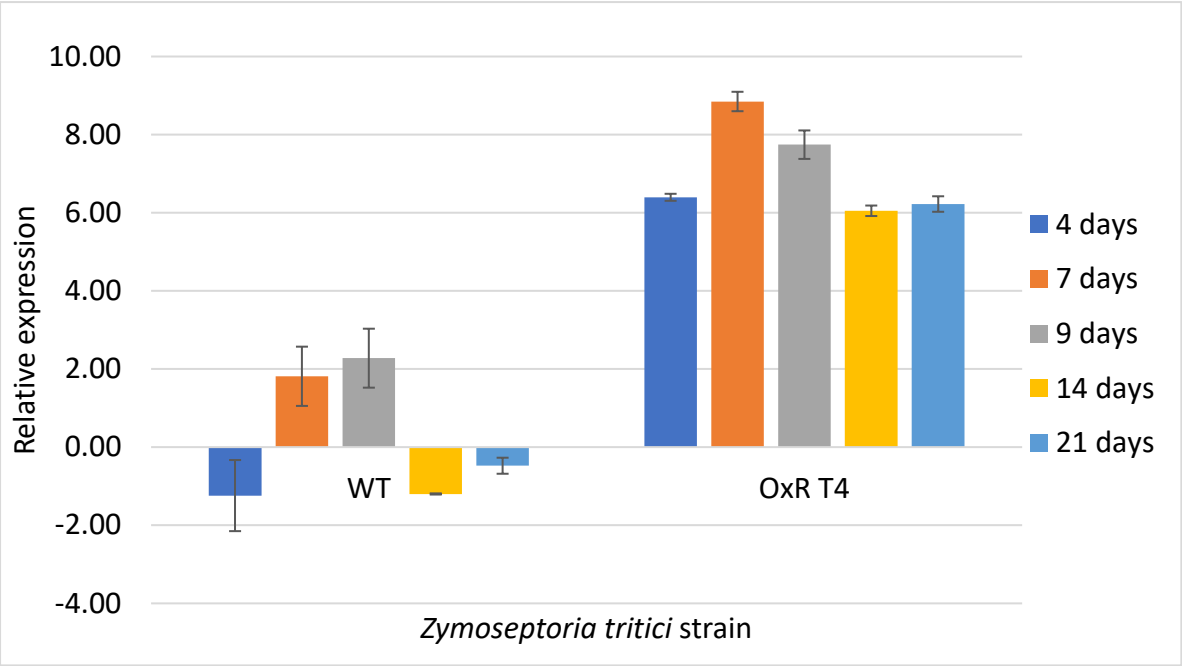

Figure 3.16 Comparison of *ZttxA* gene expression over a 21-day time course in wildtype IPO323 and the *ZttxR* overexpresser OxR T4 by qPCR.

Each strain was grown in 100ml CD+YE liquid media 20°C 200RPM for 4, 7, 9, 14 or 21 days. Colours are used to highlight the same day for each strain. Time course data for each strain are grouped – left is wildtype (WT), right is the *ZttxR* overexpresser (OxR T4). Gene expression of *ZttxA* was determined using the primers ZttxA-F/ZttxA-R. Values are ZttxA gene expression relative to the expression of *HH3* for each strain. Error bars are +/- standard error of the mean (N=3).

Overexpression of the *ZttxR* clearly increases expression of the *ZttxA* gene relative to the wildtype IPO323 *Z. tritici* strain. The impact of overexpression of *ZttxR* on other genes within the Zttx cluster was also investigated as the *ZttxR* gene product is the only proposed transcription factor encoded for within the RiPP biosynthetic gene cluster. Using RNA extracted from CD+YE wildtype IPO323 and OxR T4 cultures, nine-days post media inoculation, comparisons of gene expression of these additional cluster genes were carried out (Figure 3.17). Specific primers for each cluster gene were designed (Table 9.3), where possible these spanned introns to allow detection of genomic DNA contamination beyond the efforts already made. Two genes immediately flanking the *Zttx* cluster, labelled CLF and CLR in Figure 3.17, were also assessed to determine the span of control *ZttxR* has on gene expression and confirming the limits of the genes within biosynthetic cluster. Increased gene

expression in the OxR T4 strain is seen for all genes within the cluster (with the exception of *ZttxO*) – p-values of less than 0.1 are noted for *T, Q, P, M, Y1, Y3* and *Y4* in Mann Whitney U tests but no significance at the $p<0.05$ level is seen. Genes flanking the cluster to the left (CLF) or right (CRF) show little change or indeed show slightly reduced expression, indicating that they are not under the regulation of *ZttxR* and adding further evidence that they are not part of the biosynthetic cluster.

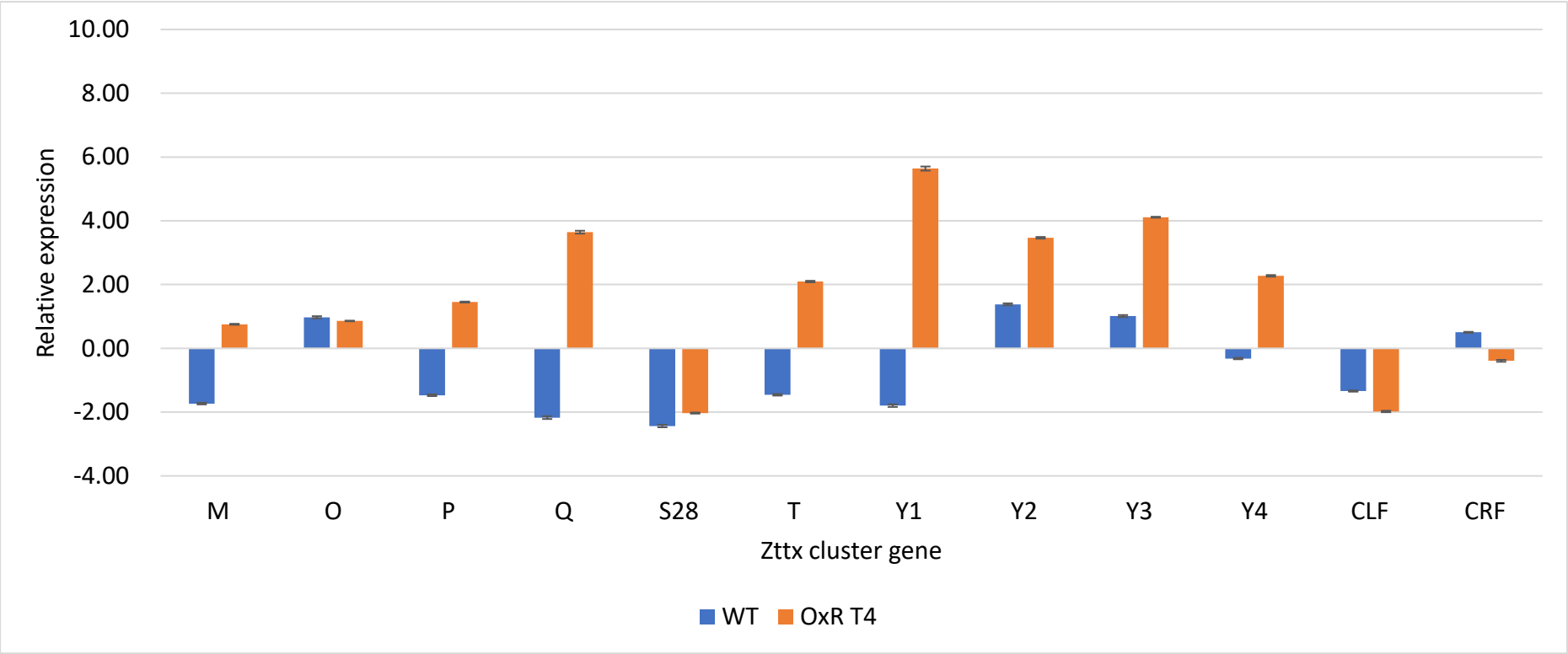

Figure 3.17 Relative transcript levels of each gene of the Zttx cluster in WT and OxR T4 showing modified expression with *ZttxR* overexpression.

Each strain was grown in 100ml CD+YE liquid media 20°C 200RPM for nine days. Colours are used to highlight data from the same *Z. tritici* strain (WT; blue and OxR T4; orange). Gene expression for each cluster gene was assessed using gene specific primers. Values are gene of interest expression relative to *HH3* gene expression. Error bars are +/- standard error of the means (N=3). Genes are labelled according to Table 3.1.

3.3.7 Isolation of the *ZttxA* RiPP peptide

Following production of the Zttx cluster knockouts the next step in the workflow was to perform largescale metabolite extractions from mycelial cultures of the various strains, isolating the mature RiPP peptide then each intermediate produced by the gene knockout strains, allowing identification of the complete method of *Z. tritici* RiPP biosynthesis. To begin, extraction efforts were directed to the mature RiPP from wildtype IPO323 *Z. tritici*. Later extractions, to mitigate the possibility of low peptide titre from the wildtype, used the OxR T4 strain which upregulates expression of several Zttx cluster genes. In each instance OxR T4 was grown alongside the ZttxA-Δ2 strain (incapable of expressing the *ZttxA* precursor peptide). All fungal extracts from this work were diluted to 10mg/ml and 10µl injected into a C18 column and analysed by LCMS as described in Chapter 2. LCMS traces were analysed for peaks present in wildtype or overexpresser chromatograms where they were absent at the equivalent timepoint in the *ZttxA* deletion strain.

Initial extraction efforts used a XAD-2 column-based method, as is routinely used for phomopsin A extraction (Ding et al., 2016, Lanigan et al., 1979, Sogahata et al., 2021). Similarity between the two peptides was predicted as they share several modifying enzymes within their biosynthetic gene clusters and differ by only one amino acid in their core sequence (Figure 3.1; Figure 3.2). Presumed differences in RiPP biosynthesis between phomopsin and the *Z. tritici* RiPP are highlighted in Figure 3.18 – namely a chlorination modification applied by the gene product of *PhomQ1*, a gene for which there is no homolog within the Zttx cluster. The phomopsin cluster also contains an additional DUF3328 containing protein (*PhomYe*) that is absent in the Zttx cluster. In spite of these differences, extraction based on the same method seemed logical.

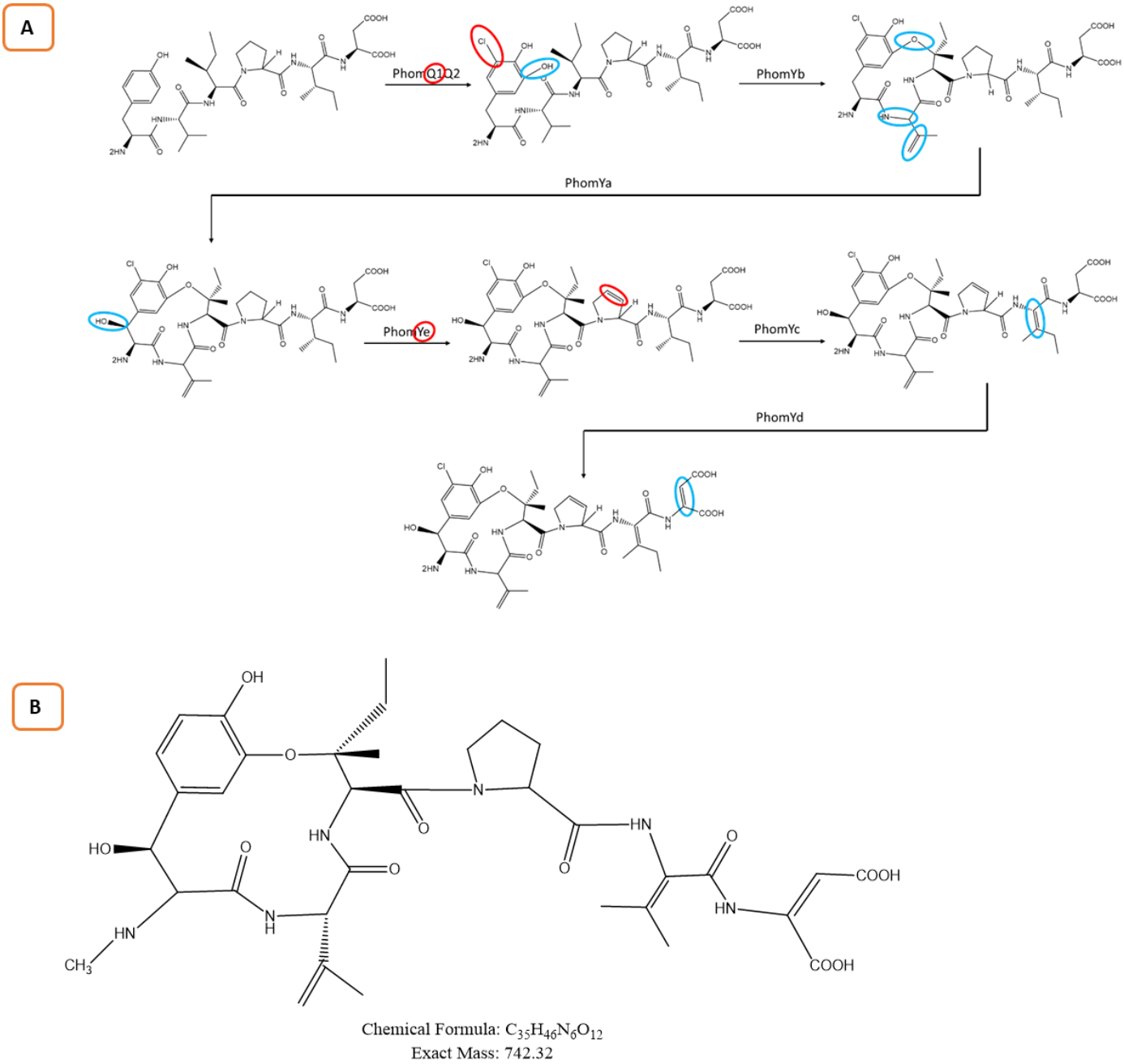

Figure 3.18 Phomopsin biosynthesis and chemical structure compared to the predicted *Z. tritici* RiPP structure.

A) Based on Sogahata et al. (2021), showing phomopsin biosynthesis and the modifications imposed by each of the phomopsin cluster genes to the chemical structure of the RiPP. Enzymes involved in phomopsin production that have no homolog in the Zttx cluster, as well as the modification they apply, are highlighted in red. Modifications in phomopsin production assumed to exist in *Z. tritici* RiPP production are highlighted blue. B) The predicted mature structure of the *Z. tritici* RiPP using the phomopsin RiPP as a model.

Predicted fragmentation patterns of the *Z. tritici* RiPP in mass spectrometry (MS) were also generated based on presumed similarity to phomopsin and the fragmentation pattern of this peptide (Figure 3.19; Table 3.3). Mass spectrometry data was analysed for these predicted masses.

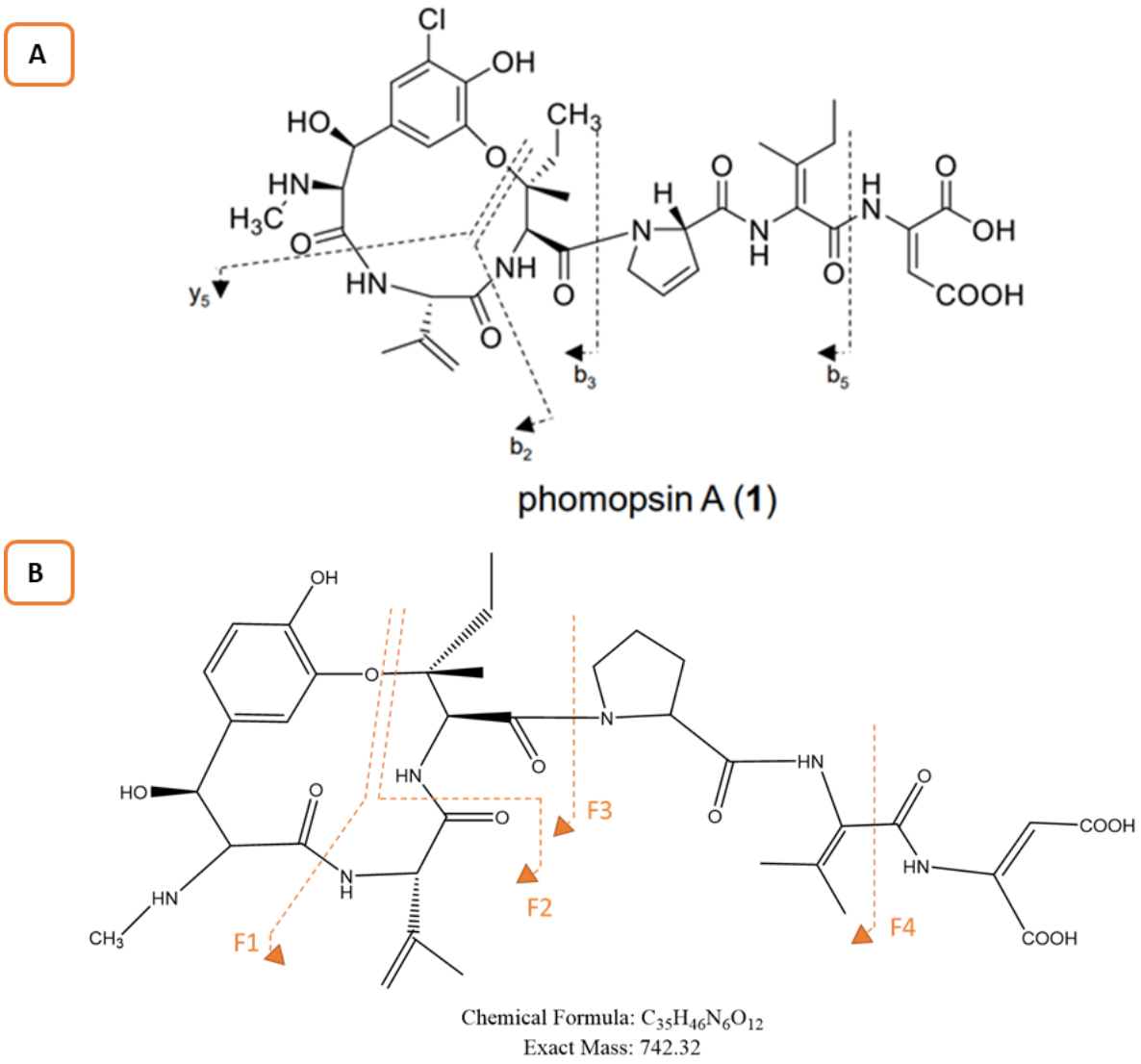

Figure 3.19. Fragmentation patterns of phomopsin and predictions for the *Z. tritici* RiPP.

584) From Sogahata et al. (2021) supplementary information. The fragmentation pattern of the phomopsin RiPP in MS analysis. B) The expected fragmentation of the *Zymoseptoria* RiPP in MS based on the phomopsin RiPP. Dashed lines indicate the points of peptide fragmentation. Arrows designate which part of the peptide is classed as a fragment. Fragments are labelled arbitrarily F1 through to F4.

Table 3.3 *Zymoseptoria tritici* RiPP fragment expected masses.

Following predictions based on the phomopsin gene cluster, masses of these fragments were generated. The fragment designations applied in Figure 3.19B are used here.

Fragment	Predicted fragment mass (m/z)
F1	533.25
F2	307.13
F3	418.20
F4	584.31

Several LCMS programmes were tested for the XAD-2 method including a 5% to 95% gradient of acetonitrile over 15 and 25 minutes, as well as an isocratic method using 30% acetonitrile for 20 minutes, all of which had been used for detection of phomopsin. However, LCMS chromatograms saw no difference in peptide profile between OxR T4 and ZttxA-Δ2 (Figure 3.20).

Therefore, several alternative means of peptide extraction were employed based on advice from experts in fungal metabolite extraction: Dr Song, Dr Prosser, and Dr Williams; as well as the available literature on dikaritin RiPP extraction. These included standard ethyl acetate extractions on both liquid and solid cultures for general metabolite purification. Extractions were also completed on both the supernatant from liquid cultures and the filtered mycelia. An acetone extraction was also conducted on the fungal mycelia alone. Plates were extracted from using the Hassani et al. (2021b) method – this was run on LCMS as in the Hassani et al. (2021b) methodology. Where possible LCMS conditions matched those noted in the papers from which the extraction technique originated, or a 5% to 95% acetonitrile gradient over 15 minutes was employed.

The final extraction method attempted was the Yoshimi et al. (2016) method used for ustiloxin B extraction. This was trialled based on the possibility that post-translational modifications of the *Z. tritici* RiPP may result in greater similarity to ustiloxin than phomopsin. Yoshimi et al. (2016) combined acetone and ethyl acetate extractions, using V8 medium for fungal growth. Both the aqueous and organic phase of the extractions were processed to be run on LCMS. This aspect of the work was hampered by repeated issues with the LCMS, with shifting baselines and intermittent faults with each of the detectors

meaning inconsistent and often incomplete data were obtained. As this was based in another lab it was beyond our control.

Chromatograms (Figure 3.20) show that the different extraction methods pull out different compounds from each other but there are no readily apparent differences between ZttxA-Δ2 and OxR T4 that would appear to be RiPPs. Notably, in Figure 3.20B, a peak in OxR T4 is seen at 8.15 minutes where this is absent in the deletion mutant. Whilst there is a difference here, further analysis showed the compound did not have the masses expected of the RiPP nor was it reproducible between replicate cultures. ELSD traces also indicated it was present in very low amounts which would have made further purification challenging. LCMS traces were analysed for each extraction, however, no peptide resembling the presumed fragmentation profile for the *Zymoseptoria tritici* RiPP was detectable in this work. The search for candidate RiPPs was also narrowed by analysing only products displaying UV absorbance profiles expected for compounds containing tyrosine residues (λmax=280nm).

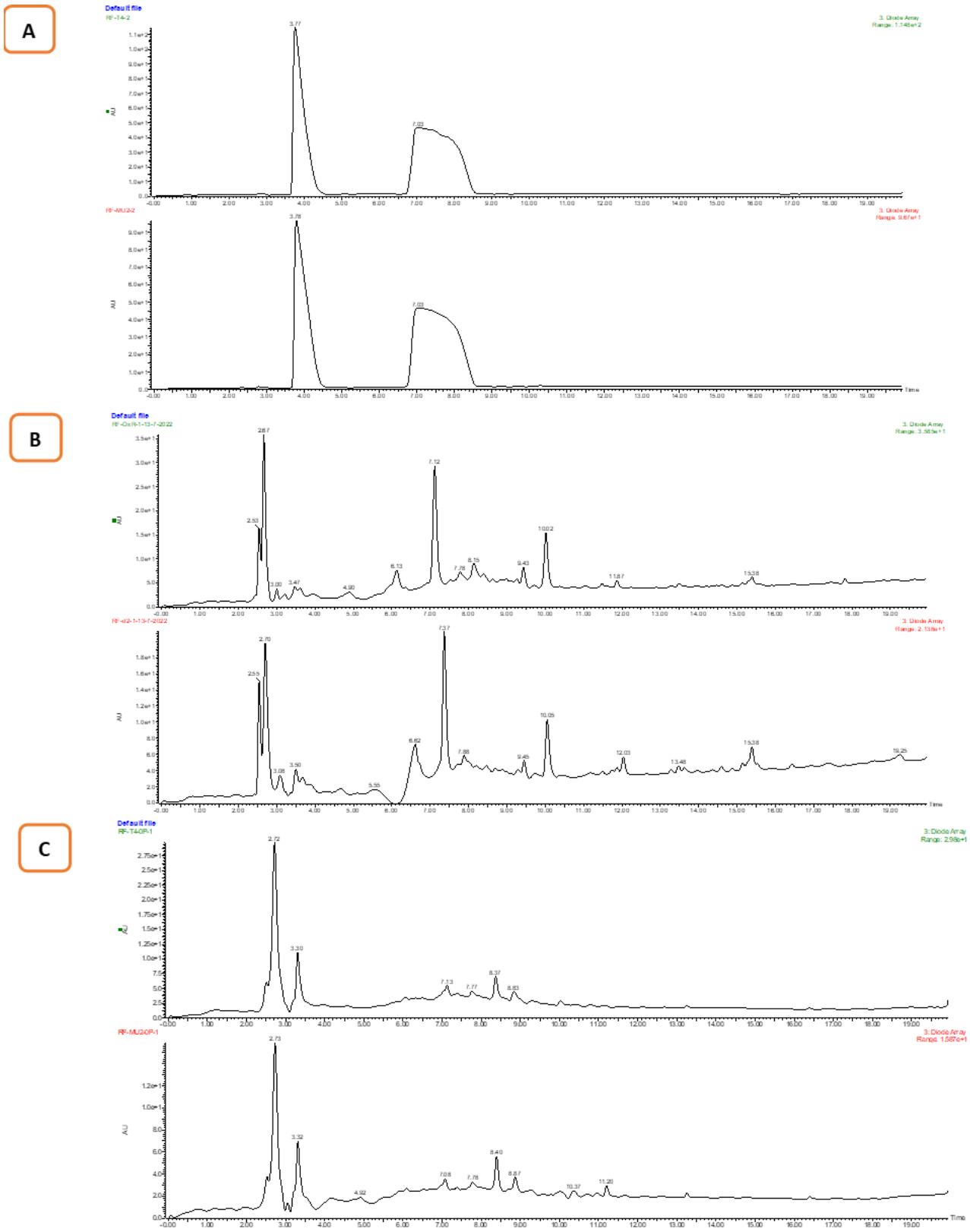

Figure 3.20 LCMS diode array chromatograms of *Zymoseptoria tritici* crude extracts.

LCMS chromatograms from several extraction methods are shown. In each instance the ZttxA-Δ2 strain chromatogram is on the bottom and the OxR T4 chromatogram on the top. A) XAD-2, B) Ethyl acetate C) Yoshimi et al. (2016) method.

3.3.8 Confirming translation of *ZttxA* gene transcripts

RT-qPCR data looking at the expression of the *ZttxA* gene alongside the associated genes within the *Zttx* cluster demonstrate that the genes presumed to be involved in RiPP biosynthesis are transcribed. However, RT-qPCR data is not informative regarding whether these transcripts are then translated in the next stage of the central dogma. Identification of the peptide by LCMS would act as confirmation of this, however, has proven difficult in this line of work and so an alternative approach was taken. Instead, a GFP fusion to the *ZttxA* gene was attempted. Initially this was trialled using the pC-G418-YR plasmid (Sidhu et al., 2015) containing the G418/geneticin resistance gene within the Ti plasmid border. This was selected as the GFP fusion was to be introduced to the OxR T4 *Z. tritici* strain (presumed to give greater GFP fluorescence than in wildtype due to regulation by the overexpressed *ZttxR*) which already contains the hygromycin resistance cassette. However, *Z. tritici* transformation attempts were unsuccessful and so efforts reverted to use of the pCAMBIA0380YA backbone alongside hygromycin resistance as selection to transform the wildtype fungal strain.

The GFP fusion plasmid was constructed in the same way as described for the overexpresser construct, using PCR to generate the fragments required for construction of the vector. These included the *ZttxA* promoter region and the gene open reading frame (ORF) amplified from wildtype IPO323 genomic DNA by the pCAM0380_ZttxAPro_F/ZttxA-R3 primer pair (including a pCAMBIA0380YA overlapping extension and removing the TAA (UAA) stop codon from the *ZttxA* gene); the *Z. tritici* codon-optimised GFP sequence (ZtGFP) amplified from pCZtGFP plasmid DNA (from Kilaru et al. (2015) using the ZttxA-ZtGFP-F/Hyg-ZtGFP-R primer pair and the hygromycin resistance cassette amplified from ZttxA-Δ2 genomic DNA using the Hyg-F/Hyg-PCAM-R primer pair (primers are outlined in Table 9.6). Together these fragments were used to generate the ZttxA-ZtGFP fusion construct (Figure 3.21). Alongside this, a control plasmid of just the *ZttxA* promoter region fused to GFP was also produced (ProZttxA-ZtGFP).

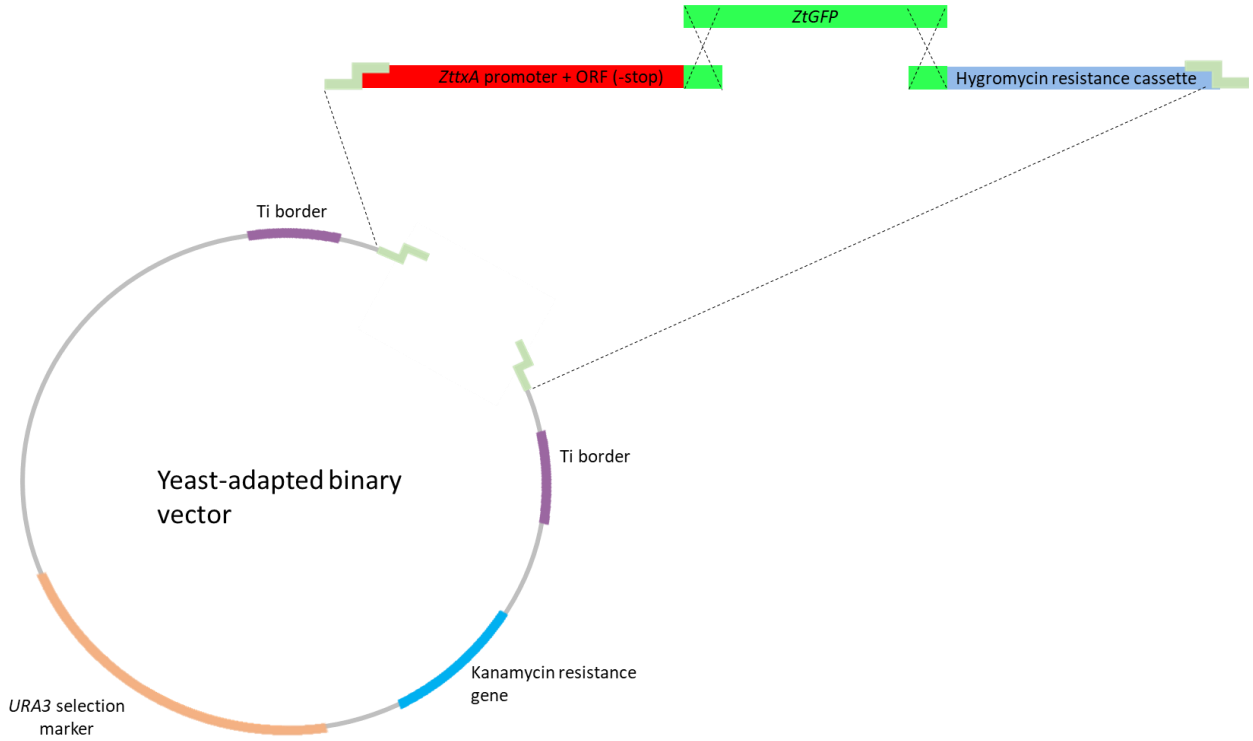

Figure 3.21 Schematic for production of the ZttxA-ZtGFP fusion construct.

Schematic for production of ZttxA-ZtGFP in pCAMBIA0380YA. ProZttxA-ZtGFP was produced in the same way but without the *ZttxA* open reading frame.

Putative *Z. tritici* transformants were grown on hygromycin selection, as done for other transformants produced in this work, and after successful growth following three successive subcultures, DNA was extracted (Liu et al., 2000). DNA was used in diagnostic PCR reactions using the primers outlined in Figure 3.22A (primer sequences are listed in Table 9.7). One successful ZttxA:ZtGFP fusion transformant was identified (Figure 3.22B); however no fluorescence was seen during fluorescence microscopy of the transformant under a range of growth conditions.

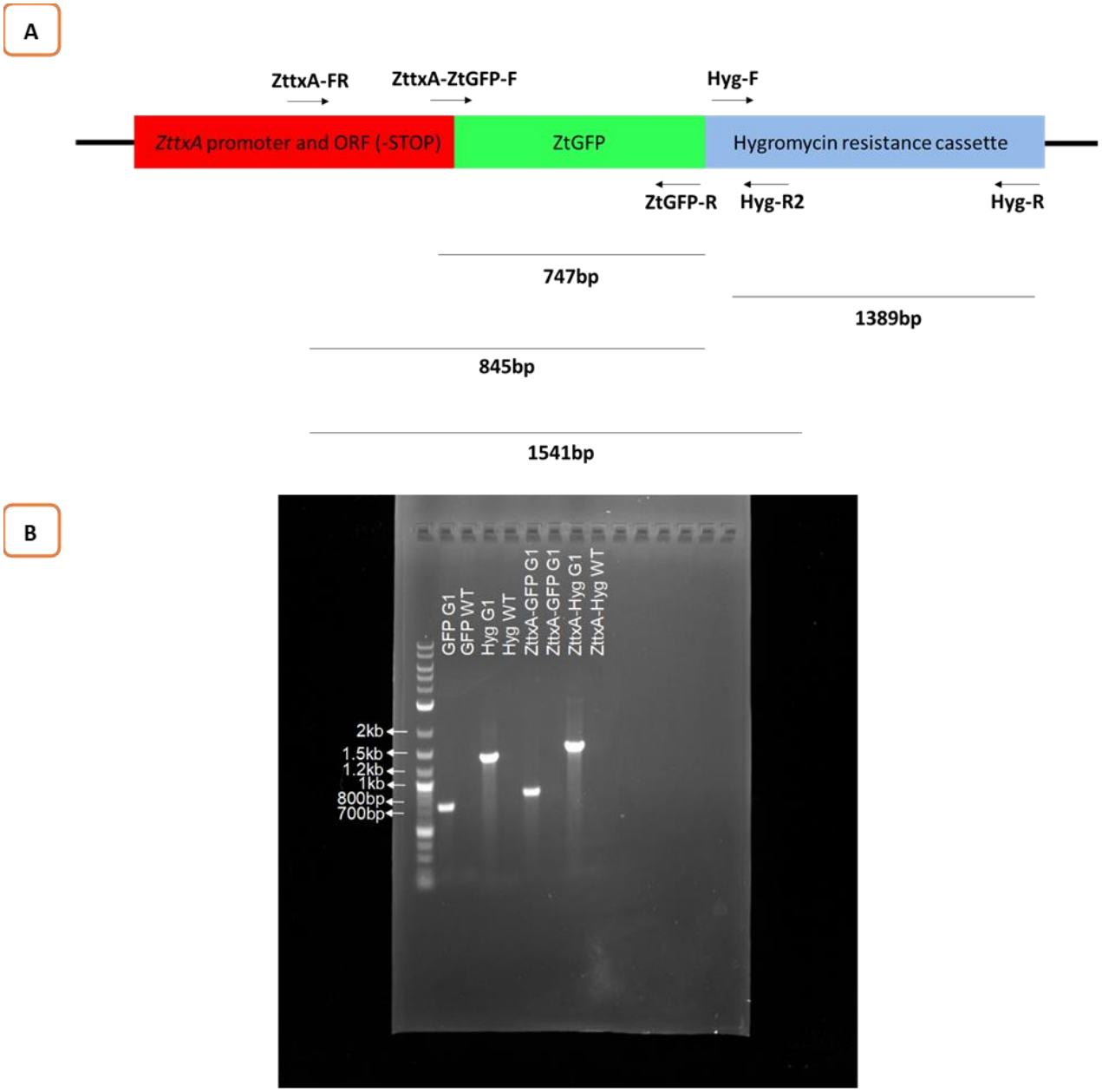

Figure 3.22 Diagnostic PCR of ZttxA:ZtGFP transformants.

A) Schematic showing the primer pairs used for ZttxA:ZtGFP transformant diagnostic PCR. Primer names are written in bold, and arrows demonstrate the orientation of the primers. Vertical lines are used to connect primer pairs with the expected amplicon size from these reactions indicated underneath. B) Putative transformant DNA was amplified with the described primers. Lane labels describe the fragment being amplified: ZttxA-ZtGFP-F/ ZtGFP-R (GFP), Hyg-F/Hyg-R (Hyg), ZttxA-FR/ZtGFP-R (ZttxA-GFP) and ZttxA-FR/Hyg-R2 (ZttxA-Hyg). Fragment descriptions are followed by the transformant name (G1) or strain name (WT; wildtype). Fragments amplify unique sequences that would be absent from the WT. Amplicons present for G1 but absent in the WT samples confirm transformation of the construct into *Z. tritici*.

3.4 Discussion

3.4.1 The Zttx RiPP-producing cluster and its dikaritin RiPP relatives.

The *Zymoseptoria tritici* RiPP cluster itself does not differ from other known RiPP cluster by the inclusion of novel genes. Indeed, all genes within the Zttx cluster have homology to those found within either the phomopsin or ustiloxin gene clusters. As such, the putative novel RiPP is not different to other known RiPPs by having increased complexity but rather in its simplicity. The greatest observable difference of the *Z. tritici* RiPP to other dikaritins is its varied core amino acid sequence of YVIPVD (Figure 3.2B). Following assignment of predicted functions to the products of the Zttx RiPP biosynthetic cluster genes, further predictions can be made in relation to what biosynthesis may look like for *Z. tritici* RiPP by comparison to known RiPP producing biosynthetic pathways.

Four enzymes containing DUF3328 have been identified in the Zttx cluster including the Y1/Yb enzyme involved in cyclisation via tyrosine residues. The exact role of each of these in RiPP production was not fully appreciated until work by Sogahata et al. (2021) elucidated the function of each in turn by gene ablation for phomopsin synthesis, showing that it is only the loss of *PhomYb* which results in complete loss of peptide intermediates, while for *PhomYa*, *PhomYc*, *PhomYd* and *PhomYe* intermediate peptide structures can be assessed in the same way as was hoped for this work. Sogahata et al. (2021) identified functions in hydroxylation of the tyrosine amino acid for *PhomYa*, and desaturation of amino acid moieties of isoleucine (5^{th} position rather than 3^{rd} position), aspartic acid and proline, for *PhomYc*, *PhomYd* and *PhomYe*, respectively. The Zttx cluster, contains a valine amino acid moiety at the 5^{th} position of the core amino acid sequence and therefore might not show the same modification imposed by the *PhomYc* gene (unless there was functional redundancy and a capability of the enzyme to desaturate different amino acid residues). Furthermore, no homolog to *PhomYe* is identifiable in the Zttx cluster, so desaturation of the proline amino acid to give a double bond would also be absent. These absent modification sites or gene homologs are some of the key differences between the Zttx cluster and the phomopsin cluster – not forgetting the phomopsin biosynthetic gene *PhomQ1,* responsible for chlorination of the aromatic ring (Sogahata et al., 2021) which is absent from the Zttx cluster.

The lack of clarity regarding the role of DUF3328 containing enzymes in RiPP production highlight the limitations of using assumed enzyme functions to piece together the

biosynthesis of a novel RiPP. It is only by production of gene cluster knockout strains and analysis of the intermediate products, as in Sogahata et al. (2021) that the real function of the enzymes in RiPP synthesis can be uncovered. Indeed, several of these required knockouts have been produced in this work already, the next stages of *Zttx* RiPP biosynthetic investigation rely on extraction of these peptides.

3.4.2 The *ZttxR* transcription factor within the Zttx gene cluster, is a transcriptional regulator for *ZttxA* and the wider Zttx cluster.

The only stage of *Z. tritici* RiPP biosynthesis that can currently be confirmed, shown in this work, is the very start of RiPP production with the *ZttxR* transcription factor regulating the transcription of the Zttx cluster genes. This work has extensively examined the impact of the *ZttxR* gene and specifically its upregulation on gene expression, ultimately determining that the gene encodes a transcription factor that modifies gene expression of all Zttx gene cluster genes, including the *ZttxA* precursor gene, generally by upregulation (Figure 3.14, Figure 3.15, Figure 3.16; Figure 3.17).

Similar results have been identified in work completed by Umemura et al. (2014) investigating the ustiloxin biosynthetic gene cluster of *Aspergillus flavus* whereby overexpression of the *ustR* gene, the homolog of the *ZttxR* gene, resulted in 4.8 times greater ustiloxin B production compared to the wildtype strain of the fungus. This increase in secondary metabolite production is also seen in other research, albeit not on RiPPs, when a C6 transcription factor is overexpressed (Bromann et al., 2012, Nakazawa et al., 2012). Hence, utilising this means of increasing peptide production of the *Z. tritici* RiPP was logical in this work.

Of interest, overexpression of *ZttxA* seemingly varied over time (Figure 3.16) despite upregulation of *ZttxR* being consistent. A constitutively expressed gene (HH3) was used to overexpress the transcription factor so the level of this modification of *ZttxA* gene expression should not vary. Yet, variation still exists because the overexpression construct inserts an additional copy of the transcription factor gene into the genome. As such, the natural variations in expression of *ZttxA* over time that are seen in the wildtype strain are also present in the *ZttxR* overexpresser strain.

Experimental investigation into the regulation of the C6 transcription factor, encoded by *phomR* within the phomopsin gene cluster, on *phomA* (the phomopsin precursor gene)

transcription or peptide production has not yet been conducted. However, given the known homology between the transcription factor genes in RiPP clusters for ustiloxin, phomopsin and the *Z. tritici* RiPP, it is likely that this role in up-regulating precursor gene transcription is shared across dikaritin RiPP-producing species. For the *Z. tritici* RiPP, the impact of upregulating the *ZttxR* gene is only understood from the perspective of transcription, how this transfers across to actual peptide production is not yet known. What the increase in *ZttxA* gene expression in this work translates to in terms of peptide titre is an area of interest upon development of a successful method for peptide extraction.

Since most of the transcriptional work assessing the *ZttxR* overexpresser revolved around quantifying the transcription of the *ZttxA* gene, this perhaps leads to questions regarding the selection of the *ZttxR* gene for overexpression rather than the *ZttxA* gene. *ZttxR* was selected for several reasons. First, only *ZttxR* overexpression could be used to assess the role of the gene product in regulating gene expression of the *Zttx* cluster – confirming the function of the protein as a transcription factor. The second, overexpression of *ZttxR* and the predicted accompanying increase in transcription and translation of all *Zttx* cluster genes would allow increased production of the necessary proteins required for mature RiPP synthesis – should the transcription factor regulate all the cluster genes in the same way as it does *ZttxA*.

Gene expression data showed the CLF and CRF transcript levels to have some of the smallest differences between wildtype and OxR T4 *Z. tritici* strains, with the changes seen being reductions in relative transcript levels in OxR T4 compared to the wildtype. This seems to indicate, given the upregulation of nearly all other Zttx cluster genes, that these genes are likely to fall outside of the Zttx biosynthetic gene cluster. Within the cluster, modification of gene expression of Zttx cluster genes by upregulation of *ZttxR* in the OxR T4 strain was not consistent and varied by gene as some genes saw much higher transcriptional upregulation than others. Hence, the control of transcription of Zttx cluster genes must be regulated for each gene by factors beyond the transcription factor alone. Beyond this, differences in regulation may be explained by the various predicted roles of the gene products, Zttx cluster genes all generate tailoring enzymes which may be differentially regulated based on their function. Furthermore, the primers used may not all amplify equally.

Intriguingly, some of the core RiPP producing genes of *ZttxQ* and *ZttxY1* (used by Ding et al. (2016) alongside *PhomM* to computationally identify further putative dikaritin RiPPs), show

some of the largest increases in transcript levels in the overexpresser strain compared to the wildtype. These genes, as well as *ZttxY3* and *ZttxY4*, all show increased transcript levels in the OxR T4 strain compared to the WT of over 250%. Without the *ZttQ* and *ZttxY1* genes, due to their involvement in forming the macrocylic structure of the RiPP – showcased from research into phomopsin (Sogahata et al., 2021) – no RiPP is produced. Hence, increased expression of these genes alongside the precursor peptide gene in an overexpresser is understandable. The relatively limited change in expression of other tailoring genes in the overexpresser compared to the wildtype, though interesting, does not explain why though the *ZttxA* gene is overexpressed, difficulties in peptide isolation still arise. Given that the tailoring enzymes produced by Zttx cluster genes are each used multiple times to modify the separate and repeated core peptides within the RiPP precursor peptide during production, it is unlikely that variances in upregulation of gene expression of these genes in the OxR T4 overexpresser would be a limiting factor in peptide production from this strain.

3.4.3 *Z. tritici* gene manipulation and phenotype

Within this work it is important to recognise that *ZttxR* overexpression, as well as Zttx cluster knockouts, do not appear to negatively impact the fungus, as this does not result in any phenotypic or growth changes, mirroring observations of the ustiloxin overexpresser in *A. flavus* by Umemura et al. (2014). It is therefore possible to grow these strains and use them in extractions. Should the peptide have been toxic to *Z. tritici*, phenotypic differences would be apparent. So too would phenotype vary if the peptide was essential to fungal survival and production was disrupted as in the knockouts. As this is not seen in this work, the peptide does not appear to be essential to the fungus and is therefore categorizable as a secondary metabolite. The relative usefulness of these overexpresser and knockout strains depends on whether the precursor peptide is ever translated from the transcripts seen within this work.

3.4.4 *Z. tritici* putative RiPP isolation

The *Z. tritici* RiPP is largely similar to phomopsin and as such, it was assumed that peptide extraction from *Z. tritici* using methods established for phomopsin would yield a quantity of the peptide suitable for LCMS. Protocols optimised for phomopsin isolation have thus far been unsuccessful in extracting the *Z. tritici* RiPP peptide from liquid or solid culture. This may be indicative of fundamental differences in the chemical properties between the two peptides as chlorination would significantly increase polarity of the molecule. Upon isolation

of the *Z. tritici* RiPP these potential differences may be investigated further and an explanation for the unsuccessful extractions determined.

Initial chemical comparisons of wildtype and *ZttxA* knockout chemical extracts, despite many attempts being made, had no readily apparent differences. It was only after extensive analyses of these that the overexpresser lines were produced. These have some hints of there being differences, but time constraints and issues with chemistry prevented this being fully analysed. Perhaps with the OxR lines and more sensitive equipment and/or larger scale extractions it might become feasible to find the compound in the future.

3.4.5 Translation of *ZttxA* mRNA transcripts

The *ZttxR* overexpresser produced in this work, does indeed deliver higher levels of *ZttxA* transcription, which naturally has the highest transcript levels at nine-days post inoculation in liquid culture as was noted *in planta* (Rudd et al., 2015), compared to the wildtype in the growth conditions used here. Though this difference is not statistically significant, any upregulation in gene expression should theoretically help to facilitate purification of the *Z. tritici* RiPP compound as in Umemura et al. (2014). However, absolute expression levels of the gene transcripts are still unknown. These absolute levels may still be low compared to other peptides if the expression of the gene is low in the wildtype. It is not enough to increase transcription of the *ZttxA* gene, peptide production is what needs to be increased to a detectable level.

Indeed, Yoshimi et al. (2016) noted, when attempting to produce ustiloxin B in *Aspergillus oryzae* (a fungus which contains the ustiloxin B biosynthetic gene cluster but does not ordinarily transcribe these genes), that in certain media types even though transcripts of the cluster genes were produced, ustiloxin B production still did not occur. However, we cannot distinguish between the peptide not being translated or it not being processed as either way there is no product to detect. Since Kex2 processing comes from the host, if it is not active in *Aspergillus oryzae* you would not get heterologous expression. However, this was also seen in *Aspergillus flavus* (Yoshimi – unpublished data)(Yoshimi et al., 2016), a known ustiloxin producer. Furthermore, Kex2 is a highly conserved enzyme which is likely to exist in the non-native host *Aspergillus oryzae*. Yoshimi et al. (2016) therefore stipulated that conditions for RiPP production may be dependent on either amino acid or vitamin availability. It is then

plausible, since extraction efforts of the *Z. tritici* RiPP have thus far proven unsuccessful, that perhaps *Z. tritici* has not been grown in the exact conditions required for the translation of *ZttxA* transcripts.

To determine whether transcripts of *ZttxA* are translated in this fungal system, a GFP fusion to the *ZttxA* gene was designed and inserted into the *Z. tritici* genome. Though ultimately peptide processing will cleave the GFP from the mature peptide, as the GFP fusion was to the C-terminal of the precursor peptide, it was assumed that the transient existence of the unprocessed peptide would allow detection of fluorescence. This would confirm translation of the precursor peptide – though not guaranteeing that this is then processed to a mature functional RiPP. Successful transformation of the construct into *Z. tritici* but absence of fluorescence, in all growth conditions examined, is however what was seen in this work. Plausibly, since we do not know absolute expression of the *ZttxA* gene, using this promoter for the fusion may result in fluorescence at a level too low to be detected – at least fluorescence is not discernible with the microscopy systems available for analysis in this work. Equally, though a range of growth conditions including liquid and solid media were employed, it is still possible that the correct growth conditions conducive to peptide translation remains elusive and under different growth regimes again, fluorescence may become apparent.

Even if the peptide is being produced there is the further complication that the precursor peptide is targeted to go through extensive processing. The ZttxA precursor has a leader sequence that will target it for secretion via processing in the golgi, and it may be that as part of this processing GFP is being targeted to the proteosome and degraded. Based on this we would not expect to see fluorescence in the cytoplasm, it would be in the golgi and vesicle systems at best, but not at all if GFP is rapidly degraded. As such, it would be of interest to examine whether a simple promoter:ZtGFP fusion, which would monitor promoter activity rather than cellular destination, fluoresces. Such a construct was made in this work, but time constraints prevented this from being completed.

Given the complexities of RiPP isolation from the native producer, it may then be beneficial to consider heterologous expression of these genes, removing the need for peptide isolation from *Z. tritici* entirely. This may use a fungal species with the biosynthetic machinery already in place for entire RiPP production such as *Aspergillus oryzae* (Yoshimi et al., 2016) or

multiple bacterial plasmids producing a single cluster gene enzyme that may be extracted and co-incubated with the immature RiPP, allowing modifications to occur outside of a living system (Ding et al., 2016). Heterologous expression has additional benefits of removing the possibility of compensatory effects of genes outside of the biosynthetic gene cluster as Tsukui et al. (2015) found that when RiPP cluster genes are deleted, proteins used in alternative peptide producing pathways with homology to those deleted can be co-opted into RiPP production. Umemura et al. (2014) noticed this in particular for the UstO movement protein and the S41 peptidase – with deletion of these genes having little to no impact on RiPP production due to this compensation. Heterologous expression has been used successfully by Ye et al. (2019) for analysis of asperipin-2a.

3.5 Summary

- The Zttx putative RiPP producing cluster within the *Z. tritici* genome shows remarkable similarity to those responsible for production of the phomopsin and ustiloxin dikaritin RiPPs.
- The *ZttxR* gene within the Zttx cluster encodes a transcription factor responsible for regulation all Zttx cluster genes. The extent of regulation varies depending on the gene but is greatest for core RiPP producing genes *ZttxA*, *ZttxY1* and *ZttxQ.*
- Nine Zttx cluster gene knockouts of IPO323 *Z. tritici* have been produced and confirmed in this work.
- Extraction attempts to purify the putative RiPP from fungal culture to date have been unsuccessful.
- A ZttxA:ZtGFP fusion construct transformed into *Z. tritici* did not produce any detectable fluorescence.

4 : On the functional role of the *Z. tritici* RiPP

This chapter discusses the role of RiPPs in general, those of fungal origin, then presents experiments looking at the RiPP from *Z. tritici.* Most of this was researched during the 2020 COVID-19 lockdown and aspects have been published in a review "Exploring fungal RiPPs from the perspective of chemical ecology" (Ford et al., 2022).

4.1 Introduction

RiPP peptides are produced by several kingdoms of life, from bacteria, animals, and, of course, fungi. Given the cost of peptide production, (energy and amino acid depletion) synthesising these peptides if they present no benefit to the producing organism would be wasteful. As such these peptides are assumed to fulfil functions that allow the producer to survive and thrive in its environment. Understanding RiPP function was particularly important when RiPP families were grouped based on shared bioactivities (Luo and Dong, 2019). Now, RiPP families are assigned based on similarity in peptide structure and biosynthesis (Arnison et al., 2013).

The activities of RiPPs can be assessed from two perspectives: the first is the natural role of the peptide (its use to the producing organism and the reason for its continued production), the second is its anthropogenic employment. It is not necessary to understand the human uses of RiPPs to group these peptides, however, it can be helpful to explore this to understand why some families have been researched in greater depth than others. For instance, RiPP families containing members with medically valuable applications have been investigated in far more detail. This is largely a result of early detection of many of these peptides having been identified as natural products during screening programmes for drug discovery – even if they were often classified as products of NRPSs rather than RiPPs. Not all RiPPs have been investigated from both perspectives, often favouring human applications, as such many ecological RiPP functions are unconfirmed but can be inferred.

4.1.1 Plant RiPPs

Biased interest in select RiPP producers is particularly the case for plant and bacterial RiPPs. Luo and Dong (2019), highlight that due to the range of activities plant RiPPs hold, they have attracted attention based on the proposed applications of these RiPPs. Plant RiPPs, known as cyclotides (Luo and Dong, 2019), are characterised as cyclic peptides with a cyclic cystine

knot (CCK) motif (Craik et al., 1999). Cyclotides were initially isolated from the Rubiaceae and Violaceae plant families (Craik et al., 1999) but have since been found in the Cucurbitaceae and Fabaceae (Arnison et al., 2013). Their natural role is assumed to be related to plant defence (Arnison et al., 2013).

This action in plant defence extends from insects to molluscs and nematodes. Cyclotide kalata B1 impacts the growth and development of *Helicoverpa punctigera* (Jennings et al., 2001) and *H. armigera* (Jennings et al., 2005) larvae as the peptide causes larval gut epithelial cells to rupture (Barbeta et al., 2008). Similarly, the kalata B1 and B2 peptides, as well as cycloviolacin O1, have shown good molluscidal activity against green apple snails (*Pomacea canaliculate*)(Plan et al., 2008). Cycloviolacin variants also effectively inhibit nematode development (of larvae) and motility (of adults) in the species *Haemonchus contortus* and *Trichostrongylus colubriformis* (Colgrave et al., 2008). Overall, plant RiPPs appear to have evolved for plant defence, further supported by the knowledge that even at concentrations of cyclotides naturally produced *in planta*, plant defence activity is still noted (Barbeta et al., 2008). The limits of cyclotide defensive activity have been assessed by testing these RiPPs against marine organisms, which would not ordinarily encounter the terrestrial RiPP producer. Even here, cycloviolacin O2 inhibits fouling barnacle (*Balanus improvisus*) settlement (Göransson et al., 2004). Together, these experiments demonstrate the ability of plant RiPPs to protect the producer from a range of threats. Since the same RiPPs have efficacy against multiple species, this activity is non-specific and can likely be applied to the natural potential pests of these plant RiPP-producers.

Cyclotides showing effective antimicrobial activity have also been identified. In fact, the antimicrobial activity of cyclotides was identified prior to the insecticidal or molluscicidal activity with Tam et al. (1999) identifying the action of kalata and CirA against gram positive bacteria, and CirB against both gram positive and gram negative bacteria. Pranting et al. (2010) extended the range of known cyclotides effective against gram negative bacteria following assessment of the antimicrobial activity of cycloviolacin O2. Some of the antibacterial cylotides are the same as those effective against eukaryotic pests highlighting the value of producing a broadscale effective defensive compound where multiple pest pressures exist. The activities of cyclotides are of interest commercially in farming and medicine – with potential uses for treating HIV (reviewed by Gustafson et al., 2004) as well

as cancers (Lindholm et al., 2002) due to their cytotoxic activity (Svangård et al., 2004). Recent advances in genome mining (Chigumba et al., 2022) guide the way towards identification of further plant RiPPs.

4.1.2 Bacterial RiPP functions

Similarly, to plant RiPPs, bacterial RiPPs have been explored in a relatively high degree of detail as these also hold promise in the agricultural and pharmaceutical sectors. Several classes of bacterial RiPPs exist including: lanthipeptides, proteusins, and cyanobactins – these and more are summarised well in a review by Arnison et al. (2013), though, new bacterial RiPP classes have emerged since this review, such as the daptides (Ren et al., 2023).

The function of many known bacterial RiPPs is antimicrobial in nature, to the extent that the lanthipeptides were previously referred to as lantibiotics (Arnison et al., 2013) before the realisation that RiPPs with other activities existed. Goto et al. (2010) first proposed the all-encompassing term lantipeptides and Arnison et al. (2013) edited this to the lanthipeptides name used now. Lantibiotics now represents a sub-group within the lanthipeptides, specific to lanthionine-containing peptides with antimicrobial activity. The most notable example of a lantibiotic is nisin, which is effective against a range of gram positive bacteria with commercial employment in food preservation (Cotter et al., 2005) and has been used for this purpose for several decades.

Bacterial RiPPs with antibiotic activity have been reviewed by Hudson and Mitchell (2018). These RiPPs likely exist in nature as a form of defence against microbial competitors (allowing bacteria to exclude competitors from a resource) or as a method of gaining resources from other microbes (González-Pastor et al., 2003). This can be translated by humans into medicinal importance. Research into bacterial RiPPs from this perspective is understandable when we consider the concerning human pathogens these RiPPs are effective against, including: methicillin-resistant *Staphylococcus aureus* (MRSA; Jabes et al., 2011), *Human Immunodeficiency Virus* (HIV; Ferir et al., 2013) and *Bacillus anthracis* (Molohon et al., 2016). Not only this, but, bacterial RiPPs also have the capability to target filamentous fungi and yeasts (Mohr et al., 2015), a further potential target of medicinal antimicrobials.

Even outside of antimicrobial activity, bacterial RiPPs have medical applications against illnesses without a pathogenic origin as the lanthipeptide, duramycin, provides effective treatment against cystic fibrosis in clinical trials by means of chloride ion channel activation (Zeitlin et al., 2004). Importantly, we must remember that as with all RiPPs these peptides have arisen to serve a purpose to its producer, rather than aid medicine. RiPPs can play key roles in the lifecycles of their producers, rather than being solely secondary metabolites which, though useful in competition and survival, are not essential for completing essential life processes. This is exemplified by the lanthipeptide SapB, which acts a biosurfactant aiding the growth of aerial hyphae, produced by the bacteria *Streptomyces coelicolor*, which is essential for spore production and dispersal (Willey et al., 2006).

4.1.3 Animal RiPP functions

Unlike the array of bacterial species capable of producing bacterial RiPPs, to date, the only RiPPs known to be produced by animals are those from marine snails. Promising RiPPs from other species upon closer analysis are often instead the product of bacteria which form symbiotic relationships with the animals from which the RiPPs were isolated (Arnison et al., 2013). However, marine snails themselves are capable of producing a large array of peptides, specifically in their venom, with snails belonging to the *Conus* genus together capable of producing a range of ~50-100,000 peptides (Buczek et al., 2005). This complex mixture of peptides within the venom includes what can be identified as RiPPs, assigning these the name conotoxins (Buczek et al., 2005). Conotoxins target aspects of the neuromuscular system including receptors (acetylcholine) and ion channels (calcium, sodium)(Olivera et al., 1990). These peptides can be employed in defence but also play a vital role in predation as injection of the toxin paralyses prey and can even cause mortality (Craig, 2000). Given that the same neuromuscular receptors and ion channels found in marine snail prey are also found in humans, the application of these RiPPs to the pharmaceutical sector has not been missed. Akondi et al. (2014) note the potential for drug development from these peptides. Indeed, some have already found success with ziconotide, a synthetic form of the conotoxin ω-MVIIA, proving effective in providing pain relief in clinical trials (Miljanich, 2004), and approved for use in the USA in 2004 (Luo and Dong, 2019).

4.1.4 Fungal RiPP functions

Fungal RiPPs were first recognised in 2007 (Hallen et al., 2007) and of those known to date, most display some level of cytotoxicity, though often the exact organisms against which the RiPP is toxic varies depending on the molecule, as does the specificity of the RiPP. Current knowledge indicates that three fungal RiPP families exist, these are the Amatoxins/Phallotoxins, the Borosins and the Dikaritins. Some families, as with the different kingdoms of life capable of producing RiPPs, have been explored in more detail than others. The ecological roles of fungal RiPPs in many cases are unknown as how peptides can be employed in medicine and agriculture is often explored before we consider the ecological importance of the peptide to its native producer. I reviewed this in detail in Ford et al. (2022) and ecological functions of many known fungal RiPPs are proposed. Broadly the ecological functions of fungal RiPPs can be divided into three main categories: defence and competition, parasitism, and symbiosis.

4.1.5 Confirmed fungal RiPP functions

4.1.5.1 Defence and competition

As a by-product of the sessile lifestyle of fungi, these organisms are incapable of escaping predation by simply moving out of the path of a consumer. Growth allows movement to an extent but is not immediate and therefore is not an appropriate response to a sudden threat. Mushroom-forming fungi in particular are prone to mycophagy due to their high visibility and also their value as a source of nutrients to foragers (Hutchison et al., 1996). As such, fungi often produce defensive compounds – chemicals that when ingested prove distasteful or are toxic and capable of causing serious illness or even death. Either effect results in an outcome whereby the consumer no longer eats the fungus due to associative learning or incapacitation.

A role of fungal RiPPs in defence is most obvious when we consider the amatoxins. Fungi producing these RiPPs are often mushroom-forming (Figure 4.1A), localising the compounds to the cap and gills of the fungal fruiting body (McKnight et al., 2010, Kaya et al., 2015, Enjalbert et al., 1993). The fungus retains the RiPP within its own body, within cell vacuoles (Luo et al., 2010), so that it does not lose the protective effect of the peptide to the environment, but also localises the peptide to the tissue most likely to be targeted by foragers. Toxicity following consumption has been confirmed in several experimental works and case studies (Yilmaz et al., 2015, Enjalbert et al., 2002, Fantozzi et al., 1986, Kaneko et

al., 2001, Wieland, 1968) and largely impacts the gastrointestinal system (Wieland, 1983), indicating a function in defence of the fungal structure from foragers. Similarly, gastrointestinal symptoms are seen following consumption of the *Gymnopus fusipes* fruiting body, a species of fungus that produces borosin RiPPs called gymnopeptides (Vanyolos et al., 2016).Therefore, this function spans multiple RiPP families.

Figure 4.1 The morphologies of RiPP-producing fungi.

From (Ford et al., 2022) showing the different morphologies of fungi capable of producing RiPPs. A) *Amanita phalloides*, B) *Phomopsis leptostromiformis* growing on lupin leaves, C) *Omphalotus olearius,* D) *Ustilaginoidea virens* on rice.

Not all fungal RiPP producers however are mushroom-forming, yet consumption of the RiPPs from these species still results in similar symptoms to those mentioned above. This is the case for phomopsin produced by *Phomopsis leptostromiformis* (Battilani et al., 2011) and

ustiloxin, produced by *Ustilaginoidea virens* (Koiso et al., 1992). These dikaritin RiPPs have a shared function in animal toxicity (Koiso et al., 1992, Peterson et al., 1987) by microtubule assembly inhibition (Koiso et al., 1994, Koiso et al., 1992, Iwasaki, 1992, Battilani et al., 2011). The defence function is still applicable here but is more subtle and can be combined with a role in competition – protecting the fungus and its food resource from predation. This most commonly applies to RiPP producers that are plant pathogenic fungi and are therefore not necessarily visible to foragers aside from as symptoms on the host plant (Figure 4.1B, 4.1D). Consumption of the fungus in these instances is unintentional, however gastrointestinal disruption in the consumer ensures the host plant will not be predated (conferring a competitive advantage to the fungus by resource domination) nor will the fungus itself be consumed (defence). Interestingly, unintentional mycophagy as an evolutionary incentive to develop RiPP peptides can apply to mushroom-forming fungal species too when fungal hyphae are consumed more often than the fruiting body. Specifically, the omphalotin borosin producer *Omphalotus olearius* (Figure 4.1C) concentrates its RiPP to its hyphae (Quijano et al., 2019), where it is most likely to interact with *Meloidogyne incognita* a plant parasitic nematode (Mayer et al., 1997, Bal et al., 2016). In accordance with the defence hypothesis, omphalotin is potently nematocidal (Quijano et al., 2019).

4.1.5.2 Parasitism

Toxicity to foragers is useful to RiPP producers for defence, however, fungi too need to consume material in order to attain energy for growth and reproduction. This has resulted in speculation that fungal RiPPs may play a role in pathogenicity, facilitating nutrient acquisition by this means. However, it was only upon the classification of victorin from *Cochliobolus victoriae* as a RiPP (Kessler et al., 2020) that this function for a fungal RiPP was confirmed. *C. victoriae* is a necrotrophic oat pathogen (Wolpert and Lorang, 2016) while victorin stimulates leaf senescence (Navarre and Wolpert, 1999), working to convert inaccessible living material into the necrotic tissue required by the pathogen.

4.1.6 Speculative fungal RiPP functions

4.1.6.1 Symbiosis

In opposition to parasitism, though not confirmed, some fungal RiPPs may aid in the formation of symbiotic associations. In particular this role has been proposed for the epichloëcyclin RiPPs based on expression data of the *GigA* gene (encoding the epichloëcyclin

RiPP precursor) when the fungus is associated with a plant (A. Koulman, G. Lane, unpublished data; 67, 75)(Johnson et al., 2015). However, this role remains to be confirmed and this possibility is limited by experimental evidence that *GigA* gene deletion does not impact the phenotype of the host plant (Johnson et al., 2015). Alternatively, given that *Epichloë* symbiosis can confer toxicity to mammals, and protection from insects and pathogens by way of alkaloid production (Caradus and Johnson, 2020, Bush et al., 1997), epichloëcyclins may also function in this role of host defence. Indeed, host-protection as the main bioactivity of these RiPPs has already been suggested by Berry et al. (2022). Ultimately the epichloëcyclins are still functionally unclassified, therefore, whether symbiosis exists as a RiPP function at all, or whether the function is in fact again defence, remains unknown. Analysing such a role *in planta* may prove challenging due to the range of toxins produced by *Epichloë* fungi.

4.1.7 Exploring novel fungal dikaritin RiPP functions

Since fungal RiPPs have been identified far more recently than RiPPs from other kingdoms of life, exploring the functions of novel fungal RiPPs presents an exciting opportunity to uncover new functions – some of which may be of use for further antibiotic development, or pharmaceutical and agricultural applications. Exploring dikaritin RiPPs in particular is an area of interest since known RiPP producers of this peptide class form impactful relationships with plant species, most often this is parasitic (the fungus being a plant pathogen) however so too do we see potential mutualistic interactions (epichloëcyclins). The functions of RiPP peptides are intimately linked with these relationships, whether this is directly in parasitism (victorin), the protection of the resource that has been parasitised (phomopsin and ustiloxin), or potentially in protection of a beneficial host (epichloëcyclins).

Specifically in relation to the *Zymoseptoria tritici* putative RiPP, as *Z. tritici* is also a plant pathogen, the role of its RiPP in this parasitic relationship is to be examined in this chapter from both perspectives of defence and nutrient attainment. A role in plant pathogenicity is of particular interest as data from Rudd et al. (2015), showed the RiPP precursor gene to have highest expression *in planta* nine days post inoculation. This timepoint coincides with the pathogen's switch to necrotrophic growth within the wheat plant. Furthermore, no fungal RiPPs to date have demonstrated antimicrobial activity, however since the ability for RiPPs across Kingdoms to fulfil this function exists, this indicates that a fungal species

producing an antimicrobial RiPP is likely to exist and as such, this was also explored for the *Z. tritici* RiPP.

4.2 Aims

- To confirm the ZttxA-Δ2 *Z. tritici* strain as an appropriate RiPP gene deletion strain for assessment of RiPP function.
- To assess the role of the putative *Z. tritici* RiPP in pathogenicity of the pathogen against wheat cultivars.
- To determine the involvement of the putative *Z. tritici* RiPP in deterring insect feeding on infected wheat leaves.
- To reveal whether the putative *Z. tritici* RiPP is the first antimicrobial fungal RiPP peptide.

4.3 Results

4.3.1 Confirmation of *ZttxA* gene knockout

In previous work conducted by Child and Bailey (unpublished), gene knockout of the *ZttxA* gene (precursor gene) was conducted in the IPO323 strain of *Z. tritici*. Knockout of this gene was completed in the same way as outlined in Chapter 3, with the hygromycin resistance cassette (*HygR*) replacing the gene of interest, yielding three likely knockout strains: ZttxA-Δ1, ZttxA-Δ2 and ZttxA-Δ3. These however needed disruption validating and so the three strains were recovered from storage and all assessed to determine if these were knockouts by diagnostic PCR as follows. DNA was extracted from the three strains, along with wildtype IPO323, using the Zymo Research YeaStar Genomic DNA kit. This DNA was then used as the template in diagnostic PCR. First the primer pair ITS1-F/ITS2 was used to confirm extracted DNA was amplifiable, thus serving as a positive control for the PCR. These primers yield a fragment of 259bp in the IPO323 strain of *Z. tritici* (Figure 4.2A) and as such a band of this size is present for all strains tested – this is unaffected by transformation of the genomic DNA as it amplifies the ribosomal ITS region. A water control was also employed for this reaction as a negative control.

Reactions using the ZttxA-F1/ZttxA-R, LF-5'F/ Hyg-R2 and Hyg-F2/3'-R primers were also employed (Figure 4.2B, 4.2C; sequences are listed in Table 9.8). ZttxA-F1/ZttxA-R primers amplify within the *ZttxA* gene and therefore will only amplify in samples containing this gene. Accordingly, a fragment of this size is visualised in the wildtype (WT) genomic DNA template sample (Figure 4.3). This amplicon was absent from all knockout samples confirming the knockout strains to be deficient in this gene. Since the *ZttxA* gene was replaced with the hygromycin resistance cassette, amplification with the LF-5'-F/ Hyg-R2 and Hyg-F2/3'-R primer sets confirm not only presence of the hygromycin resistance cassette, but also the correct insertion of this fragment within the genome in place of *ZttxA*. These primer pairs amplify from before/after the *ZttxA* gene flanking genomic regions used for transformation, into the hygromycin resistance cassette fragment. As expected, a fragment corresponding to this predicted size is absent from the IPO323 strain but is present in all transformed strains confirming replacement of *ZttxA* with the hygromycin resistance cassette in each instance (Figure 4.3). This confirms the three strains to be knockouts of the *ZttxA* gene and therefore suitable for use in assessing the function of the *Z. tritici* RiPP by comparative analysis.

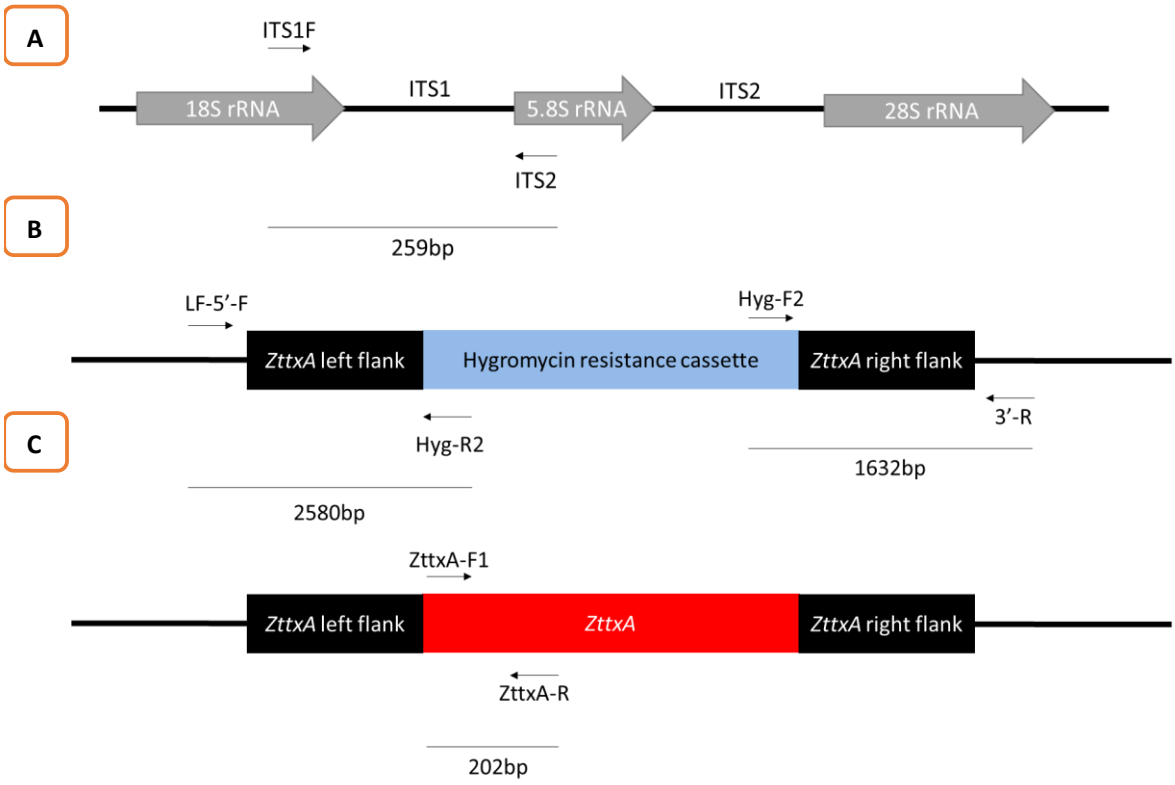

Figure 4.2 Schematic of primer binding sites for ZttxA-Δ2 diagnostic PCR.

A) ITS primer binding sites flanking the internal transcribed spacer 1 region (ITS1) yielding a 259bp fragment. B) Primer binding sites for amplification from outside of the primer designated left and right flanks used for transformation (coloured black) into the hygromycin resistance cassette (expected amplicons are 2580bp for left flank; 1632bp for right flank) to detect *ZttxA* gene knockouts. C) Sites for detection of the *ZttxA* gene within the wildtype IPO323 strain of *Z. tritici* (202bp).

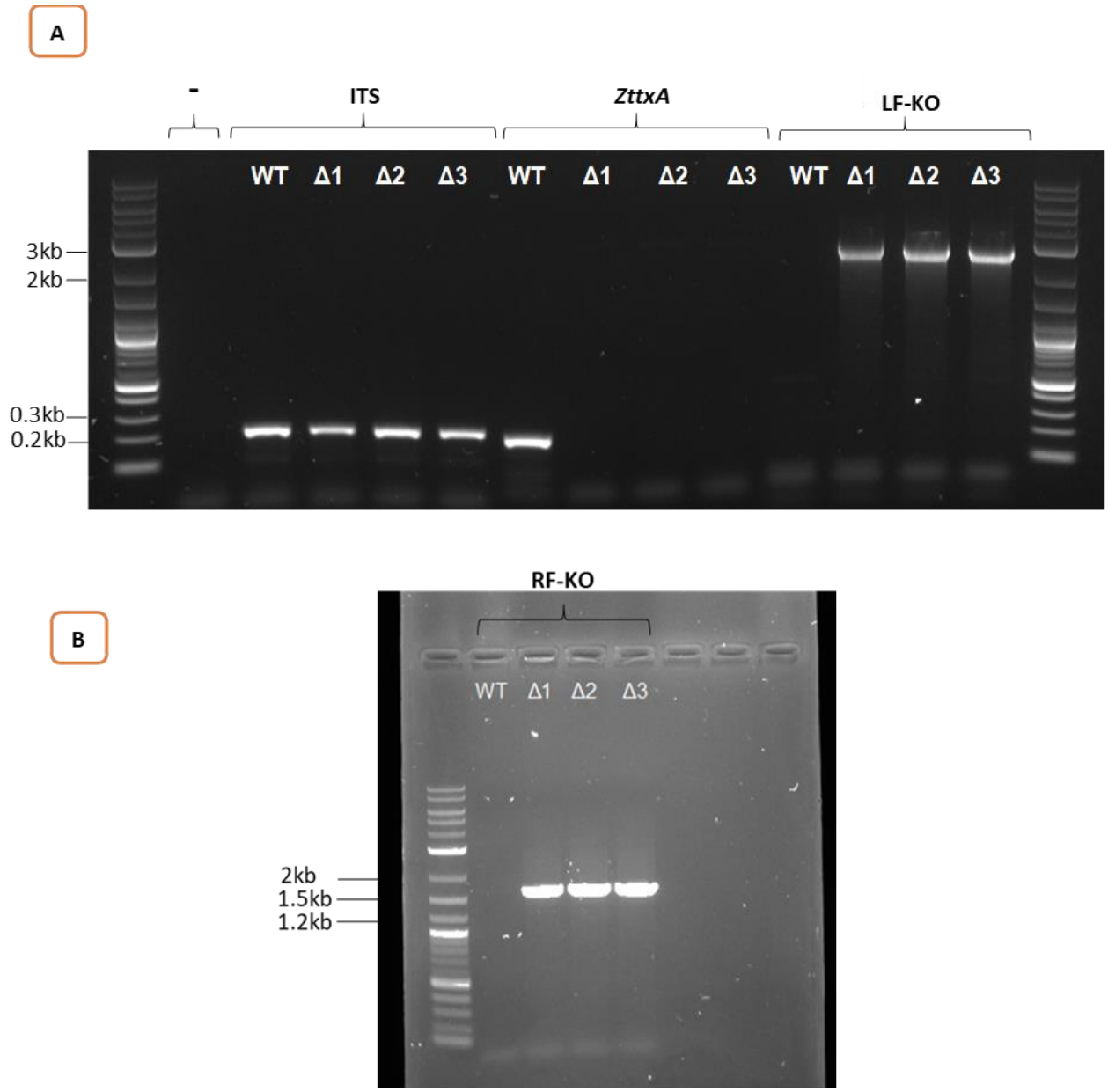

Figure 4.3 Diagnostic PCR confirming *ZttxA* deletion of transformed strains.

PCR using ITS primers ITS1-F/ITS2 confirmed DNA was of amplifiable quality, a negative water control was used for this primer pair. All DNA samples were also amplified with the **A)** ZttxA-F1/ZttxA-R (*ZttxA*), LF-5'F/ Hyg-R2 (LF-KO) and **B)** Hyg-F2/3'R (RF-KO) primer pairs, yielding products of an expected size of 202bp, 2580bp, and 1632bp respectively. The amplification of DNA from primers specific to the *ZttxA* gene in the wildtype and absence in the transformants confirm this gene to be absent from all knockout strains; amplification across the left flank or right flank region into hygromycin and absence in the wildtype IPO323 strain indicate the *ZttxA* gene to be replaced successfully with the hygromycin resistance cassette. Sizes of PCR products are compared to a NEB 1kb 2-log ladder with key sizes labelled.

4.3.2 Impact of *ZttxA* deletion on disease progression

To determine the significance of the *ZttxA* gene (and by extension the *Z. tritici* RiPP) to Septoria tritici blotch disease progression, three-week-old Riband wheat plants were inoculated with wildtype IPO323 and the three *ZttxA* knockout strains. Inoculations were carried out by painting individual wheat leaves using a cotton bud dipped in spore suspension adjusted to $4x10^6$ spores/ml in 0.5% tween 80 – following the method refined by Tiley (2016). After inoculation, Septoria tritici blotch symptom development was monitored at regular intervals from nine days onwards. Tween controls were employed to confirm symptoms presented were the result of *Z. tritici* infection rather than extraneous abiotic factors within the growing environment. Symptoms were manually assessed according to the predefined scale (Figure 2.2). The experiment was terminated when all leaves (except the tween control leaves) had reached the highest level on the disease assessment scoring system (4).

Symptoms of disease began to appear on wheat leaves 9 to 11 days post inoculation (dpi) and progressed until 44 dpi at which point all infected leaves had completely senesced (Figure 4.4). At each timepoint strains showed small variations in their mean disease symptom score but not to any large extent. Analysis of disease symptom data overall, showed the *Z. tritici* RiPP to have no obvious impact on disease progression of *Z. tritici* in Riband wheat. Lack of influence of *ZttxA* loss on Riband infection was noticeable from Figure 4.4 and as such no statistical analyses were conducted on these data.

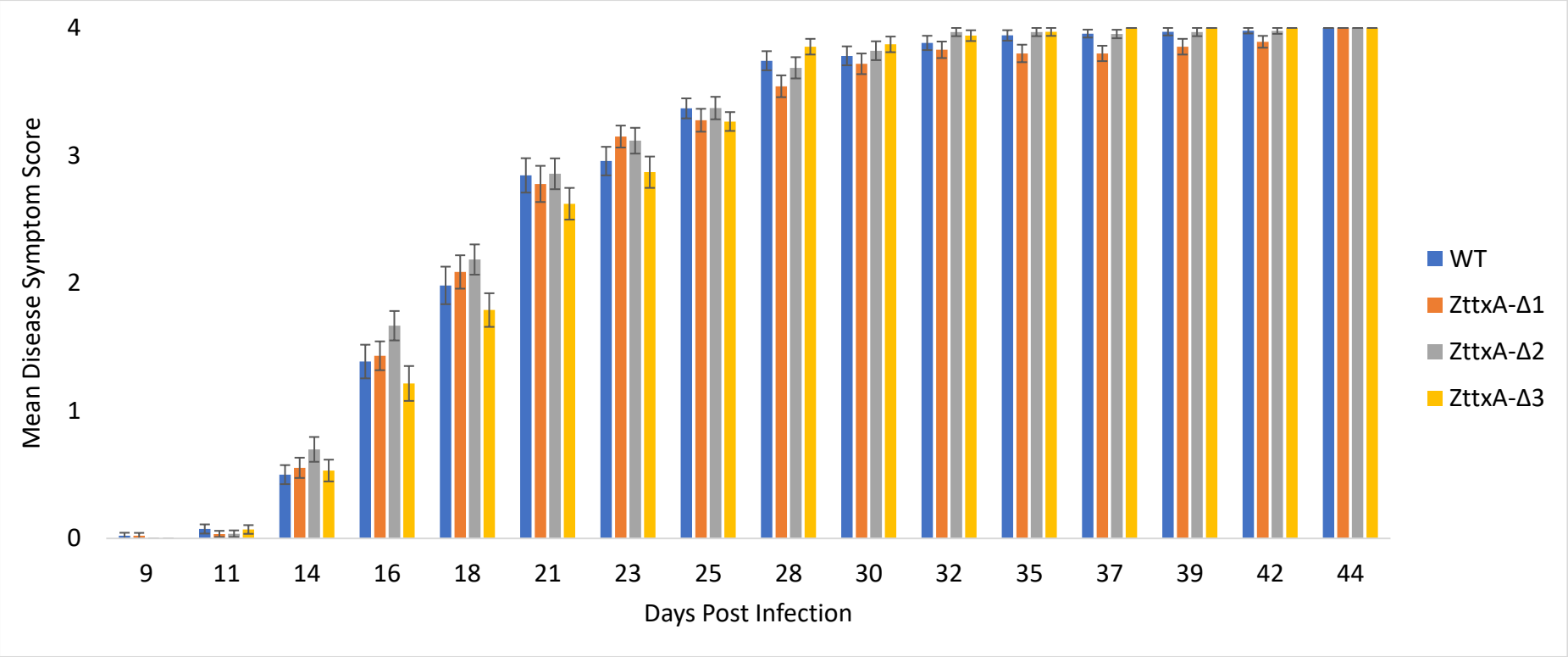

Figure 4.4 Time-course of *Z. tritici* infection symptom development for wildtype IPO323 and *ZttxA* knockout strains, showing loss of *ZttxA* has no impact on disease development.

Z. tritici strains wildtype IPO323 (WT), ZttxA-Δ1 (Δ1), ZttxA-Δ2 (Δ2), and ZttxA-Δ3 (Δ3) were inoculated onto three-week-old Riband wheat leaves. Disease progression was assessed over a 44-day time-course by assigning leaves a disease symptom score from 0 (no symptoms) to 4 (complete leaf senescence). The mean disease symptom score for each *Z. tritici* strain at each given timepoint was determined and plotted. Data are mean ± standard error of the mean (S.E.M), N=9-12

4.3.3 Quantifying *Z. tritici* infection

The time-course experiment used a visual scoring of symptoms to determine disease progression over 44 days. This experiment could not give detailed, accurate metrics of *Z. tritici* infection such as how many pycnidia were produced during infection. Further assessments of the impact of the *Z. tritici* RiPP on pathogenicity were then made using an automated system within ImageJ (Stewart and McDonald, 2014, Stewart et al., 2016, Karisto et al., 2018). Inoculation of Riband wheat leaves with wildtype *Z. tritici* and the ZttxA-Δ2 strain was repeated and extended to include overexpresser strains produced in Chapter 3 (OxR T4, OxR T7 and OxR T8). In this instance *Z. tritici* was again inoculated onto three-week-old Riband wheat but instead of checking these at regular intervals, at 21 dpi leaves were excised, pressed for 48 hours, then scanned (Figure 4.5).

Strain-dependent variations in the number of pycnidia per cm^2 leaf area was observed as shown in Figure 4.6. Leaves painted with overexpresser strains had fewer pycnidia per cm^2 leaf area when compared to wildtype or ZttxA-Δ2 inoculated leaves. Kruskal-Wallis testing identified a significant difference in pycnidia per cm^2 leaf area based on the inoculating isolate ($p<0.05$). Pairwise comparisons between groups using Dunn's test (with correction for multiple pairwise tests using the Benjamini-Hochberg procedure) revealed that only the OxR T8 isolate significantly differed from the wildtype in pycnidia number per cm^2 leaf area ($p<0.05$). Significant differences between ZttxA-Δ2 and OxR T4 ($p<0.05$), as well ZttxA-Δ2 and OxR T8 ($p<0.05$), can also be noted.

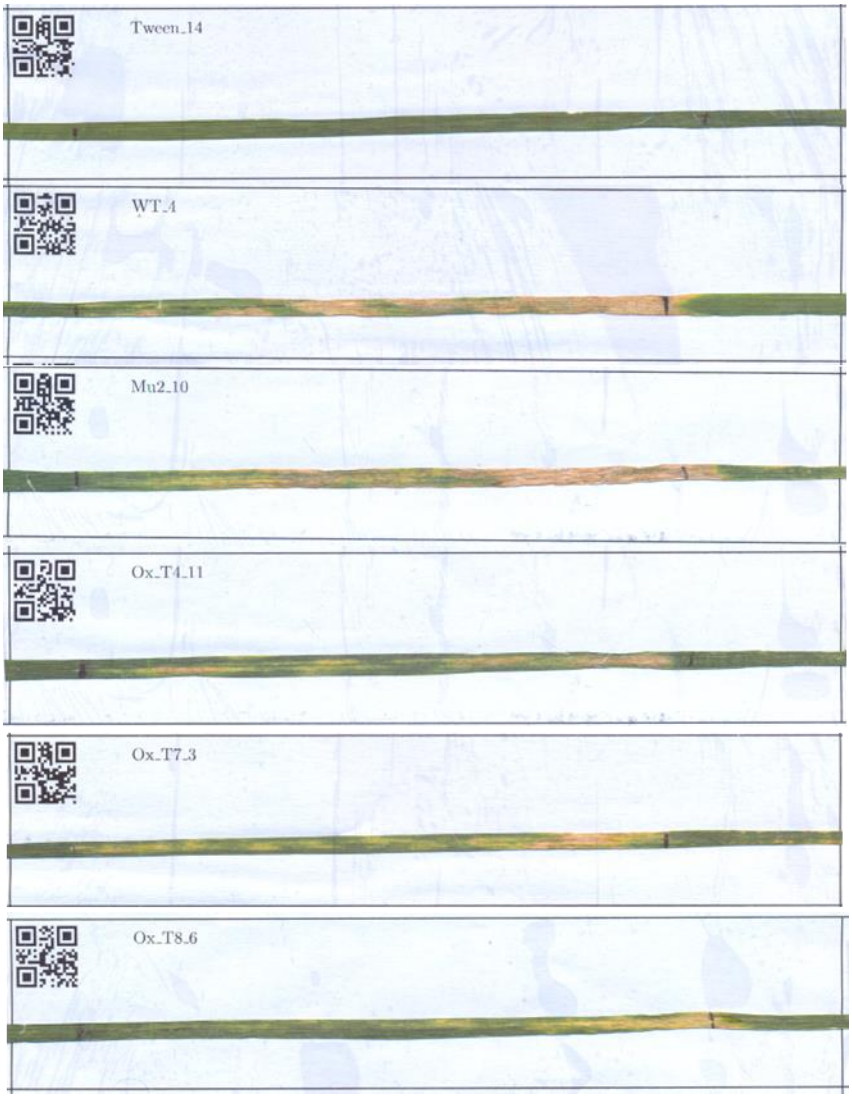

Figure 4.5 Riband wheat leaves inoculated with *Zymoseptoria tritici* IPO323 strains with genetic differences in relation to the Zttx cluster.

Representative Riband wheat leaves inoculated with either a tween negative control (top) or *Zymoseptoria tritici* isolates with genetic differences within the Zttx gene cluster. Following the tween control is the wildtype *Z. tritici* strain followed by the *ZttxA* gene deletion strain, and the *ZttxR* overexpresser strains OxR T4, OxR T7 and OxR T8 (at the bottom of the image).

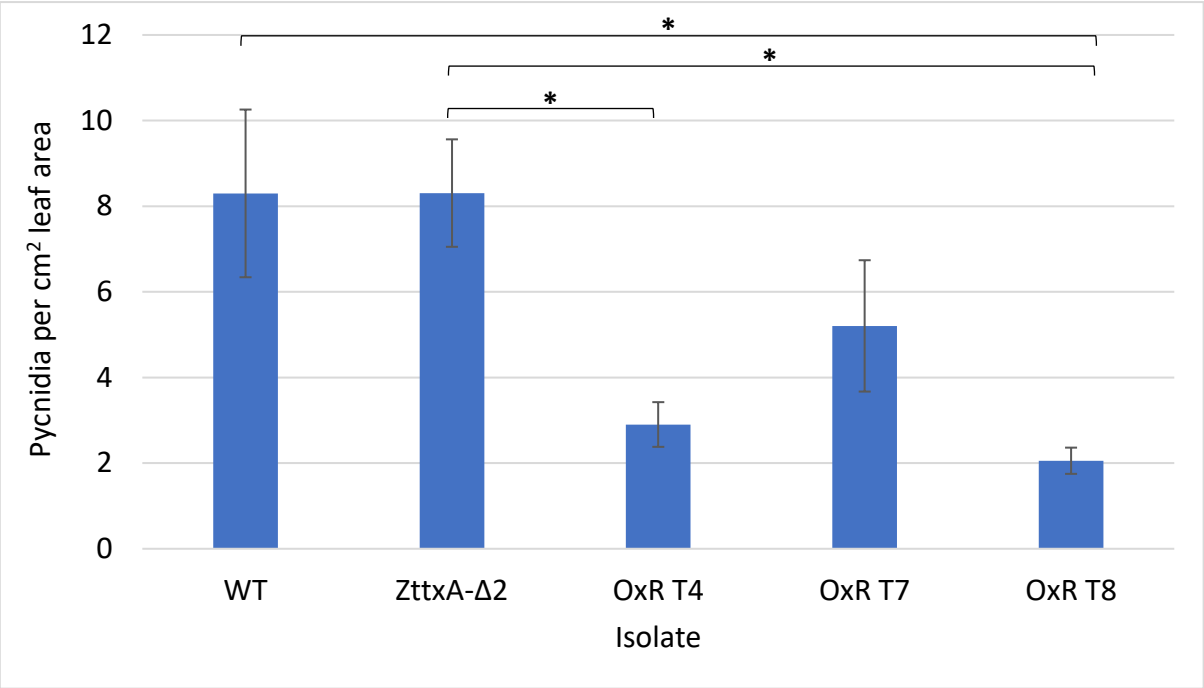

Figure 4.6 Effect of deletion or overexpression of the *ZttxA* gene on pycnidia production per cm^2 leaf area.

Zymoseptoria tritici pycnidia per cm^2 leaf area for Riband wheat leaves inoculated with WT, ZttxA-Δ2, OxR T4, OxR T7 and OxR T8. Error bars are +/- standard error of the mean (S.E.M), N=15. Horizontal bars with an asterisk specify conditions which statistically differ at the $p<0.05$ level.

4.3.4 Investigating cultivar and isolate specific interactions in relation to *ZttxA*

Given that *Z. tritici* virulence is quantitative and disease severity is known to be cultivar and isolate specific (with some cultivars of wheat containing resistance genes specific to the virulence factors produced by certain *Z. tritici* isolates), the possibility that *ZttxA* may be an avirulence gene was explored. Since *ZttxA* overexpression leads to reduced pycnidiation in the Riband cultivar of wheat, this was an area of particular interest. The virulence and pycnidia producing potential of wildtype and mutant *Z. tritici* strains was then tested on different wheat cultivars – presuming that gene knockout of an avirulence factor would result in increased virulence. Wheat leaves of cultivars: Alchemy, Bobwhite and Cadenza (with known differing susceptibilities to *Z. tritici* infection); were inoculated with wildtype or ZttxA-Δ2 *Z. tritici* isolates by painting a 4x10^6 spores/ml onto leaves. Again, tween control inoculated leaves were employed (Figure 4.7).

For all cultivars tested, pycnidia per cm^2 leaf area was similar for both the wildtype and ZttxA-Δ2 inoculated leaf types. The different cultivars showed variations in pycnidia per cm^2 leaf area, with Bobwhite leaves displaying the greatest number of pycnidia per cm^2 leaf area and Cadenza leaves having the fewest (Figure 4.8). In part this was expected knowing that Cadenza has the Stb6 resistance gene corresponding to avrStb6 in IPO323. Significance testing was performed using a Kruskal-wallis test ($p<0.05$). Pairwise comparisons using Dunn's test, with Benjamini-Hochberg correction, showed pycnidia per cm^2 leaf area did not significantly differ by isolate but by cultivar. Wildtype inoculated Bobwhite leaves had significantly greater pycnidia numbers per cm^2 leaf area compared to wildtype inoculated Alchemy or Cadenza leaves ($p<0.05$). For the ZttxA-Δ2 inoculations, the pycnidia number on Cadenza leaves was significantly reduced compared to the number on both Alchemy and Bobwhite leaves ($p<0.05$ in each instance).

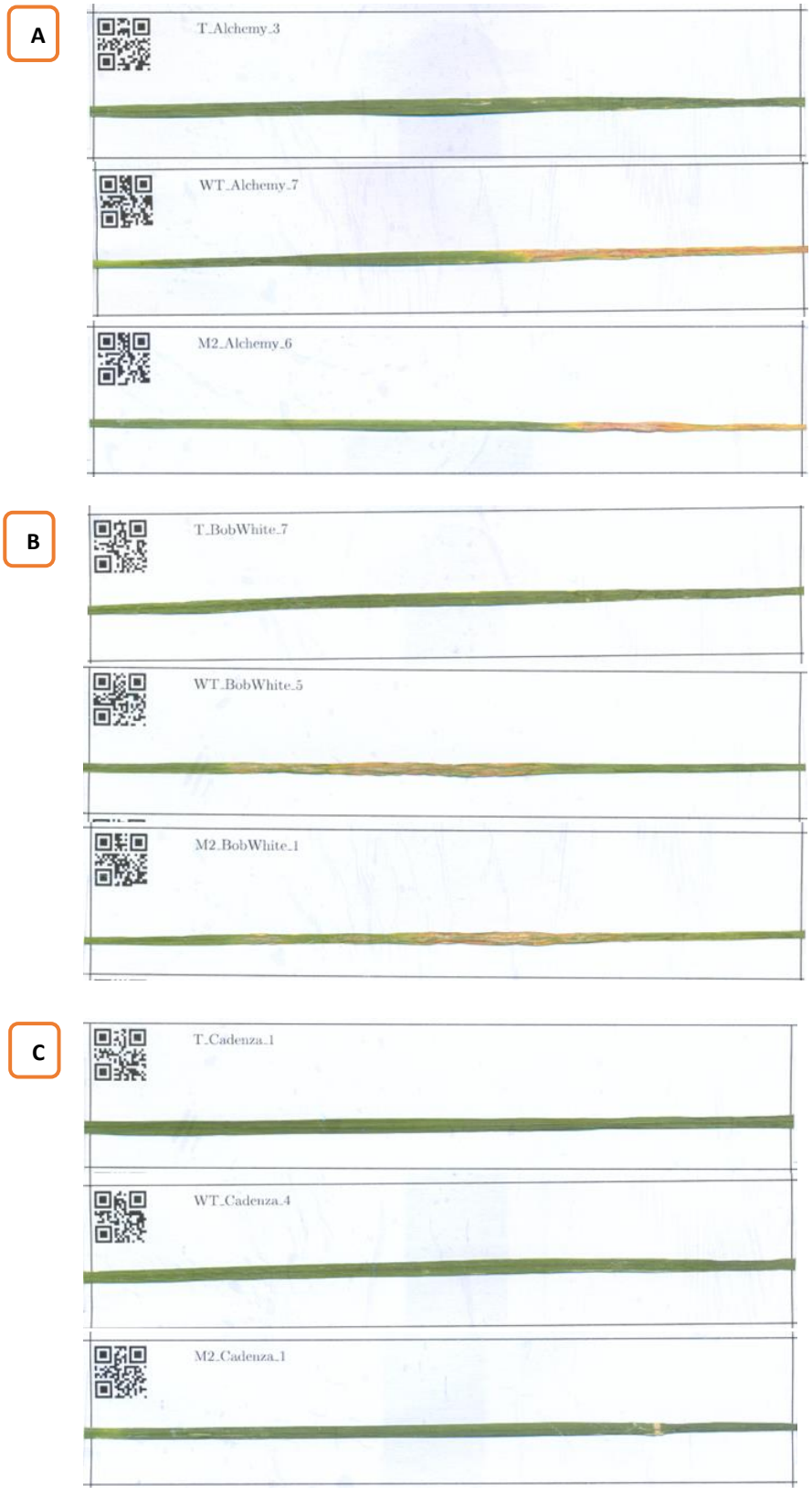

Figure 4.7 Wheat leaves inoculated with wildtype or *ZttxA* knockout *Zymoseptoria tritici* IPO323 strains.

Representative wheat leaves inoculated with either a tween negative control (top), wildtype *Zymoseptoria tritici* (middle), or the *ZttxA* knockout fungal strain (bottom). Different wheat cultivars were inoculated with these *Z. tritici* strains: A) Alchemy, B) Bobwhite, C) Cadenza.

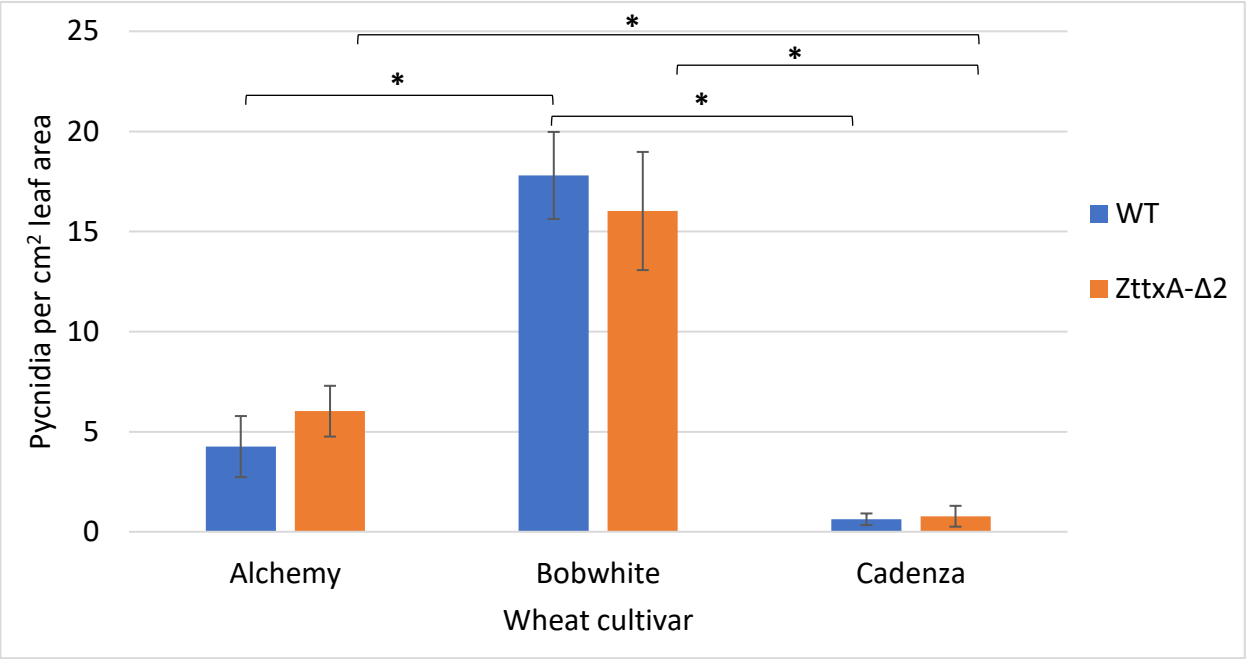

Figure 4.8 Effect of *ZttxA* deletion on pycnidia production in wheat cultivars Alchemy, Bobwhite and Cadenza.

Zymoseptoria tritici pycnidia number per cm^2 leaf area for different cultivar WT or ZttxA-Δ2 infected wheat leaves: Alchemy, Bobwhite and Cadenza. Data are grouped by cultivar and by *Z. tritici* isolate: wildtype (WT; blue) and ZttxA-Δ2 (orange). Error bars are +/- standard error of the mean (S.E.M), N=10. Horizontal bars with an asterisk specify conditions which statistically differ at the $p<0.05$ level.

In a separate inoculation experiment, conducted in the same way, Alchemy, Bobwhite and Cadenza wheat cultivars were inoculated with wildtype *Z. tritici* and the three overexpresser isolates: OxR T4, OxR T7 and OxR T8 (Figure 4.9). Tween controls were employed as standard. The wildtype trend of greatest pycnidia number per cm^2 leaf area in the Bobwhite wheat cultivar, followed by Alchemy, and fewest pycnidia for the Cadenza strain is maintained in this experiment (Figure 4.10). A significant difference in pycnidia number depending on cultivar and isolate combination was identified by a Kruskal-wallis test ($p<0.05$). Pairwise comparisons were completed using Dunn's test, with Benjamini-Hochberg correction. For the wildtype inoculated conditions, only wildtype IPO323 inoculated Bobwhite leaves and wildtype inoculated Cadenza leaves significantly differed in pycnidia number ($p<0.05$).

Figure 4.9. Representative leaves from plant assays investigating the interaction between wheat cultivar and *Zymoseptoria tritici* strain.

Leaves shown are those inoculated with tween as a negative control (at the top of the image) followed by wildtype IPO323, then the three ZttxR overexpresser strains: OxR T4, OxR T7, and OxR T8 (at the bottom of the image). Different wheat cultivars were inoculated with these *Z. tritici* strains: A) Alchemy, B) Bobwhite, C) Cadenza.

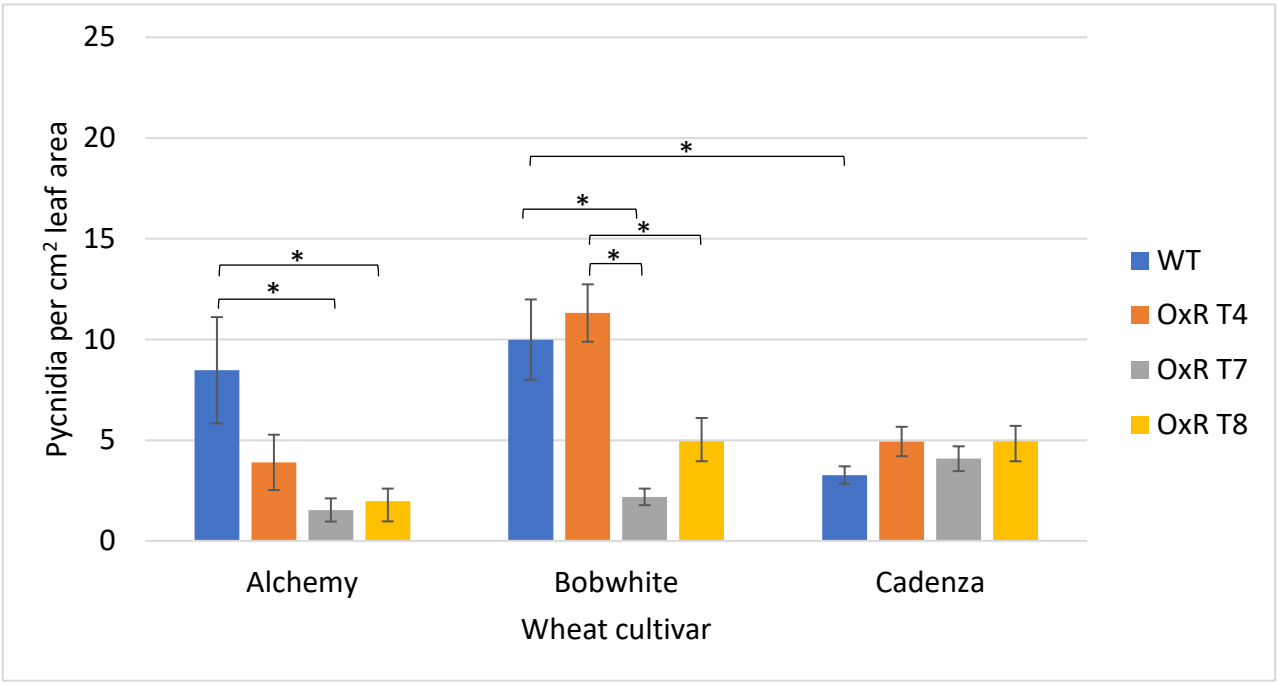

Figure 4.10. Effect of *ZttxA* overexpression (from strains OxR T4, OxR T7 and OxR T8) on pycnidia production in wheat cultivars Alchemy, Bobwhite and Cadenza.

Zymoseptoria tritici pycnidia per cm^2 leaf area for different cultivar wheat leaves: Alchemy, Bobwhite and Cadenza. Data are grouped by cultivar and by *Z. tritici* isolate: wildtype (WT; blue) and OxR T4 (orange), OxR T7 (grey), OxR T8 (yellow). Error bars are +/- standard error of the mean (S.E.M), N=9. Horizontal bars with an asterisk specify conditions which statistically differ at the $p<0.05$ level.

Though like Riband, Alchemy infected leaves showed the same reduction in pycnidia for all overexpresser strains, no consistent pattern was seen for the overexpresser strains in all cultivars. Pycnidia numbers produced by the overexpresser strains varied between cultivars, however, generally the OxR T4 strain produced greatest pycnidia numbers in infected leaves followed by OxR T8. Excluding the cultivar Riband, OxR T7 consistently produced fewest pycnidia regardless of the wheat cultivar inoculated. For the Bobwhite cultivar overexpresser strains significantly differed in their pycnidia number per cm^2 leaf area with OxR T7 and OxR T8 inoculated leaves showing significantly fewer pycnidia than OxR T4 inoculated leaves ($p<0.05$); not only this but OxR T7 inoculated Bobwhite wheat leaves had significantly fewer pycnidia than wildtype inoculated Bobwhite leaves ($p<0.05$). The difference in pycnidia number produced by infections of the wildtype and the OxR T7 strain is also seen for the cultivar Alchemy ($p<0.05$) but not for Cadenza. For Alchemy, OxR T8

infected leaves also had significantly fewer pycnidia than those inoculated by wildtype IPO323 *Z. tritici* ($p<0.05$).

4.3.5 Antimicrobial activity of the putative *Z. tritici* RiPP *in vivo*

To assess potential antimicrobial activity of the *Z. tritici* RiPP, wildtype *Z. tritici*, ZttxA-Δ2 and OxR T4 strains were grown on CDV8 agar for five days before taking 7mm agar plugs and placing them onto TSAb agar plates, allowing growth for a further five days. At this point TSAg overlays containing *Saccharomyces cerevisiae*, *Escherichia coli* and *Bacillus subtilis* cells were added to the plates alongside MTT or TTC dyes to assess cell viability. Rudd et al. (2015) indicate the *Z. tritici* RiPP to be a secreted peptide and as such, should antimicrobial activity exist, clearing zones around the fungal plugs would be identified so long as the peptide diffused into the agar. No zones of inhibition were identified after several days of growth (Figure 4.11). This experiment was repeated with nine-day old CD+YE liquid media – TSAb was overlaid with TSAg (impregnated with *S. cerevisiae, E. coli* or *B. subtilis*) and a 7mm plug removed from the centre of the plate, this was then filled with 40µl liquid culture. No zones of inhibition were seen here either.

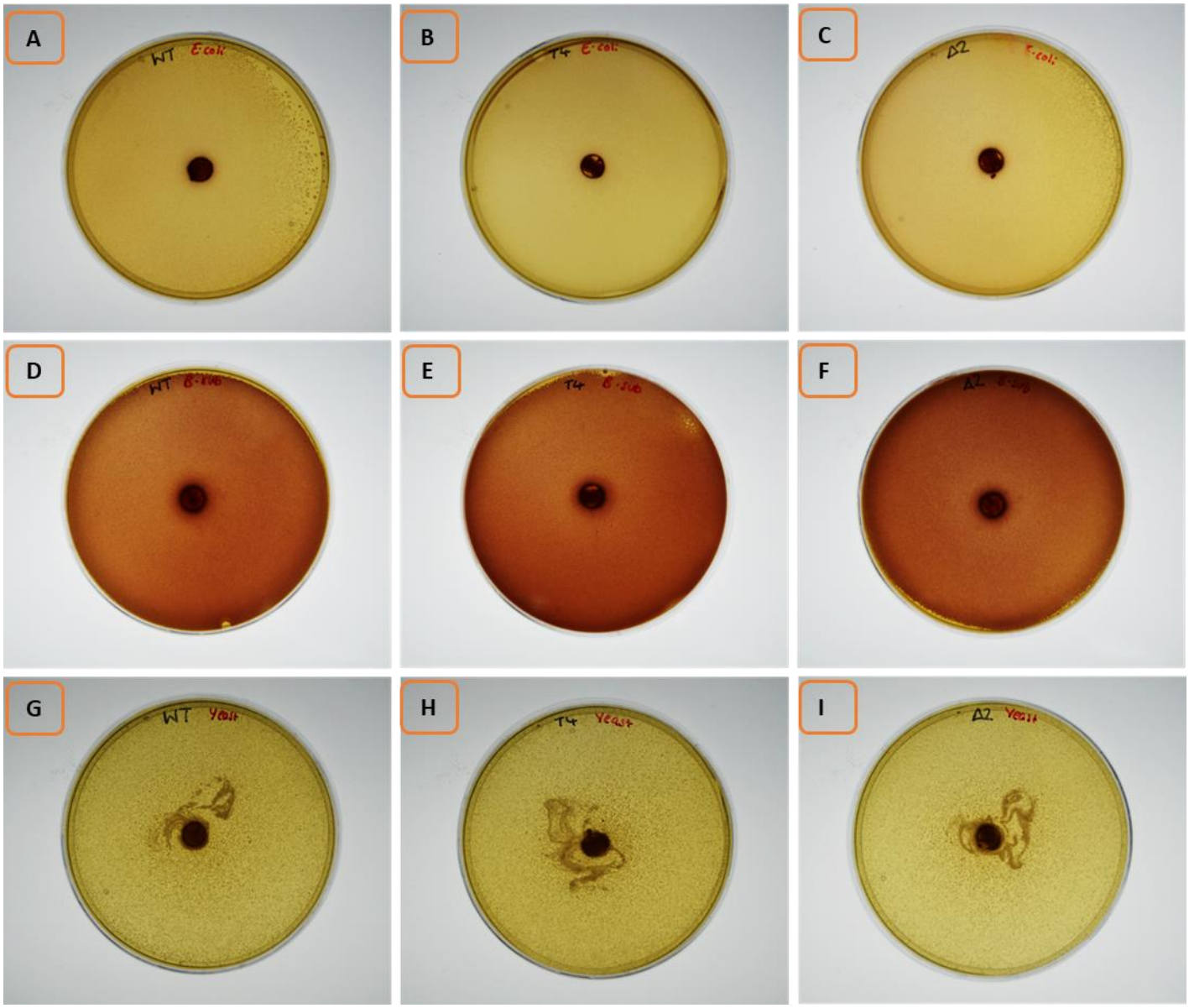

Figure 4.11 *In vitro* bioassay plates assessing antimicrobial activity of the *Z. tritici* RiPP.

Solid culture bioassay plates seven-days post-overlay. Plates A, D, G show wildtype IPO323 *Zymoseptoria tritici*; plates B, E, H show the OxR T4 strain and plates C, F, I show the ZttxA-Δ2 strain. For all organisms: *Escherichia coli* (A, B, C), *Bacillus subtilis* (D, E, F), and *Saccharomyces cerevisiae* (G, H, I); no clearing zones were observed demonstrating a lack of antibiotic or antifungal activity by secreted *Zymoseptoria* peptides.

4.3.6 Determination of *ZttxA* RiPP antifeedant activity against insects

Given the toxic nature of other known dikaritin RiPPs, this is also presumed to be the most likely function of the *Z. tritici* RiPP – similarity to phomopsin in core peptide sequence and post-translational modifications adds fuel to this theory. This was assessed by conducting an insect feeding study, infecting Riband wheat with wildtype, ZttxA- Δ2 and OxR T4 *Z. tritici* strains and feeding heavily infected dried leaf material (presenting pycnidia) in a choice of feeding experiment to ten third Instar *Schistocerca gregaria* locusts. Leaf material was placed in seed trays with five repeats per strain type – 50mg material was added to each cell. After five days of feeding, locust preference for a given material type was assessed by comparing the amount of wheat consumed for each inoculation type. A Kruskal-Wallis test ($p<0.05$) showed that wheat leaves were differentially consumed based on the *Z. tritici* isolate used to inoculate the wheat. Pairwise comparisons with Benjamini-Hochberg correction determined that leaves infected with ZttxA-Δ2 or OxR T4 *Z. tritici* were consumed to a greater extent than those inoculated with wildtype *Z. tritici* ($p<0.05$; Figure 4.12). As the knockout and overexpresser strain did not differ from each other no clear effect of *ZttxA* on feeding was found.

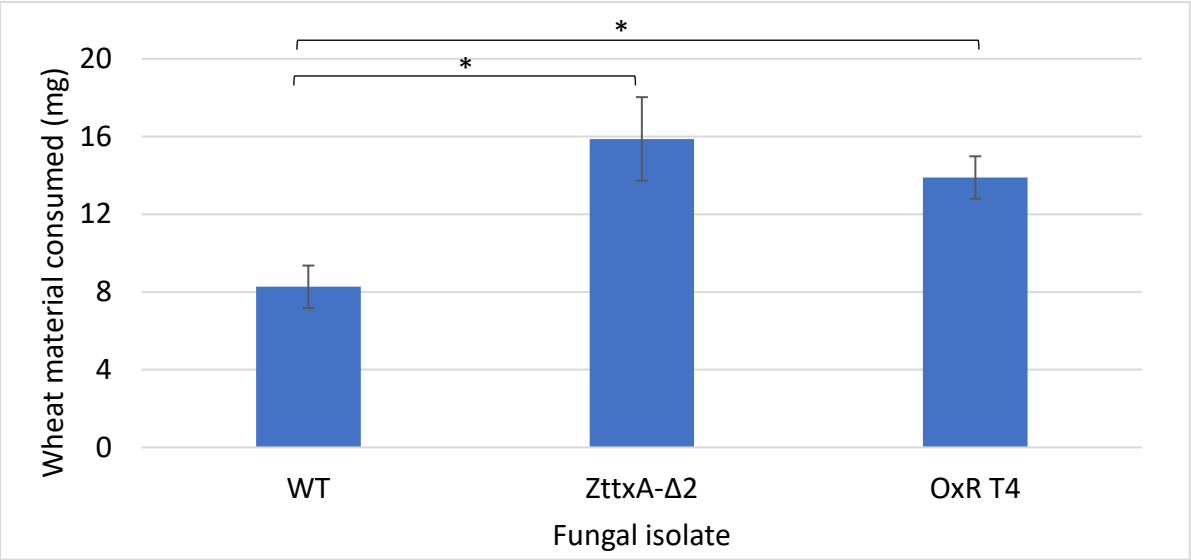

Figure 4.12 Determination of *Z. tritici* RiPP insect antifeedant activity based on *Schistocerca gregaria* locust feeding preference.

The consumption (milligrams) of *Z. tritici* (wildtype; WT, ZttxA-Δ2, and OxR T4) infected Riband wheat leaves after five days of uninhibited *Schistocerca gregaria* feeding. Data are mean ± standard error of the mean (S.E.M), N=5. Horizontal bars with an asterisk specify conditions which statistically differ at the $p<0.05$ level.

4.4 Discussion

The possible function of the *Z. tritici* RiPP was explored by investigating whether this peptide shared any of the roles of other known RiPPs such as: aiding pathogen virulence as well as antibiotic and antifeedant activity.

4.4.1 *ZttxA* gene absence and Septoria tritici blotch disease progression

Following wheat inoculation, time course data saw symptoms of *Zymoseptoria tritici* infection (for both wildtype and *ZttxA* knockout fungal strains) become visible on wheat leaves from 9 to 11 dpi – this is in line with the results seen in alternative works (Kema et al., 1996a, Keon et al., 2007). It is at this stage in the infection cycle that the latent phase of the fungal lifecycle ends and a transition to necrotrophic feeding by the fungus takes place (Rudd et al., 2015, Keon et al., 2007). Hence, signs of disease in the plant become more easily visible due to a suddenly exacerbated progression of infection. It was for this reason that timepoints prior to nine dpi were not scored using the disease symptom index.

Over the 44-day time course used in this work to determine whether disease progression was influenced by presence or absence of the *ZttxA* gene (Figure 4.4), small variations between fungal isolates in disease symptom scores at given timepoints can be noted. ZttxA-Δ1 at 25-42 dpi and ZttxA-Δ3 at 16-25 dpi, seem delayed in their development of disease symptoms on wheat compared to the wildtype, while 1-23 dpi Septoria tritici blotch appears to develop faster in the ZttxA-Δ2 strain. However, lack of consistency of this deviation from the wildtype in all deletion strains, with the same *ZttxA* deletion and *HygR* insertion at the *ZttxA* locus, indicate that this is a result of natural variation rather than a real difference. These data demonstrate that the *Z. tritici* RiPP does not play an essential role in disease progression.

Other small metabolites can be essential to virulence, such as HC-toxin which is a host-selective toxin produced by *Cochliobolus carbonum*, a pathogen of maize (Brosch et al., 1995). RiPPs can act in the same way, the victorin RiPP, from *Cochliobolus victoriae,* is key to infection of oats containing the *Vb* gene (Navarre and Wolpert, 1999, Wolpert and Macko, 1989). Abolishing victorin production, prevents a virulence phenotype from developing in susceptible cultivars (Zainudin et al., 2015). Given this, deletion of the *ZttxA* gene, if instrumental to *Z. tritici* infection, would obviously impact virulence phenotype. Such a change in virulence phenotype is not seen for the *Z. tritici* RiPP here.

4.4.2 Quantifying *Z. tritici* pathogenicity and the influence of *ZttxA* on metrics of Septoria tritici blotch infection in Riband wheat

Time course data confirmed that loss of the *ZttxA* gene does not influence disease progression, however this is only one aspect of *Z. tritici* infection. If the *ZttxA* gene plays a role in pycnidia production, deleting this gene will ultimately reduce the pathogenicity of the fungus as it is unable to spread without generation of spores within these structures (Tiley et al., 2018). As such, an automated method of counting pycnidia per cm^2 leaf area was employed to quantify pathogenicity. Intriguingly, it was not deletion of the *ZttxA* gene that reduced pycnidia number, but rather overexpression of this gene with all *ZttxR* overexpresser strains producing fewer pycnidia than the wildtype IPO323 strain on Riband wheat (Figure 4.6). This indicates a possible function of the peptide as a weak avirulence factor – a virulence factor that the host has become able to detect and respond defensively to. Overexpression of the peptide might allow easier detection of the fungal molecule by the

host plant. In turn, earlier recognition allows plant defences to be put into place and the pathogen's potential for pycnidia production is reduced.

A statistically significant reduction in pycnidia per cm^2 leaf area was seen only for the OxR T8 strain compared to the wildtype, rather than for all overexpresser strains, indicating that this difference may not be the result of overexpression of the *Z. tritici* RiPP but rather the consequence of undirected insertion of the *ZttxR* overexpression construct into the *Zymoseptoria tritici* genome. Since all overexpresser strains upregulate the *ZttxA* gene to a similar extent (Figure 3.14), we hypothesise that the RiPP titre in these strains would be similar. Extending this logic, we would expect the difference in pycnidia per cm^2 leaf area to also be similar between these three strains, which was not what was observed. However, it must be appreciated that transcript data was attained from *in vitro* experimentation, therefore, this result may not hold *in planta*.

In the case of OxR T8, perhaps the impact of *ZttxA* overexpression is compounded by the genomic context of the insertion to produce the statistically significant result that is absent from the other overexpresser strains. Should the OxR T8 construct have inserted into a genomic region involved in pycnidia production and disrupted this, as well as overexpressing the *ZttxR* gene, this would explain the result seen here. It may then be of interest to undertake whole genome sequencing of these overexpresser strains to understand the genomic context of the *ZttxR* overexpression construct insertion site and how this may act as a confounding factor when assessing *Z. tritici* RiPP function.

Given the proposed role of the *Z. tritici* RiPP as a virulence factor, it is surprising that loss of the *ZttxA* gene does not impact pycnidiation. However, as *Z. tritici* virulence is quantitative and the result of the combined influence of genes of both small and large effects (Stewart et al., 2018), not all virulence genes will generate a large impact on overall pathogenicity. All virulence genes do not need to be present for Septoria tritici blotch to ensue, with different combinations of these genes proving equally damaging depending on the host context (Stewart et al., 2018). Deletion of the *ZttxA* gene from the IPO323 genome may not significantly impact overall infection severity as other genes contributing to total virulence are still at play.

It must be recognised that testing virulence based on *ZttxA* on one cultivar of wheat is simplistic, especially since avirulence factors typically have cultivar specific effects – such as ACE1 from *Magnaporthe grisea* which cannot infect *Pi33* containing cultivars. Host specificity of *Z. tritici* strains has already been noted too (Kema and van Silfhout, 1997) with the outcome of *Z. tritici* infection of wheat dependent on the exact combination of genes within the infecting isolate as well as genes within the host plant. The IPO323 strain of *Z. tritici* is known to be virulent on the cultivar Riband (Brown et al., 2001, Rudd et al., 2008), yet alternative wheat cultivars exist with different genetic backgrounds. Breeding of these cultivars to be resistant against local *Z. tritici* strains may mean that susceptibility to other virulence factors may have slipped through, similarly to how resistance to *Fusarium* disease lessens following breeding of dwarf wheat (Srinivasachary et al., 2008). As such, the role and significance of the *Z. tritici* RiPP in infection may change depending on the cultivar it is tested against.

4.4.3 The role of the *Z. tritici* RiPP in pycnidia production in cultivar and isolate specific interactions

To determine whether the importance of *ZttxA* in *Z. tritici* infection was cultivar specific, the IPO323 strain (both wildtype and *ZttxA* knockout) was raised against several additional wheat cultivars of Alchemy, Cadenza and Bobwhite. These were chosen based on understood difference in resistance genes, specifically relating to Stb6 as IPO323 is avirulent on cultivars containing this gene (Brading et al., 2002, Kema et al., 2000). In a gene-for-gene interaction between wheat and *Z. tritici,* the fungus has to secrete the AvrStb6 effector protein (Zhong et al., 2017) in order for this to be detected by the wheat Stb6 receptor-like kinase (Brading et al., 2002) and a defence response mounted by the plant. Lack of either gene from the plant or fungus results in a shift in infection dynamics. As such, the cultivars each vary in their susceptibility to this strain of the fungus with Bobwhite and Alchemy cultivars being susceptible (Saintenac et al., 2018, Stephens et al., 2021), while the Cadenza cultivar is not (Arraiano and Brown, 2006).

Data relating to the susceptibility of these cultivars to IPO323 *Z. tritici* is therefore as expected (Figure 4.8) with the Cadenza cultivar showing fewest pycnidia, followed by Alchemy and Bobwhite. *Z. tritici* infection of wheat is indeed host specific, however these data also confirm that for no cultivar inoculated is the *ZttxA* gene playing a significant role in

pathogen virulence as no difference between the wildtype and deletion strain was identified. Hence, the *Z. tritici* RiPP does not appear to be a virulence factor, or at least not one of large effect. To further support this result, alternate isolates of *Z. tritici* should be tested against these cultivars, using the *ZttxA* knockout construct to transform these strains if there is sufficient conservation of the flanking regions used to this means across different strains.

This work was extended by applying overexpresser strains to the Alchemy, Cadenza and Bobwhite cultivars, to determine if the reduction in pycnidia in the overexpresser strains seen in Riband was consistent across cultivars. This trend however was not consistent. In particular, for the Cadenza wheat cultivar, all strains gave similar low numbers of pycnidia on infected leaves. This is perhaps unsurprising given that the Cadenza wheat cultivar is resistant to IPO323 *Z. tritici,* thanks to possession of the Stb6 gene (Arraiano and Brown, 2006) and all overexpresser isolates are transformants of this strain.

The avirulence factor hypothesis holds for the Alchemy cultivar which, as in Riband, saw reduced pycnidiation for all overexpresser strains compared to the wildtype – though only statistically significant for OxR T7 and OxR T8. The cultivar: isolate interaction on Bobwhite, however, yields an unexpected result. Two of three OxR strains showed significantly less pycnidia per cm^2 leaf area on the susceptible cultivar Bobwhite. This pattern generally matches what was observed for the susceptible cultivar Riband, however the third OxR strain, OxR T4 did not show this reduction. Data were produced from an average of three replicate experiments conducted at separate points in time over which this result was consistent. No readily apparent explanation is available for this result, beyond possible implications of the genomic context of the insertion in the OxR T4 strain (as discussed for OxR T8 in the context of Riband wheat infection). However, overall, data on the role of the *Z. tritici* RiPP in pathogenicity is largely inconclusive.

4.4.4 *Z. tritici* RiPP antimicrobial activity

Under the conditions used in this work the *Z. tritici* RiPP does not appear to be a secreted antibiotic. This result may be a consequence of several possible reasons. The first, the peptide is being produced in too low concentrations to be sufficient for inhibition of test organism growth. Low peptide titre is not outside of the realms of possibility given that extractions from these fungi do not allow for the RiPP peptide to be detected by LCMS.

Second, the *in vitro* assay assumes the RiPP to be secreted. However, the possibility exists that, despite indications to the contrary by Rudd et al. (2015), the peptide is retained within the fungus similar to amatoxin/phallotoxin and omphalotin (McKnight et al., 2010, Kaya et al., 2015, Enjalbert et al., 1993, Quijano et al., 2019). Thirdly, the assay assumes expression/translation of transcripts on this media, which, as explored in Chapter 3, may not necessarily occur. Conclusions regarding this activity cannot be decisively made until the peptide is purified and tested as a pure extract.

Lack of antibiotic activity would not be unsurprising given that presumably similar RiPPs of ustiloxin and phomopsin are not cytotoxic against bacterial and fungal cells (Koiso et al., 1994, Li et al., 1992), nor are there any known antibacterial fungal RiPPs to date. Phomopsin and ustiloxin, specifically, are cytotoxic to mammalian cell types through tubulin binding and the knock-on effects of preventing spindle formation on mitosis (Battilani et al., 2011, Koiso et al., 1992, Li et al., 1995). Bacteria, however, do not have standard tubulins (Jenkins et al., 2002). Though, tubulin homologs have been identified, these differ significantly to those in eukaryotes (Jenkins et al., 2002, Pilhofer et al., 2011).

Beyond the *Z. tritici* RiPP, these data indicate that no other compound secreted by *Z. tritici* shows any antimicrobial activity to the organisms tested in this work. However, conclusions regarding the antibiotic activity of the *Z. tritici* RiPP, and other secreted *Z. tritici* chemicals, can only be made in relation to the peptide at natural concentrations. This does not however guarantee a lack of antimicrobial activity under different circumstances. Indeed, Kettles et al. (2018) have shown that *Z. tritici* does produce an antimicrobial protein but used a recombinant protein expression system to demonstrate this.

4.4.5 *Z. tritici* RiPP antifeedant activity

This work investigated the antifeedant activity of the *Z. tritici* RiPP against *Schistocerca* locusts and identified a significant difference in wheat leaf consumption based on the inoculating strain of *Z. tritici*. However, as leaves containing the RiPP (inoculated with OxR T4) as well as those lacking the peptide (inoculated with ZttxA-Δ2) were consumed to a similar extent, this feeding preference is clearly not due to RiPP distastefulness or acute toxicity. If the RiPP were indeed distasteful or toxic to *Schistocerca* locusts, a reduction in feeding on OxR T4 inoculated leaves would be expected relative to the wildtype and knockout.

The experimental evidence supporting apparent lack of antifeedant activity of the RiPP is however limited for several reasons. The first is based on experimental design in that this method tests for distastefulness or acute toxicity and assumes that consumption of infected material over a few days is sufficient to reveal feeding preferences. If the effect of the proposed toxin was not immediate, nor was the RiPP distasteful (Clay, 1996), no differences would be noted. The impact of peptide consumption on different locust growth stages or over a longer time period was not assessed – nor was an impact on overall insect health determined, as the peptide may not be toxic but instead influence insect life processes such as reproduction (Battilani et al., 2011), ensuring fewer insects would exist to feed on the fungal infected material over generations.

The investigation, similarly to the antimicrobial investigation, also assumes that the RiPP is produced in sufficient quantities to generate an effect – though other RiPPs need only small quantities to be lethal (Yilmaz et al., 2015, Vetter, 1998) – given that this RiPP cannot be detected by LCMS following extraction it follows that the peptide titre may be too low to have any influence on the test organism. It can however be concluded that the natural RiPP concentration generated by *Z. tritici* is not sufficient to be acutely insecticidal to locusts (since no locust mortality was recorded) or deter feeding. This is perhaps surprising given that the effect of alternative dikaritin RiPPs at natural concentrations is toxic (Van Warmelo et al., 1971, Zhou et al., 2012). However, to our knowledge, insect toxicity has not been assessed for dikaritin RiPPs – though insect toxicity has been observed for the amatoxins (Kunzler, 2018, Jaenike et al., 1983, Jaenike, 1985).

Despite these results, the predicted chemical structure of the *Z. tritici* RiPP indicates the most likely function of the peptide to be inhibition of microtubule assembly. Koiso et al. (1994)M note that a shared cyclic structural element between ustiloxin and phomopsin is assumed to interact with tubulin. As this same cyclic element is predicted to exist in the *Z. tritici* RiPP (Figure 4.13) this function is presumed here, as such, the name “zymoseptorin” is proposed for the *Z. tritici* RiPP in line with the designations of mammalian toxic dikaritin RiPPs assigned already. Indeed, zymoseptorin is predicted to share a cyclic core with these toxic dikaritins, with differential tailoring of this structure altering the pharmacokinetic properties of the molecule. It may then be this tailoring that determines the specificity of the RiPP to a given organism. Here, locusts were selected as the test organism but since the

specificity of zymoseptorin is unknown, selecting the organism against which the peptide is toxic by chance is small.

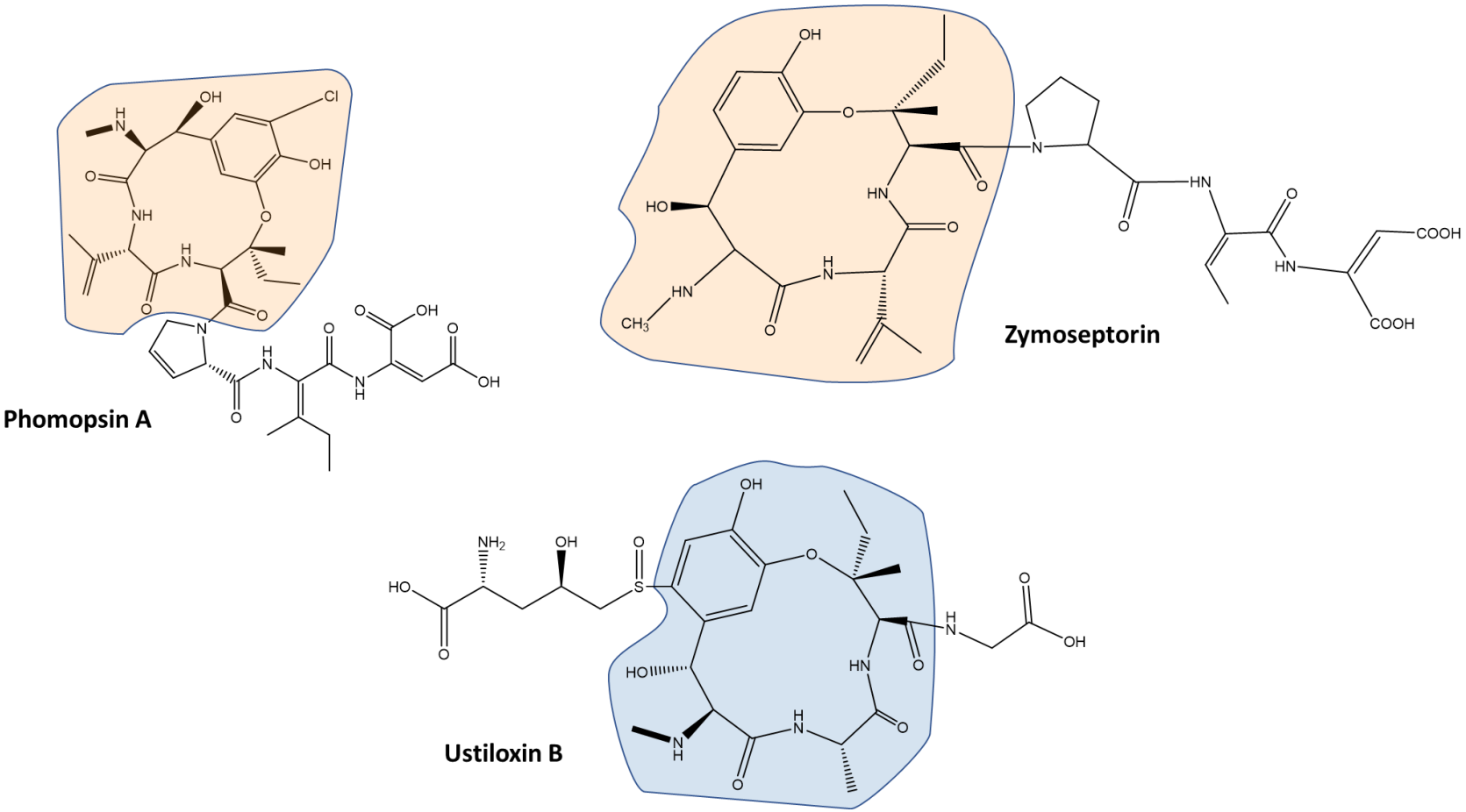

Figure 4.13 Chemical structures of phomopsin A, ustiloxin B and proposed zymoseptorin.

The toxic dikaritin RiPP chemical structures are displayed alongside the predicted chemical structure of zymoseptorin. The cyclic region of the ustiloxin peptide indicated to interact with tubulin by Koiso et al. (1994) is highlighted blue. The corresponding cyclic elements in the phomopsin and zymoseptorin molecules are highlighted orange.

Understanding the potential toxicity of the *Z. tritici* RiPP is of high importance in terms of food safety. As *Z. tritici* is a foliar-specific wheat pathogen, the grain of infected plants is unlikely to contain the RiPP (despite its presumed secretion into the plant), therefore, fungal infection of wheat is not a concern for human safety but rather animal safety since wheat straw can be used as animal bedding and feed. Regulations of phomopsin in food have already been put into place for humans (van Egmond et al., 2007, van Egmond and Jonker, 2004, Cheung and Mehta, 2015) and animals (Bhat et al., 2010), with concerns over ustiloxin safety in feed rising (Wang et al., 2017, Miyazaki, 2006, Uka et al., 2020). This is however, placated by the knowledge that no toxicosis outbreaks from ustiloxin have occurred to date (Nakamura et al., 1994), nor has toxicosis from an unknown wheat contaminant yet been documented.

4.5 Summary

- Deletion of the *ZttxA* gene from IPO323 *Z. tritici* does not influence Septoria tritici blotch disease progression.
- Pycnidia production from wildtype *Z. tritici* varies depending on the wheat cultivar infected.
- Pycnidia production on Riband wheat decreases with increased *ZttxA* expression but only significantly for the OxR T8 *Z. tritici* strain. This trend is not consistent across cultivars and the role of the *ZttxA* RiPP as an avirulence factor is inconclusive.
- At the natural concentration produced by the fungus, the *Z. tritici* RiPP does not show antimicrobial activity against *Saccharomyces cerevisiae, Escherichia coli* or *Bacillus subtilis*, under the conditions used in this work.
- At the concentration of the *Z. tritici* RiPP produced by the fungus naturally, locust feeding on infected wheat leaves was not deterred – zymoseptorin is not acutely toxic or distasteful to this organism.

5 : Bioinformatic investigation of the *Z. tritici* RiPP and genome mining for novel dikaritin RiPPs

Since its initial cluster identification (Child and Bailey, unpublished, Ding et al., 2016), no further investigation of the *Z. tritici* RiPP has been conducted. As seen in Chapters 3 and 4, this may largely be due to the difficulties in assessing peptide function as well as extracting the peptide from the fungus in order to chemically characterise the compound. However, it is still possible to investigate the peptide from a bioinformatic perspective, looking specifically here at the RiPP precursor peptide gene within the cluster. This chapter explores the precursor peptide gene in multiple *Z. tritici* isolates and uses the proposed zymoseptorin biosynthetic cluster genes as a starting point from which other RiPP producing species may be identified.

5.1.1 The *Z. tritici* genome

The complete genome of *Z. tritici* (strain: IPO323) was first published in 2011, revealing the existence of 21 chromosomes – including eight dispensable chromosomes – totalling 39.7 Mb in size (Goodwin et al., 2011). The genome size of *Z. tritici* was therefore far bigger than first anticipated with McDonald and Martinez (1991) estimating a genome size of 31Mb shared among 17 or 18 chromosomes prior to sequencing. As such, at that time, *Z. tritici* was determined to have one of the highest chromosome numbers of the filamentous ascomycetes (Mehrabi et al., 2007, Wittenberg et al., 2009). Since the first *Z. tritici* genome was published, at the time of writing, 59 additional strains have been sequenced and this information made available on the National Centre for Biotechnology Information (NCBI; Zymoseptoria tritici - Assembly - NCBI (nih.gov)). These genomic sequences are all assembled to various levels (scaffold, contig, chromosome), however, regardless of this, these data serve to confirm that the genome size of this fungus varies to a large degree between strains (Table 5.1). Aside from the “core” chromosomes which do not vary, often chromosomes of these strains can differ in length (McDonald and Martinez, 1991) or chromosomes can be lacking from the genome entirely (Mehrabi et al., 2007). It should be noted that lost chromosomes are dispensable, or ‘accessory chromosomes’, with research indicating that

these often have only small impacts on host infection by the fungus (Habig et al., 2017, Stewart et al., 2018). Loss of these chromosomes does not hugely negatively impact the fungus (under lab conditions) since for several years these chromosomes were not known to have any function or importance to the pathogen. Though, recent work by Chen et al. (2023) indicates that effector proteins encoded by genes on accessory chromosomes may also be important in the wheat:*Zymoseptoria* interaction.

It is however clear that isolates within this species have a large degree of genomic variability, something that is further demonstrated in Table 5.1 showing genomes of the sequenced strains to vary from 31.79Mb to 42.96Mb. Clearly the genomic DNA sequence is not identical for all strains, however, what is interesting is where these DNA variances exist and what their significance can be.

Table 5.1 A comparison of *Z. tritici* isolates showing differences in genome sizes.

The genome sizes of *Z. tritici* strains available on NCBI. Strains are those that have been naturally collected, rather than those which have been generated from experimental crosses.

Strain	**Size (Mb)**
WAI323	39.9548
3D1	40.6575
3D7	37.8614
1A5	39.6987
1E4	38.6284
Zt05	41.9532
Zt10	39.329
Zt289	37.9869
Zt71	41.0388
Zt74	39.7207
Zt36	39.3901
Zt80	38.0262
Zt48	39.2195
Zt88	37.8425
Zt92	39.0017

Zt55	39.6131
553.11	38.343
Einstein-Oak	39.1941
560.11	38.7934
Lion-Oak	37.4874
Zt153	36.8452
Zt155	36.9113
Zt150	38.4303
Zt148	36.9978
Lion-Cork	39.8001
Zt151	37.4326
Zt04	38.03
Cordiale-Cork	40.4094
Cordiale-Oak	38.6902
Zt07	37.2616
Zt154	36.656
IPO323	39.6863
WAI321	40.0101
WAI332	40.6494
Zt469	42.9646
Zt02	37.5177
STIR04_A48b	31.7941
STIR04_A26b	32.6413

5.1.2 The zymoseptorin biosynthetic gene cluster

The zymoseptorin biosynthetic gene cluster, encompassing the 12 genes BLAST searched in Chapter 3, is located on chromosome 4, a 'core' chromosome (Goodwin et al., 2011). The cluster spans 25028bp from location 4:1681686 to 4:1706713. Full information on the genomic locations of the Zttx cluster genes is shown in Table 3.1. Within this work, genomic variations within the *ZttxA* gene coding sequence are of particular interest since it is this gene that encodes the putative RiPP precursor peptide.

5.1.3 Core peptide sequence repetition and titre

The initial reporting of the putative *Z. tritici* RiPP by Ding et al. (2016) noted the existence of a repetitive sequence within the *ZttxA* gene. This translated to a 9-fold repeated amino acid sequence within the precursor peptide of "AEAVEDYVIPVDKTKR". Within this 16-amino acid sequence lies the YVIPVD core peptide – assuming processing is similar to phomopsin. Zymoseptorin is a multicore RiPP, as defined by Rubin and Ding (2020), because the precursor gene encodes multiple core peptide repeats within the larger precursor peptide. This RiPP characterisation spans the kingdoms of life and is used for any such peptide showing repeated units within the precursor (Rubin and Ding, 2020). The existence of multicore RiPPs in fungi was initially believed to be a unique feature of a select few fungal RiPPs (Umemura et al., 2014) – though common in bacteria (Sardar et al., 2015, Ziemert et al., 2008, Noike et al., 2015). Multicore RiPPs do not appear in other fungal classes beyond the dikaritins, in which instance, all identified RiPPs to date are multicore (Vogt and Kunzler, 2019). Repeat number within the precursor has been suggested to determine the quantity of mature RiPP synthesised (Umemura et al., 2014). Though, this may be an important factor, we also now know that there is control of transcription and translation of the precursor gene beyond this (Yoshimi et al., 2016, Umemura et al., 2020). Aside from directly increasing or decreasing peptide abundance, core unit repeats add a layer of redundancy to peptide production. Modification to any one repeat does not stop the others from being produced, albeit at a slightly reduced quantity, but does allow different peptides with potentially altered bioactivities to be produced from a single precursor (Vogt and Kunzler, 2019, Rubin and Ding, 2020).

The exact quantity of RiPP produced is likely under tight control and optimised to the needs of the producing organism. Indeed, different fungal species capable of producing the same RiPP have varying numbers of core peptide repeats within their peptide precursors. In the instance of the ustiloxin B producers *Aspergillus flavus* and *Ustilaginoidea virens* the former contains 16 YAIG repeats (Umemura et al., 2014), while the latter contains only three (Tsukui et al., 2015). Beyond this, *U. virens* also produces ustiloxin A with the core peptide sequence of YVIG (Tsukui et al., 2015).

As discussed above, different species that produce the same RiPP can carry precursor peptides with different total numbers of the core peptide repeat. This is also seen when

looking at different strains of the same species (Table 5.2)(Ding et al., 2016). It is less common to see completely unique RiPP core sequences specific to given strains of the fungal RiPP producer. So, whilst sequence is typically conserved within strains, repeat number is quite variable.

Table 5.2 Data from Ding et al. (2016) showing RiPP core subunit repeat numbers of different strains of identified putative RiPP producers.

Putative RiPP producing species are identified as well as the strains analysed in the work by Ding et al. (2016). The number of repeats of each core subunit are noted revealing variations in repeat unit number between strains to be common among dikaritin RiPP producers.

Species and core subunit	**Strain name/accession number**	**Repeat number**
Neurospora crassa (YVIEVD/YAIGVD/YVISVD/YVIAVD)	73 (KHE86654.1)	3/3/1/1
	OR74A (EAA30507.1)	4/4/1/1
Beauveria bassiana (YAIPVN/YVISVN)	D1-5 (KGQ06486.1)	6
	ARSEF 2860 (EJP63461.1)	4/3
Neurospora tetrasperma (YVIEVD/YAIGVD)	FGSC 2509 (EGZ72581.1)	3/3
	FGSC 2508 (EGO55879.1)	5/4
Aspergillus oryzae (YAIG)	RIB40 (BAE63088.1)	15
	3.042 (EIT79501.1)	7
Ustilaginoidea virens (YAIG/YVIG)	UV-8b (KDB11630.1)	3/4
	IPU010 (GAO17429.1)	3/4

Bioinformatic investigation of the *ZttxA* gene allows us to understand whether other *Z. tritici* strains showed variation in either the precursor peptide sequence or the total number of repeats. In fact, indication that this may be the case has already been seen. In research by Rudd et al. (2010), investigating tandem repeat proteins produced by *Z. tritici*, different PCR product sizes were noted when genomic DNA of various strains was targeted with primers spanning the repetitive region of the *ZttxA* gene – annotated by them as TRP11. Analysis of

this region is expanded upon within this work since it is not known whether these variances in fragment lengths result from intronic or exonic DNA changes as the primers employed by Rudd et al. (2010) span an intron.

5.1.4 RiPP discovery by genome mining

Beyond exploring the different strains of known RiPP producers, we must also look to uncover new RiPPs. Novel RiPP discovery by genome mining has been used extensively for bacteria and is made possible by easy identification of conserved modifying enzymes or gene motifs within bacterial RiPP classes. New peptides are then detected by identifying similar genes in other species. This has proven successful for several bacterial RiPP classes (Letzel et al., 2014) including the lasso peptides (Hegemann et al., 2013, Maksimov et al., 2012) and the lanthipeptides (Begley et al., 2009, Singh and Sareen, 2014). Finding novel bacterial RiPPs is made easier again by bioinformatic tools such as DeepRIPP (Merwin et al., 2020), RiPPquest (Mohimani et al., 2014) and RiPPMiner-Genome (Agrawal et al., 2021).

Attempts have been made to extend these tools, namely RiPPMiner-Genome, to fungal RiPPs (Vignolle et al., 2020), however as they are trained on bacterial RiPP classes (Agrawal et al., 2021) the predictive power for fungal RiPPs is limited. Notably, RiPPMiner-Genome is unable to recognise phomopsin (a confirmed RiPP) as a RiPP (Ding et al., 2016). Yet, coercing bacterial RiPP mining tools to look for fungal RiPPs is unsurprising given the lack of such software for fungi, with this largely due to the limited information we have on fungal RiPPs (Vignolle et al., 2020). Indeed, due to greater research into bacterial RiPPs, genome mining tools for bacteria were being employed around the time fungal RiPPs were first discovered (Hallen et al., 2007) and certainly before dikaritin RiPPs were uncovered (Umemura et al., 2014).

More recent improved understanding of the characteristic features of dikaritin RiPPs and the conserved genes and motifs that unite this class (discussed in Chapter 3) allows a degree of genome mining based on these conserved elements, however, this has lacked automation. Ding et al. (2016) identified novel dikaritin RiPPs by performing multiple Protein BLAST searches using PhomA, PhomQ and PhomM as query sequences and manually analysing the genomic context of the coding sequences of these hits for homologous biosynthetic genes to those in the phomopsin cluster – identifying the *Z. tritici* RiPP by this means. Since genomic databases are constantly being updated the possibility for uncovering novel RiPP producers

is always expanding. Not only this but, in short spaces of time, large advances in the bioinformatic tools available are being made. Indeed, even during the course of completing this project, novel tools have become available and are utilised here to identify novel ascomycete RiPPs with similarity to zymoseptorin (Gilchrist et al., 2021, Gilchrist and Chooi, 2021).

5.2 Aims

- To determine whether genomic differences between *Z. tritici* isolates within the precursor peptide coding region exist.
- To understand whether core subunit number impacts transcript levels of the *ZttxA* gene.
- To identify additional putative RiPPs, beyond those already identified, based on similarity to proposed RiPP biosynthetic cluster genes in the *Z. tritici* genome.

5.3 Results

5.3.1 Determining variation across *Z. tritici* strains in core unit repeat number within the RiPP precursor peptide

Following on from work by Rudd et al. (2010), identifying repetitive regions within *Z. tritici* proteins, the repetitive region of the *ZttxA* gene was analysed in more detail. In this work, I have assembled a selection of *Z. tritici* strains diverse in terms of their geographical origin, and additionally UK isolates which span several years of collection. To assess whether these strains substantially varied from one another in the selected genomic region (a subsection of the *ZttxA* gene), a PCR and gel electrophoresis method was employed. *Z. tritici* DNA of each strain was extracted from mycelia as described by Liu et al. (2000). Each DNA extraction was used as the template in separate PCR reactions using the ZttxA-F1/ZttxA-R2 primer pair, designed to sit outside of the repeat region (Figure 5.1A) and therefore capable of capturing the complete picture of genomic variation in this region. As in Rudd et al. (2010), however, this necessitates the primers to amplify across an intron. In the IPO323 strain of the fungus this reaction was predicted to yield a 673bp fragment based on available sequence information (Goodwin et al., 2011). The PCR extension time was extended relative to this to account for potential varying amplified fragment lengths dependent on repeat unit number differences between the strains.

Using Dream *Taq* DNA polymerase, fragments were amplified and run on a 2% agarose gel. As expected, the IPO323 sample generated a ~673bp amplicon, but amplicons of alternate strains differed from this fragment length (Figure 5.1B). This confirmed the existence of variations in genomic DNA sequences between strains. Though the core repeat unit encoding “YVIPVD” is only 18bp in length, this is encapsulated within a larger repeated section encoding “AEAVEDYVIPVDKTKR”. This 48bp sequence is large enough to visually assess the presence of additional or fewer repeat units compared to the IPO323 strain by gel electrophoresis separation of amplicons. The resultant predicted core subunit repeat numbers for each strain are outlined in Table 5.3. Using the same method of analysis core repeat numbers of the Rudd et al. (2010) strains can also be estimated (Table 9.9).

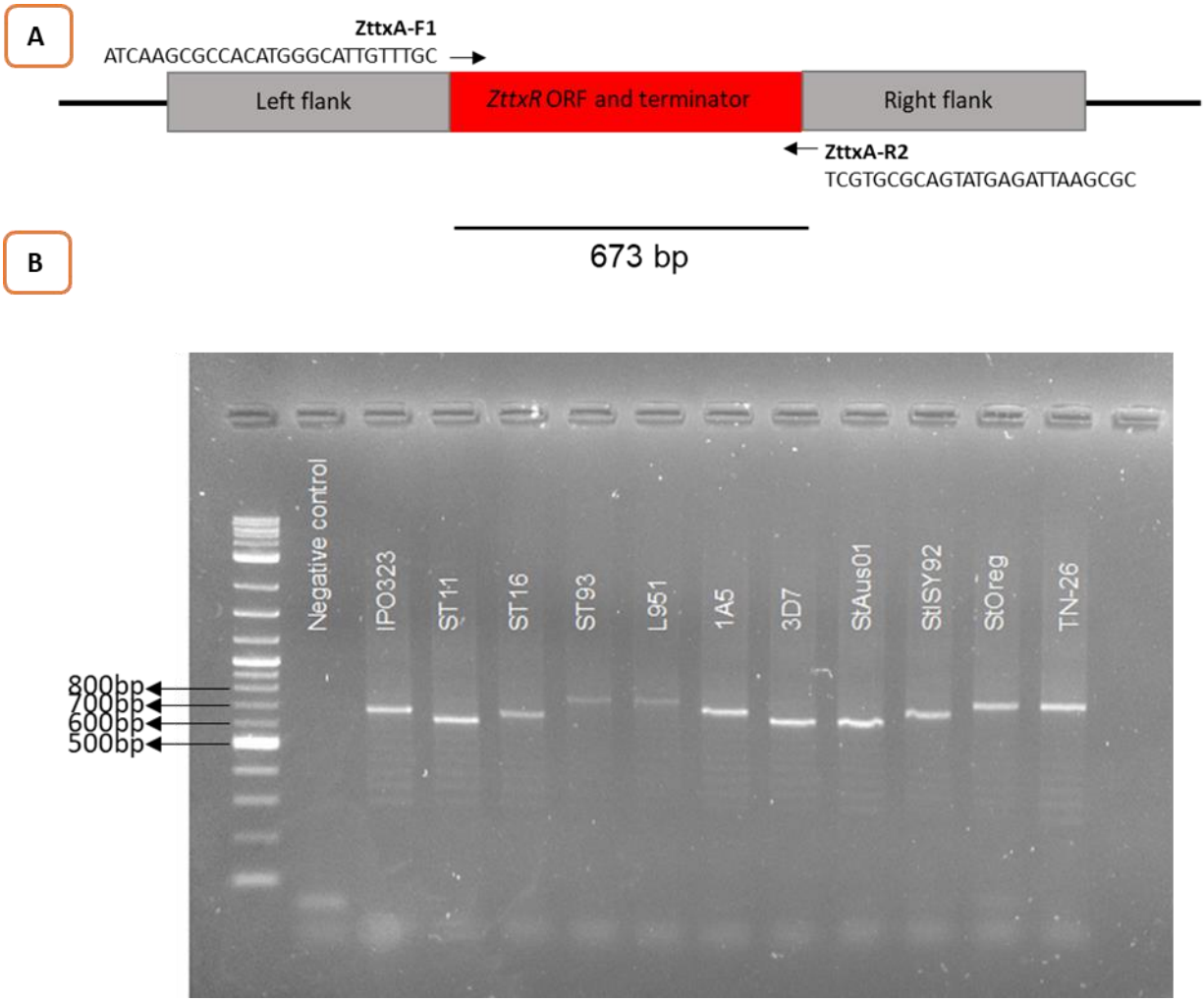

Figure 5.1 Amplification of the *Z. tritici* RiPP core repeat sequence unit from different isolates showing genomic variation in this region between strains.

A) Schematic map of PCR primer binding sites to the *Z. tritici ZttxA* genomic region (primers are named alongside their sequence). The site of primer annealing to the genomic *Z. tritici* DNA template is indicated by arrows and primer pairs are connected by a solid line – the expected amplicon size is stated and is based on the IPO323 strain. B) Gel electrophoresed PCR products from amplification of genomic DNA isolated from IPO323, L951, ST11, ST16, ST93, 1A5, 3D7, StAus01, StISY92, StOreg, and TN-26 *Zymoseptoria tritici* isolates with the ZttxA-F1/ZttxA-R2 primer pair. No template DNA was used in a negative control reaction to ensure no contamination had occurred. Band sizes are seen compared to an NEB 1kb 2-log ladder. Key molecular weights of the ladder are labelled.

Table 5.3 Predicted RiPP core subunit repeat numbers of *Z. tritici* strains based on gel electrophoresis.

An asterisk is used to denote repeat numbers that have been assigned from pre-existing sequence information (Goodwin et al., 2011). It was determined whether the amplicon size was greater than the IPO323 strain (>), equal to IPO323 (=) or less than IPO323 (<) in each instance. Each ~50bp size modification was assumed to represent a single core repeat change and total repeat unit number estimated based on this scheme.

Zymoseptoria tritici isolate	**Amplicon size relative to IPO323 (>/=/<)**	**Estimated core repeat unit number**
IPO323		9*
ST11	<	8
ST16	=	9
St93	>	11
L951	>	11
1A5	=	9
3D7	<	8
StAus01	<	8
StISY92	=	9
StOreg	>	10
TN-26	>	10

The PCR and gel electrophoresis-based method can only estimate repeat unit number and does not eliminate the possibility that variations in amplicon length between strains arise due to sequence differences within the *ZttxA* gene but outside of the repeat region. Similarly, since primers used in this work span an intron, genomic differences may exist in this region rather than the exon itself. As such, a bioinformatic approach was additionally undertaken. For *Z. tritici* isolates IPO323, L951, ST11, ST16, ST93, 1A5, 3D7, StAus01, StISY92, StOreg, and TN-26 this required that the DNA be used as a template in PCR using the proofreading Phusion *Taq* enzyme and once again the ZttxA-F1/ZttxA-R2 primer pair. The generated products were cloned into the pJET1.2 plasmid and transformed into chemically competent *E. coli* before sequencing with the pJET1.2F and pJET1.2R primers (Table 9.5).

Resultant sequences were manually searched for DNA encoding the 6-amino acid “YVIPVD” core repeat within the precursor peptide (Figure 5.2).

Alongside this, additional *Z. tritici* strains with publicly available genome sequences, were analysed. This was completed as above, identifying the *ZttxA* gene and searching this region for DNA encoding the YVIPVD repeat. Strains were initially identified by BLAST searching the IPO323 *ZttxA* gene sequence (BLASTn)(Altschul et al., 1990), limiting the results to *Z. tritici.* This yielded information on the 3D1 (GCA_900184105.1) and 1E4 (GCA_900184115.1*) Z. tritici* strains – as well as 1A5 (GCA_900099495.1) and 3D7 (GCA_900091695.1) which were experimentally investigated. At the time of investigation (March 2020), 19 assemblies existed on NCBI, including the IPO323 sequence and two assemblies of the same strain - Zt10 (STIR04_A26b). These assemblies were individually BLAST searched using the *ZttxA* gene sequence as a query. Only three additional strains with appropriate sequence data for analysis of variation within the *ZttxA* gene were identified – Zt05 (GCA_002937425.1) and Zt10 (GCA_002937415.1) and ST00Arg1D1a1 (GCA_902712725.1). Due to the repetitive nature of the sequence, assembly issues when using short-read sequencing methods was common (Table 5.4).

Combined, bioinformatic data based on known and novel *ZttxA* sequences, indicate that core repeat unit number does vary between strains. In this work, a range of 6 to 11 repeats across strains was noted (Figure 5.2). Of the 16 strains that could be analysed in this work, the majority had repeat numbers greater than or equal to 10 repeats with four strains displaying 11 repeats and six strains encoding 10 repeats. Smaller repeat unit numbers were less frequently seen in the *Z. tritici* strains examined here – only one strain had 6 repeat units, two strains had 8 repeats and three strains had 9 repeats. Higher repeat unit numbers were most common for the strain selection analysed in this work.

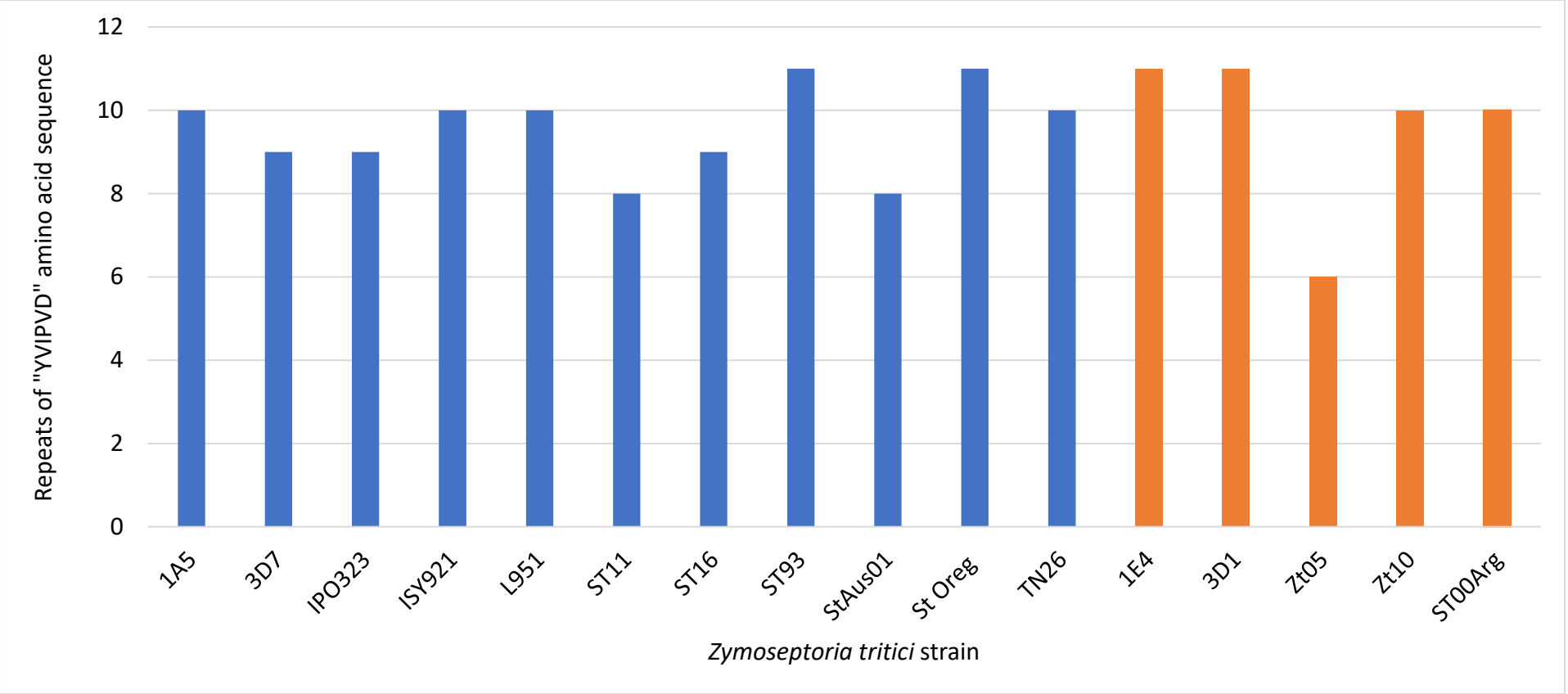

Figure 5.2 RiPP core peptide sequence repeat number variations across *Zymoseptoria* tritici strains.

Repeat number of the DNA sequence encoding the "YVIPVD" RiPP core amino acid peptide sequence in 16 *Zymoseptoria tritici* strains. Blue bars are used for strains which have been sequenced in this work following cloning the *ZttxA* gene into pJET1.2. Orange bars are used for strains for which the *ZttxA* genomic region had already been sequenced and were available on NCBI. The IPO323 strain *ZttxA* region was sequenced in this work to ensure the repeat number allied with that from Goodwin et al. (2011).

Table 5.4 *Zymoseptoria tritici* genome assemblies lacking sufficient data for RiPP core peptide sequence repetition analysis.

The *Zymoseptoria tritici* strains for which genome assemblies are available on NCBI but have insufficient information to accurately determine repeat number within the *ZttxA* gene are listed. The issue preventing RiPP core unit investigation is noted alongside the sequencing technology used in these works to generate sequence data.

Strain and genbank identifier	**Assembly issue**	**Genome sequencing technology**
Zt02 (GCA_003611065.1)	The start and end of the *ZttxA* gene are found on two different scaffolds. Scaffolds overlap only over repeat region indicating a loss of repeat information.	Illumina HiSeq
Zt04 (GCA_003611135.1)	The start and end of the *ZttxA* gene are found on two different scaffolds. Scaffolds overlap only over repeat region indicating a loss of repeat information.	Illumina HiSeq
Zt07 (GCA_003613095.1)	The start and end of the *ZttxA* gene are found on two different scaffolds. Scaffolds overlap only over repeat region indicating a loss of repeat information.	Illumina HiSeq
Zt148 (GCA_003611175.1)	The start and end of the *ZttxA* gene are found on two different scaffolds. Scaffolds overlap only over repeat region indicating a loss of repeat information.	Illumina HiSeq
Zt150 (GCA_003611055.1)	The start and the end of the *ZttxA* gene is found on the same scaffold but the central portion of the gene contains a long stretch of N reads.	Illumina HiSeq
Zt151 (GCA_003611075.1)	The start and the end of the *ZttxA* gene is found on the same scaffold but the central portion of the gene contains a long stretch of N reads.	Illumina HiSeq
Zt153 (GCA_003611115.1)	The start and end of the *ZttxA* gene are found on two different scaffolds. Scaffolds overlap only over repeat region indicating a loss of repeat information.	Illumina HiSeq
Zt154 (GCA_003611185.1)	The start and end of the *ZttxA* gene are found on two different scaffolds. Scaffolds overlap only over repeat region indicating a loss of repeat information.	Illumina HiSeq
Zt155 (GCA_003611125.1)	The start and end of the *ZttxA* gene are found on two different scaffolds. Scaffolds overlap only over repeat region indicating a loss of repeat information.	Illumina HiSeq
STIR04 A48b (GCA_000223625.2)	Only the end of the *ZttxA* gene is identified when BLAST searched with the IPO323 *ZttxA* gene sequence.	Illumina

5.3.2 Geographic localisation of *Z. tritici* strains and RiPP core peptide sequence repeat number

Strains L951, St11, St16 and St93 were all isolated from Long Ashton research station over several years – 1995 for the first three strains and 1993 for St93. These strains therefore demonstrate that there is no association between repeat number and geographic localisation as none of the strains have the same repeat number. Unfortunately, the wheat cultivars from which these strains were isolated are unknown and therefore any link between repeat number and the infected cultivar cannot be determined.

5.3.3 Sequence analysis of *Z. tritici* strains

Searching sequence data for the YVIPVD amino acid sequence (encoded within the DNA) alone, does not take into account the potential for alternative core peptide sequences to exist in alternate *Z. tritici* strains. As such, *ZttxA* genomic information from the different strains was translated (excluding introns) and the amino acid sequences aligned against each other, as well as the IPO323 strain, using BioEdit (Hall, 1999)(Figure 5.3). Sequences from NCBI were aligned from the start codon encoded methionine amino acid onwards while sequences amplified with ZttxA-F1 and cloned into pJET, and as such lacking the ATG start codon, were aligned from the first in frame codon (encoding the 4th amino acid in the precursor peptide sequence). This was the case for all cloned sequences except for TN26, for which sequencing data was only of sufficient quality for alignment from the 6th amino acid onwards (Figure 5.3). Untranslated DNA sequences were also aligned (Figure 9.1).

DNA sequence comparisons showed synonymous mutations within the repeat region, namely a substitution of GTG for GTC (both resulting in a valine amino acid) in strain 3D1 and TN26. Amino acid sequence comparisons between strains serve to further highlight the repetitive nature of the precursor peptide and how core repeat unit number varies between strains. Amino acid sequences were largely conserved within the precursor peptide, with only three non-synonymous mutations observed across strains. The DNA sequence for Zt10 showed a five base pair deletion at position 187, which causes a frame shift of the coding sequence. This results in the insertion of an early stop codon and likely a non-functional protein (Figure 5.3). Single amino acid substitutions are noticeable in the L951 and 3D1 strains. For L951 this exists within the core repeat unit with the 3rd position isoleucine being replaced by a methionine. Therefore, this strain has 10 YVIPVD repeats as well as one YVMPVD unit. In the instance of 3D1, the substitution occurs outside of the core repeat unit,

and changes a Kex2 KR processing residue to KG. This nonsynonymous substitution could impact the protease recognition site and prevent this protein from releasing all the encoded peptides.

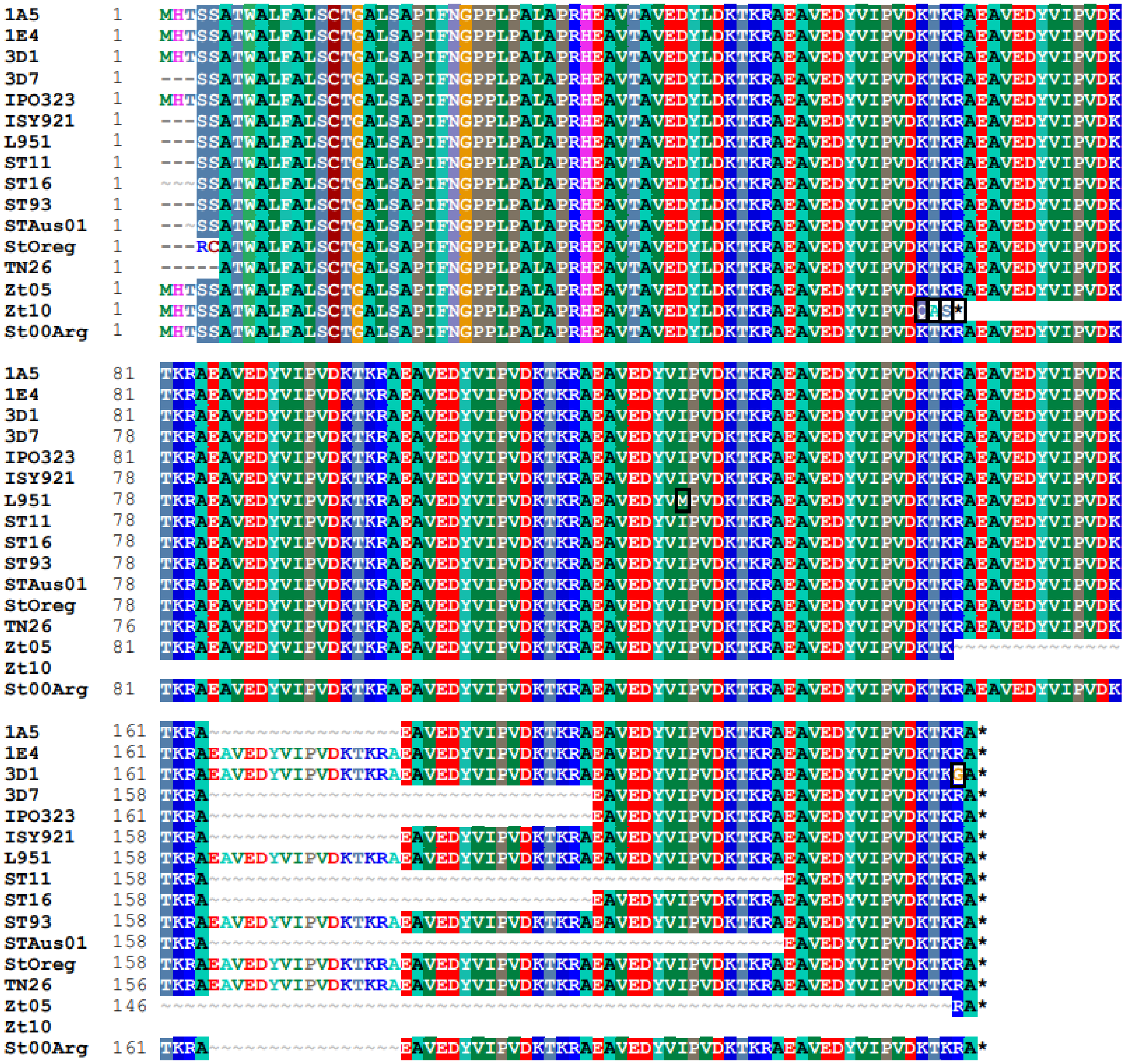

Figure 5.3 Amino acid sequence alignment of the translated *Z. tritici ZttxA* gene in several strains.

The zymoseptorin precursor peptide is highly conserved across strains. Of the 16 strains analysed only one showed massive disruption of the *ZttxA* gene sequence to the extent of loss of the core RiPP subunit amino acid sequence. The Zt10 strain has a DNA deletion in the *ZttxA* gene resulting in a frameshift. In the other strains only few amino acid substitutions can be noted, these are highlighted by black boxes. In L951 this single amino acid change results in a YVMPVD core variant and in 3D1 a Kex2 KR recognition site is lost.

5.3.4 The impact of core peptide repeat number on transcription of the *ZttxA* gene

It had previously been proposed by Umemura et al. (2014) that increased repeat number of the core peptide sequence within the precursor results in greater final RiPP titre. However, due to difficulties extracting zymoseptorin from *Z. tritici*, this could not be tested within this work. Instead, RT-qPCR was completed to determine whether strains with varying numbers of repeats within the precursor are capable of regulating the transcription of the *ZttxA* gene to compensate for these differences – potentially resulting in similar overall peptide titres but by different methods. The IPO323 (9 repeats), StAus01 (8 repeats), 3D7 (9 repeats), TN26 (10 repeats), and St93 (11 repeats) strains were selected for qPCR based on their varied repeat numbers. The IPO323 and 3D7 strains, both with nine repeats were selected to compare gene expression levels of strains with the same number of repeats too. cDNA produced from nine-day old CD+YE liquid cultures was used in qPCR and primed with the ZttxA-F/ZttxA-R primer pair (not in the repeat region)(Figure 5.4). The *HH3* gene was used as a reference gene.

ZttxA gene expression was shown to significantly differ by strain in a Kruskal-Wallis test ($p<0.05$). A Dunn post-hoc test with Benjamini-Hochberg correction revealed that only the IPO323 and TN26 strains of *Z. tritici* significantly differed from one another ($p<0.05$) with TN26 showing a reduction in relative gene expression levels compared to the IPO323 strain of ~446%. Overall, transcript levels of the *ZttxA* gene vary between strains with no clear pattern relative to copy number – strains with fewest repeats did not upregulate gene expression, nor did strains with the greatest number of repeats consistently downregulate gene expression.

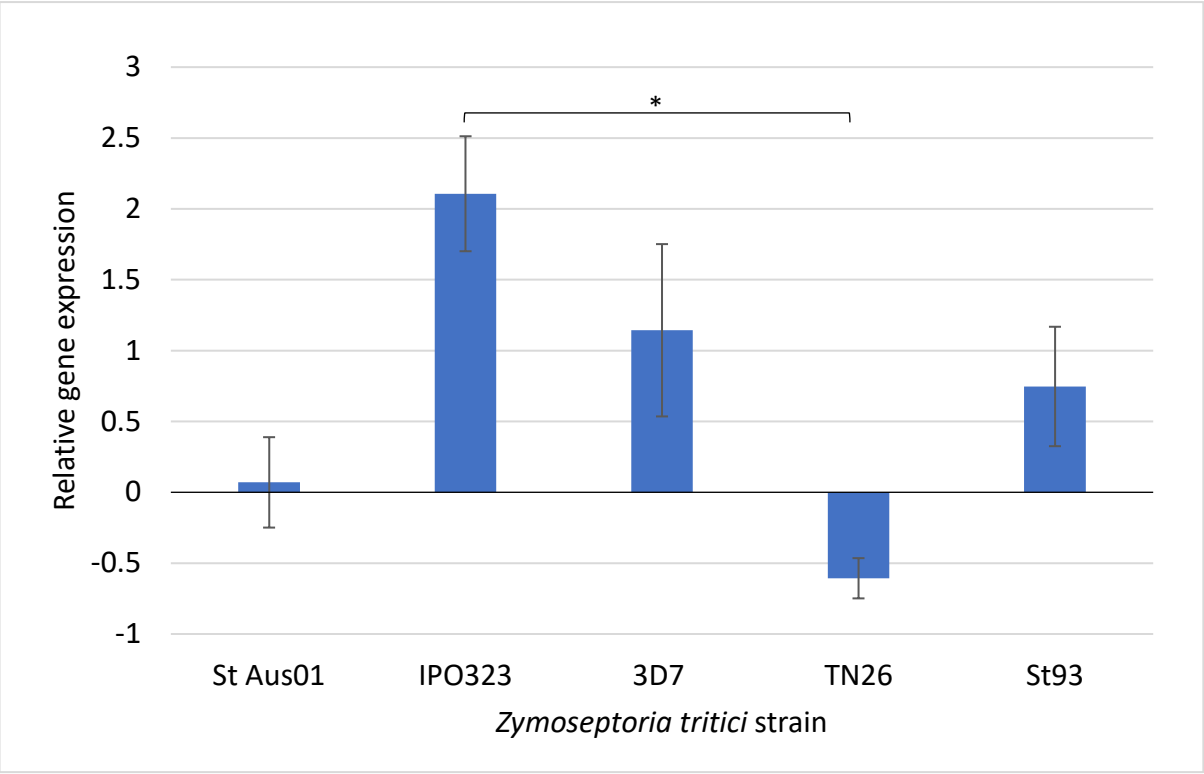

Figure 5.4 Gene expression of the *ZttxA* gene in *Zymoseptoria tritici* strains with varying numbers of core peptide sequence repeats.

Gene expression of the five selected strains after growth for nine days in CD+YE liquid media. Strains are presented in order of repeat unit numbers (least on the left and greatest on the right). Relative gene expression of the *ZttxA* gene was determined using the primers ZttxA-F/ZttxA-R. Values are *ZttxA* gene expression relative to *HH3* for each strain. Error bars are +/- standard error of the means (N=3). Horizontal lines topped with an asterisk indicate strains which significantly differ from each other at the $p<0.05$ level.

5.3.5 Finding novel dikaritin RiPPs

The approach taken by Ding et al. (2016) using protein BLAST searches with the phomopsin biosynthetic cluster proteins was repeated in this work. Here, the *Z. tritici* cluster proteins ZttxA, ZttxQ, and ZttxY1 were used as queries in protein BLAST in order to identify further putative RiPPs from their similarity to the *Zymoseptoria tritici* RiPP cluster rather than the phomopsin cluster. These proteins were selected based on their known importance to dikaritin RiPP generation in other species with loss of any one of these proteins abolishing mature RiPP production (Ding et al., 2016, Sogahata et al., 2021, Nagano et al., 2016) – this

is through loss of the cyclisation modification applied by the Ust/PhomQ and PhomY1/UstYb proteins; or loss of the precursor peptide. BLAST searches were limited to Ascomycete fungal species and the E value cut-offs of $1E^{-10}$ used for ZttxA and ZttxY1 and $1E^{-20}$ for ZttxQ. Species with homologs for these genes were recorded and a database formulated. Species that had homologs of all three proteins were identified, and their genomes examined to uncover if the genes were contiguous - forming a putative RiPP biosynthetic gene cluster.

30 species were shown to possess RiPP protein homologs, but for only 25 species did the genes encoding these form potential biosynthetic clusters. Of these 25 species, several had previously been identified as known dikaritin RiPP producers, namely *Ustilaginoidea virens (Tsukui et al., 2015), Aspergilus flavus (Nagano et al., 2016, Ye et al., 2016)* and *Phomopsis leptostromiformis*, (Ding et al., 2016). A further eight had been uncovered from genome mining conducted by Ding et al. (2016)(Table 9.10) or were alternative producer strains of those highlighted by Ding et al. (2016), including: *Aspergillus oryzae, Aspergillus parasiticus, Aspergillus flavus*. Three additional RiPPs had been identified as Kex2-processed repeat proteins (KEPs) in Umemura (2020): *Aspergillus arachidicola*, *Cordyceps fumosorosea ARSEF 2679* and *Penicillium polonicum* (Table 9.11). From my analysis, seven additional putative novel RiPP producers were identified: *Aspergillus pseudocaelatus, Aspergillus pseudonomius, Cordyceps militaris, Aspergillus sergii, Aspergillus novoparasiticus, Aspergillus minisclerotigenes and Aspergillus coremiiformis*.

Following the completion of this work in 2020, a novel bioinformatics resource called Cblaster was developed (Gilchrist et al., 2021) which allows multiple protein BLAST analysis to be automated. The protein query sequences were again employed however the tool itself analyses the genome for contiguous genes. Cblaster was queried with the ZttxA, ZttxQ and ZttxY1 protein sequences and the results corroborated with those garnered from the manual database comparisons. The Cblaster search was completed 26/5/23. This yielded 39 possible RiPP producing clusters. Removing those already identified by other research groups, as noted above, left 10 possible novel dikaritin RiPP producers (Table 5.5). Again, alternative strains for species which are already known to produce dikaritin RiPPs were identified but were not analysed in detail. Only species *Icmadophila ericetorum, Lecanicillium fungicola* and *Penicillium freii* were not identified by the database but highlighted by Cblaster.

Table 5.5 Blast outputs generated from using the ZttxA, ZttxQ, and ZttxY1 Zttx cluster proteins as query sequences.

Accession number and species	ZttxA				ZttxQ				ZttxY1			
	Bit score	E-value	Percent Coverage	Percent Identity	Bit score	E-value	Percent Coverage	Percent Identity	Bit score	E-value	Percent Coverage	Percent Identity
Aspergillus coremiiformis (KAE8351272.1)	95.1	2.12E-19	77.55	48.03	257	2.22E-76	64.36	59.14	127	1.01E-34	86.99	49.61
Aspergillus minisclerotigenes (KAB8276095.1)	103	2.93E-23	95.41	39.68	265	2.55E-79	100	44.98	120	1.44E-30	58.9	61.63
Aspergillus novoparasiticus (KAB8217959.1)	104	1.30E-23	93.37	35.84	291	6.70E-89	100	48.1	120	5.82E-31	58.9	60.47
Aspergillus pseudocaelatus (KAE8418376.1)	104	1.94E-24	68.88	57.78	377	2.06E-127	100	57.78	202	1.91E-62	100	60.27
Aspergillus pseudonomiae (XP_031938991.1)	110	8.21E-26	95.41	40.21	375	8.89E-127	100	58.13	120	5.75E-31	58.9	60.47
Aspergillus sergii (KAE8325628.1)	109	2.44E-25	93.37	41.08	330	3.89E-104	100	52.25	121	3.17E-31	58.9	60.47
Cordyceps militaris (ATY60394.1)	119	8.26E-27	77.55	52.76	353	6.21E-118	99.65	57.99	184	2.14E-55	98.63	56.94
Diaporthaceae sp. PMI_573 (KAH8785180.1)	188	1.16E-56	77.55	77.78	369	7.76E-124	99.65	60.07	191	5.09E-58	98.63	29.72

Icmadophila ericetorum (MCJ1357632.1)	182	5.09E-53	96.43	52.67	261	2.45E-83	69.2	60.5	190	1.40E-57	98.63	55.56
Lecanicillium fungicola (KAJ2978183.1)	82	4.49E-16	61.73	51.24	377	1.54E-127	99.65	58.33	86.3	5.04E-17	91.78	36.13

The precursor peptide of each putative RiPP cluster was analysed further for each producer. The homologous proteins identified from Cblaster searches were manually examined for repetitive core peptide sequences, identifying core peptides six amino acids in length and flanked at the C-terminal by Kex2 recognition sites (Table 5.6). The genomic regions identified by Cblaster within which the contiguous sequences existed were used as query sequences in antiSMASH fungal version (Blin et al., 2023) and the entire RiPP cluster visualised alongside zymoseptorin using clinker (Gilchrist and Chooi, 2021)(Figure 5.5).

Table 5.6 Putative dikaritin RiPP producers identified from homology to the zymoseptorin RiPP biosynthetic gene cluster and the precursor peptide amino acid sequence.

The newly uncovered putative RiPP producers are listed alongside the accession number for the protein analysed. Repetitive suspected core peptide subunits are shown in bold, different colours are used for each different repeat variant seen across species. The number of repeat units within each precursor is identified in relation to the entire amino acid sequence length of the precursor peptide. Only repeats flanked with a KR, RR, or KK residue were determined to be core RiPP units. The *Cordyceps militaris* RiPP cluster was previously reported by Zhang et al. (2022a), however the precursor peptide was not investigated – this sequence is analysed here.

Accession number and species	**Length (bp)/ Repeats**	**Sequence**
Aspergillus coremiiformis (KAE8351272.1)	**294/17 YAIGVD; 2 YAIGIN; 3 YAIGID**	MKLLLSLFVSGLCVLAAPRPKPSGVQD**YAIGVD**KRGSVED**YAIGVD**KRGVED**YAIGVD**KRSVED**YAIGIN**KRGSVED**YAIGVD**KRNSVED**YAIGVD**KRGSVED**YAIGID**KRSVED**YAIGID**KRSVED**YAIGVD**KRGSVED**YAIGID**KRSVED**YAIGVD**KRGVED**YAIGVD**KRSVED**YAIGVD**KRGVED**YAIGVD**KRSVED**YAIGVD**KRGVED**YAIGVD**KRSVED**YAIGVD**KRGVED**YAIGVD**KRGVED**YAIGVD**KRGVED**YAIGVD**KRGSVED**YAIGIN**KRSVED**YAIGVD**KRH
Aspergillus minisclerotigenes (KAB8276095.1)	**211/ 14 YAIGID**	MKLILTLLVSGLCALAAPAAKRDGVED**YAIGID**KRNSVED**YAIGID**KRNSVED**YAIGID**KRNTVED**YAIGID**KRNSVED**YAIGID**KRNTVED**YAIGID**KRNSVED**YAIGID**KRNSVED**YAIGID**KRGGSVED**YAIGID**KRNSVED**YAIGID**KRNSVED**YAIGID**KKRNSVED**YAIGID**KRGSVED**YAIGID**KRGGSVED**YAIGID**KRHGGH
Aspergillus novoparasiticus (KAB8217959.1)	**225/ 15 YAIGID**	MKLMLTLLVSGLCALAAPAAKRDGIED**YAIGID**KRNSVED**YAIGID**KRNSVED**YAIGID**KRNSVED**YAIGID**KRGGSVED**YAIGID**KRNTVED**YAIGID**KRNSVED**YAIGID**KRNSVED**YAIGID**KRNSVED**YAIGID**KRNTVED**YAIGID**KRNSVED**YAIGID**KKRNSVED**YAIGID**KRNSVED**YAIGID**KRGGSVED**YAIGID**KRGGSVED**YAIGID**KRHAGH

Aspergillus pseudocaelatus (KAE8418376.1)	**155/ 9** **YVIEVG**	MKLVPTLLVSGLCVLAAPMAESNAVED**YVIEVG**KRDGGVED**YVIEVG**KRDAIED**YVIEVG**KRDAVED**YVIEVG**KRDEGVED**YVIEVG**KRDEGVED**YVIEVG**KRDEGVED**YVIEVG**KRDEGVED**YVIEVG**KRDEGVED**YVIEVG**KRDAIEDYVIEV
Aspergillus pseudonomiae (XP_031938991.1)	**218/ 13** **YAIGID**	MKLMLTLLVSGLCALAAPAAKRDGIED**YAIGID**KRSSVED**YAIGID**KRNSVED**YAIGID**KRGGSVED**YAIGID**KRNSVED**YAIGID**KRGGSVED**YAIGID**KRNSVED**YAIGID**KRGGSVED**YAIGID**KRNSVEDYAIGIDMCGFSVED**YAIGID**KRNSVED**YAIGID**KKRNSVEDYAID**YAIGID**KRNSVED**YAIGID**KRGGSVED**YAIGID**KRHAGH
Aspergillus sergii (KAE8325628.1)	**239/ 16** **YAIGID**	MKLMLTLLVSGLCALAAPAAKRDGIED**YAIGID**KRNSVED**YAIGID**KRNSVED**YAIGID**KRNSVED**YAIGID**KRNSVED**YAIGID**KRNSVED**YAIGID**KRGGSVED**YAIGID**KKRSSVED**YAIGID**KRNSVEDYAIGIDKRGGSVED**YAIGID**KRNSVED**YAIGID**KRNTVED**YAIGID**KRNSVED**YAIGID**KKRNSVED**YAIGID**KRGSVED**YAIGID**KRGGSVED**YAIGID**KRHAGH
Cordyceps militaris (ATY60394.1)	**185/3** **YAIAVD; 1** **YVIAVD; 6** **YAIGVD, 1** **YVIQVD**	MKLSLIAVLAVGGAIAAPTRLDNAVED**YAIAVD**KRGSVED**YAIAVD**KRGSVED**YVIAVD**KRGSVED**YAIAVD**KRGGSVED**YAIGVD**KRGGSVED**YAIGVD**KRGGSVED**YAIGVD**KRGGSVED**YAIGVD**KRGGSVED**YAIGVD**KRGGSVED**YAIGVD**KRGGSVQD**YVIQVD**KRGGSVEDYAIGVDQ
Diaporthaceae sp. PMI_573 (KAH8785180.1)	**202/11** **YVIPID**	MRFTPAIIVAAFCSLATAAPAAKAVARAASEAVED**YVIPID**KRSEAVED**YVIPID**KKRGEAVED**YVIPID**KRSEAVED**YVIPID**KKRGEAVED**YVIPID**KKRGEAVED**YVIPID**KRSEAVED**YVIPID**KRGEAVEDYVIPIDKKRGEAVED**YVIPID**KRSEAVED**YVIPID**KKRGEAVEDYVIPIDKKRGEAVEDYVIPIDK
Icmadophila ericetorum (MCJ1357632.1)	**295/13** **YVIPVD; 2** **YIIPVD; 1** **YVIPID**	MKYTTAFLFAALCTGSLAAPAPRANAFNNLFEPVEKRAQSVED**YVIPVD**KRAQSVED**YIIPVD**KRHESVED**YVIPVD**KRAQSVED**YVIPVD**KRAQSVED**YVIPVD**KRHESVED**YVIPVD**KRAQSVED**YVIPVD**KRAQSVED**YIIPVD**KRHESVED**YVIPVD**KRHESVED**YVIPVD**KRHESVED**YVIPVD**KRHNMVEDFFTPLNKRAQSVED**YVIPID**KKARRAQSVED**YVIPVD**KRHESVED**YVIPVD**RRGVSVED**YVIPVD**KKVKRGVSVEDYVIPVDKV
Lecanicillium fungicola (KAJ2978183.1)	**124/3** **YAIAVD; 3** **YAIGVG**	MKVSLISALAAGIAIAAPTPSANSIQD**YAIAVD**RRNAVED**YAIGVG**KRGGAVED**YAIAVD**KRNAVED**YAIAVD**KRNAVEDYAIGRNAVED**YAIGVG**KRNAVED**YAIGVG**KRGGAVQDYVIEVDK

Across the species identified here, 11 different core subunit variants were identified. Core peptide subunits can be shared across species. Indeed, the YVIPVD core unit of zymoseptorin is also found in *Icmadophila ericetorum,* while the YVIPID phomopsin subunit is also noted for *Diaporthaceae sp*. Of the novel RiPPs identified, YAIGVD is shared by *Aspergillus coremiiformis* and *Cordyceps militaris*; and YAIAVD *by Cordyceps militaris* and *Lecanicillium fungicola*. Notably, with the exception of *A. pseudocaelatus* for which the repeat unit is YVIEVG, all *Aspergillus sp.* identified in this work have the YAIGID repeat unit making this the most common subunit identified in this work. However, *Aspergillus* species clearly do not exclusively produce this subunit and in addition to YAIGID, *Aspergillus coremiiformis* also has YAIGVD and YAIGIN units – YAIGVD is the predominant repeat within this species and the other variants are produced to lesser extents. Indeed, the precursor peptide encompassing multiple RiPP core subunits is not uncommon here as only six species produced just one core subunit type. Of the remaining four putative RiPP producers most precursors hold just two subunit types, though two species have greater variation than this (*Aspergillus coremiiformis* and *Cordyceps militaris* – the latter containing four repeat types).

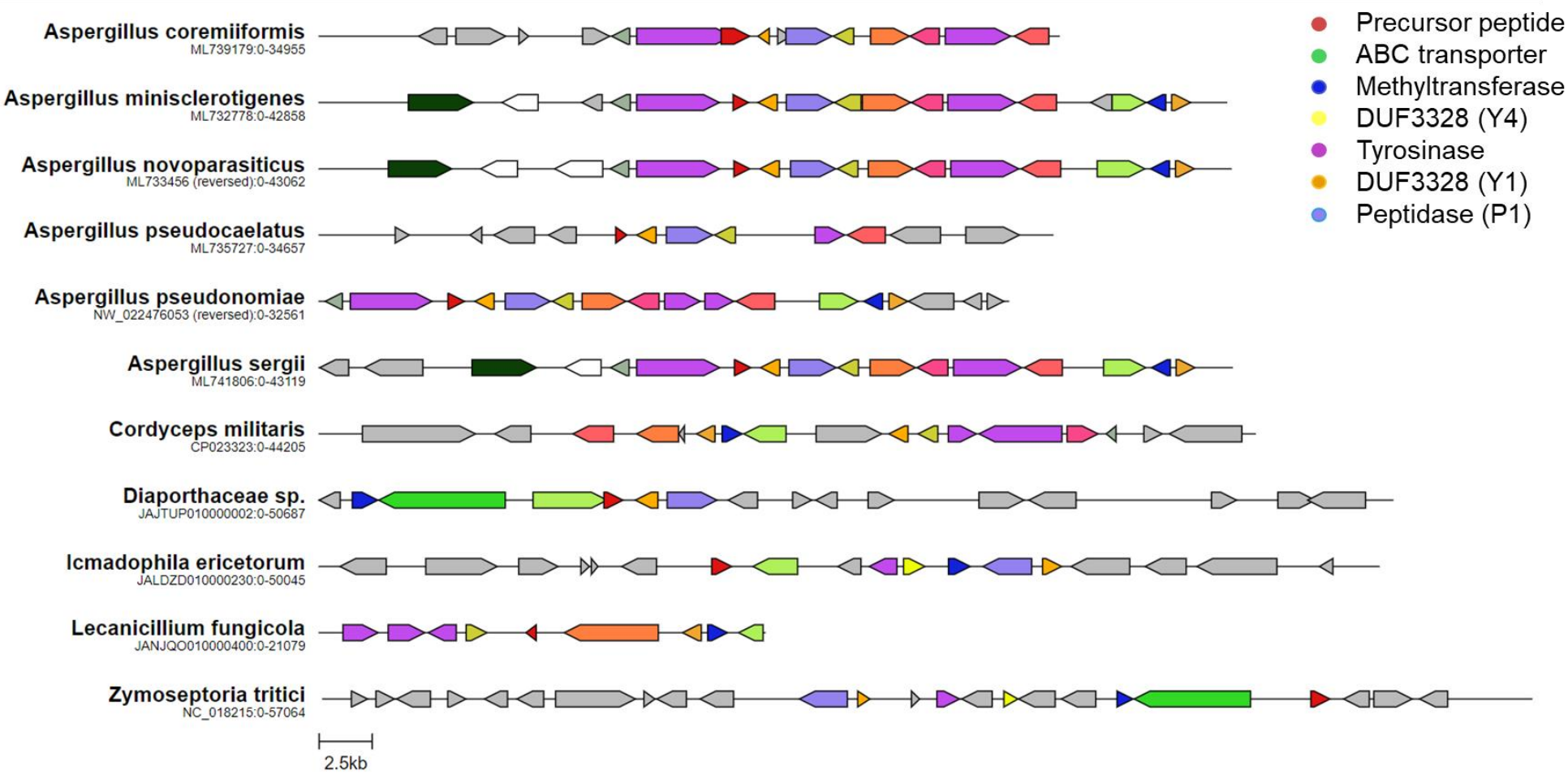

Figure 5.5 Clinker generated image highlighting similarities in putative RiPP biosynthetic cluster genes between species.

Colours are used to highlight cluster genes with similarity and the predicted function of these shown in the key. The information submitted to clinker is from gene cluster information generated by antiSMASH using publicly available genome sequences. For the IPO323 strain, the *ZttxR* gene is not shown in the cluster as this has not been annotated in the IPO323 assembly.

5.4 Discussion

5.4.1 RiPP core unit repeat variation between *Z. tritici* strains

Zymospetoria tritici strains, prior to this work, were already known to vary in regard to internal tandem repeats within protein coding sequences (Rudd et al., 2010). Indeed, in work by Rudd et al. (2010), unbeknownst to the authors, the TRP11 sequence analysed was that encoding the zymoseptorin precursor peptide. As such, just as other RiPP producing species have been shown to vary in core peptide subunit repeat number between strains (Table 5.2)(Ding et al., 2016) so too had this been intimated for *Zymoseptoria tritici*. However, the true extent of this variation was not verified until the completion of this work. In Rudd et al. (2010), comparisons were made to the IPO323 fully sequenced *Z. tritici* strain, as in this work, sequencing only the repetitive region of the *ZttxA* gene for one further strain - IPO92006. Analysis of this sequence data reveals 12 repeats of the core unit to exist within the IPO92006 strain with this being the highest repeat number of all strains investigated genomically.

Within Rudd et al. (2010), beyond IPO323 and IPO92006, seven further *Z. tritici* strains were investigated using the gel electrophoresis-based method also employed in this work. However, here we have seen that analysing genomic DNA based on sequence length is not always accurate (since gel electrophoresis-based estimations of strain repeat numbers aligned with sequence data only half of the time) and cannot fully inform regarding the final peptide produced. Indeed, alternative sequences within the repetitive region can exist, as for the L951 strain. So too can insertions or deletions in the coding sequence result in total disruption of the subsequent protein produced – as in Zt10 (Figure 5.3). In these instances, PCR product sizes would be unchanged, or undetectable, by gel electrophoresis, highlighting the necessity of genomic sequence analysis. It is important to note though that, the gel electrophoresis-based method for predicting repeat unit number still holds value as a means of identifying potential errors in sequencing since an expected total sequence length is identified.

Despite the importance of accurate genomic information to this investigation and others, during this work it was noted that for many publicly available assemblies this data is incomplete (Table 5.4). Though often assembled to the scaffold level, and both the start and end of the *ZttxA* gene identifiable on two separate scaffolds, the repeat numbers identified

across the two are consistently lower than those seen in any other strain. However, it is only these two scaffolds that are identified from BLAST searching the IPO323 *ZttxA* gene against the assembly. Therefore, it appears as though sequence generation using Illumina sequencing and assembly of this information results in data loss – with all unusable assemblies using Illumina sequencing generated data. Since Illumina sequencing generates ~300bp reads (Yoshinaga et al., 2018), this certainly does not span the 664bp genomic region over which the *ZttxA* gene exists. It is then likely that the short read nature of Illumina sequencing, leads to real reads of the repeat region being interpreted by assembly programmes as the same section sequenced multiple times rather than greater coverage of the genome. This mismatched alignment is not unique to *Z. tritici* genomes and is seen for multiple alignment software's applied to repetitive genomic regions when Illumina sequencing data has been used (Yu et al., 2012).

With this in mind, alongside the knowledge that several tandem repeat regions exist across the *Z. tritici* genome (Rudd et al., 2010), it may be beneficial when generating genomic data on further strains of the fungus to employ long read technologies. Specifically for further analysis of the zymoseptorin precursor gene it would be useful to repeat the PCR, cloning and sequencing work conducted here for Illumina sequenced strains to determine if the assumed data loss is a real difference in repeat number or a consequence of the technology used in these analyses. Following this we may see that fewer or more repeats and modifications to those identified within this work exist. Indeed, after the completion of this analysis, additional *Z. tritici* assemblies have become available on NCBI, including: WAI321, WAI332, WAI323, Zt469, Zt289, 553.11, 560.11 – in these strains alone a new minimum of five repeats was identified.

The existence of repeat unit variation in *Z. tritici* strains is confirmed here, but the purpose of this remains elusive. Umemura et al. (2022) have argued that the repeat functions to stabilise gene transcripts – though exactly how this occurs is not yet known. Perhaps a much simpler explanation comes from natural selection. It seems more likely that the function of the RiPP peptide, though currently unknown, is directing selection for greater or fewer repeats when they arise by spontaneous mutation. If more repeats result in greater titre, should the peptide be of use to the fungus, mutant strains with higher repeat numbers will

be selected for. Equally if the peptide is no longer of use and rather a costly artefact to produce, reducing repeat number would be advantageous.

A similar argument can be applied for the novel YVMPVD core unit found within the L951 *Z. tritici* strain. Multiple instances of this mutation arising in different strains would indicate that this mutation is useful to the fungus and worth maintaining. However, as this mutation is not seen in any other strain, this is unlikely to be the case. Indeed, given the conserved amino acid residues on which dikaritins are known to be cyclised (Vogt and Kunzler, 2019), this amino acid substitution may prevent peptide processing and the production of a mature RiPP. What is more conceivable then is that the L951 strain, which already has 10 YVIPVD repeats is not massively negatively impacted by the variant and therefore there is so no real incentive to lose it quickly. Though we cannot be certain that YVIPVD is the original core unit sequence, given that no other RiPP producer identified in this work produces a YVMPVD core while additional species to *Z. tritici* have a YVIPVD sequence, this order of evolution seems the most parsimonious.

5.4.2 The impact of zymoseptorin core repeat unit number on RiPP precursor gene expression

Though it has not been possible within this work to realise the impact of different RiPP core repeat unit numbers between strains on actual peptide titre, it has also been shown that analysing transcript levels of the precursor gene can hold value. In fact, Umemura et al. (2022), following production of synthetic forms of the *Aspergillus flavus* ustiloxin B precursor gene with varying core repeat numbers, found that the impact of this on transcript levels differed from the effect had on peptide production. A linear increase on transcript levels with increasing repeat number was identified in the first instance and a quadratic increase in peptide tire noted in the second. As such, given the naturally existing variation in core repeats found within the *Z. tritici* strains examined in this work, this was investigated here too. However, the relationship between repeat number and transcript levels in *Z. tritici* was not as simple as in *A. flavus*. Here, the linear increase in transcript levels of the precursor gene was not identified and strains with 8 or 11 repeats did not significantly differ from each other in this respect (Figure 5.4). Indeed, the only significant difference in transcript levels noted was between the IPO323 and TN26 strains ($p<0.05$) with the latter having significantly reduced levels of *ZttxA* gene transcripts. Yet, the TN26 strain has a higher number of repeats

than IPO323 (10 and 9, respectively) and this effect is not consistent across strains with greater than 9 repeat units – ST93 with 11 repeats does not have significantly reduced *ZttxA* transcript levels. However, as the conditions which best induce *ZttxA* expression are still unknown, this trend may differ for samples grown in different media and could be better visualised with the addition of strains with more varied repeat numbers again.

Importantly, though Umemura et al. (2022) investigated the impact of repeat number in isolation, the use of synthetic genes replacing the native precursor gene each within the same strain of *A. flavus* (A1421) calls into question the applicability of these results to a real-life context. Strains, will seldom differ in just one gene and therefore, looking at repeat unit number alone is perhaps uninformative since it does not take other modifications between strains into account. Transcriptional data generated here, clearly demonstrates that beyond repeat unit number there are other factors at play influencing final rates of RiPP transcription and that these vary by strain.

5.4.3 Using zymoseptorin as a basis for novel RiPP discovery

Beyond understanding the *Z. tritici* RiPP, given that zymoseptorin was identified from genome mining based on similarity to the phomopsin cluster, use of the *Z. tritici* biosynthetic gene cluster to continue dikaritin RiPP discovery based on similarity to this cluster seemed logical. Not only this but since the Ding et al. (2016) work was completed, further genomic sequences will have become available and BLAST searchable. Searches for novel RiPPs in this work, though initially using the same method as Ding et al. (2016) did differ in its focus, using protein queries of ZttxA, ZttxY1 and ZttxQ (compared to PhomA, PhomQ and PhomM). Following the formation of databases of species capable of producing proteins with homology to those in the *Z. tritici* biosynthetic cluster in early 2020, greater understanding of the phomopsin biosynthetic cluster has been provided by Sogahata et al. (2021). This has made clear which genes are essential to dikaritin RiPP biosynthesis with experimental research also confirming this since, removing any one of the genes selected in this work abolishes peptide production (Nagano et al., 2016, Sogahata et al., 2021, Ding et al., 2016). Though involved in the post-translational modification defining the peptide class the methyltransferase gene (PhomM in the phomopsin cluster) is not essential to peptide production and post-translational modifications can be found in other forms (Sogahata et al., 2021). Equally, for some dikaritin RiPPs not all genes are required to be in the cluster – for

asperipin 2a, peptidases are absent, and this role fulfilled by peptidases encoded outside of the cluster (Nagano et al., 2016). As such, limiting the search to these identified core *ZttxA*, *ZttxY1* and *ZttxQ* genes avoids overlooking more diverse novel dikaritin peptides.

Of those novel dikaritin RiPPs identified here, there was a near equal split of precursor peptides with only one core repeat type and those with multiple. It therefore appears to be equally common for multiple different repeat units to exist within a precursor peptide, adding support to recent suggestions that this is more common than previously assumed (Vogt and Kunzler, 2019). What is somewhat unique among certain RiPPs, or at least less common, is the existence of more than two core repeat types, seen in only two of the precursor peptides identified here. In all instances where multiple core repeat sequence variants exist what can clearly be noted is the predominance of one repeat type over others. This is even clearer for those precursors with greater than two variations where often some variants exist only once or twice within the wider sequence. This seems to indicate that these less common variants have arisen more recently by mutation of the original DNA encoding sequence – especially as these amino acid sequences differ from others seen within the precursor usually by only one or two amino acids. However, sequencing of several strains would need to be conducted to confirm this.

Amino acid sequence similarity of repeats is largely unsurprising since even across species, precursor peptide amino acid sequences share similarities (Table 5.6). All identified in this work (except for L951), and by Ding et al. (2016), have a 1st position tyrosine residue and a 3rd position isoleucine amino acid – these being the known moieties on which a tyrosinase modification is applied and through which peptide cyclisation is achieved (Ding et al., 2016, Nagano et al., 2016); and all are flanked by Kex2 endoprotease recognition sites at the C-terminal of the core peptide (Julius et al., 1984). The impact of additional amino acids outside of the core sequence but before the Kex2 recognition motif is not yet understood. In *P. leptostromiformis* core repeats are flanked by KKR motifs; in *Z. tritici* core repeats are flanked by KTKR, but without the extracted compound the relevance of these differences, if any, cannot be assessed.

In addition to conserved 1st and 3rd position amino acid residues and processing motifs, often different species also share the same core repeat. Most obviously this is seen for *Aspergillus* species with nearly all having several repeats of the YAIGID core. The conserved

nature of this repeat indicates that the RiPP existed in the ancestor of all *Aspergillus* species with modifications of this sequence being indicative or more recent changes. Similarly, *Diaporthaceae sp. PMI_573*, an unclassified ascomycete species belonging to the *Diaporthaceae* family, shares the YVIPID repeat sequence with phomopsin (Ding et al., 2016, Sogahata et al., 2021). Given that *Phomopsis leptostromiformis*, has recently been renamed to that of its teleomorph *Diaporthe toxica* (Williamson et al., 1994, Ksiazkiewicz et al., 2020), so too is the phomopsin RiPP produced by a member of the *Diaporthaceae* family. As such perhaps the likelihood of sharing RiPP precursor core subunits can be predicted to the family taxonomical group level.

Notably, RiPP core units can also be seen in species that do not share a genus, specifically the YVIPVD zymoseptorin sequence is also found in *Icmadophila ericetorum* and *Penicillium freii*. However, it is important to note that a shared core unit does not necessarily equate to the same peptide being produced. Post-translational modifications are key to RiPPs and therefore fewer or greater modifying proteins in the biosynthetic gene cluster will result in slight changes to the mature RiPP. Though it cannot be denied that the basic amino acid sequence does confer a degree of similarity with Jingwei et al. (2022) arguing that the impact of these modifications on the final peptide is small. To address this, these peptides (and their biosynthetic clusters) should be investigated in greater detail to determine if they do in fact share a common chemical structure and function despite possible differences in processing.

Currently, little is known about the *Icmadophila ericetorum* and *Penicillium freii* clusters – the former identified in this work and the latter uncovered by Umemura (2020). Indeed, *Icmadophila ericetorum,* as well as *Lecanicillium fungicola,* were not initially detected as possible RiPP producers using the Ding et al. (2016) methodology based on a database formulated in 2020. The species were flagged, however, by Cblaster which searches all available sequences at the time of the query. Given that genomic data for these species became available post-2020 (2022/04/04 and 2023/01/09 for *Icmadophila ericetorum* and *Lecanicillium fungicola*, respectively), this result is unsurprising. The power of Cblaster is clearly demonstrable in this instance, providing up to date results in a matter of minutes – which manually takes several weeks.

However, it is interesting to note that in the two and a half years between the initial database formation and the Cblaster search only data for two further putative RiPP-producing species have become available. We must consider though that the default parameters of Cblaster were employed here, specifically the maximum intergenic distance of 20,000bp (Gilchrist et al., 2021). Given that *P. leptostromiformis* is not identified by Cblaster searches of ZttxA, ZttxQ, ZttY1 but rather ZttxA, ZttxQ, ZttY1 and ZttM, this lack of detection is likely due to using only few genes with these Cblaster default parameters. In future genome mining, a balance needs to be struck between using core genes so as not to exclude diversity, but also taking into account that using fewer genes can equally result in false negative results. Beyond this, novel RiPP discovery is clearly reliant on the availability of genomic information - many more RiPPs and RiPP producers than those identified in this work or others likely exist but without genomic data we cannot find them. The quality of this genomic information is however of high importance. Given the problems identified in this work of sequencing a repetitive region such as the precursor peptide gene, it is possible that homologous precursor genes are missed from BLAST searches due to short-read assembled genomes being of inadequate quality.

Similarly, in this work detection of whole fungal RiPP clusters, beyond the genes used in Cblaster searches, was based on antiSMASH fungal version (fungiSMASH) (Medema et al., 2011) – which is not always perfect. Indeed, antiSMASH is only capable of identifying novel clusters based on similarity to those that are already known to exist and have been characterised and annotated (Vignolle et al., 2020). In fact, initial investigations of the *Cordyceps fumosorosea* RiPP region yielded an NRPS match in earlier versions of the programme (Blin et al., 2021). It was not until more recent updates (Blin et al., 2023), that a RiPP cluster match was identifiable. Hence, the advancement of such software is continually making novel RiPP discovery easier and more reliable. Not only this, but as we find more clusters, there is a greater pool from which similarity can be found.

5.5 Summary

- *Z. tritici* strains from diverse geographical locations and collection dates differ in the number of tandem repeats within the RiPP precursor peptide.

- Mutations within the *ZttxA* gene between *Z. tritici* strains can result in modifications in the translated precursor peptide.
- Tandem repeat number across strains does not have a predictable influence on transcript levels of the *ZttxA* gene.
- Using the zymoseptorin biosynthetic gene cluster for comparison, 10 novel putative RiPP precursors and clusters were identified.
- Putative RiPP precursors both share RiPP repeat regions to known RiPP precursors as well as extend the current database of known RiPP core repeat units.

6 : *Zymoseptoria* and the environment

6.1 Introduction

The fungus *Zymoseptoria tritici* as a pathogen of wheat has been explored in previous chapters of this thesis – namely Chapter 1 and to some extent in Chapter 4. As a living organism, the fungus represents a biotic stress to wheat plants. However, wheat does not experience one stress at a time and often sees attack from multiple biotic stresses – whether this is different strains of the same pathogen (Curran et al., 2023) or a different organism entirely (Zhang et al., 2022b). In fact, Chapter 4 of this thesis hypothesised that this overlap of biotic stresses may have been the catalyst for plant pathogen evolution of toxic RiPPs, to prevent unintentional mycophagy and exclude other organisms (other sources of biotic stress).

Living organisms are just one source of stress to growing plants – the environment and its abiotic conditions can equally impact plant health and resultant growth with the disease triangle (Figure 6.1) being a key concept in plant pathology. Not only this, but just as a host plant is exposed to abiotic stresses, so too is the fungus, as different environmental conditions also effect fungal growth. In turn, the environment can modulate the plant response to infection and the pathogen's ability to infect a host. Therefore, this biotic interaction can be shifted and shaped by abiotic factors. The abiotic conditions impacting wheat and *Z. tritici* can be varied, however, within this work there is a focus on salinity, pH, light, and wind.

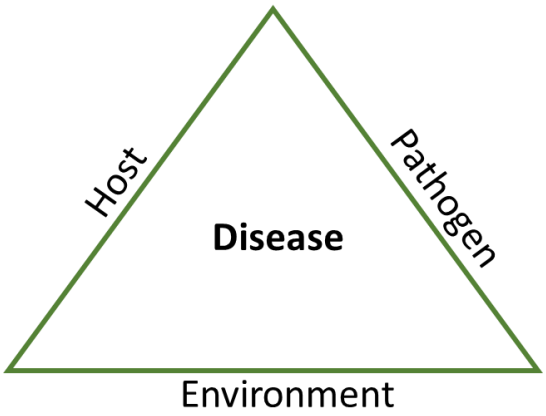

Figure 6.1 Schematic diagram showing the disease triangle concept.

The host, pathogen, and environment interact to produce final disease symptoms.

6.1.1 Wheat and the environment

The issue of high salinity levels in agricultural soils has existed for a long time (Boyer, 1982). Salt stress in plants can limit crop productivity, or in extreme cases lead to plant death (Allakhverdiev et al., 2000). Wheat is not exempt from this, though salt tolerant cultivars have been identified (Goudarzi and Pakniyat, 2008), with salinity stressed plants showing reduced biomass and grain yield (Sairam et al., 2002, Rajpar et al., 2005). Recent work has indicated that fertiliser application can help to limit the negative effects of salinity on wheat (Ibrahim et al., 2018). However, this can have negative implications on other abiotic conditions which can be equally damaging to plant health.

Soil pH can become acidified upon fertiliser application (Ghimire et al., 2017, Aula et al., 2016) with soil pH inversely correlated with soil aluminium saturation (Schroder et al., 2011). Plant toxic soluble Al^{3+} ions exist in soils with a pH range between 4.7 to 6.5 (Kariuki et al., 2007). Therefore, it is of no surprise that wheat yield when plants are grown in low pH soils is reduced compared to plants grown at a neutral pH (Kariuki et al., 2007). Soil pH can also influence the biotic community within wheat fields with greatest community stability seen in neutral pH soils (Fan et al., 2018). This could impact rhizosphere bacteria that may counter root infection and also nitrogen fixing organisms. pH changes could then lead to knock-on effects on wheat yield through reduced plant protection or nitrogen availability.

One of the lesser understood abiotic conditions influencing wheat is wind. Early investigations have shown that hot, dry wind applied at different stages of growth reduces wheat yield (Smika and Shawcroft, 1980). Equally, wheat lodging (wind induced displacement of wheat stems from a perpendicular position (Mondal, 2020)) lowers cereal yield and quality (Sterling et al., 2003, Fischer and Stapper, 1987, Acreche and Slafer, 2011). Lodging is the result of extreme winds, however, the impact of varying wind speeds on wheat is only starting to be appreciated with Araghi et al. (2022) seeing significant changes to wheat yield in the field depending on wind speed. This impact is perhaps unsurprising since we know wind can impact plant evaporation and transpiration as well as cause mechanical damage (Araghi et al., 2022). Responding to this stimulus may force the plant to sequester resources that would otherwise be channelled into growth resulting in this shift in productivity.

6.1.2 *Zymoseptoria tritici* and the environment

The necessity for *Z. tritici* to respond to and modify its behaviour in different biotic and abiotic contexts is well appreciated – we know that the fungus behaves differently *in planta* compared to *in vitro* at least from a transcriptional perspective (Kellner et al., 2014) – and equally the fungus shows distinct morphological changes under environmental stress (Francisco et al., 2019). Namely, morphotypes more conducive to survival (chlamydospores) are seen under abiotic stress conditions (Francisco et al., 2019, Francisco et al., 2023). Not only this, but environmental stresses such as nutrient-limited conditions may stimulate expression of potential virulence genes (Francisco et al., 2019). As such, the environment can not only impact upon fungal growth, but also virulence.

Fungi detect light and use this abiotic factor to regulate gene expression of important fungal processes (Yu and Fischer, 2019). Light, and its recognition by the white-collar complex, has even been implicated in the wheat infection process, potentially synchronising hyphal growth with the opening of wheat leaf stomata (Kilaru et al., 2022, Tiley et al., 2022, Tiley et al., 2019). Outside of the plant interaction, a light stimulus may allow fungi to prepare for stressful conditions, by stimulating the expression of DNA repair enzymes (Berrocal-Tito et al., 1999), since light itself can be a source of stress (Fuller et al., 2015). Fungi can also experience salt stress under which growth rates can be restricted (Stapley and McDonald, 2022) and cell metabolism disrupted (Hohmann, 2002). Equally, when *Z. tritici* is grown at low pH levels, reduced or no fungal growth is identified (Lynch et al., 2016). *Zymoseptoria tritici* is adapted and specialised to the pH and salt concentrations of its natural environment which is regulated by the plant during the latent phase of infection. During the necrotrophic stage of infection, the host no longer controls the conditions of the necrotic lesions and so the fungus may experience a range of conditions.

Rather than stress, abiotic factors can beneficially impact fungi. Given that *Z. tritici* ascospores are wind dispersed (Shaw and Royle, 1989), without this force, spores would not be liberated and spread, limiting fungal dispersal. Strong winds would permit greater spread and dislodging of spores, however, even wind speeds of 0.5m/s can disperse spores to downwind leaves (Mukherjee et al., 2021). In addition, wind can damage wheat leaves, with areas of damage (as well as stomata) providing a means of entry to the plant apoplastic space for the fungus (Fones et al., 2017).

6.1.3 Intersectionality of wheat and *Zymoseptoria tritici* in relation to the environment.

So far, the impact of abiotic factors on wheat and *Zymoseptoria tritici* have been investigated separately, both within this work and in research more widely (Sairam et al., 2002, Zhan and McDonald, 2011, Deihimi et al., 2013, Francisco et al., 2019, Stapley and McDonald, 2022). Often the impact of the environment is just in relation to the response of the plant or just the fungus rather than considering the intersectionality of abiotic stresses and the plant-pathogen interaction. The response of a plant and pathogen to an abiotic stress may be similar, for example in both instances growth may be reduced, however, when the abiotic factor coincides with this biotic interaction the result may be different.

Investigations into wheat responses to biotic and abiotic stresses (*Zymoseptoria tritici* infection and salt stress) indicate that the same proteins may be produced as a result of both (Deihimi et al., 2013). Indeed, if abiotic factors trigger the same changes in gene expression as those instigated by a biotic factor, such as a pathogen, this could serve to prime plant defences. Then, subsequent contact with a pathogen may not result in as high levels of infection. In the same way, diverse environmental factors can influence fungal infection processes with different species being differentially impacted (Xu et al., 2008). As such it is clear that overall infection of a host is dependent on the host's response as well as the pathogen's response to the environment.

6.2 Aims:

- To understand whether the ability of *Zymoseptoria tritici* to withstand fungicide application is light dependent.
- To determine whether priming plants with wind influences disease dynamics of *Z. tritici.*
- To appreciate whether different abiotic conditions that may be impacted by climate change significantly affect the capacity of *Z. tritici* to infect wheat.

6.3 Results

6.3.1 Light and fungicide sensitivity

The light-entrained plant circadian clock moderates a plant's sensitivity to herbicides (Belbin et al., 2019). As fungi can respond to light by promoting a stress response and DNA repair, the influence of light presence or absence on fungal growth during fungicide treatment was assessed (to determine whether fungicide sensitivity was similarly affected). Different concentrations of the fungus were grown on PDA media supplemented with varied concentrations of hygromycin fungicide from 0 to 12.5µg/ml. This could determine in turn whether the timing of fungicide application during the day (in relation to light presence or absence) could influence susceptibility of the fungus to the chemical. The impact on growth was determined by assessing colony size after five days growth at 20°C in either constant light or darkness. Differences between light and dark grown fungi were visually noticeable (Figure 6.2).

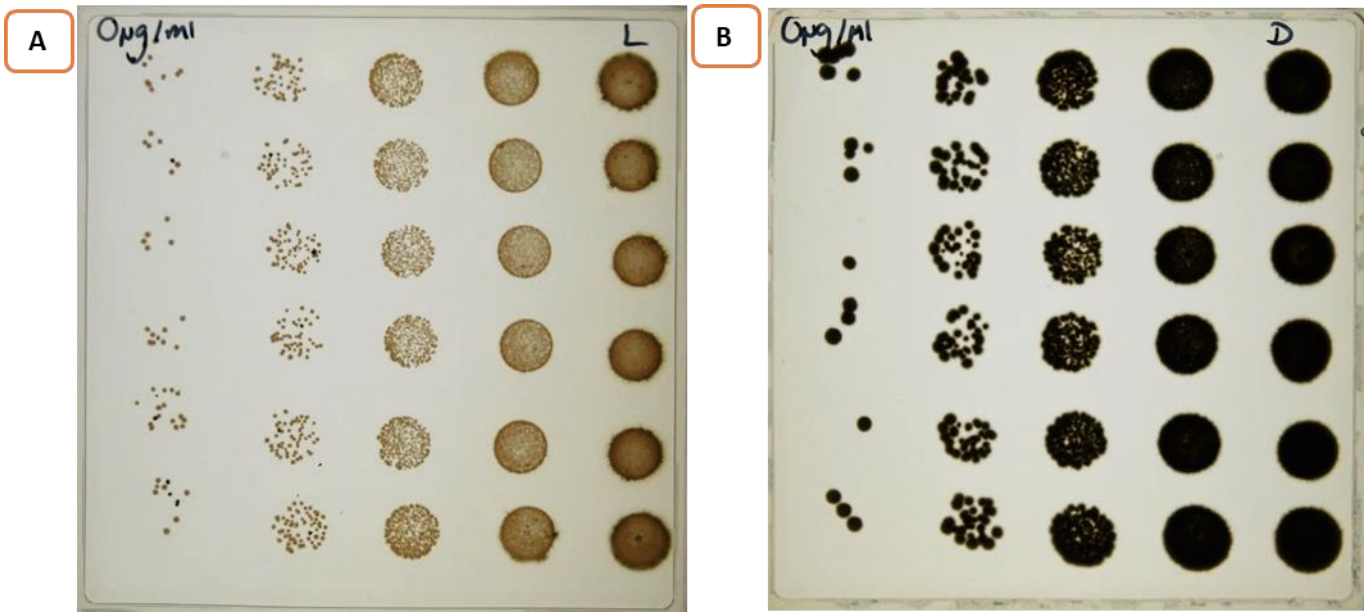

Figure 6.2 Visual differences in *Zymoseptoria tritici* growth under constant light or darkness conditions.

A) *Z. tritici* grown in constant light without hygromycin supplemented. B) *Z. tritici* grown in constant darkness without hygromycin supplemented. Within each plate are varying concentrations of the fungus. Each column is the same fungus concentration replicated six times, from left to right: $1x10^3$, $1x10^4$, $1x10^5$, $1x10^6$, $1x10^7$ spores/ml.

Looking at the $1x10^6$spores/ml fungal concentration, in both light and dark conditions increasing hygromycin concentrations resulted in a decrease in fungal colony area (Figure 6.3A). At concentrations of 1.25µg/ml and higher no growth was seen for fungi in either light treatment. The difference between light and dark grown fungi was significant, as determined by Mann-Whitney U tests ($p<0.05$), for fungicide concentrations of 0µg/ml, 0.0125µg/ml and 0.125µg/ml. The percentage reduction in fungal growth under fungicide treatment was calculated in relation to the no fungicide control for each light condition showing light to have no effect on fungicide sensitivity. No significant difference in percentage growth reduction based on light regime was detected for any fungicide concentration in Mann-Whitney U tests.

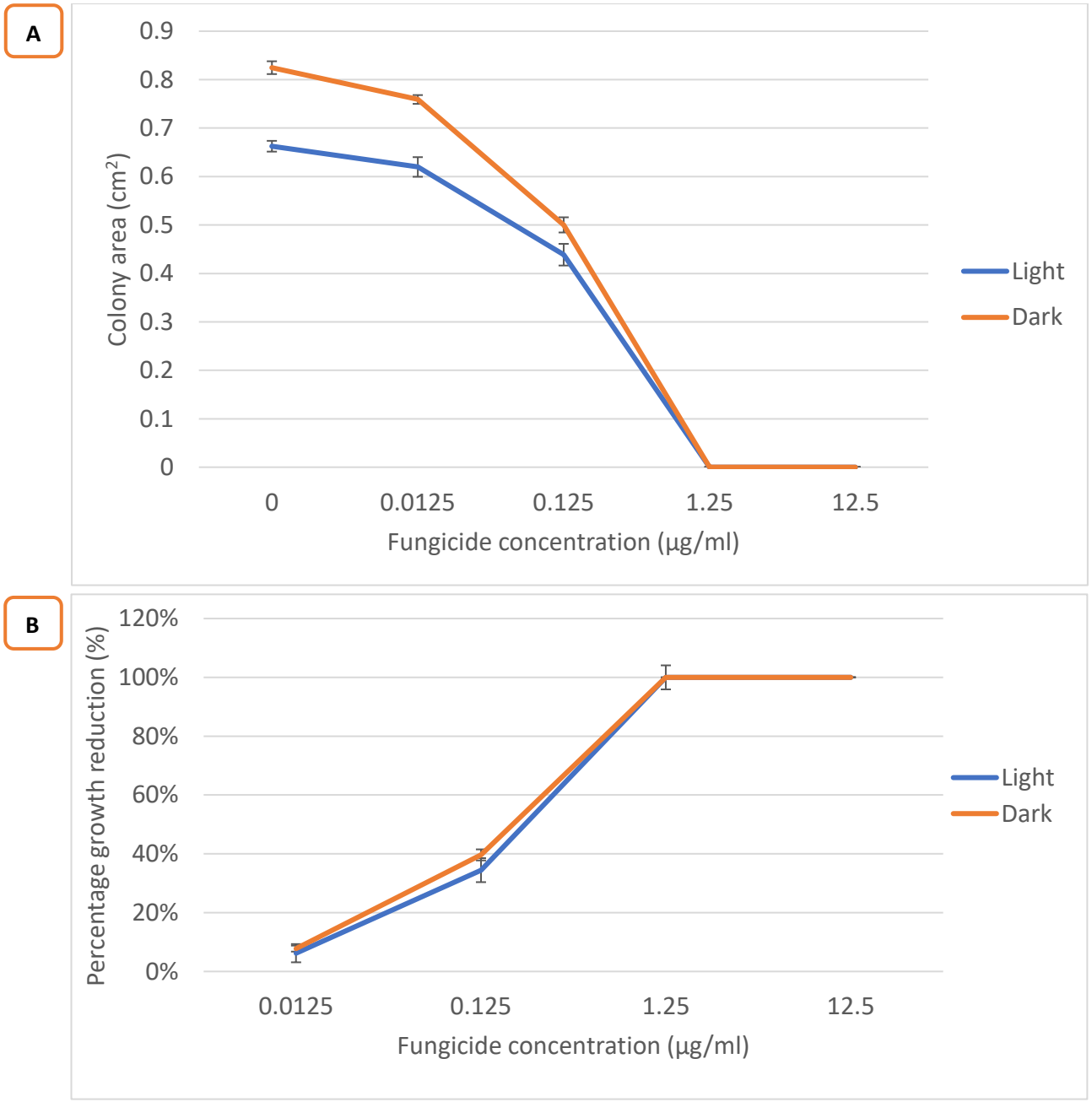

Figure 6.3 Colony size of *Zymoseptoria tritici* IPO323 strain grown under different hygromycin concentrations and light conditions.

Zymoseptoria tritici at a concentration of $1x10^6$ was pipetted in 3µl aliquots onto PDA agar. A) Colony growth under the different fungicide and light treatments was measured. Regardless of light condition increasing fungicide concentration resulted in a reduction in fungal colony size. Error bars are +/- S.E.M. N=12. B) Percentage reduction in colony area from fungicide application was calculated for each light condition showing the reduction in colony size to be consistent across light treatments.

6.3.2 Wind priming wheat and *Z. tritici* infection.

Zymoseptoria tritici is a wind and rain-splash transmitted plant pathogen. Evidence indicates that sound vibrations, similar to those made by the chewing of an insect transmission vector, can prime a plant's defences in readiness for potential infection resulting in reduced pathogenicity of the insect-associated pathogen (Choi et al., 2017). The ability of other means for pathogen spread to prime plant defences prior to infection was investigated here. Specifically, whether wind-primed plants are more resistant to *Zymoseptoria tritici* infection, using pycnidial coverage of leaves as an indicator. Several wind speeds were tested: 2.23m/s, 2.63m/s and 3.15m/s (Figure 6.4 and 6.5). In each instance three-week-old wheat plants were exposed to six hours of wind per day for one week prior to inoculation with the fungus. After 21 days infected leaves were collected and scanned as in Chapter 4.

At wind speeds below 3.15m/s Mann-Whitney U tests determined that the difference in pycnidia number per cm^2 leaf area did not significantly differ between wind and untreated wheat leaves. However, wheat leaves treated with a wind speed of 3.15m/s presented significantly fewer pycnidia compared to their non-wind treated counterpart ($p<0.05$).

3.15m/s wind treated wheat plants visually differed from untreated plants (Figure 6.6) – plants were shorter compared to unprimed controls and also duller. Therefore, characteristics of plants grown under the two different wind regimes were investigated. Several aspects of wheat phenotypes were investigated including weight, height, moisture content and chlorophyll content (Figure 6.7). For height measurements wheat plants were measured from their point of soil emergence to the tip of the second true leaf. For weight measurements, groups of five young wheat plants were cut from the soil and dried to give dry weight – moisture content was determined as the percentage difference between wet biomass and dry weight. Total chlorophyll content was determined by spectrophotometry following extraction.

Figure 6.4. Representative images of Riband wheat leaves from the three wind speed treatment disease assays.

A) Wheat leaves treated with 2.23m/s wind prior to inoculation. B) Wheat leaves treated with 2.63m/s wind prior to inoculation. C) Wheat leaves treated with 3.15m/s wind prior to inoculation**.** Leaves on the left are controls which have been inoculated with tween; leaves on the right are those inoculated with wildtype *Zymoseptoria tritici*. In each instance, wind treated leaves are on top while non-wind treated leaves are on the bottom of each image set.

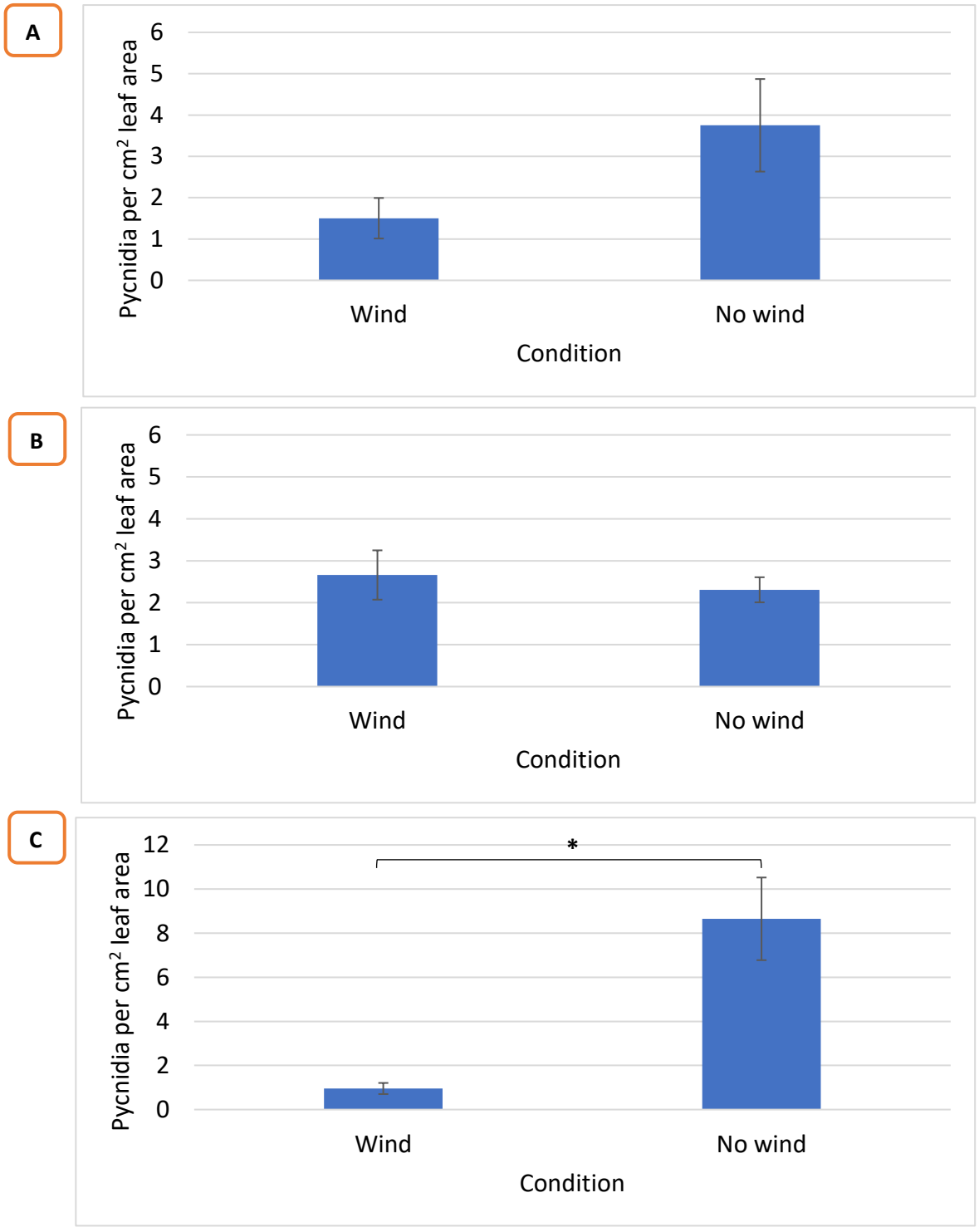

Figure 6.5 Wheat plants primed with wind and *Z. tritici* pycnidia presentation on leaves.

A) Wheat plants treated with 2.23m/s wind prior to inoculation. B) Wheat plants treated with 2.63m/s wind prior to inoculation. C) Wheat plants treated with 3.15m/s wind prior to inoculation**.** Only wind plants treated with the highest wind speed of 3.15m/s significantly differed from an untreated control in terms of pycnidia number per cm^2 wheat leaf area. Horizontal bars with asterisks indicate groups which significantly differ from each other. Error bars are +/- S.E.M. N=11-15.

Figure 6.6 The impact of wind treatment on wheat plant phenotype.

3.15m/s wind treated wheat plants (left); untreated wheat plants (right).

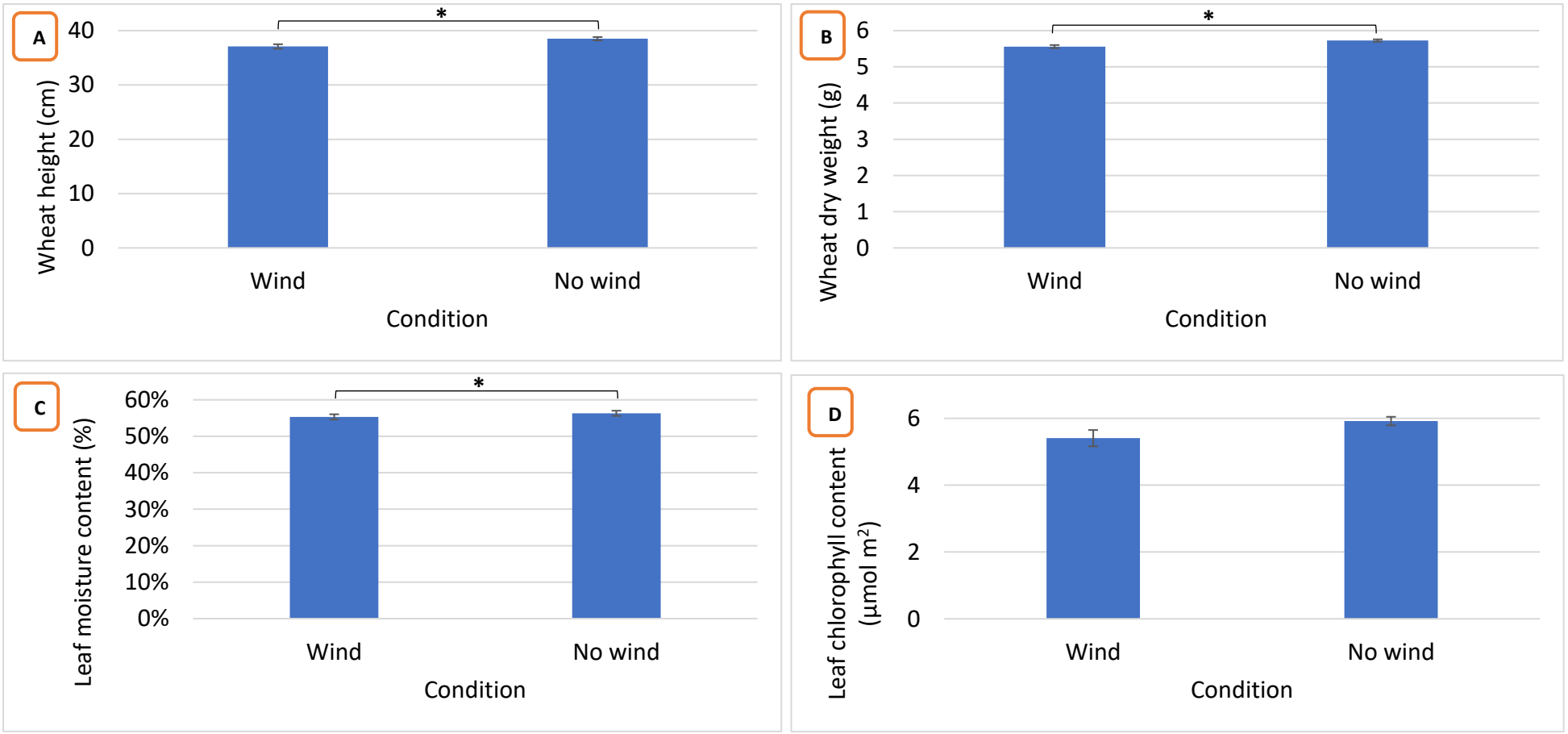

Figure 6.7 Comparisons of 3.15m/s wind treated wheat with untreated controls.

A) Height of wheat plants N=32. B) Weight of wheat plants. N=5. C) Moisture content of wheat plants. N=5. D) Chlorophyll content of wheat leaves. N=6. Wheat plant height, weight and moisture content significantly differed between control and treated plants with wind primed plants showing reduced height, weight, and moisture content comparatively. In all instances error bars are +/- S.E.M. Horizontal bars with asterisks are used to denote significant differences between groups.

Of the four wheat characteristics assessed, leaf height, weight and moisture content significantly differed between wind treated and untreated plants as determined by Mann Whitney U testing ($p<0.05$). Wind treated plants were shorter, weighed less and had reduced moisture content compared to their untreated counterparts. An estimated difference between treatments of 1.37cm, 0.16g and 1% was produced using the Hodges Lehmann estimator for height, weight, and moisture content, respectively.

RNA was also extracted from four-week-old plants that had been wind treated as described previously as well as untreated controls. cDNA was generated from this RNA and RT-qPCR completed using the primers outlined in Table 9.4. Primers amplified several genes implicated in the wheat plant abiotic stress (salt and temperature stress) response: *TaNAC69-1*, *TtNAMB-2* (Baloglu et al., 2012), as well as *Triticum aestivum* Thaumatin like protein (*TaTLP*) which is additionally involved in the wheat response to *Z. tritici* (Deihimi et al., 2013). Gene expression was assessed relative to *Ta54227* (Paolacci et al., 2009). Relative expression of these genes varied between wind and untreated controls (Figure 6.8).

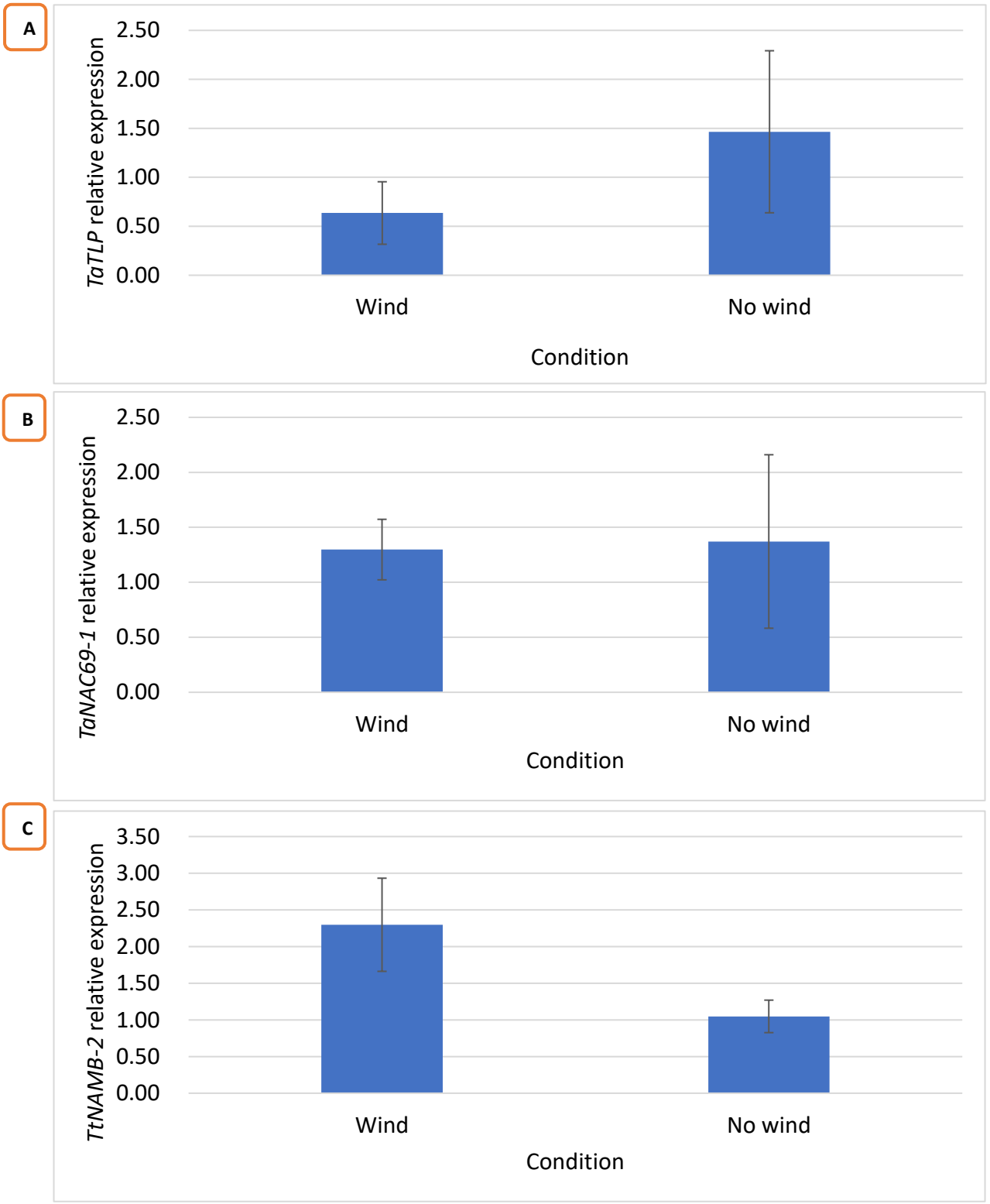

Figure 6.8 Relative expression of wheat genes involved in the abiotic stress response in wind and untreated wheat plants.

A) *TaTLP* relative gene expression, N=3. B) *TaNAC69-1* relative gene expression, N=3. C) *TtNAMB-2* relative gene expression, N=3. Error bars are +/- S.E.M. Gene expression is relative to the *Ta54227* housekeeping gene identified by Paolacci et al. (2009). Wind treatment results in changes in wheat gene expression.

6.3.3 Soil salinity and STB

In a similar line of experiments, wheat plants were primed with another abiotic stress – salt. The impact of salinity on plant growth (Rajpar et al., 2005) and *Zymoseptoria tritici* growth is appreciated (Stapley and McDonald, 2022), however, whether soil salinity can impact the progression of Septoria tritici blotch is not known. To this end, wheat plants were watered with varying concentrations of salt solution (NaCl)(Figure 6.9).

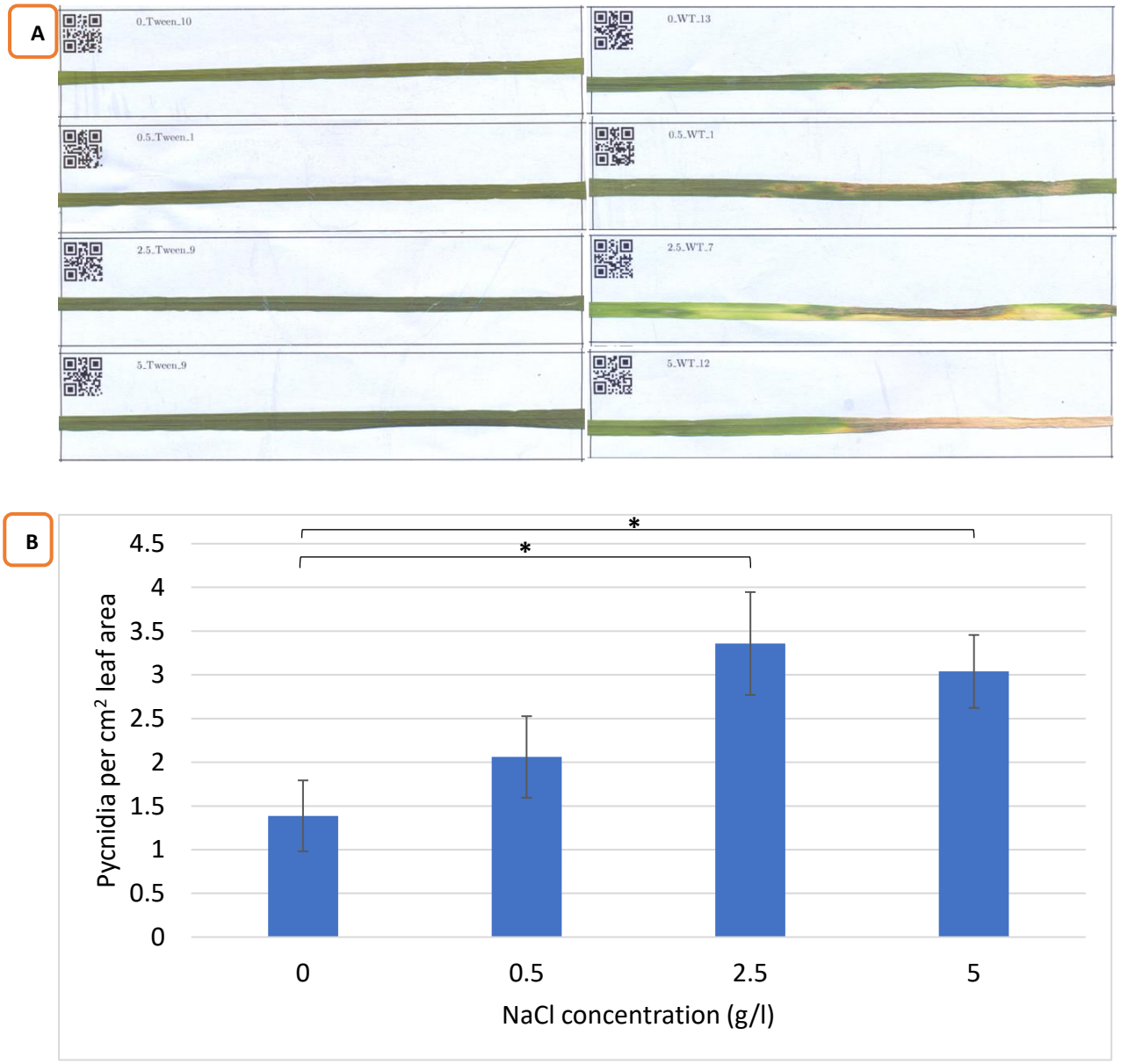

Figure 6.9 The impact of soil salinity on wheat susceptibility to Septoria tritici blotch.

Wheat plants were watered with NaCl concentrations from no NaCl (0g/l) to 5g/l NaCl – influencing the soil salinity. A) Representative images of wheat leaves under each treatment type. Leaves on the left of the image set are uninoculated tween controls, those on the right were inoculated with wildtype *Zymoseptoria tritici.* The lowest salt level, 0g/l is at the top of the image, followed by 0.5g/l, 2.5g/l, with 5g/l on the bottom. B) The number of pycnidia produced by the fungus (after three weeks of infection) calculated. Errors bars are +/- S.E.M. N=11-15. Horizontal bars with asterisks denote groups which significantly differ from each other.

Salt concentration had a significant impact on pycnidia per cm^2 leaf area, as determined by Kruskal-Wallis testing ($p<0.05$). A Dunn post hoc with p-value adjustment using the Benjamini-Hochberg method revealed that salt concentrations of 2.5g/L and 5g/L in wheat plant irrigation water resulted in a significant increase in pycnidia per cm^2 leaf area ($p<0.05$).

6.3.4 pH and Septoria tritici blotch

Along the same vein – examining the impact of soil conditions on the vulnerability of wheat plants to STB – pH was investigated. Wheat plants were grown in an inorganic substrate (perlite) and watered with Letcombe nutrient solution pH adjusted to three different levels (Figure 6.10), including levels at which plant toxic Al^{3+} ions are solubilised in soil (Kariuki et al., 2007), or unadjusted – giving a pH 6.58 treatment. Aluminium ions were not present in Letcombe solution but rather in the perlite substrate. pH treatments, however, were intended to act as a stress to the plant rather than be lethal. The pycnidia per cm^2 leaf area of inoculated wheat plants did not significantly differ based on the pH adjusted Letcombe solution applied in a Kruskal-Wallis test. However, a general trend of decreasing pycnidia numbers with increasing pH can be noted.

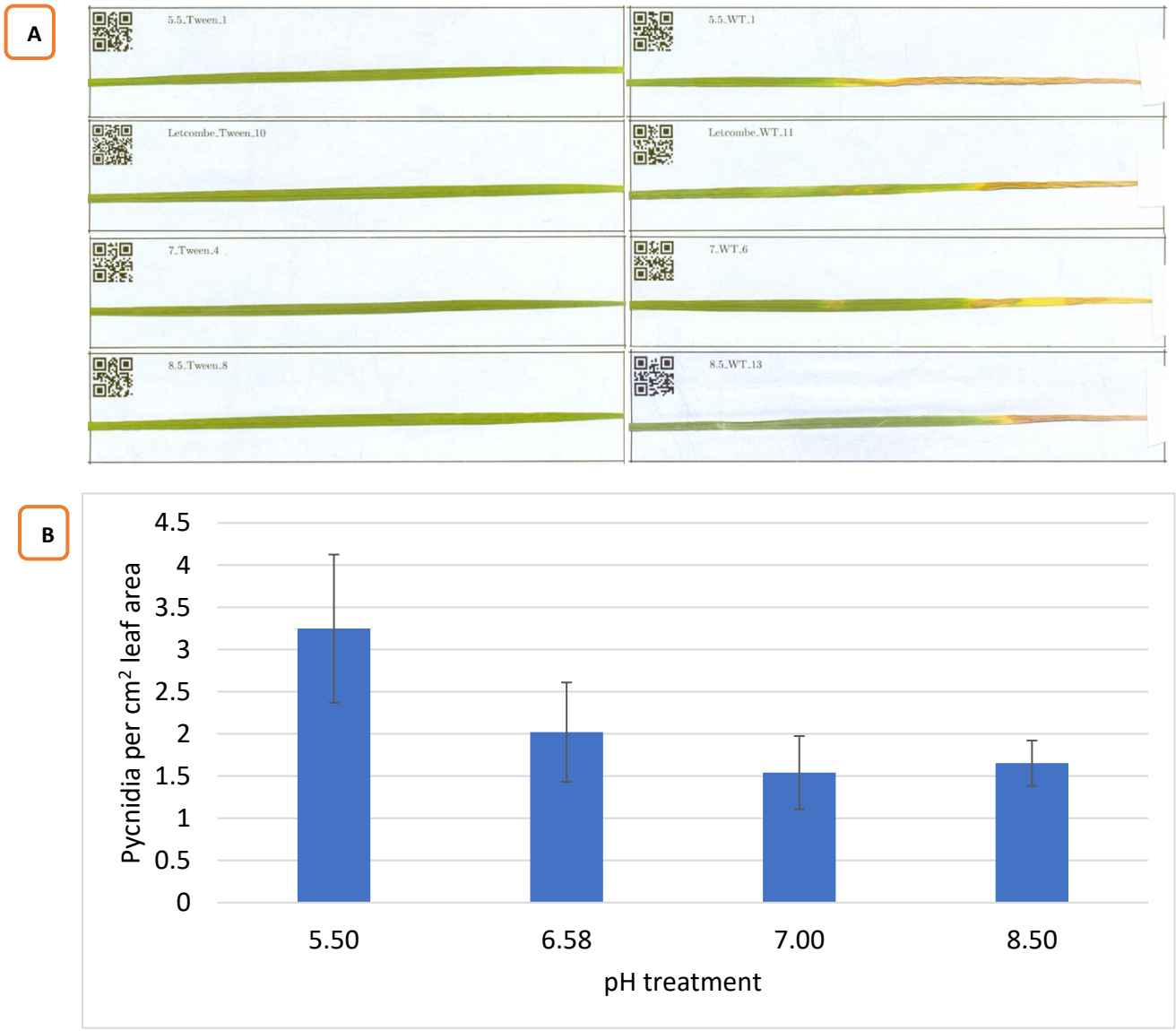

Figure 6.10 The impact of pH on wheat tolerance to Septoria tritici blotch.

The different pH treatments were used to water wheat plants grown in perlite. A) Representative images of wheat leaves under each treatment type. Leaves on the left of the image set are uninoculated tween controls, those on the right were inoculated with wildtype *Zymoseptoria tritici.* The lowest pH, 5.5, is at the top of the image, followed by 6.58, 7, with pH 8 on the bottom. B) The number of pycnidia produced on wheat leaves under each pH treatment were measured. Error bars are +/- S.E.M. N=15. None of the pH treatments significantly differed from one another.

6.4 Discussion

6.4.1 Climate change

The impact of abiotic factors on *Zymoseptoria tritici* infection will only serve to be exacerbated by climate change. The effect of higher temperatures on wheat yield has already been discussed within this thesis, but climate change extends beyond this into increased frequencies of severe weather including storms (Fones et al., 2017) as well as potentially higher soil salinity affecting drylands and irrigated arable land (Hassani et al., 2021a, Talat, 2020). The impact of climate change on these abiotic factors can be both direct and indirect, in some instances resulting from our attempts to respond to the negative effects of climate change. For example, reduced yield from higher temperatures (Ortiz et al., 2008) could lead to greater fertiliser inputs to try to minimise losses – which in turn can modify soil pH. The results of this work, looking at the impact of abiotic factors on *Zymoseptoria tritici* infection of wheat, will therefore be considered in the context of climate change.

6.4.2 Light and fungicide efficacy

Beyond infection, the environment may modulate other fungal processes. For example, light may interact with the effect of fungicides on fungal growth, in a similar way to how the light-entrained circadian clock influences plant herbicide sensitivity (Belbin et al., 2019). Understanding the exact conditions under which fungicides are most effective not only helps better control STB – but also can serve to reduce the quantity of fungicides utilised as the light regulated circadian oscillator of fungi could be used to target chemical treatments used in control to when the fungus is most susceptible (Steed et al., 2021). When the negative implications of fungicide use are taken into consideration (Marques et al., 2016) the benefit of this to the environment is apparent.

Evidence from this investigation indicated that light condition significantly impacted the growth of the fungus (even in the absence of fungicides) and further demonstrates the ability of the fungus to sense and respond to light (Tiley et al., 2022). This alongside the melanisation seen for darkness grown fungi alone confirms differences in gene expression occur in response to light, corroborating the findings of McCorison and Goodwin (2020). Fungi grown in complete darkness had larger colony sizes at all fungicide concentrations where growth was still possible. Fungi grown alongside 0.0125μg/ml and 0.125μg/ml hygromycin also significantly differed in their growth in light and dark conditions. However,

this is likely due to the light condition alone rather than intersectionality between light condition and fungicide application since the same trend was seen where fungicides were not present – and similar percentage growth reductions for hygromycin grown colonies were noted. The difference between fungal growth under light and dark treatments decreased with increasing fungicide concentration though this is simply indicative of fungicide efficacy. As such, light does not serve to protect the fungus from damage from this fungicide.

However, others with different modes of action may vary. Indeed, during photosynthesis, which usually occurs under light conditions, reactive oxygen species (ROS) can be liberated (Foyer, 2018) and therefore any infecting fungus will also encounter ROS. It would then be beneficial for the pathogen to upregulate genes for protection from ROS in light conditions and as such ROS defence may impact the efficiency of fungicides that induce accumulation of ROS (Mesa-Arango et al., 2014, Wang et al., 2022, Xing et al., 2003). Therefore, the fungal response may be specific to the type of fungicide tested. If there were more time, a wider range of fungicides with varying modes of action would be tested.

6.4.3 Wind and Septoria tritici blotch

Perhaps the most unexpected result from this work is the demonstrated impact of wind on Septoria tritici blotch. Given that *Z. tritici* can enter wheat leaves through sites of wind-induced damage (Fones et al., 2017), it was expected that increasing wind speeds would result in increased symptoms of STB. If this were the case then this information could be used to inform decisions regarding the timing of fungicide applications after high risk periods of severe winds (Gladders et al., 2001). What was instead identified was that wheat pre-treated with a threshold wind speed (greater than 3.15m/s) showed fewer pycnidia per cm^2 leaf area compared to untreated controls. It should be noted that this wind speed equates to ~7mph and so is not an unrealistic field condition, falling below the 2022 UK average daily wind speed of just under 10mph (GOV.UK, 2023).

Analysis of the characteristics of wheat plants treated with this wind speed revealed significant differences in leaf architecture were instigated by wind treatment – indicative of more largescale transcriptional differences triggered by this abiotic stress. A few abiotic stress-induced candidate genes were investigated in this work, including *TaTLP* which has also been indicated in the wheat response to *Z. tritici* (Deihimi et al., 2013), with these showing small changes in gene expression between control and treated samples and so wind

is impacting gene expression at some level. RT-qPCR data from this work alone cannot explain differences in disease symptoms between plants under still conditions or with air movement – especially as *TaTLP* expression is reduced relative to the untreated control. As such, it may be of benefit to conduct RNAseq on these samples as an informative means of understanding changes in gene expression between plants under still conditions or with air movement. As differences in gene expression ultimately alter phenotype, including leaf characteristics, looking more widely at transcriptional changes between control and wind-treated plants may allow identification of the exact genes responsible for the response to wind seen here. This data may be used to select cultivars with greater expression of these genes, under all conditions, for breeding – providing there are no detrimental effects since wind treated plants were dwarfed, although it is well known that dwarfing has been shown to be largely beneficial for wheat yields (Rebetzke et al., 2011).

Though not the expected result, these data can still feed into decision making regarding spray application of fungicides since under prolonged still conditions wheat plants might be more susceptible to infection by *Z. tritici.* Therefore, applications at these times would likely prove beneficial in reducing STB levels. The impact of climate change on wind speed is not fully understood with both reductions and increases in wind speeds projected (Greene et al., 2010, Sydeman et al., 2014). If wind speeds are increased, it is possible that this factor may ultimately result in lower levels of STB and may prevent epidemics if fewer reproductive cycles can be completed by the fungus over the course of the growing season. However, as only one wheat growth stage was tested here, whether the reduced pycnidiation result would be seen for all growth stages is yet to be determined but would be interesting to investigate further. Equally, higher wind speeds than 3.15m/s were not investigated and since there is a threshold below which wind speed does not impact STB levels, there may too be a cutoff point after which wind becomes too damaging and results in higher STB levels. Future investigations should employ these higher speeds to determine if this is in fact the case. Extreme winds impact wheat yield by lodging, therefore, presumably past a certain wind speed the benefit of reduced STB symptoms may be outweighed by the detriment of lodging.

The implications of this result can potentially exist more widely than allowing for predictions for STB under differing climatic conditions. Indeed, as this abiotic condition can significantly

alter the pycnidia number presenting on treated wheat leaves, even at relatively moderate wind speeds, in field trials of novel fungicides or tests of gene knockouts and their impact on virulence how can we be sure that this result is not one that has resulted from abiotic conditions (not just for wheat but for other crops if this is a broadly applicable response). Of course, efforts are made to take any confounding environmental factors into account, and this would not be an issue for cabinet grown wheat plants. However, as the impact of the abiotic factor on its host is only just starting to be appreciated, this calls into question how well wind would be accounted for in field experiments.

6.4.4 Soil abiotic factors and STB

Armed with the knowledge that abiotic factors in combination with the wheat-*Zymoseptoria* biotic interaction can result in shifted and unexpected outcomes, the impact of alternative abiotic factors on STB was determined. This was conducted for soil abiotic factors of pH and salinity. The expectation was that plants that have activated stress-response pathways might display more resistance, and so support fewer pycnidia under extreme acid or high salt conditions, but this was not the case.

In the first instance, pH had no significant impact on STB levels, even for pH levels at which plant toxic Al^{3+} ions would be solubilised (Kariuki et al., 2007). However, as these ions exist within the 4.7 to 6.5 range, perhaps an adequate stress to trigger plant defences was not provided. Some reports suggest that toxicity is alleviated at pH 5.5 (Ernani et al., 2002) and this was the lowest pH used in this study. Future research should look at STB on plants grown in more acidic pH environments. However, given the aforementioned toxicity to the plant, the ability to use pH adjusted soil as a treatment for STB if pycnidia levels are found to be reduced in more acidic pH treatments is limited. Any benefit to the plant in terms of reduced STB might be lost from the damage to the plant from toxicity. However, the trend that appears to be developing in this data is reduced pycnidiation as the substrate pH becomes more alkaline – potentially due to alleviating the toxicity experienced at acidic pH levels and increasing overall plant health. It would then be interesting to repeat this work with a wider pH range, testing this relationship by linear regression.

On the other hand, soil salinity did significantly impact STB levels on inoculated wheat plants. Single applications of 2.5g/lor 5g/l sodium chloride resulted in significant increases in pycnidia per cm^2 leaf area compared to controls. For this abiotic factor, triggering a stress

response appears to be detrimental rather than beneficial to the plant, which is surprising given the work by Deihimi et al. (2013) showing the same defence gene to be induced in response to salt and *Z. tritici* stress. As such, the condition of the soil should be a serious consideration to wheat farmers to avoid losses to STB, especially given the implications of climate change on increased soil salinity – a particular issue in areas where plants are not accustomed to this stress. Though salt tolerant cultivars exist (Goudarzi and Pakniyat, 2008), and may react differently in this experiment, these would not be grown in areas where soil salinity has not previously been a problem. The Riband wheat used here has not been bred for salt tolerance as a cultivar, and in the past was commonly sown in the UK, therefore the result seen in this experiment is representative of a salt response where tolerance has not been selected for. The increase in soil salinity in novel areas is expected due to rising sea levels, more use of irrigation, and frequent droughts (Hossain et al., 2019). This is predicted to reduce the available land for wheat production (Kheir et al., 2019) as salt intrudes into groundwater (McGranahan et al., 2016)

It must be noted that no statistically significant differences existed between the 2.5g/l and 5g/l salt treated plants – increasing salt concentration from 2.5g/l to 5g/l did not result in even greater numbers of pycnidia. There could however still be a benefit in expanding future research to encompass even greater salt concentrations beyond 5g/l if these may be realistically expected in worst-case scenarios – knowing the presumed outcome of this on the wheat-*Zymoseptoria* interaction may then be useful. Equally, it would be worthwhile to examine the impact of soil water salt concentrations between 0.5g/L to 2.5g/L to determine the point at which soil salinity becomes detrimental to wheat defences against STB and whether this is salt per se, or the osmotic potential (i.e., drought simulation) that the salt gives. The latter can be assessed using things like mannitol or sorbitol to alter the osmolarity of soils but without altering the salt levels.

6.4.5 Abiotic influence on STB is not consistent.

Here, we see that the resulting level of STB (the outcome of the wheat-*Zymoseptoria* biotic interaction) is not consistent across abiotic stresses. For wind stress, STB levels are reduced; for salt stress, STB levels are increased. It is then clear that the wheat host does not respond in the same way to all abiotic stresses and therefore we would expect different genes to be expressed during the plant reaction to the environment. The ability for some stimuli to

reduce STB symptoms, seems to further indicate, alongside evidence from Deihimi et al. (2013), that some of these genes may also undergo increased expression when the plant is challenged by *Z. tritici.* Though a protective effective of this was not realised in the case of salt stress, it may be true of other genes induced by alternative abiotic stresses.

6.5 Summary

- Light does not impact fungicide efficacy against *Z. tritici.*
- Priming wheat plants with a moderate wind speed one week prior to infection significantly reduces the number of *Z. tritici* pycnidia which develop on wheat leaves.
- High soil salt concentrations significantly increase the number of pycnidia identified on wheat leaves – salt stress increases wheat susceptibility to *Z. tritici.*
- Soil pH's tested in this work do not impact the susceptibility of wheat to *Z. tritici.*

7 : General Discussion

7.1 Introduction

Despite the significance of *Zymoseptoria tritici* as a plant pathogen and the research conducted into the fungus, the genes (of which there are likely many) involved in pathogen virulence remain largely elusive. As such, in terms of the battle for food security, we are fighting against an enemy which is still poorly understood. The urgency to understand the pathogen is exacerbated by the growing human population putting even greater pressure and demand on limited, and potentially dwindling, food supplies. Compounded with this is the added impact of climate change. Just as we are beginning to understand the wheat-*Zymoseptoria* interaction, the environment in which the host and the pathogen exist is shifting and what this means for STB is hard to predict. Overall, there are many known unknowns for the *Zymoseptoria tritici* pathogen. This thesis has therefore aimed to gain deeper insight into the fungus as an organism and as a pathogen.

7.2 Understanding the zymoseptorin biosynthetic cluster.

One of the main aims of this work was to better understand a putative RiPP peptide, zymoseptorin, encoded for by a biosynthetic gene cluster on chromosome 4 of the *Zymoseptoria tritici* genome. To this means, BLAST searches were completed, and possible functions assigned based on homology to characterised proteins. Often, proteins within the zymoseptorin biosynthetic gene cluster showed greatest similarity to those produced by other dikaritin RiPP producers – namely *Phomopsis leptostromiformis, Aspergillus flavus,* and *Ustilaginoidea virens*.

The existence of similar genes in diverse fungal species calls into question how these peptides have come about in fungi. Of course, the kexin processing of the precursor peptide has attracted comparison to the processing of yeast pheromones (Mizuno et al., 1989, Brenner and Fuller, 1992, Vogt and Kunzler, 2019, Umemura, 2020), therefore a possible evolution of these RiPPs from their fungal mating pheromones may be considered (Ford et al., 2022). This may be true of KEPs which do not require post-translational modifications to produce an active compound – of which there are many (Umemura, 2020). However, it seems unlikely that such similar RiPP biosynthetic gene clusters would have arisen independently especially when there are often 10 or more genes involved in peptide

synthesis and processing. As a result, the more likely answer to the question of how this mechanism of peptide synthesis has arisen in several fungal classes (Table 7.1) is horizontal gene transfer (HGT). This is especially clear when we consider the existence of the same RiPP across fungal classes with ustiloxin B produced by both *Ustilaginoidea virens* and *Aspergillus flavus* (Tsukui et al., 2015, Umemura et al., 2014). This is hypothesised for several further RiPPs in Chapter 5 of this thesis, including zymoseptorin.

Table 7.1 The taxonomic classes of known dikaritin RiPP producers to date.

Fungal RiPP producer	**Class**
Phomopsis leptostromiformis	Sordariomycetes
Ustilaginoidea virens	Sordariomycetes
Aspergillus flavus	Eurotiomycetes
Epichloë festucae	Sordariomycetes
Cochliobolus victoriae	Dothideomycetes

Indeed, horizontal gene transfer of nuclear genes is possible between eukaryotes and can occur across kingdoms (Richards et al., 2009), as well as within them (Wisecaver and Rokas, 2015). Given the existence of RiPPs throughout the different kingdoms of life, HGT then seems plausible as the means by which this method of peptide synthesis has proliferated – especially since HGT can be of whole gene clusters (Wisecaver and Rokas, 2015). Interestingly, HGT between fungal species has already been proposed for fungal RiPPs, including the amatoxins (Drott et al., 2023, Walton, 2018, Luo et al., 2018) and the dikaritin RiPP victorin (from *Cochliobolus victoriae*) which is believed to have acquired the genes for peptide synthesis from *Cochliobolus carbonum* (Rosewich and Kistler, 2000).

Horizontal gene transfer is usually of genes with importance including those that allow tolerance of specific environments (Bucknell and McDonald, 2023) or, as with victorin, those that permit virulence (Wisecaver and Rokas, 2015). Therefore, though perhaps not always obvious now, RiPPs were likely ecologically important to their producer in order for horizontal gene transfer to have occurred. Indeed, horizontal gene transfer may not have

occurred recently (though not impossible) and the existence of several putative RiPP producers within the genus *Aspergillus* probably points to the transfer of a RiPP cluster to a common ancestor prior to the branching of new and separate species.

7.2.1 Predicted zymoseptorin biosynthetic pathway

As for the other dikaritin RiPPs, the *Z. tritici* precursor peptide contains core peptide sequences flanked by lysine and arginine amino acids (KR), the recognition site for Kex2 endoprotease enzymes (Jalving et al., 2000). Kex2 endoproteases, though absent from dikaritin gene clusters, are instrumental to RiPP production, since deletion of KexB in *A. oryzae* has been shown to result in a significant reduction in Ustiloxin B titre (Yoshimi et al., 2016). These Kex2 endoprotease enzymes, encoded elsewhere in the genome, exist in the golgi, therefore, before the larger precursor unit is hydrolysed and cleaved at the C-terminal of Kex2 recognition sites (liberating the smaller core peptide sequences), the precursor peptide must be transported to this organelle (Yoshimi et al., 2016). The peptide is presumably translated and enters the golgi as the larger precursor as it is this peptide that contains the signal sequence for golgi localisation. It is unclear where in the cell the additional tailoring steps are based as well as whether they are applied before or after the peptide enters the golgi. However, to remove amino acids outside of the presumed core RiPP sequence region (YVIPVD), including the KR Kex2 recognition sites, additional peptidases are required with this proteolysis likely undertaken by the two peptidase enzymes within the Zttx cluster: S41 family peptidase and S28 serine carboxypeptidase, encoded by the *ZttxP* and *S28* (also known as *P2*) genes, respectively. Given that this processing would remove the golgi signal peptide, this modification is likely to occur following Kex2 processing.

The order of application of the remaining post-translational modifications, based on the additional genes present within the *Zttx* cluster, is however less easily theorised. Yet, these post-translational modifications can be core to the production of the mature RiPP. Specifically, cyclisation of the peptide by the tyrosinase enzyme (from *ZttxQ*) at tyrosine and isoleucine amino acid side chains (Umemura et al., 2014) is essential, a modification without which mature RiPP peptides cannot be produced (Ding et al., 2016). As with the other known dikaritin RiPPs, a tyrosine in the 1st position of the core sequence and an isoleucine in the 3rd position is also conserved in the zymoseptorin RiPP core sequence and as such

cyclisation here is logical. RiPP cyclisation is also dependent on the *Y1/Yb* gene DUF3328 containing product with deletion of the gene in *Phomopsis leptostromiformis* preventing production of the mature Phomopsin RiPP (Sogahata et al., 2021) – the same is noted for ustiloxin (Nagano et al., 2016). Though the *Z. tritici* RiPP cluster lacks the chlorination modifying enzyme within the phomopsin cluster, it does contain the *ZttM* gene encoding an S-Adenosylmethionine dependent methyltransferase. In phomopsin production this enzyme methylates the peptide at its N-terminus (Ding et al., 2016). Since, the N-terminus of the peptide remains unchanged in the *Z. tritici* core sequence, methylation likely occurs on the same residues.

Though functions of the zymoseptorin genes have been assigned bioinformatically and a pathway for RiPP production proposed, this can only be confirmed experimentally by gene knockout, assessing the impact of gene loss on the resultant mature peptide – as in Sogahata et al. (2021). Within this work several knockout strains of the zymoseptorin biosynthetic cluster genes were produced. However, since no method of extracting the mature peptide from the fungus has yet been developed, there is no mature peptide against which presence or absence of modification provided by the enzymes encoded by the cluster genes can be determined. As such upon development of a successful extraction method, future work should repeat such extractions with these knockout strains in order to piece together the steps of zymoseptorin biosynthesis. In addition, intermediate compounds in zymoseptorin production may possess novel and interesting biological activities.

7.3 Chemical characterisation of zymoseptorin

Isolation of the zymoseptorin peptide was a principal objective of this work, which would have allowed the compound to be chemically characterised and compared structurally to other known RiPPs. To help achieve this aim, overexpresser strains of the zymoseptorin transcription factor (encoded by *ZttxR*) were produced. Investigation of the transcript levels of the *ZttxA* gene in the wildtype compared to the overexpresser fungal strains showed the overexpresser strains consistently increase transcript levels but not significantly.

The overexpression construct was designed by incorporating a region upstream of the *Zymoseptorita tritici* Histone H3 (*HH3*) gene, a constitutively expressed gene (Umemura et al., 2020) – at least in *Aspergillus oryzae*. The region selected was supposed to represent the promoter region of the *HH3* gene and therefore incorporation of this into the overexpression

construct as the promoter region for the *ZttxR* gene would increase transcription of this copy of the gene when inserted into the fungal genome, as completed for ustiloxin (Umemura et al., 2020). However, whether the region selected encompassed the entirety of the *HH3* promoter region or just a subsection of the promoter is unknown. Furthermore, overexpression it is not necessarily this simple. In work by Umemura et al. (2020), despite putting the ustiloxin transcription factor gene, *UstR*, under the regulation of constitutive promoters, different culture conditions resulted in varying levels of *UstR* transcripts and ustiloxin production. Even when relative gene expression of the transcription factor was high, this was not necessarily reflected in peptide yield (Umemura et al., 2020). Therefore, producing an overexpresser construct alone is not sufficient for RiPPs, various culture conditions need to be trialled and the most conducive to increased transcript levels and peptide production identified. Peptide production is not just a case of increasing transcription, further conditions during fungal growth must also be met. It is then not surprising that using the overexpresser produced in this work (OxR T4) in peptide extraction experiments has not given any hugely obvious indications of chemical differences between extracts of the overexpresser strain and the knockout. As such, the GFP:*ZttxA* fusion strain produced in this work may be used to permit the optimisation of peptide extraction protocols as different media conditions, beyond those examined here, may be trialled and those under which greatest fluorescence is noted used for purifications.

For all conditions employed in this research, it seems as though the concentration of the peptide is either low or non-existent (since no fluorescence was detected), and as such the peptide does not necessarily exist as a peak on a chromatogram. It is assumed that incorporating a different or larger portion of the *HH3* promoter into the overexpression construct will result in even greater upregulation of the *ZttxA* gene. This, as intended for the overexpresser strains produced here, should facilitate purification of the peptide by making differences between the knockout and overexpresser more obvious. Additionally, multiple new overexpresser constructs could be designed using different promoter regions from different genes to induce the highest possible levels of gene expression. However, prior to this it must first be determined whether the peptide is produced at all. Upregulating gene expression can only go so far – if the gene transcript is never translated to a peptide no matter what promoter region is used, we will never see a peak on a chromatogram. Indeed,

though transcripts of the *ZttxA* gene clearly do exist – as evidenced in this work – it cannot be said for certain that this is ever translated into a mature peptide due to regulation at later stages of peptide production – which we also know to occur in ustiloxin (Umemura et al., 2020). If the peptide is not produced however, it is then hard to explain why the RiPP is conserved in a wide range of strains from different countries and collection dates, and why the same, or similar clusters are found in such a wide range of fungi. To have this degree of conservation the peptide must be produced and doing something. Perhaps then it is our analytical facilities that are not sufficiently sensitive. Indeed, LCMS analyses were repeatedly hindered by various components of the machine failing, therefore isolation of the peptide in the future is not outside of the realms of possibility.

7.4 Functional characterisation of zymoseptorin

Given these difficulties, purified zymoseptorin could not be used in functional analyses. This has however permitted the impact of natural concentrations of the peptide on plants, insects, and microorganisms to be assessed. Ecologically, this is more informative than understanding the role of the peptide when using inflated concentrations that would never exist in a real situation. As the OxR T4 overexpresser strain increases transcript levels of the *ZttxA* gene, though peptide extraction has not yet been possible, functional analyses were also completed with this strain to presumably exaggerate the phenotype caused by zymoseptorin in place of being able to define the concentration of the purified peptide.

At native concentrations the peptide has no obvious role in plant pathogenicity when compared to the knockout strain of the fungus. Though a possible role in controlling pycnidia formation, based on OxR T4 wheat inoculation data, has been put forward, this is not consistent across cultivars, nor does removing regulation by this gene (the knockout strain) result in greater numbers of pycnidia. Equally, the RiPP, at the natural concentrations generated during infection, does not act as an antifeedant against *Schistocerca gregaria* locusts and is not acutely toxic to this species – nor does the RiPP show any antibiotic properties during co-incubation of fungal and bacterial cultures. However, this does not guarantee a lack of antifeedant activity or toxicity to all organisms since other RiPPs show specific toxicity to nematodes and mammals (Quijano et al., 2019, Battilani et al., 2011, Koiso et al., 1992, Li et al., 1995). The omphalotin RiPP was shown to have high specificity to the *Meloidogyne incognata* nematode (Sterner et al., 1997), just as victorin is only effective

against oat cultivars containing the *Vb* gene (Meehan and Murphy, 1947, Wolpert and Macko, 1989). This specificity makes finding the exact organism against which a novel, bioinformatically identified peptide is effective appreciably difficult. Simply testing the peptide against an array of organisms may never yield the exact species against which the RiPP is effective.

The bottom-up approach to peptide discovery whereby the peptide gene cluster is identified prior to the natural product itself (Luo et al., 2014b), specifically for RiPPs, appears to be challenging. To our knowledge, despite their identification in 2016, none of the RiPPs identified by Ding et al. (2016) have been isolated or chemically and functionally characterised, therefore the difficulties experienced in this work are not unique. Though many putative RiPPs exist, perhaps the concentrations of these produced by most fungal species are low – as is their relative importance to the producer. Indeed, if the peptides were produced in any large quantities, with significant ecological effects, logically these would have already been identified by the same top-down approach of other RiPPs.

7.4.1 Assessing methods of monitoring Septoria tritici blotch

Within this work multiple methods of assessing *Z. tritici* infection were employed – these were visual assessments of Septoria tritici blotch symptoms using a simple scale and automated pycnidia counts from Image J analysis (Karisto et al., 2018, Stewart and McDonald, 2014, Stewart et al., 2016). The use of both methods was necessary since no single method can give the full picture of infection. The visual scale method was most beneficial for time course analyses as it allowed repeated measurements of the same leaves, something that is not possible when performing image analysis which requires leaves to be detached, mounted, and scanned. As such, image analysis of scanned leaves can only give a final measure of disease severity after a specific incubation period.

However, this quantitative method perhaps gives more reliable data regarding pathogenicity since it gives counts of pycnidia per cm^2 leaf area, which provides an indication of the likelihood of spread of the pathogen as well as severity of disease for the inoculation in question. Though lesions can be measured by automated image analysis, here, pycnidia number was determined to be a more accurate measure since, despite efforts to determine if leaf symptoms were due to abiotic factors, leaf chlorosis and necrosis can be induced by these conditions (as well as other pests). Measuring pycnidia alone confirms that these are

symptoms caused by fungal infection. This method is relatively new compared to other quantitative methods such as real time qPCR (which gives an indication of fungal biomass) (Rudd et al., 2008), but is unique in its identification of these pycnidia as well as its time and cost efficiency. As such this method is gaining popularity for investigations of *Z. tritici* pathogenicity (Fones et al., 2015, Karisto et al., 2018, Fones et al., 2017).

So too are chlorophyll fluorescence measurements becoming a popular means of garnering an indication of overall plant health (Tischler et al., 2018, Bellow et al., 2013, Cséfalvay et al., 2009). Since Septoria tritici blotch negatively impacts this, chlorophyll fluorescence can inform regarding the progress of infection (Mihailova et al., 2019) and, since it does not require leaf excision, can be employed in time course analysis. Unlike the scale or scanner-based methods, however, this does require specialist equipment and as a result has not been completed in this work due to availability of the equipment only at the end of the project. It would be beneficial to repeat the time course analysis with this quantitative method and determine whether chlorophyll fluorescence can reliably assess damage from *Z. tritici,* and if data are comparable to manual assessments. This is key as the chlorophyll fluorescence method is liable to confoundment by abiotic factors as it does not use an index specific to fungal infection.

Just as the methods of detecting infection can be assessed, so too must the methods of inoculation used in this work be considered. As data from this work determines that wind, a source of mechanical disruption, can influence disease susceptibility, inoculation methods that similarly disturb the plant may result in a modified response. The impact of inoculation method may not necessarily parallel the result of the wind treatment especially since inoculating wheat leaves by brushing them with spore solution could provide damage sites through which the fungus can enter the leaf (Fones et al., 2017) – which may instead increase plant susceptibility to infection since there are more entry sites than just stomatal apertures. The inoculation method was consistent within experiments and therefore, differences in pycnidia numbers (or lack thereof) between control and treated groups, or wildtype and knockout strains still stand. However, the levels of pycnidia seen in this work may not be the same as those seen on a field level where inoculum is naturally delivered to wheat leaves.

7.4.2 The importance of understanding RiPP function as a means of identifying novel RiPPs

From our understanding of fungal RiPP function to date it is clear that selective pressures applied by the immediate surroundings of the fungus, namely biotic stresses, are the main driving forces in the evolution of RiPP functions. Where fungi are consumed frequently, fungal RiPPs likely evolve as toxins and where nutrient acquisition by the fungus is the main concern, fungal RiPPs evolve to be virulence factors. RiPP function matters because it gives an indication of the environmental conditions conducive to RiPP evolution. It then follows that other fungi, under similar ecological circumstances, may produce similar RiPPs, having evolved under the same selection pressures. As such, understanding RiPP function may be key to finding novel RiPPs since in genome mining, we may narrow the search to fungi which exist in specified niches.

Genome mining, as the name implies, relies on genome availability, therefore searches for novel fungal RiPPs to date are limited to fungi with genomes that have been sequenced. However, as far more fungi exist in nature than have even been named and characterised (O'Brien et al., 2005, Hawksworth, 1991), RiPP producing species likely exist outside of those identifiable from genomic databases. Therefore, understanding RiPP function may also allow us to identify candidate ecological locations to simultaneously look for novel RiPPs and unidentified fungi. Beyond novel RiPP discovery, understanding fungal RiPP function is key to their anthropogenic employment (Spiteller, 2015).

7.4.3 Future work in functional analysis of zymoseptorin

Fungi are known to produce a wide array of compounds with extremely varied functions; therefore, it is not unsurprising that the limited activities tested here did not permit functional characterisation. The possible roles tested were logical and based on those already known to exist for RiPPs, however, even within these categories there are multiple avenues to explore. For pathogenicity for example, the impact of the RiPP was assessed only in terms of one aspect of the fungal lifecycle – the asexual cycle. The potential role of the peptide in the sexual cycle, growth and survivability in necrotic tissue and on stubble, as well as in competition with other organisms *in planta*, were not investigated, therefore the true purpose of zymoseptorin could lie here.

Though this work has made progress in narrowing down the possible role of zymoseptorin – for animal toxicity and antibiotic activity, purifying the peptide, as for chemical

characterisation, would be beneficial. Ecologically, the peptide may not have an obvious function at natural concentrations, however, at inflated concentrations a different result may be seen. Indeed, most research into antimicrobial compounds, including bacterial RiPPs, use inflated concentrations beyond that which would be produced naturally (Tenland et al., 2018, Kombrink et al., 2019, Li and Rebuffat, 2020). Not only this but peptide extraction may allow investigations of toxicity of different cell types to take place without carrying out feeding studies. Specifically, for investigation of toxicity to mammalian cell types, against which phomopsin and ustiloxin RiPPs exert their toxic effect, microtubule assembly assays may be performed (Koiso et al., 1994, Li et al., 1995) which would remove the need for animal experiments - making this the more ethical choice of study based on the principles of the Three R's.

7.5 Bioinformatic investigation of the *Z. tritici* RiPP

Within this work, zymoseptorin was explored bioinformatically from multiple perspectives, ultimately aiming to understand the *Z. tritici* RiPP in better detail and expand the range of currently known putative RiPP producers and compounds. In the first instance, bioinformatic tools allowed functional predictions for enzymes produced by genes within the Zttx biosynthetic gene cluster to be made and determined that *Z. tritici* strains not only vary in ZttxA core peptide repeat number within the precursor peptide but also in sequence. The second, used a subset of these biosynthetic cluster genes (and their translated amino acid sequences) to find fungi which produce homologous proteins.

7.5.1 The future of RiPP dikaritin genome mining

Within this work 10 further putative dikaritin RiPP producing clusters have been identified. This, alongside the 27 clusters highlighted by (Ding et al., 2016), demonstrate the capacity to find novel RiPPs using a bottom-up approach. Yet, Hetrick and van der Donk (2017) have noted that for fungal RiPPs the most common approach is top-down, identifying the peptide prior to the gene cluster (Luo et al., 2014b). Perhaps, this serves to highlight two things, the first is the progress in developing bioinformatic tools which facilitate natural product discovery, the second is the difficulty in linking genetic information to peptide synthesis – as is true for all conventional secondary metabolites. What this means for RiPPs in particular, is that no fungal RiPP identified bioinformatically has yet been functionally characterised.

The value of genome mining is often stressed – highlighting potential uses in novel drug discovery and even the potential identification of new secondary metabolite classes entirely (Gilchrist et al., 2018). However, the limitation often stated for these genomic techniques in relation to RiPPs is their reliance on homology to already characterised RiPP classes (Vignolle et al., 2020). As such, using this method will only yield similar RiPP clusters with potentially shared functions (Jingwei et al., 2022). Though novel bacterial RiPP classes have been identified from genome mining (Ren et al., 2023) and efforts are being made to minimise the need for homology in fungal RiPP genome mining (Jingwei et al., 2022), given the lag in fungal RiPP research behind that of bacteria it may be some time before computational methods for fungi catch up. Not only this, but we are also faced with the reality that translating genome mining to real peptide discovery does not appear to be straightforward – else genomically identified RiPPs would already have been isolated. Indeed, this certainly has been the case for zymoseptorin. As with conventional secondary metabolites, heterologous expression might present a way forward, as discussed in Chapter 3.

7.5.2 RiPP classifications

Given the novelty of fungi as RiPP producers, it is not surprising that fungal RiPP classifications are constantly shifting. This can be in overall group name, with some referring to the amatoxin/phallotoxin family as cycloamanides (Ozaki et al., 2023), as well as some contention over whether the dikaritin group should instead be known as Ust-RiPS (Umemura, 2020, Nagano et al., 2016, Vogt and Kunzler, 2019). Not only this, but the epichloëcyclins, which once represented a group of their own (Vogt and Kunzler, 2019) have since been moved into the dikaritin class (Kessler and Chooi, 2021). Undoubtedly, as more fungal RiPPs are identified additional family groups may be named, and subgroups within the pre-defined family groups formed.

Specifically in relation to the dikaritin RiPP class, one of the defining features of this group is processing by Kex2 endoproteases (Nagano et al., 2016). Previously cyclisation at tyrosine and isoleucine residues or tyrosine and phenylalanine residues (Vogt and Kunzler, 2019) has been stated as a common feature too of dikaritins. All novel putative dikaritin RiPPs found within this work have cyclisation at tyrosine and isoleucine residues, and the same can be said of those RiPPs identified by Ding et al. (2016). Yet, victorin and the epichloëcyclins, which also show kexin endoprotease recognition sites flanking the RiPP core sequence, do

not have these amino acids at which cyclisation can occur. In the case of the epichloëcyclins the structures of these peptides have not been fully elucidated (Ozaki et al., 2023) and so the exact amino acids at which the peptides are cyclised are unknown.

This serves to demonstrate that though RiPPs can be grouped as dikaritins based on the presence of kex2 recognition sites – variations within this group can and do exist. Therefore, it is proposed here that several subgroups within the dikaritins be formed based on how these peptides are cyclised. The first, encompassing dikaritin RiPPs cyclised at tyrosine and isoleucine residues named YI-dikaritins. Similarly, for RiPPs cyclised on phenylalanine and tyrosine residues, namely asperipins, FY-dikaritins is proposed. Peptides with similar sequences, with cyclisation on the same amino acid residues, are more likely to have similar functions so grouping by this means may be helpful in terms of bioinformatic identification of novel RiPPs.

7.5.3 The future of fungal RiPPs

To date, only one fungal RiPP has been identified as a main determinant of virulence against its host – this is victorin produced by *Cochliobolus victoriae* (Kessler et al., 2020). The novel ascomycete RiPP producers identified so far both in this work and others (Ding et al., 2016, Umemura, 2020) have been either molds, coprophilous, or pathogens of insects, plants or mushrooms. No human pathogenic fungal RiPP producers have yet been identified nor have bacterial RiPPs involved in human pathogenicity been found. However, bacterial RiPPs from species in the human microbiome are known (Fobofou and Savidge, 2022). As we are aware these peptides can be vital to a pathogenic relationship, and ascomycete pathogens of humans do exist, it is perhaps only a matter of time until a RiPP human virulence factor is found. It is then important to understand these peptides to the best of our abilities using those currently known as a basis for this to prepare for this potentiality.

7.6 *Zymoseptoria* and the environment

The impact of several abiotic conditions on *Zymoseptoria tritici* and its infection of wheat are understood. Specifically, as we explore the impact of climate change on future STB epidemics, temperature and drought have been major areas of interest. However, the environment will be modified by climate change beyond this. As such, it is important to investigate additional abiotic factors so a better picture of the extent of STB in the future can be put together. Naturally, under stress, changes in plant gene expression occur. If this

environmental stimulus results in expression of defence genes before a pathogen is delivered to the host, this could be beneficial – permitted that the same defence genes are involved in protection from the biotic threat. Equally, stressful conditions for the plant can lead to the diversion of resources away from battling a pathogen, and so the detriment of poor environmental conditions to a plant can be two-fold.

This research saw the impact of the environment on plant responses to challenge by *Zymoseptoria tritici* and determined that this was inconsistent. The problem here is that though the impact of single abiotic conditions on STB have been examined, abiotic conditions and stresses do not often exist in isolation. As a result, the benefit of one condition may be countered by the negative effect of another. The overall level of STB presented on a wheat plant is the consequence of the combined effect of all abiotic conditions. Though it is useful to understand how all of these environmental factors may interact to give the greatest natural protection to wheat plants against STB – using just the plants own response to the environment – applying this knowledge to agriculture is far more complex. It is one thing to have tight control of environmental variables in a laboratory experiment and another to try to maintain this control to a field scale.

7.7 Conclusion

This work has extended our understanding of *Zymoseptoria tritici* both in terms of a novel putative RiPP and the influence of the environment on its ability to infect its plant host. Equipped with the knowledge that a fungal RiPP involved in plant pathogenicity exists, and that the genetic components of *Zymoseptoria tritici* infection of wheat are largely unknown, this role for the *Z. tritici* RiPP was tested alongside other known RiPP functions of animal toxicity and antibiotic activity. Though the zymoseptorin RiPP has not been functionally characterised in this research, given the limitations of these analyses (discussed in section 7.4.3), space exists to explore peptide function in greater detail.

Beyond this, due to the novelty of fungal RiPPs, various aspects of zymoseptorin were explored, from its biosynthetic gene cluster to the multicore nature of the peptide precursor. These were investigated bioinformatically but also experimentally. Knockouts of the zymoseptorin cluster genes were produced in this work for future use upon development of a method for peptide purification. Repeat number of the YVIPVD core sequence within the zymoseptorin precursor peptide was determined to vary across strains and expression of the *ZttxA* gene in strains with different repeat numbers examined, however no obvious relationship between repeat number and *ZttxA* transcript levels was seen.

Finally, the ability of additional abiotic factors, beyond temperature and drought, to moderate *Z. tritici* infection of wheat was investigated. In each instance, wheat was exposed to an abiotic stress and whether this triggered plant defences, that also served to protect the plant against STB, or negatively impacted plant health and increased plant susceptibility to STB, determined. Wind priming was shown to help limit symptoms of STB on wheat, while salt treating the soil in which wheat plants were grown increased symptoms. Importantly, if outcomes of bioassays are so prone to being impacted by abiotic factors, in publications the detail included in 'Materials and Methods' sections regarding these is key to the reproducibility of experiments between research groups. Otherwise, small differences in experimental set-ups could lead to misunderstanding. Yet, tight control of environmental conditions does not reflect real life and if laboratory conditions no longer serve as a proxy for field conditions, laboratory-based experiments may cease to hold any real value. Field resistance is the totality of many factors (host, pathogen, and the environment) and therefore it is the impact on wheat production seen in the field that matters to farmers.

8 References

ACRECHE, M. M. & SLAFER, G. A. 2011. Lodging yield penalties as affected by breeding in Mediterranean wheats. *Field Crops Research,* 122**,** 40-48.

AGRAWAL, P., AMIR, S., DEEPAK, BARUA, D. & MOHANTY, D. 2021. RiPPMiner-Genome: A Web Resource for Automated Prediction of Crosslinked Chemical Structures of RiPPs by Genome Mining. *Journal of Molecular Biology,* 433**,** 1-10.

AKONDI, K. B., MUTTENTHALER, M., DUTERTRE, S., KAAS, Q., CRAIK, D. J., LEWIS, R. J. & ALEWOOD, P. F. 2014. Discovery, synthesis, and structure-activity relationships of conotoxins. *Chemical Reviews,* 114**,** 5815-47.

ALI, S. J. 2015. *Investigating secondary metabolism in Zymoseptoria tritici.* Degree of Doctor of Philosophy (Ph.D), University of Bristol.

ALLAKHVERDIEV, S. I., SAKAMOTO, A., NISHIYAMA, Y., INABA, M. & MURATA, N. 2000. Ionic and Osmotic Effects of NaCl-Induced Inactivation of Photosystems I and II in Synechococcus sp.1. *Plant Physiology,* 123**,** 1047-1056.

ALLEN, J. G., WOOD, P. M., CROCKER, K. & HAMBLIN, J. 1979. Lupinosis: a disease still with us. *Journal of the Department of Agriculture, Western Australia, Series 4,* 20**,** 10-13.

ALLIOUI, N., DRISS, F., DHOUIB, H., JLAIL, L., TOUNSI, S. & FRIKHA-GARGOURI, O. 2021. Two Novel Bacillus Strains (subtilis and simplex Species) with Promising Potential for the Biocontrol of Zymoseptoria tritici, the Causal Agent of Septoria Tritici Blotch of Wheat. *Biomed Research International,* 2021**,** 6611657.

ALLIOUI, N., SIAH, A., BRINIS, L., REIGNAULT, P. & HALAMA, P. 2016. Identification of Qol fungicide-resistant genotypes of the wheat pathogen Zymoseptoria tritici in Algeria. *Phytopathologia Mediterranea***,** 89-97.

ALMAGRO ARMENTEROS, J. J., TSIRIGOS, K. D., SONDERBY, C. K., PETERSEN, T. N., WINTHER, O., BRUNAK, S., VON HEIJNE, G. & NIELSEN, H. 2019. SignalP 5.0 improves signal peptide predictions using deep neural networks. *Nature Biotechnology,* 37**,** 420-423.

ALMEIDA, H., TSANG, A. & DIALLO, A. B. Supporting supervised learning in fungal Biosynthetic Gene Cluster discovery: new benchmark datasets. 2019 IEEE International Conference on Bioinformatics and Biomedicine (BIBM), 2019. IEEE, 1280-1287.

ALTSCHUL, S. F., GISH, W., MILLER, W., MYERS, E. W. & LIPMAN, D. J. 1990. Basic local alignment search tool. *Journal of Molecular Biology,* 215**,** 403-410.

ARAGHI, A., MAGHREBI, M. & OLESEN, J. E. 2022. Effect of wind speed variation on rainfed wheat production evaluated by the CERES-Wheat model. *International Journal of Biometeorology,* 66**,** 225-233.

ARNISON, P. G., BIBB, M. J., BIERBAUM, G., BOWERS, A. A., BUGNI, T. S., BULAJ, G., CAMARERO, J. A., CAMPOPIANO, D. J., CHALLIS, G. L., CLARDY, J., COTTER, P. D., CRAIK, D. J., DAWSON, M., DITTMANN, E., DONADIO, S., DORRESTEIN, P. C., ENTIAN, K. D., FISCHBACH, M. A., GARAVELLI, J. S., GORANSSON, U., GRUBER, C. W., HAFT, D. H., HEMSCHEIDT, T. K., HERTWECK, C., HILL, C., HORSWILL, A. R., JASPARS, M., KELLY, W. L., KLINMAN, J. P., KUIPERS, O. P., LINK, A. J., LIU, W., MARAHIEL, M. A., MITCHELL, D. A., MOLL, G. N., MOORE, B. S., MULLER, R., NAIR, S. K., NES, I. F., NORRIS, G. E., OLIVERA, B. M., ONAKA, H., PATCHETT, M. L., PIEL, J., REANEY, M. J., REBUFFAT, S., ROSS, R. P., SAHL, H. G., SCHMIDT, E. W., SELSTED, M. E., SEVERINOV, K., SHEN, B., SIVONEN, K., SMITH, L., STEIN, T., SUSSMUTH, R. D., TAGG, J. R., TANG, G. L., TRUMAN, A. W., VEDERAS, J. C., WALSH, C. T., WALTON, J. D., WENZEL, S. C., WILLEY, J. M. & VAN DER DONK, W. A. 2013. Ribosomally synthesized and post-translationally modified peptide natural products: overview and recommendations for a universal nomenclature. *Natural Product Reports,* 30**,** 108-60.

ARRAIANO, L. S. & BROWN, J. K. M. 2006. Identification of isolate-specific and partial resistance to septoria tritici blotch in 238 European wheat cultivars and breeding lines. *Plant Pathology,* 55**,** 726-738.

AULA, L., MACNACK, N., OMARA, P., MULLOCK, J. & RAUN, W. 2016. Effect of Fertilizer Nitrogen (N) on Soil Organic Carbon, Total N, and Soil pH in Long-Term Continuous Winter Wheat (Triticum AestivumL.). *Communications in Soil Science and Plant Analysis,* 47**,** 863-874.

AUSTIN, R. B. 1999. Yield of Wheat in the United Kingdom: Recent Advances and Prospects. *Crop Science,* 39**,** 1604-1610.

AVENOT, H. F. & MICHAILIDES, T. J. 2010. Progress in understanding molecular mechanisms and evolution of resistance to succinate dehydrogenase inhibiting (SDHI) fungicides in phytopathogenic fungi. *Crop Protection,* 29**,** 643-651.

AYDOGDU, M. 2020. Impact of Seedling Infection of Septoria Tritici Blotch on Bread Wheat. *The Journal of Animal and Plant Sciences,* 31.

BADET, T., OGGENFUSS, U., ABRAHAM, L., MCDONALD, B. A. & CROLL, D. 2020. A 19-isolate reference-quality global pangenome for the fungal wheat pathogen Zymoseptoria tritici. *BMC Biology,* 18**,** 12.

BAKER BRACHMANN, C., DAVIES, A., COST, G. J., CAPUTO, E., LI, J., HIETER, P. & BOEKE, J. D. 1998. Designer deletion strains derived from Saccharomyces cerevisiae S288C: a useful set of strains and plasmids for PCR-mediated gene disruption and other applications. *Yeast,* 14**,** 115-132.

BAL, A., ANIL, M., YILMAZ, I., AKATA, I. & ATILLA, O. D. 2016. An outbreak of non-fatal mushroom poisoning withOmphalotus olearіusamong Syrian refugees in Izmir, Turkey. *Toxin Reviews,* 35**,** 1-3.

BALOGLU, M. C., OZ, M. T., OKTEM, H. A. & YUCEL, M. 2012. Expression Analysis of TaNAC69-1 and TtNAMB-2, Wheat NAC Family Transcription Factor Genes Under Abiotic Stress Conditions in Durum Wheat (Triticum turgidum). *Plant Molecular Biology Reporter,* 30**,** 1246-1252.

BANKE, S. & MCDONALD, B. A. 2005. Migration patterns among global populations of the pathogenic fungus Mycosphaerella graminicola. *Molecular Ecology,* 14**,** 1881-96.

BANKE, S., PESCHON, A. & MCDONALD, B. A. 2004. Phylogenetic analysis of globally distributed Mycosphaerella graminicola populations based on three DNA sequence loci. *Fungal Genetics and Biology,* 41**,** 226-38.

BANKS, A. M., SONG, L., CHALLIS, G. L., BAILEY, A. M. & FOSTER, G. D. 2020. Bovistol B, bovistol D and strossmayerin: Sesquiterpene metabolites from the culture filtrate of the basidiomycete Coprinopsis strossmayeri. *PLoS One,* 15**,** e0229925.

BANNON, F. J. & COOKE, B. M. 1998. Studies on dispersal of Septoria tritici pycnidiospores in wheat?clover intercrops. *Plant Pathology,* 47**,** 49-56.

BARBETA, B. L., MARSHALL, A. T., GILLON, A. D., CRAIK, D. J. & ANDERSON, M. A. 2008. Plant cyclotides disrupt epithelial cells in the midgut of lepidopteran larvae. *Proceedings of the National Academy of Sciences of the United States of America,* 105**,** 1221-1225.

BARTLETT, D. W., CLOUGH, J. M., GODWIN, J. R., HALL, A. A., HAMER, M. & PARR-DOBRZANSKI, B. 2002. The strobilurin fungicides. *Pest Management Science,* 58**,** 649-62.

BATTILANI, P., GUALLA, A., DALL'ASTA, C., PELLACANI, C., GALAVERNA, G., GIORNI, P., CAGLIERI, A., TAGLIAFERRI, S., PIETRI, A. & DOSSENA, A. 2011. Phomopsins: An overview of phytopathological and chemical aspects, toxicity, analysis and occurrence. *World Mycotoxin Journal,* 4**,** 345-359.

BEARCHELL, S. J., FRAAIJE, B. A., SHAW, M. W. & FITT, B. D. 2005. Wheat archive links long-term fungal pathogen population dynamics to air pollution. *Proceedings of the National Academy of Sciences,* 102**,** 5438-5442.

BEGLEY, M., COTTER, P. D., HILL, C. & ROSS, R. P. 2009. Identification of a novel two-peptide lantibiotic, lichenicidin, following rational genome mining for LanM proteins. *Applied and Environmental Microbiology,* 75**,** 5451-60.

BELBIN, F. E., HALL, G. J., JACKSON, A. B., SCHANSCHIEFF, F. E., ARCHIBALD, G., FORMSTONE, C. & DODD, A. N. 2019. Plant circadian rhythms regulate the effectiveness of a glyphosate-based herbicide. *Nature Communications,* 10**,** 3704.

BELLOW, S., LATOUCHE, G., BROWN, S. C., POUTARAUD, A. & CEROVIC, Z. G. 2013. Optical detection of downy mildew in grapevine leaves: daily kinetics of autofluorescence upon infection. *Journal of Experimental Botany,* 64**,** 333-41.

BERROCAL-TITO, G., SAMETZ-BARON, L., EICHENBERG, K., HORWITZ, B. A. & HERRERA-ESTRELLA, A. 1999. Rapid blue light regulation of a Trichoderma harzianum photolyase gene. *Journal of Biological Chemistry,* 274**,** 14288-94.

BERRY, D., LEE, K., WINTER, D., MACE, W., BECKER, Y., NAGABHYRU, P., TREINDL, A. D., BOGANTES, E. V., YOUNG, C. A., LEUCHTMANN, A., JOHNSON, L. J., JOHNSON, R. D., COX, M. P., SCHARDL, C. L. & SCOTT, B. 2022. Cross-species transcriptomics identifies core regulatory changes differentiating the asymptomatic asexual and virulent sexual life cycles of grass-symbiotic Epichloe fungi. *G3 (Bethesda),* 12.

BHAT, R., RAI, R. V. & KARIM, A. A. 2010. Mycotoxins in food and feed: present status and future concerns. *Comprehensive reviews in food science and food safety,* 9**,** 57-81.

BLIN, K., SHAW, S., AUGUSTIJN, H. E., REITZ, Z. L., BIERMANN, F., ALANJARY, M., FETTER, A., TERLOUW, B. R., METCALF, W. W., HELFRICH, E. J. N., VAN WEZEL, G. P., MEDEMA, M. H. & WEBER, T. 2023. antiSMASH 7.0: new and improved predictions for detection, regulation, chemical structures and visualisation. *Nucleic Acids Research*.

BLIN, K., SHAW, S., KLOOSTERMAN, A. M., CHARLOP-POWERS, Z., VAN WEZEL, G. P., MEDEMA, M. H. & WEBER, T. 2021. antiSMASH 6.0: improving cluster detection and comparison capabilities. *Nucleic Acids Research***,** 1-7.

BOYER, J. S. 1982. Plant productivity and environment. *Science,* 218**,** 443-448.

BRADING, P. A., VERSTAPPEN, E. C. P., KEMA, G. H. J. & BROWN, J. K. M. 2002. A Gene-for-Gene Relationship Between Wheat and Mycosphaerella graminicola, the Septoria Tritici Blotch Pathogen. *Phytopathology,* 92**,** 439-445.

BRAKHAGE, A. A. 2013. Regulation of fungal secondary metabolism. *Nature Reviews Microbiology,* 11**,** 21-32.

BRENNAN, C. J., BENBOW, H. R., MULLINS, E. & DOOHAN, F. M. 2019. A review of the known unknowns in the early stages of septoria tritici blotch disease of wheat. *Plant Pathology,* 68**,** 1427-1438.

BRENNER, C. & FULLER, R. S. 1992. Structural and enzymatic characterization of a purified prohormone-processing enzyme: secreted, soluble Kex2 protease. *Proceedings of the National Academy of Sciences of the United States of America,* 89**,** 922-926.

BROMANN, K., TOIVARI, M., VILJANEN, K., VUORISTO, A., RUOHONEN, L. & NAKARI-SETALA, T. 2012. Identification and characterization of a novel diterpene gene cluster in Aspergillus nidulans. *PLoS One,* 7**,** e35450.

BROSCH, G., RANSOM, R., LECHNER, T., WALTON, J. D. & LOIDL, P. 1995. Inhibition of maize histone deacetylases by HC toxin, the host-selective toxin of Cochliobolus carbonum. *The Plant Cell,* 7**,** 1941-1950.

BROWN, J. K., CHARTRAIN, L., LASSERRE-ZUBER, P. & SAINTENAC, C. 2015. Genetics of resistance to Zymoseptoria tritici and applications to wheat breeding. *Fungal Genetics and Biology,* 79**,** 33-41.

BROWN, J. K. M., KEMA, G. H. J., FORRER, H. R., VERSTAPPEN, E. C. P., ARRAIANO, L. S., BRADING, P. A., FOSTER, E. M., FRIED, P. M. & JENNY, E. 2001. Resistance of wheat cultivars and breeding lines to septoria tritici blotch caused by isolates of Mycosphaerella graminicola in field trials. *Plant Pathology,* 50**,** 325-338.

BRUECKNER, F. & CRAMER, P. 2008. Structural basis of transcription inhibition by alpha-amanitin and implications for RNA polymerase II translocation. *Nature Structural & Molecular Biology,* 15**,** 811-8.

BUCKNELL, A. H. & MCDONALD, M. C. 2023. That's no moon, it's a Starship: Giant transposons driving fungal horizontal gene transfer. *Molecular Microbiology,* 120**,** 555-563.
BUCZEK, O., BULAJ, G. & OLIVERA, B. M. 2005. Conotoxins and the posttranslational modification of secreted gene products. *Cellular and Molecular Life Sciences,* 62**,** 3067-79.
BUNDOCK, P. & HOOYKAAS, P. J. J. 1996. Integration of Agrobacterium tumefaciens T-DNA in the Saccharomyces cerevisiae genome by illegitimate recombination. *Proceedings of the National Academy of Sciences of the United States of America,* 93**,** 15272–15275.
BUSH, L. P., WILKINSON, H. H. & SCHARDL, C. L. 1997. Bioprotective Alkaloids of Grass-Fungal Endophyte Symbioses. *Plant Physiology,* 114**,** 1-7.
CARADUS, J. R. & JOHNSON, L. J. 2020. Epichloe Fungal Endophytes-From a Biological Curiosity in Wild Grasses to an Essential Component of Resilient High Performing Ryegrass and Fescue Pastures. *Journal of Fungi (Basel),* 6.
CHARTRAIN, L., BRADING, P., MAKEPEACE, J. & BROWN, J. 2004. Sources of resistance to septoria tritici blotch and implications for wheat breeding. *Plant Pathology,* 53**,** 454-460.
CHARTRAIN, L., BRADING, P. A. & BROWN, J. K. M. 2005. Presence of the Stb6 gene for resistance to septoria tritici blotch (Mycosphaerella graminicola) in cultivars used in wheat-breeding programmes worldwide. *Plant Pathology,* 54**,** 134-143.
CHEN, H., KING, R., SMITH, D., BAYON, C., ASHFIELD, T., TORRIANI, S., KANYUKA, K., HAMMOND-KOSACK, K., BIERI, S. & RUDD, J. 2023. Combined pangenomics and transcriptomics reveals core and redundant virulence processes in a rapidly evolving fungal plant pathogen. *BMC Biology,* 21**,** 24.
CHEN, Q., BAKHSHI, M., BALCI, Y., BRODERS, K. D., CHEEWANGKOON, R., CHEN, S. F., FAN, X. L., GRAMAJE, D., HALLEEN, F., JUNG, M. H., JIANG, N., JUNG, T., MAJEK, T., MARINCOWITZ, S., MILENKOVIC, I., MOSTERT, L., NAKASHIMA, C., NURUL FAZIHA, I., PAN, M., RAZA, M., SCANU, B., SPIES, C. F. J., SUHAIZAN, L., SUZUKI, H., TIAN, C. M., TOMSOVSKY, M., URBEZ-TORRES, J. R., WANG, W., WINGFIELD, B. D., WINGFIELD, M. J., YANG, Q., YANG, X., ZARE, R., ZHAO, P., GROENEWALD, J. Z., CAI, L. & CROUS, P. W. 2022. Genera of phytopathogenic fungi: GOPHY 4. *Studies in Mycology,* 101**,** 417-564.
CHEN, R.-S. & MCDONALD, B. A. 1996. Sexual reproduction plays a major role in the genetic structure of populations of the fungus Mycosphaerella graminicola. *Genetics,* 142**,** 1119-1127.
CHEUNG, P. C. K. & MEHTA, B. M. 2015. *Handbook of food chemistry*, Springer Berlin Heidelberg.
CHIGUMBA, D. N., MYDY, L. S., DE WAAL, F., LI, W., SHAFIQ, K., WOTRING, J. W., MOHAMED, O. G., MLADENOVIC, T., TRIPATHI, A., SEXTON, J. Z., KAUTSAR, S., MEDEMA, M. H. & KERSTEN, R. D. 2022. Discovery and biosynthesis of cyclic plant peptides via autocatalytic cyclases. *Natural Chemical Biology,* 18**,** 18-28.
CHILD, H. T. & BAILEY, A. unpublished. *Investigation of a novel ribosomal peptide with a potential function during the host-pathogen interaction of Zymoseptoria tritici.* Unpublished, University of Bristol, Bristol, UK.
CHOI, B., GHOSH, R., GURURANI, M. A., SHANMUGAM, G., JEON, J., KIM, J., PARK, S. C., JEONG, M. J., HAN, K. H., BAE, D. W. & BAE, H. 2017. Positive regulatory role of sound vibration treatment in Arabidopsis thaliana against Botrytis cinerea infection. *Scientific Reports,* 7**,** 1-14.
CLAY, K. 1996. Interactions among fungal endophytes, grasses and herbivores. *Researches on Population Ecology,* 38**,** 191-201.
COLGRAVE, M. L., KOTZE, A. C., IRELAND, D. C., WANG, C. K. & CRAIK, D. J. 2008. The anthelmintic activity of the cyclotides: natural variants with enhanced activity. *ChemBioChem,* 9**,** 1939-45.
COOK, R. J., POLLEY, R. W. & THOMAS, M. R. 1991. Disease-induced losses in winter wheat in England and Wales 1985–1989. *Crop Protection,* 10**,** 504-508.
COOLS, H. J. & FRAAIJE, B. A. 2008. Are azole fungicides losing ground against Septoria wheat disease? Resistance mechanisms in Mycosphaerella graminicola. *Pest Management Science,* 64**,** 681-4.

COOLS, H. J., MULLINS, J. G., FRAAIJE, B. A., PARKER, J. E., KELLY, D. E., LUCAS, J. A. & KELLY, S. L. 2011. Impact of recently emerged sterol 14{alpha}-demethylase (CYP51) variants of Mycosphaerella graminicola on azole fungicide sensitivity. *Applied Environmental Microbiology,* 77**,** 3830-7.

COTTER, P. D., HILL, C. & ROSS, R. P. 2005. Bacteriocins: developing innate immunity for food. *Nature Reviews Microbiology,* 3**,** 777-788.

COUSIN, A., MEHRABI, R., GUILLEROUX, M., DUFRESNE, M., T, V. D. L., WAALWIJK, C., LANGIN, T. & KEMA, G. H. 2006. The MAP kinase-encoding gene MgFus3 of the non-appressorium phytopathogen Mycosphaerella graminicola is required for penetration and in vitro pycnidia formation. *Molecular Plant Pathology,* 7**,** 269-78.

CRAIG, A. G. 2000. The Characterization of Conotoxins. *Journal of Toxicology: Toxin Reviews,* 19**,** 53-93.

CRAIK, D. J., DALY, N. L., BOND, T. & WAINE, C. 1999. Plant cyclotides: a unique family of cyclic and knotted proteins that defines the cyclic cystine knot structural motif. *Journal of Molecular Biology,* 294**,** 1327-1336.

CROPMONITOR. 2020. *Defra Winter Wheat Commercial Crops Disease Survey 2019 Highlights* [Online]. Available: http://www.cropmonitor.co.uk/cmsReport.cfm?id=59 [Accessed 4 February 2020].

CROUS, P. W., BRAUN, U. & GROENEWALD, J. Z. 2007. Mycosphaerella is polyphyletic. *Studies in Mycology,* 58**,** 1-32.

CSÉFALVAY, L., DI GASPERO, G., MATOUŠ, K., BELLIN, D., RUPERTI, B. & OLEJNÍČKOVÁ, J. 2009. Pre-symptomatic detection of Plasmopara viticola infection in grapevine leaves using chlorophyll fluorescence imaging. *European Journal of Plant Pathology,* 125**,** 291-302.

CURRAN, E., BURKE, J. I. & FEECHAN, A. 2023. Mixed infections of Zymoseptoria tritici lead to reduced Septoria tritici blotch disease symptoms. *Plant Pathology,* 00**,** 1-16.

CZEKSTER, C. M., LUDEWIG, H., MCMAHON, S. A. & NAISMITH, J. H. 2017. Characterization of a dual function macrocyclase enables design and use of efficient macrocyclization substrates. *Nature Communications,* 8**,** 1045.

DEAN, R., VAN KAN, J. A., PRETORIUS, Z. A., HAMMOND-KOSACK, K. E., DI PIETRO, A., SPANU, P. D., RUDD, J. J., DICKMAN, M., KAHMANN, R., ELLIS, J. & FOSTER, G. D. 2012. The Top 10 fungal pathogens in molecular plant pathology. *Molecular Plant Pathology,* 13**,** 414-30.

DEFRA. 2022. *Cereal and oilseed production in the United Kingdom 2022* [Online]. Available: https://www.gov.uk/government/statistics/cereal-and-oilseed-rape-production/cereal-and-oilseed-production-in-the-united-kingdom-2022 [Accessed 07/08/23 2023].

DEFRA. 2023. *Total income from farming in the UK in 2022* [Online]. Available: https://www.gov.uk/government/statistics/total-income-from-farming-in-the-uk/total-income-from-farming-in-the-uk-in-2022#about-these-statistics [Accessed 07/08/2023 2023].

DEIHIMI, T., NIAZI, A. & EBRAHIMIE, E. 2013. Identification and expression analysis of TLPs as candidate genes promoting the responses to both biotic and abiotic stresses in wheat. *Plant Omics,* 6**,** 107-115.

DERBYSHIRE, M. C., GOHARI, A. M., MEHRABI, R., KILARU, S., STEINBERG, G., ALI, S., BAILEY, A., HAMMOND-KOSACK, K., KEMA, G. H. J. & RUDD, J. J. 2018. Phosphopantetheinyl transferase (Ppt)-mediated biosynthesis of lysine, but not siderophores or DHN melanin, is required for virulence of Zymoseptoria tritici on wheat. *Scientific Reports,* 8**,** 17069.

DIAZ, J. H. 2018. Amatoxin-Containing Mushroom Poisonings: Species, Toxidromes, Treatments, and Outcomes. *Wilderness & Environmental Medicine,* 29**,** 111-118.

DILLEN, S., VERDONCK, R., ZELS, S., VAN WIELENDAELE, P. & VANDEN BROECK, J. 2014. Identification of the short neuropeptide F precursor in the desert locust: evidence for an inhibitory role of sNPF in the control of feeding. *Peptides,* 53**,** 134-9.

DING, W., LIU, W. Q., JIA, Y., LI, Y., VAN DER DONK, W. A. & ZHANG, Q. 2016. Biosynthetic investigation of phomopsins reveals a widespread pathway for ribosomal natural products in

Ascomycetes. *Proceedings of the National Academy of Sciences of the United States of America,* 113**,** 3521-6.
DROTT, M. T., PARK, S. C., WANG, Y. W., HARROW, L., KELLER, N. P. & PRINGLE, A. 2023. Pangenomics of the death cap mushroom Amanita phalloides, and of Agaricales, reveals dynamic evolution of toxin genes in an invasive range. *The ISME Journal,* 17**,** 1236-1246.
DUBIN, H. J. & RAJARAM, S. 1996. BREEDING DISEASE-RESISTANT WHEATS FOR TROPICAL HIGHLANDS AND LOWLANDS. *Annual Review of Phytopathology,* 34**,** 503-526.
DUNCAN, K. E. & HOWARD, R. J. 2000. Cytological analysis of wheat infection by the leaf blotch pathogen Mycosphaerella graminicola. *Mycological Research,* 104**,** 1074-1082.
ENJALBERT, F., CASSANAS, G., RAPIOR, S., RENAULT, C. & CHAUMONT, J. P. 2004. Amatoxins in wood-rotting Galerina marginata. *Mycologia,* 96**,** 720-9.
ENJALBERT, F., GALLION, C., JEHL, F. & MONTEIL, H. 1993. Toxin content, phallotoxin and amatoxin composition of Amanita phalloides tissues. *Toxicon,* 31**,** 803-807.
ENJALBERT, F., RAPIOR, S., NOUGUIER-SOULE, J., GUILLON, S., AMOUROUX, N. & CABOT, C. 2002. Treatment of Amatoxin Poisoning: 20-year Retrospective Analysis. *Clinical Toxicology,* 40**,** 715-757.
ERNANI, P. R., BAYER, C. & MAESTRI, L. 2002. Corn Yield as Affected by Liming and Tillage System on an Acid Brazilian Oxisol. *Agronomy Journal,* 94**,** 305-309.
EYAL, Z. 1999. Breeding for Resistance to Septoria and Stagonospora Diseases of Wheat. *In:* LUCAS, J. A., BOWYER, P. & ANDERSON, H. M. (eds.) *Septoria on Cereals: a Study of Pathosystems.* Wallingford, Oxon, United Kingdom: CAB International.
FAN, K., WEISENHORN, P., GILBERT, J. A., SHI, Y., BAI, Y. & CHU, H. 2018. Soil pH correlates with the co-occurrence and assemblage process of diazotrophic communities in rhizosphere and bulk soils of wheat fields. *Soil Biology and Biochemistry,* 121**,** 185-192.
FANTOZZI, R., LEDDA, F., CARAMELLI, L., MORONI, F., BLANDINA, P., MASINI, E., BOTTI, P., PERUZZI, S., ZORN, M. & MANNAIONI, P. 1986. Clinical findings and follow-up evaluation of an outbreak of mushroom poisoning—survey of Amanita phalloides poisoning. *Klinische Wochenschrift,* 64**,** 38-43.
FERIR, G., PETROVA, M. I., ANDREI, G., HUSKENS, D., HOORELBEKE, B., SNOECK, R., VANDERLEYDEN, J., BALZARINI, J., BARTOSCHEK, S., BRONSTRUP, M., SUSSMUTH, R. D. & SCHOLS, D. 2013. The lantibiotic peptide labyrinthopeptin A1 demonstrates broad anti-HIV and anti-HSV activity with potential for microbicidal applications. *PLoS One,* 8**,** e64010.
FEURTEY, A., LORRAIN, C., MCDONALD, M. C., MILGATE, A., SOLOMON, P. S., WARREN, R., PUCCETTI, G., SCALLIET, G., TORRIANI, S. F. F., GOUT, L., MARCEL, T. C., SUFFERT, F., ALASSIMONE, J., LIPZEN, A., YOSHINAGA, Y., DAUM, C., BARRY, K., GRIGORIEV, I. V., GOODWIN, S. B., GENISSEL, A., SEIDL, M. F., STUKENBROCK, E. H., LEBRUN, M. H., KEMA, G. H. J., MCDONALD, B. A. & CROLL, D. 2023. A thousand-genome panel retraces the global spread and adaptation of a major fungal crop pathogen. *Nature Communications,* 14**,** 1059.
FIGUEROA, M., HAMMOND-KOSACK, K. E. & SOLOMON, P. S. 2018. A review of wheat diseases-a field perspective. *Molecular Plant Pathology,* 19**,** 1523-1536.
FISCHER, R. A. & STAPPER, M. 1987. Lodging effects on high-yielding crops of irrigated semidwarf wheat. *Field Crops Research,* 17**,** 245-258.
FOBOFOU, S. A. & SAVIDGE, T. 2022. Microbial metabolites: cause or consequence in gastrointestinal disease? *The American Journal of Physiology-Gastrointestinal and Liver Physiology,* 322**,** G535-G552.
FONES, H. & GURR, S. 2015. The impact of Septoria tritici Blotch disease on wheat: An EU perspective. *Fungal Genetics and Biology,* 79**,** 3-7.
FONES, H. N., EYLES, C. J., KAY, W., COWPER, J. & GURR, S. J. 2017. A role for random, humidity-dependent epiphytic growth prior to invasion of wheat by Zymoseptoria tritici. *Fungal Genetics and Biology,* 106**,** 51-60.

FONES, H. N., STEINBERG, G. & GURR, S. J. 2015. Measurement of virulence in Zymoseptoria tritici through low inoculum-density assays. *Fungal Genetics and Biology,* 79**,** 89-93.
FORD, R. E., FOSTER, G. D. & BAILEY, A. M. 2022. Exploring fungal RiPPs from the perspective of chemical ecology. *Fungal Biology and Biotechnology,* 9**,** 12.
FOYER, C. H. 2018. Reactive oxygen species, oxidative signaling and the regulation of photosynthesis. *Environmental and Experimental Botany,* 154**,** 134-142.
FRAAIJE, B., BURNETT, F., CLARK, W., MOTTERAM, J. & LUCAS, J. Resistance development to QoI inhibitors in populations of Mycosphaerella graminicola in the UK. Modern fungicides and antifungal compounds IV: 14th International Reinhardsbrunn Symposium, Friedrichroda, Thuringia, Germany, April 25-29, 2004, 2005a. British Crop Protection Council, 63-71.
FRAAIJE, B. A., BAYON, C., ATKINS, S., COOLS, H. J., LUCAS, J. A. & FRAAIJE, M. W. 2012. Risk assessment studies on succinate dehydrogenase inhibitors, the new weapons in the battle to control Septoria leaf blotch in wheat. *Molecular Plant Pathology,* 13**,** 263-75.
FRAAIJE, B. A., COOLS, H. J., FOUNTAINE, J., LOVELL, D. J., MOTTERAM, J., WEST, J. S. & LUCAS, J. A. 2005b. Role of Ascospores in Further Spread of QoI-Resistant Cytochrome b Alleles (G143A) in Field Populations of Mycosphaerella graminicola. *Phytopathology,* 95**,** 933-941.
FRAAIJE, B. A., COOLS, H. J., KIM, S. H., MOTTERAM, J., CLARK, W. S. & LUCAS, J. A. 2007. A novel substitution I381V in the sterol 14alpha-demethylase (CYP51) of Mycosphaerella graminicola is differentially selected by azole fungicides. *Molecular Plant Pathology,* 8**,** 245-54.
FRANCISCO, C. S., MA, X., ZWYSSIG, M. M., MCDONALD, B. A. & PALMA-GUERRERO, J. 2019. Morphological changes in response to environmental stresses in the fungal plant pathogen Zymoseptoria tritici. *Scientific Reports,* 9**,** 9642.
FRANCISCO, C. S., MCDONALD, B. A. & PALMA-GUERRERO, J. 2023. A transcription factor and a phosphatase regulate temperature-dependent morphogenesis in the fungal plant pathogen Zymoseptoria tritici. *Fungal Genetics and Biology,* 167.
FULLER, K. K., LOROS, J. J. & DUNLAP, J. C. 2015. Fungal photobiology: visible light as a signal for stress, space and time. *Current Genetics,* 61**,** 275-88.
GARCIA, J., COSTA, V. M., CARVALHO, A., BAPTISTA, P., DE PINHO, P. G., DE LOURDES BASTOS, M. & CARVALHO, F. 2015. Amanita phalloides poisoning: Mechanisms of toxicity and treatment. *Food and Chemical Toxicology,* 86**,** 41-55.
GARDES, M. & BRUNS, T. D. 1993. ITS primers with enhanced specificity for basidiomycetes-application to the identification of mycorrhizae and rusts. *Molecular Ecology,* 2**,** 113-118.
GARDINER, M. 1975. Lupinosis. *Journal of the Department of Agriculture, Western Australia, Series 4,* 16**,** 26-30.
GHIMIRE, R., MACHADO, S. & BISTA, P. 2017. Soil pH, Soil Organic Matter, and Crop Yields in Winter Wheat–Summer Fallow Systems. *Agronomy Journal,* 109**,** 706-717.
GIETZ, R. D. & SCHIESTL, R. H. 2007. High-efficiency yeast transformation using the LiAc/SS carrier DNA/PEG method. *Nature Protocols,* 2**,** 31-4.
GIETZ, R. D. & WOODS, R. A. 2002. Transformation of yeast by lithium acetate/single-stranded carrier DNA/polyethylene glycol method. *Methods in Enzymology.* Elsevier.
GILCHRIST, C. L., BOOTH, T. J., VAN WERSCH, B., VAN GRIEKEN, L., MEDEMA, M. H. & CHOOI, Y.-H. 2021. Cblaster: a remote search tool for rapid identification and visualization of homologous gene clusters. *Bioinformatics Advances,* 1**,** vbab016.
GILCHRIST, C. L. M. & CHOOI, Y. H. 2021. clinker & clustermap.js: automatic generation of gene cluster comparison figures. *Bioinformatics,* 37**,** 2473-2475.
GILCHRIST, C. L. M., LI, H. & CHOOI, Y. H. 2018. Panning for gold in mould: can we increase the odds for fungal genome mining? *Organic and Biomolecular Chemistry,* 16**,** 1620-1626.
GISI, U., CHIN, K. M., KNAPOVA, G., KÜNG FÄRBER, R., MOHR, U., PARISI, S., SIEROTZKI, H. & STEINFELD, U. 2000. Recent developments in elucidating modes of resistance to phenylamide, DMI and strobilurin fungicides. *Crop Protection,* 19**,** 863-872.

GISI, U. & SIEROTZKI, H. 2008. Fungicide modes of action and resistance in downy mildews. *European Journal of Plant Pathology,* 122**,** 157-167.
GISI, U., SIEROTZKI, H., COOK, A. & MCCAFFERY, A. 2002. Mechanisms influencing the evolution of resistance to Qo inhibitor fungicides. *Pest Management Science,* 58**,** 859-67.
GLADDERS, P., PAVELEY, N. D., BARRIE, I. A., HARDWICK, N. V., HIMS, M. J., LANGTON, S. & TAYLOR, M. C. 2001. Agronomic and meteorological factors affecting the severity of leaf blotch caused by Mycosphaerella graminicola in commercial wheat crops in England. *Annals of Applied Biology,* 138**,** 301-311.
GONZÁLEZ-PASTOR, J. E., HOBBS, E. C. & LOSICK, R. 2003. Cannibalism by sporulating bacteria. *Science,* 301**,** 510-513.
GOODWIN, S. B. 2007. Back to basics and beyond: increasing the level of resistance to Septoria tritici blotch in wheat. *Australasian Plant Pathology,* 36**,** 532-538.
GOODWIN, S. B., M'BAREK S, B., DHILLON, B., WITTENBERG, A. H., CRANE, C. F., HANE, J. K., FOSTER, A. J., VAN DER LEE, T. A., GRIMWOOD, J., AERTS, A., ANTONIW, J., BAILEY, A., BLUHM, B., BOWLER, J., BRISTOW, J., VAN DER BURGT, A., CANTO-CANCHE, B., CHURCHILL, A. C., CONDE-FERRAEZ, L., COOLS, H. J., COUTINHO, P. M., CSUKAI, M., DEHAL, P., DE WIT, P., DONZELLI, B., VAN DE GEEST, H. C., VAN HAM, R. C., HAMMOND-KOSACK, K. E., HENRISSAT, B., KILIAN, A., KOBAYASHI, A. K., KOOPMANN, E., KOURMPETIS, Y., KUZNIAR, A., LINDQUIST, E., LOMBARD, V., MALIEPAARD, C., MARTINS, N., MEHRABI, R., NAP, J. P., PONOMARENKO, A., RUDD, J. J., SALAMOV, A., SCHMUTZ, J., SCHOUTEN, H. J., SHAPIRO, H., STERGIOPOULOS, I., TORRIANI, S. F., TU, H., DE VRIES, R. P., WAALWIJK, C., WARE, S. B., WIEBENGA, A., ZWIERS, L. H., OLIVER, R. P., GRIGORIEV, I. V. & KEMA, G. H. 2011. Finished genome of the fungal wheat pathogen Mycosphaerella graminicola reveals dispensome structure, chromosome plasticity, and stealth pathogenesis. *PLoS Genetics,* 7**,** e1002070.
GÖRANSSON, U., SJÖGREN, M., SVANGÅRD, E., CLAESON, P. & BOHLIN, L. 2004. Reversible antifouling effect of the cyclotide cycloviolacin O2 against barnacles. *Journal of Natural Products,* 67**,** 1287-1290.
GOTO, Y., LI, B., CLAESEN, J., SHI, Y., BIBB, M. J. & VAN DER DONK, W. A. 2010. Discovery of unique lanthionine synthetases reveals new mechanistic and evolutionary insights. *PLoS Biology,* 8**,** e1000339.
GOUDARZI, M. & PAKNIYAT, H. 2008. Evaluation of wheat cultivars under salinity stress based on some agronomic and physiological traits. *Journal of Agriculture & Social Sciences,* 4**,** 35-38.
GOV.UK. 2023. *Average wind speed and deviations from the long term mean (ET 7.2)* [Online]. Available: https://www.gov.uk/government/statistics/energy-trends-section-7-weather [Accessed 16/08/23 2023].
GRAFTON, R. Q., DAUGBJERG, C. & QURESHI, M. E. 2015. Towards food security by 2050. *Food Security,* 7**,** 179-183.
GREEN, K. A., BERRY, D., FEUSSNER, K., EATON, C. J., RAM, A., MESARICH, C. H., SOLOMON, P., FEUSSNER, I. & SCOTT, B. 2020. Lolium perenne apoplast metabolomics for identification of novel metabolites produced by the symbiotic fungus Epichloe festucae. *New Phytologist,* 227**,** 559-571.
GREENE, S., MORRISSEY, M. & JOHNSON, S. E. 2010. Wind Climatology, Climate Change, and Wind Energy. *Geography Compass,* 4**,** 1592-1605.
GU, D., ANDREEV, K. & DUPRE, M. E. 2021. Major trends in population growth around the world. *China CDC weekly,* 3**,** 604.
GUSTAFSON, K. R., MCKEE, T. C. & BOKESCH, H. R. 2004. Anti-HIV cyclotides. *Current Protein and Peptide Science,* 5**,** 331-40.
HABIG, M., BAHENA-GARRIDO, S. M., BARKMANN, F., HAUEISEN, J. & STUKENBROCK, E. H. 2020. The transcription factor Zt107320 affects the dimorphic switch, growth and virulence of the fungal wheat pathogen Zymoseptoria tritici. *Molecular Plant Pathology,* 21**,** 124-138.

HABIG, M., QUADE, J. & STUKENBROCK, E. H. 2017. Forward Genetics Approach Reveals Host Genotype-Dependent Importance of Accessory Chromosomes in the Fungal Wheat Pathogen Zymoseptoria tritici. *mBio,* 8.

HABIG, M., SCHOTANUS, K., HUFNAGEL, K., HAPPEL, P. & STUKENBROCK, E. H. 2021. Ago1 Affects the Virulence of the Fungal Plant Pathogen Zymoseptoria tritici. *Genes (Basel),* 12.

HAJIEGHRARI, B., TORABI-GIGLOU, M., MOHAMMADI, M. R. & DAVARI, M. 2008. Biological potantial of some Iranian Trichoderma isolates in the control of soil borne plant pathogenic fungi. *African Journal of Biotechnology,* 7.

HALL, T. A. BioEdit: a user-friendly biological sequence alignment editor and analysis program for Windows 95/98/NT. Nucleic acids symposium series, 1999. [London]: Information Retrieval Ltd., c1979-c2000., 95-98.

HALLEN, H. E., ADAMS, G. C. & EICKER, A. 2002. Amatoxins and phallotoxins in indigenous and introduced South African Amanita species. *South African Journal of Botany,* 68**,** 322-326.

HALLEN, H. E., LUO, H., SCOTT-CRAIG, J. S. & WALTON, J. D. 2007. Gene family encoding the major toxins of lethal Amanita mushrooms. *Proceedings of the National Academy of Sciences of the United States of America,* 104**,** 19097-19101.

HAMMOND-KOSACK, K. E. & RUDD, J. J. 2008. Plant resistance signalling hijacked by a necrotrophic fungal pathogen. *Plant Signaling & Behavior,* 3**,** 993-5.

HARDWICK, N. V., JONES, D. R. & SLOUGH, J. E. 2001. Factors affecting diseases of winter wheat in England and Wales, 1989-98. *Plant Pathology,* 50**,** 453-462.

HARLAN, J. R. & ZOHARY, D. 1966. Distribution of wild wheats and barley: the present distribution of wild forms may provide clues to the regions of early cereal domestication. *Science,* 153**,** 1074-1080.

HASSANI, A., AZAPAGIC, A. & SHOKRI, N. 2021a. Global predictions of primary soil salinization under changing climate in the 21st century. *Nature Communications,* 12**,** 6663.

HASSANI, M. A., OPPONG-DANQUAH, E., FEURTY, A., TASDEMIR, D. & STUKENBROCK, E. H. 2021b. Differential regulation and production of secondary metabolites among isolates of the fungal wheat pathogen Zymoseptoria tritici. *bioRxiv*.

HAWKSWORTH, D. L. 1991. The fungal dimension of biodiversity: magnitude, significance, and conservation. *Mycological Research,* 95**,** 641-655.

HEGEMANN, J. D., ZIMMERMANN, M., ZHU, S., KLUG, D. & MARAHIEL, M. A. 2013. Lasso peptides from proteobacteria: Genome mining employing heterologous expression and mass spectrometry. *Biopolymers,* 100**,** 527-42.

HEICK, T. M., JUSTESEN, A. F. & JØRGENSEN, L. N. 2017. Anti-resistance strategies for fungicides against wheat pathogen Zymoseptoria tritici with focus on DMI fungicides. *Crop Protection,* 99**,** 108-117.

HETRICK, K. J. & VAN DER DONK, W. A. 2017. Ribosomally synthesized and post-translationally modified peptide natural product discovery in the genomic era. *Current Opinion in Chemical Biology,* 38**,** 36-44.

HOHMANN, S. 2002. Osmotic stress signaling and osmoadaptation in yeasts. *Microbiology and Molecular Biology Reviews,* 66**,** 300-72.

HOSSAIN, M. A., NAHAR, K. & HASANUZZAMAN, M. 2019. *Wheat Production in Changing Environments: Responses, Adaptation and Tolerance*, Springer.

HOWELL, C. 2003. Mechanisms employed by Trichoderma species in the biological control of plant diseases: the history and evolution of current concepts. *Plant Disease,* 87**,** 4-10.

HUDSON, G. A. & MITCHELL, D. A. 2018. RiPP antibiotics: biosynthesis and engineering potential. *Current Opinion in Microbiology,* 45**,** 61-69.

HUNTER, COKER & ROYLE 1999a. The teleomorph stage, Mycosphaerella graminicola, in epidemics of septoria tritici blotch on winter wheat in the UK. *Plant Pathology,* 48**,** 51-57.

HUNTER, T., COKER, R. R. & ROYLE, D. J. 1999b. Studies on the Sexual Phase of Leaf Blotch in UK Winter Wheat. *In:* LUCAS, J. A., BOWYER, P. & ANDERSON, H. M. (eds.) *Septoria on Cereals: a Study of Pathosystems.* Wallingford, Oxon, United Kingdom: CAB International.

HUTCHISON, L. J., MADZIA, S. E. & BARRON, G. L. 1996. The presence and antifeedant function of toxin-producing secretory cells on hyphae of the lawn-inhabiting agaric Conocybe lactea. *Canadian Journal of Botany,* 74**,** 431-434.

IBRAHIM, M. E. H., ZHU, X., ZHOU, G., ALI, A. Y. A., AHMAD, I. & FARAH, G. A. 2018. Nitrogen fertilizer alleviated negative impacts of NaCl on some physiological parameters of wheat. *Pakistan Journal of Botany,* 50**,** 2097-2104.

INOUE, H., NOJIMA, H. & OKAYAMA, H. 1990. High efficiency transformation of Escherichia coli with plasmids. *Gene,* 96**,** 23-28.

IWASAKI, S. 1992. Chemistry and biological activity of the mycotoxins interfering with tubulin function. *JSM Mycotoxins,* 1992**,** 1-6.

JABES, D., BRUNATI, C., CANDIANI, G., RIVA, S., ROMANO, G. & DONADIO, S. 2011. Efficacy of the new lantibiotic NAI-107 in experimental infections induced by multidrug-resistant Gram-positive pathogens. *Antimicrobial Agents and Chemotherapy,* 55**,** 1671-6.

JAENIKE, J. 1985. Parasite pressure and the evolution of amanitin tolerance in Drosophila. *Evolution,* 39**,** 1295-1301.

JAENIKE, J., GRIMALDI, D. A., SLUDER, A. E. & GREENLEAF, A. L. 1983. α-Amanitin tolerance in mycophagous Drosophila. *Science,* 221**,** 165-167.

JALVING, R., VAN DE VONDERVOORT, P. J., VISSER, J. & SCHAAP, P. J. 2000. Characterization of the Kexin-Like Maturase ofAspergillus niger. *Applied and Environmental Microbiology,* 66**,** 363-368.

JENKINS, C., SAMUDRALA, R., ANDERSON, I., HEDLUND, B. P., PETRONI, G., MICHAILOVA, N., PINEL, N., OVERBEEK, R., ROSATI, G. & STALEY, J. T. 2002. Genes for the cytoskeletal protein tubulin in the bacterial genus Prosthecobacter. *Proceedings of the National Academy of Sciences of the United States of America,* 99**,** 17049-17054.

JENNINGS, C., WEST, J., WAINE, C., CRAIK, D. & ANDERSON, M. 2001. Biosynthesis and insecticidal properties of plant cyclotides: the cyclic knotted proteins from Oldenlandia affinis. *Proceedings of the National Academy of Sciences of the United States of America,* 98**,** 10614-10619.

JENNINGS, C. V., ROSENGREN, K. J., DALY, N. L., PLAN, M., STEVENS, J., SCANLON, M. J., WAINE, C., NORMAN, D. G., ANDERSON, M. A. & CRAIK, D. J. 2005. Isolation, solution structure, and insecticidal activity of kalata B2, a circular protein with a twist: do Möbius strips exist in nature? *Biochemistry,* 44**,** 851-860.

JING, H. C., LOVELL, D., GUTTERIDGE, R., JENK, D., KORNYUKHIN, D., MITROFANOVA, O. P., KEMA, G. H. J. & HAMMOND-KOSACK, K. E. 2008. Phenotypic and genetic analysis of the Triticum monococcum-Mycosphaerella graminicola interaction. *New Phytologist,* 179**,** 1121-1132.

JINGWEI, L., ZIXIN, D. & QI ZHANG, W. D. 2022. Identification of RiPPs precursor peptides and cleavage sites based on deep learning. *Synthetic Biology Journal,* 3**,** 1262.

JOHNSON, R. D., LANE, G. A., KOULMAN, A., CAO, M., FRASER, K., FLEETWOOD, D. J., VOISEY, C. R., DYER, J. M., PRATT, J., CHRISTENSEN, M., SIMPSON, W. R., BRYAN, G. T. & JOHNSON, L. J. 2015. A novel family of cyclic oligopeptides derived from ribosomal peptide synthesis of an in planta-induced gene, gigA, in Epichloe endophytes of grasses. *Fungal Genetics and Biology,* 85**,** 14-24.

JØRGENSEN, H. J. L. & SMEDEGAARD-PETERSEN, V. 1999. Host-Pathogen Interactions in the Septoria-Disease Complex. *In:* LUCAS, J. A., BOWYER, P. & ANDERSON, H. M. (eds.) *Septoria on Cereals: a Study of Pathosystems.* Wallingford, Oxon, United Kingdom: CAB International.

JØRGENSEN, L., MATZEN, N., SEMASKIENE, R., KORBAS, M., DANIELEWICZ, J., GLAZEK, M., MAUMENE, C., RODEMANN, B., WEIGAND, S. & HESS, M. Azoles have different strengths and

perform diversely across Europe. Modern Fungicides and Antifungal Compounds. Abstracts of the 18th International Reinhardsbrunn Symposium 2016, 2017. 129-134.
JØRGENSEN, L. N., MATZEN, N., HEICK, T. M., HAVIS, N., HOLDGATE, S., CLARK, B., BLAKE, J., GLAZEK, M., KORBAS, M., DANIELEWICZ, J., MAUMENE, C., RODEMANN, B., WEIGAND, S., KILDEA, S., BATAILLE, C., BRAUNA-MORŽEVSKA, E., GULBIS, K., BAN, R., BERG, G., SEMASKIENE, R. & STAMMLER, G. 2020. Decreasing azole sensitivity of Z. tritici in Europe contributes to reduced and varying field efficacy. *Journal of Plant Diseases and Protection,* 128**,** 287-301.
JULIUS, D., BRAKE, A., BLAIR, L., KUNISAWA, R. & THORNER, J. 1984. Isolation of the putative structural gene for the lysine-arginine-cleaving endopeptidase required for processing of yeast prepro-α-factor. *Cell,* 37**,** 1075-1089.
KANEKO, H., TOMOMASA, T., INOUE, Y., KUNIMOTO, F., FUKUSATO, T., MURAOKA, S., GONMORI, K., MATSUMOTO, T. & MORIKAWA, A. 2001. Amatoxin poisoning from ingestion of Japanese Galerina mushrooms. *Journal of Toxicology: Clinical Toxicology,* 39**,** 413-6.
KAPLAN, C. D., LARSSON, K.-M. & KORNBERG, R. D. 2008. The RNA Polymerase II Trigger Loop Functions in Substrate Selection and Is Directly Targeted by α-Amanitin. *Molecular Cell,* 30**,** 547-556.
KARISTO, P., HUND, A., YU, K., ANDEREGG, J., WALTER, A., MASCHER, F., MCDONALD, B. A. & MIKABERIDZE, A. 2018. Ranking Quantitative Resistance to Septoria tritici Blotch in Elite Wheat Cultivars Using Automated Image Analysis. *Phytopathology,* 108**,** 568-581.
KARIUKI, S. K., ZHANG, H., SCHRODER, J. L., EDWARDS, J., PAYTON, M., CARVER, B. F., RAUN, W. R. & KRENZER, E. G. 2007. Hard Red Winter Wheat Cultivar Responses to a pH and Aluminum Concentration Gradient. *Agronomy Journal,* 99**,** 88-98.
KAYA, E., KARAHAN, S., BAYRAM, R., YAYKASLI, K. O., COLAKOGLU, S. & SARITAS, A. 2015. Amatoxin and phallotoxin concentration in Amanita phalloides spores and tissues. *Toxicology and Industrial Health,* 31**,** 1172-1177.
KELLER, N. P. 2019. Fungal secondary metabolism: regulation, function and drug discovery. *Nature Reviews Microbiology,* 17**,** 167-180.
KELLNER, R., BHATTACHARYYA, A., POPPE, S., HSU, T. Y., BREM, R. B. & STUKENBROCK, E. H. 2014. Expression profiling of the wheat pathogen Zymoseptoria tritici reveals genomic patterns of transcription and host-specific regulatory programs. *Genome Biology and Evolution,* 6**,** 1353-65.
KEMA, G., ANNONE, J., SAYOUD, R. & VAN SILFHOUT, C. 1996a. Genetic variation for virulence and resistance in the wheat-Mycosphaerella graminicola pathosystem. I. Interactions between pathogen isolates and host cultivars. *Phytopathology,* 86**,** 200-212.
KEMA, G. H., VERSTAPPEN, E. C., TODOROVA, M. & WAALWIJK, C. 1996b. Successful crosses and molecular tetrad and progeny analyses demonstrate heterothallism in Mycosphaerella graminicola. *Current Genetics,* 30**,** 251-258.
KEMA, G. H., VERSTAPPEN, E. C. & WAALWIJK, C. 2000. Avirulence in the wheat Septoria tritici leaf blotch fungus Mycosphaerella graminicola is controlled by a single locus. *Molecular Plant-Microbe Interactions,* 13**,** 1375-1379.
KEMA, G. H., YU, D., RIJKENBERG, F. H., SHAW, M. W. & BAAYEN, R. P. 1996c. Histology of the pathogenesis of Mycosphaerella graminicola in wheat. *Phytopathology,* 86**,** 777-786.
KEMA, G. H. J. & VAN SILFHOUT, C. H. 1997. Genetic Variation for Virulence and Resistance in the Wheat-Mycosphaerella graminicola Pathosystem III. Comparative Seedling and Adult Plant Experiments. *Phytopathology,* 87**,** 266-272.
KEON, J., ANTONIW, J., CARZANIGA, R., DELLER, S., WARD, J. L., BAKER, J. M., BEALE, M. H., HAMMOND-KOSACK, K. & RUDD, J. J. 2007. Transcriptional Adaptation of Mycosphaerella graminicola to Programmed Cell Death (PCD) of Its Susceptible Wheat Host. *Molecular Plant-Microbe Interactions,* 20**,** 178-193.
KESSLER, S. C. & CHOOI, Y. H. 2021. Out for a RiPP: challenges and advances in genome mining of ribosomal peptides from fungi. *Natural Product Reports*.

KESSLER, S. C., ZHANG, X., MCDONALD, M. C., GILCHRIST, C. L. M., LIN, Z., RIGHTMYER, A., SOLOMON, P. S., TURGEON, B. G. & CHOOI, Y. H. 2020. Victorin, the host-selective cyclic peptide toxin from the oat pathogen *Cochliobolus victoriae*, is ribosomally encoded. *Proceedings of the National Academy of Sciences of the United States of America,* 117**,** 24243-24250.

KETTLES, G. J., BAYON, C., CANNING, G., RUDD, J. J. & KANYUKA, K. 2017. Apoplastic recognition of multiple candidate effectors from the wheat pathogen Zymoseptoria tritici in the nonhost plant Nicotiana benthamiana. *New Phytologist,* 213**,** 338-350.

KETTLES, G. J., BAYON, C., SPARKS, C. A., CANNING, G., KANYUKA, K. & RUDD, J. J. 2018. Characterization of an antimicrobial and phytotoxic ribonuclease secreted by the fungal wheat pathogen Zymoseptoria tritici. *New Phytologist,* 217**,** 320-331.

KETTLES, G. J. & KANYUKA, K. 2016. Dissecting the Molecular Interactions between Wheat and the Fungal Pathogen Zymoseptoria tritici. *Front in Plant Science,* 7**,** 508.

KHEIR, A. M. S., EL BAROUDY, A., AIAD, M. A., ZOGHDAN, M. G., ABD EL-AZIZ, M. A., ALI, M. G. M. & FULLEN, M. A. 2019. Impacts of rising temperature, carbon dioxide concentration and sea level on wheat production in North Nile delta. *Science of the Total Environment,* 651**,** 3161-3173.

KILARU, S., FANTOZZI, E., CANNON, S., SCHUSTER, M., CHALONER, T. M., GUIU-ARAGONES, C., GURR, S. J. & STEINBERG, G. 2022. Zymoseptoria tritici white-collar complex integrates light, temperature and plant cues to initiate dimorphism and pathogenesis. *Nature Communications,* 13**,** 5625.

KILARU, S., SCHUSTER, M., STUDHOLME, D., SOANES, D., LIN, C., TALBOT, N. J. & STEINBERG, G. 2015. A codon-optimized green fluorescent protein for live cell imaging in Zymoseptoria tritici. *Fungal Genetics and Biology,* 79**,** 125-31.

KILDEA, S., MARTEN-HEICK, T., GRANT, J., MEHENNI-CIZ, J. & DOOLEY, H. 2019. A combination of target-site alterations, overexpression and enhanced efflux activity contribute to reduced azole sensitivity present in the Irish Zymoseptoria tritici population. *European Journal of Plant Pathology,* 154**,** 529-540.

KOAY, B. T. 2010. *Investigating polyketide synthase genes of the wheat pathogenic fungus Mycosphaerella graminicola.* M. Sc., University of Bristol.

KOISO, Y., LI, Y., IWASAKI, S., HANAKA, K., KOBAYASHI, T., SONODA, R., FUJITA, Y., YAEGASHI, H. & SATO, Z. 1994. Ustiloxins, antimitotic cyclic peptides from false smut balls on rice panicles caused by Ustilaginoidea virens. *The Journal of Antibiotics,* 47**,** 765-773.

KOISO, Y., NATORI, M., IWASAKI, S., SATO, S., SONODA, R., FUJITA, Y., YAEGASHI, H. & SATO, Z. 1992. Ustiloxin: A phytotoxin and a mycotoxin from false smuth balls on rice panicles. *Tetrahedron Letters,* 33**,** 4157-4160.

KOMBRINK, A., TAYYROV, A., ESSIG, A., STOCKLI, M., MICHELLER, S., HINTZE, J., VAN HEUVEL, Y., DURIG, N., LIN, C. W., KALLIO, P. T., AEBI, M. & KUNZLER, M. 2019. Induction of antibacterial proteins and peptides in the coprophilous mushroom Coprinopsis cinerea in response to bacteria. *The ISME Journal,* 13**,** 588-602.

KRAMER, B., THINES, E. & FOSTER, A. J. 2009. MAP kinase signalling pathway components and targets conserved between the distantly related plant pathogenic fungi Mycosphaerella graminicola and Magnaporthe grisea. *Fungal Genetics and Biology,* 46**,** 667-81.

KSIAZKIEWICZ, M., WOJCIK, K., IRZYKOWSKI, W., BIELSKI, W., RYCHEL, S., KACZMAREK, J., PLEWINSKI, P., RUDY, E. & JEDRYCZKA, M. 2020. Validation of Diaporthe toxica resistance markers in European Lupinus angustifolius germplasm and identification of novel resistance donors for marker-assisted selection. *Journal of Applied Genetics* 61**,** 1-12.

KUNZLER, M. 2018. How fungi defend themselves against microbial competitors and animal predators. *PLoS Pathogens,* 14**,** e1007184.

LANIGAN, G., PAYNE, A., SMITH, L., WOOD, P. M. & PETTERSON, D. 1979. Phomopsin A production by Phomopsis leptostromiformis in liquid media. *Applied and Environmental Microbiology,* 37**,** 289-292.

LATCH, G. C. M. 1993. Physiological interactions of endophytic fungi and their hosts. Biotic stress tolerance imparted to grasses by endophytes. *Agriculture, Ecosystems & Environment,* 44**,** 143-156.

LATZ, M. A. C., JENSEN, B., COLLINGE, D. B. & LYNGS JØRGENSEN, H. J. 2020. Identification of two endophytic fungi that control Septoria tritici blotch in the field, using a structured screening approach. *Biological Control,* 141.

LEE, W. S., RUDD, J. J., HAMMOND-KOSACK, K. E. & KANYUKA, K. 2014. Mycosphaerella graminicola LysM effector-mediated stealth pathogenesis subverts recognition through both CERK1 and CEBiP homologues in wheat. *Molecular Plant-Microbe Interactions,* 27**,** 236-43.

LEIGH, A., COSGROVE, M. J. & NICOTRA, A. B. 2006. Reproductive allocation in a gender dimorphic shrub: anomalous female investment in Gynatrix pulchella? *Journal of Ecology,* 94**,** 1261-1271.

LETZEL, A.-C., PIDOT, S. J. & HERTWECK, C. 2014. Genome mining for ribosomally synthesized and post-translationally modified peptides (RiPPs) in anaerobic bacteria. *BMC Genomics,* 15**,** 983.

LI, Y., KOBAYASHI, H., HASHIMOTO, Y. & IWASAKI, S. 1992. Binding selectivity of rhizoxin, phomopsin A, vinblastine, and ansamitocin P-3 to fungal tubulins: differential interactions of these antimitotic agents with brain and fungal tubulins. *Biochemical and Biophysical Research Communications,* 187**,** 722-729.

LI, Y., KOISO, Y., KOBAYASHI, H., HASHIMOTO, Y. & IWASAKI, S. 1995. Ustiloxins, new antimitotic cyclic peptides: interaction with porcine brain tubulin. *Biochemical Pharmacology,* 49**,** 1367-1372.

LI, Y. & REBUFFAT, S. 2020. The manifold roles of microbial ribosomal peptide-based natural products in physiology and ecology. *Journal of Biological Chemistry,* 295**,** 34-54.

LICHTENTHALER, H. K. & BUSCHMANN, C. 2001. Extraction of phtosynthetic tissues: chlorophylls and carotenoids. *Current Protocols in Food Analytical Chemistry,* 1**,** F4. 2.1-F4. 2.6.

LIERMANN, J. C., OPATZ, T., KOLSHORN, H., ANTELO, L., HOF, C. & ANKE, H. 2009. Omphalotins E-I, Five Oxidatively Modified Nematicidal Cyclopeptides fromOmphalotus olearius. *European Journal of Organic Chemistry,* 2009**,** 1256-1262.

LINDE, C. C., ZHAN, J. & MCDONALD, B. A. 2002. Population structure of Mycosphaerella graminicola: from lesions to continents. *Phytopathology,* 92**,** 946-955.

LINDHOLM, P., GORANSSON, U., JOHANSSON, S., CLAESON, P., GULLBO, J., LARSSON, R., BOHLIN, L. & BACKLUND, A. 2002. Cyclotides: a novel type of cytotoxic agents. *Molecular Cancer Therapeutics,* 1**,** 365-369.

LIU, D., COLOE, S., BAIRD, R. & PEDERSEN, J. 2000. Rapid Mini-Preparation of Fungal DNA for PCR. *Journal of Clinical Microbiology,* 38**,** 471-471.

LIVAK, K. J. & SCHMITTGEN, T. D. 2001. Analysis of Relative Gene Expression Data Using Real-Time Quantitative PCR and the 2−ΔΔCT Method. *Methods,* 25**,** 402-408.

LOBELL, D. B., SCHLENKER, W. & COSTA-ROBERTS, J. 2011. Climate trends and global crop production since 1980. *Science,* 333**,** 616-620.

LOVELL, D. J., HUNTER, T., POWERS, S. J., PARKER, S. R. & VAN DEN BOSCH, F. 2004. Effect of temperature on latent period of septoria leaf blotch on winter wheat under outdoor conditions. *Plant Pathology,* 53**,** 170-181.

LUO, H., CAI, Q., LÜLI, Y., LI, X., SINHA, R., HALLEN-ADAMS, H. E. & YANG, Z. L. 2018. The MSDIN family in amanitin-producing mushrooms and evolution of the prolyl oligopeptidase genes. *IMA Fungus,* 9**,** 225-242.

LUO, H., HALLEN-ADAMS, H. E., SCOTT-CRAIG, J. S. & WALTON, J. D. 2010. Colocalization of amanitin and a candidate toxin-processing prolyl oligopeptidase in *Amanita* basidiocarps. *Eukaryotic Cell,* 9**,** 1891-1900.

LUO, H., HALLEN-ADAMS, H. E., SCOTT-CRAIG, J. S. & WALTON, J. D. 2012. Ribosomal biosynthesis of alpha-amanitin in Galerina marginata. *Fungal Genetics and Biology,* 49**,** 123-9.

LUO, H., HALLEN-ADAMS, H. E. & WALTON, J. D. 2009. Processing of the Phalloidin Proprotein by Prolyl Oligopeptidase from the Mushroom *Conocybe albipes*. *Journal of Biological Chemistry,* 284**,** 18070-18077.

LUO, H., HONG, S. Y., SGAMBELLURI, R. M., ANGELOS, E., LI, X. & WALTON, J. D. 2014a. Peptide macrocyclization catalyzed by a prolyl oligopeptidase involved in alpha-amanitin biosynthesis. *Chemistry & Biology,* 21**,** 1610-1617.

LUO, S. & DONG, S. H. 2019. Recent Advances in the Discovery and Biosynthetic Study of Eukaryotic RiPP Natural Products. *Molecules,* 24**,** 15.

LUO, Y., COBB, R. E. & ZHAO, H. 2014b. Recent advances in natural product discovery. *Current Opinion in Biotechnology,* 30**,** 230-7.

LUTTRELL, E. 1974. Parasitism of Fungi on Vascular Plants. *Mycologia,* 66**,** 1-15.

LYNCH, K. M., ZANNINI, E., GUO, J., AXEL, C., ARENDT, E. K., KILDEA, S. & COFFEY, A. 2016. Control of Zymoseptoria tritici cause of septoria tritici blotch of wheat using antifungal Lactobacillus strains. *Journal of Applied Microbiology,* 121**,** 485-94.

M'BAREK, S. B., CORDEWENER, J. H., GHAFFARY, S. M. T., VAN DER LEE, T. A., LIU, Z., GOHARI, A. M., MEHRABI, R., AMERICA, A. H., ROBERT, O. & FRIESEN, T. L. 2015. FPLC and liquid-chromatography mass spectrometry identify candidate necrosis-inducing proteins from culture filtrates of the fungal wheat pathogen Zymoseptoria tritici. *Fungal Genetics and Biology,* 79**,** 54-62.

MAKSIMOV, M. O., PELCZER, I. & LINK, A. J. 2012. Precursor-centric genome-mining approach for lasso peptide discovery. *Proceedings of the National Academy of Sciences of the United States of America,* 109**,** 15223-8.

MARQUES, A., REGO, A., GUILHERME, S., GAIVAO, I., SANTOS, M. A. & PACHECO, M. 2016. Evidences of DNA and chromosomal damage induced by the mancozeb-based fungicide Mancozan((R)) in fish (Anguilla anguilla L.). *Pesticide Biochemistry and Physiology,* 133**,** 52-58.

MARSHALL, R., KOMBRINK, A., MOTTERAM, J., LOZA-REYES, E., LUCAS, J., HAMMOND-KOSACK, K. E., THOMMA, B. P. & RUDD, J. J. 2011. Analysis of two in planta expressed LysM effector homologs from the fungus Mycosphaerella graminicola reveals novel functional properties and varying contributions to virulence on wheat. *Plant Physiology,* 156**,** 756-69.

MAYER, A., ANKE, H. & STERNER, O. 1997. Omphalotin, A New Cyclic Peptide with Potent Nematicidal Activity fromOmphalotus OleariusI. Fermentation and Biological Activity. *Natural Product Letters,* 10**,** 25-32.

MAYER, A., KILIAN, M., HOSTER, B., STERNER, O. & ANKE, H. 1999a. In-vitro and in-vivo nematicidal activities of the cyclic dodecapeptide omphalotin A. *Pesticide Science,* 55**,** 27-30.

MAYER, A., KILIAN, M., HOSTER, B., STERNER, O. & ANKE, H. 1999b. In-vitro and in-vivo nematicidal activities of the cyclic dodecapeptide omphalotin A. *Pesticide Science,* 55**,** 27-30.

MCCORISON, C. B. & GOODWIN, S. B. 2020. The wheat pathogen Zymoseptoria tritici senses and responds to different wavelengths of light. *BMC Genomics,* 21**,** 513.

MCDONALD, B. A. & MARTINEZ, J. 1991. Chromosome length polymorphisms in a Septoria tritici population. *Current Genetics,* 19**,** 265-271.

MCDONALD, M. C., MCGINNESS, L., HANE, J. K., WILLIAMS, A. H., MILGATE, A. & SOLOMON, P. S. 2016. Utilizing Gene Tree Variation to Identify Candidate Effector Genes in Zymoseptoria tritici. *G3 (Bethesda),* 6**,** 779-91.

MCDONALD, M. C., RENKIN, M., SPACKMAN, M., ORCHARD, B., CROLL, D., SOLOMON, P. S. & MILGATE, A. 2019. Rapid Parallel Evolution of Azole Fungicide Resistance in Australian Populations of the Wheat Pathogen Zymoseptoria tritici. *Applied and Environmental Microbiology,* 85.

MCGRANAHAN, G., BALK, D. & ANDERSON, B. 2016. The rising tide: assessing the risks of climate change and human settlements in low elevation coastal zones. *Environment and Urbanization,* 19**,** 17-37.
MCKENDRY, A., HENKE, G. & FINNEY, P. 1995. Effects of Septoria leaf blotch on soft red winter wheat milling and baking quality. *Cereal Chemistry,* 72**,** 142-146.
MCKNIGHT, T. A., MCKNIGHT, K. B. & SKEELS, M. C. 2010. Amatoxin and phallotoxin concentration in amanita bisporigera spores. *Mycologia,* 102**,** 763-5.
MEDEMA, M. H., BLIN, K., CIMERMANCIC, P., DE JAGER, V., ZAKRZEWSKI, P., FISCHBACH, M. A., WEBER, T., TAKANO, E. & BREITLING, R. 2011. antiSMASH: rapid identification, annotation and analysis of secondary metabolite biosynthesis gene clusters in bacterial and fungal genome sequences. *Nucleic Acids Research,* 39**,** W339-46.
MEEHAN, F. & MURPHY, H. C. 1947. Differential Phytotoxicity of Metabolic By-Products of *Helminthosporium victoriae*. *Science,* 106**,** 270-271.
MEHRABI, R., BEN M'BAREK, S., VAN DER LEE, T. A., WAALWIJK, C., DE WIT, P. J. & KEMA, G. H. 2009. G(alpha) and Gbeta proteins regulate the cyclic AMP pathway that is required for development and pathogenicity of the phytopathogen Mycosphaerella graminicola. *Eukaryotic Cell,* 8**,** 1001-13.
MEHRABI, R. & KEMA, G. H. 2006. Protein kinase A subunits of the ascomycete pathogen Mycosphaerella graminicola regulate asexual fructification, filamentation, melanization and osmosensing. *Molecular Plant Pathology,* 7**,** 565-77.
MEHRABI, R., TAGA, M. & KEMA, G. H. J. 2007. Electrophoretic and cytological karyotyping of the foliar wheat pathogen Mycosphaerella graminicola reveals many chromosomes with a large size range. *Mycologia,* 99**,** 868-876.
MEHRABI, R., VAN DER LEE, T., WAALWIJK, C. & KEMA, G. H. 2006a. MgSlt2, a cellular integrity MAP kinase gene of the fungal wheat pathogen Mycosphaerella graminicola, is dispensable for penetration but essential for invasive growth. *Molecular Plant-Microbe Interactions,* 19**,** 389-398.
MEHRABI, R., ZWIERS, L.-H., DE WAARD, M. A. & KEMA, G. H. 2006b. MgHog1 regulates dimorphism and pathogenicity in the fungal wheat pathogen Mycosphaerella graminicola. *Molecular Plant-Microbe Interactions,* 19**,** 1262-1269.
MEJRI, S., SIAH, A., COUTTE, F., MAGNIN-ROBERT, M., RANDOUX, B., TISSERANT, B., KRIER, F., JACQUES, P., REIGNAULT, P. & HALAMA, P. 2018. Biocontrol of the wheat pathogen Zymoseptoria tritici using cyclic lipopeptides from Bacillus subtilis. *Environmental Science and Pollution Research,* 25**,** 29822-29833.
MERWIN, N. J., MOUSA, W. K., DEJONG, C. A., SKINNIDER, M. A., CANNON, M. J., LI, H., DIAL, K., GUNABALASINGAM, M., JOHNSTON, C. & MAGARVEY, N. A. 2020. DeepRiPP integrates multiomics data to automate discovery of novel ribosomally synthesized natural products. *Proceedings of the National Academy of Sciences of the United States of America,* 117**,** 371-380.
MESA-ARANGO, A. C., TREVIJANO-CONTADOR, N., ROMAN, E., SANCHEZ-FRESNEDA, R., CASAS, C., HERRERO, E., ARGUELLES, J. C., PLA, J., CUENCA-ESTRELLA, M. & ZARAGOZA, O. 2014. The production of reactive oxygen species is a universal action mechanism of Amphotericin B against pathogenic yeasts and contributes to the fungicidal effect of this drug. *Antimicrobial Agents and Chemotherapy,* 58**,** 6627-38.
MIHAILOVA, G., STOYANOVA, Z., RODEVA, R., BANKINA, B., BIMSTEINE, G. & GEORGIEVA, K. 2019. Physiological changes in winter wheat genotypes in response to the Zymoseptoria tritici infection. *Photosynthetica,* 57**,** 428-437.
MILJANICH, G. 2004. Ziconotide: neuronal calcium channel blocker for treating severe chronic pain. *Current Medicinal Chemistry,* 11**,** 3029-3040.
MIRZADI GOHARI, A., MEHRABI, R., ROBERT, O., INCE, I. A., BOEREN, S., SCHUSTER, M., STEINBERG, G., DE WIT, P. J. & KEMA, G. H. 2014. Molecular characterization and functional analyses of

ZtWor1, a transcriptional regulator of the fungal wheat pathogen Zymoseptoria tritici. *Molecular Plant Pathology,* 15**,** 394-405.
MIYAZAKI, S. 2006. Phytoalexins and endophyte related mycotoxins as hazards to the animal industry. *Mycotoxins,* 56.
MIZUNO, K., NAKAMURA, T., OHSHIMA, T., TANAKA, S. & MATSUO, H. 1989. Characterization of KEX2-encoded endopeptidase from yeast Saccharomyces, cerevisiae. *Biochemical and Biophysical Research Communications,* 159**,** 305-311.
MOHAMMADI, N., MEHRABI, R., MIRZADI GOHARI, A., MOHAMMADI GOLTAPEH, E., SAFAIE, N. & KEMA, G. H. J. 2017. The ZtVf1 transcription factor regulates development and virulence in the foliar wheat pathogen Zymoseptoria tritici. *Fungal Genetics and Biology,* 109**,** 26-35.
MOHAMMADI, N., MEHRABI, R., MIRZADI GOHARI, A., ROOSTAEI, M., MOHAMMADI GOLTAPEH, E., SAFAIE, N. & KEMA, G. H. J. 2020. MADS-Box Transcription Factor ZtRlm1 Is Responsible for Virulence and Development of the Fungal Wheat Pathogen Zymoseptoria tritici. *Frontiers in Microbiology,* 11**,** 1976.
MOHD KHALID, R. 2011. *Linking genes and secondary metabolites in Mycosphaerella graminicola.* Degree of Doctor of Philosophy (Ph.D), University of Bristol.
MOHD KHALID, R., BAILEY, A. & COX, R. J. 2015. Annotations and domain analysis of polyketide synthase genes in fungal wheat pathogen, *Mycosphaerella graminicola Jurnal Teknologi,* 77.
MOHIMANI, H., KERSTEN, R. D., LIU, W. T., WANG, M., PURVINE, S. O., WU, S., BREWER, H. M., PASA-TOLIC, L., BANDEIRA, N., MOORE, B. S., PEVZNER, P. A. & DORRESTEIN, P. C. 2014. Automated genome mining of ribosomal peptide natural products. *ACS Chemical Biology,* 9**,** 1545-51.
MOHR, K. I., VOLZ, C., JANSEN, R., WRAY, V., HOFFMANN, J., BERNECKER, S., WINK, J., GERTH, K., STADLER, M. & MULLER, R. 2015. Pinensins: the first antifungal lantibiotics. *Angewandte Chemie International Edition in English,* 54**,** 11254-8.
MOLOHON, K. J., SAINT-VINCENT, P. M. B., PARK, S., DOROGHAZI, J. R., MAXSON, T., HERSHFIELD, J. R., FLATT, K. M., SCHROEDER, N. E., HA, T. & MITCHELL, D. A. 2016. Plantazolicin is an ultra-narrow spectrum antibiotic that targets the Bacillus anthracis membrane. *ACS Infectious Diseases,* 2**,** 207-220.
MONDAL, T. 2020. Lodging in wheat: Its causes, ill effects and management for higher productivity and profitability. *Indian Farmer,* 7**,** 832-837.
MOTTERAM, J., KÜFNER, I., DELLER, S., BRUNNER, F., HAMMOND-KOSACK, K. E., NÜRNBERGER, T. & RUDD, J. J. 2009. Molecular characterization and functional analysis of MgNLP, the sole NPP1 domain–containing protein, from the fungal wheat leaf pathogen Mycosphaerella graminicola. *Molecular Plant-Microbe Interactions,* 22**,** 790-799.
MUKHERJEE, R., GRUSZEWSKI, H. A., BILYEU, L. T., SCHMALE, D. G., 3RD & BOREYKO, J. B. 2021. Synergistic dispersal of plant pathogen spores by jumping-droplet condensation and wind. *Proceedings of the National Academy of Sciences of the United States of America,* 118**,** 1-8.
MÜLLENBORN, C., STEINER, U., LUDWIG, M. & OERKE, E.-C. 2007. Effect of fungicides on the complex of Fusarium species and saprophytic fungi colonizing wheat kernels. *European Journal of Plant Pathology,* 120**,** 157-166.
MURIA-GONZALEZ, M. J., CHOOI, Y.-H., BREEN, S. & SOLOMON, P. S. 2015. The past, present and future of secondary metabolite research in the Dothideomycetes. *Molecular Plant Pathology,* 16**,** 92-107.
NAGANO, N., UMEMURA, M., IZUMIKAWA, M., KAWANO, J., ISHII, T., KIKUCHI, M., TOMII, K., KUMAGAI, T., YOSHIMI, A., MACHIDA, M., ABE, K., SHIN-YA, K. & ASAI, K. 2016. Class of cyclic ribosomal peptide synthetic genes in filamentous fungi. *Fungal Genetics and Biology,* 86**,** 58-70.
NAKAMURA, K. I., IZUMIYAMA, N., OHTSUBO, K. I., KOISO, Y., IWASAKI, S., SONODA, R., FUJITA, Y., YAEGASHI, H. & SATO, Z. 1994. “Lupinosis”-Like lesions in mice caused by ustiloxin, produced by Ustilaginoieda virens: A morphological study. *Natural Toxins,* 2**,** 22-28.

NAKAZAWA, T., ISHIUCHI, K., PRASEUTH, A., NOGUCHI, H., HOTTA, K. & WATANABE, K. 2012. Overexpressing transcriptional regulator in Aspergillus oryzae activates a silent biosynthetic pathway to produce a novel polyketide. *ChemBioChem,* 13**,** 855-61.

NAVARRE, D. A. & WOLPERT, T. J. 1999. Victorin Induction of an Apoptotic/Senescence–like Response in Oats. *The Plant Cell,* 11**,** 237-249.

NELSON, G. C., ROSEGRANT, M. W., PALAZZO, A., GRAY, I., INGERSOLL, C., ROBERTSON, R., TOKGOZ, S., ZHU, T., SULSER, T. B. & RINGLER, C. 2010. *Food security, farming, and climate change to 2050: scenarios, results, policy options*, International Food Policy Research Institute.

NOIKE, M., MATSUI, T., OOYA, K., SASAKI, I., OHTAKI, S., HAMANO, Y., MARUYAMA, C., ISHIKAWA, J., SATOH, Y., ITO, H., MORITA, H. & DAIRI, T. 2015. A peptide ligase and the ribosome cooperate to synthesize the peptide pheganomycin. *Nature Chemical Biology,* 11**,** 71-6.

NOVELLO, F., FIUME, L. & STIRPE, F. 1970. Inhibition by α-amanitin of ribonucleic acid polymerase solubilized from rat liver nuclei. *Biochemical Journal,* 116**,** 177.

O'BRIEN, H. E., PARRENT, J. L., JACKSON, J. A., MONCALVO, J.-M. & VILGALYS, R. 2005. Fungal community analysis by large-scale sequencing of environmental samples. *Applied and Environmental Microbiology,* 71**,** 5544-5550.

O'DRISCOLL, A., KILDEA, S., DOOHAN, F., SPINK, J. & MULLINS, E. 2014. The wheat-Septoria conflict: a new front opening up? *Trends in Plant Science,* 19**,** 602-10.

O'HANLON, K. A., KNORR, K., JØRGENSEN, L. N., NICOLAISEN, M. & BOELT, B. 2012. Exploring the potential of symbiotic fungal endophytes in cereal disease suppression. *Biological Control,* 63**,** 69-78.

OERKE, E. C. 2005. Crop losses to pests. *The Journal of Agricultural Science,* 144**,** 31-43.

OLIVERA, B. M., RIVIER, J., CLARK, C., RAMILO, C. A., CORPUZ, G. P., ABOGADIE, F. C., MENA, E. E., WOODWARD, S. R., HILLYARD, D. R. & CRUZ, L. J. 1990. Diversity of Conus neuropeptides. *Science,* 249**,** 257-263.

ORTEGA, M. A. & VAN DER DONK, W. A. 2016. New Insights into the Biosynthetic Logic of Ribosomally Synthesized and Post-translationally Modified Peptide Natural Products. *Cell Chemical Biology,* 23**,** 31-44.

ORTIZ, R., SAYRE, K. D., GOVAERTS, B., GUPTA, R., SUBBARAO, G. V., BAN, T., HODSON, D., DIXON, J. M., IVÁN ORTIZ-MONASTERIO, J. & REYNOLDS, M. 2008. Climate change: Can wheat beat the heat? *Agriculture, Ecosystems & Environment,* 126**,** 46-58.

ORTON, E. S., DELLER, S. & BROWN, J. K. 2011. Mycosphaerella graminicola: from genomics to disease control. *Molecular Plant Pathology,* 12**,** 413-24.

OZAKI, T., MINAMI, A. & OIKAWA, H. 2023. Recent advances in the biosynthesis of ribosomally synthesized and posttranslationally modified peptides of fungal origin. *The Journal of Antibiotics* 76**,** 3-13.

PALMA-GUERRERO, J., TORRIANI, S. F., ZALA, M., CARTER, D., COURBOT, M., RUDD, J. J., MCDONALD, B. A. & CROLL, D. 2016. Comparative transcriptomic analyses of Zymoseptoria tritici strains show complex lifestyle transitions and intraspecific variability in transcription profiles. *Molecular Plant Pathology,* 17**,** 845-59.

PAOLACCI, A. R., TANZARELLA, O. A., PORCEDDU, E. & CIAFFI, M. 2009. Identification and validation of reference genes for quantitative RT-PCR normalization in wheat. *BMC Molecular Biology,* 10**,** 11.

PERELLÓ, A. E., MORENO, M. V., MÓNACO, C., SIMÓN, M. R. & CORDO, C. 2008. Biological control of Septoria tritici blotch on wheat by Trichoderma spp. under field conditions in Argentina. *BioControl,* 54**,** 113-122.

PETERSON, J., JAGO, M., PAYNE, A. & STEWART, P. 1987. The toxicity of phomopsin for sheep. *Australian Veterinary Journal,* 64**,** 293-298.

PILHOFER, M., LADINSKY, M. S., MCDOWALL, A. W., PETRONI, G. & JENSEN, G. J. 2011. Microtubules in bacteria: Ancient tubulins build a five-protofilament homolog of the eukaryotic cytoskeleton. *PLoS Biology,* 9**,** e1001213.

PLAN, M. R. R., SASKA, I., CAGAUAN, A. G. & CRAIK, D. J. 2008. Backbone cyclised peptides from plants show molluscicidal activity against the rice pest Pomacea canaliculata (golden apple snail). *Journal of Agricultural and Food Chemistry,* 56**,** 5237-5241.

PONOMARENKO, A., GOODWIN, S. B. & KEMA, G. H. J. 2011. Septoria tritici blotch (STB) of wheat. Available: https://www.apsnet.org/edcenter/disandpath/fungalasco/pdlessons/Pages/Septoria.aspx [Accessed 26/6/23].

POPPE, S., DORSHEIMER, L., HAPPEL, P. & STUKENBROCK, E. H. 2015. Rapidly Evolving Genes Are Key Players in Host Specialization and Virulence of the Fungal Wheat Pathogen Zymoseptoria tritici (Mycosphaerella graminicola). *PLoS Pathogens,* 11**,** e1005055.

PORRA, R., THOMPSON, W. & KRIEDEMANN, P. 1989. Determination of accurate extinction coefficients and simultaneous equations for assaying chlorophylls a and b extracted with four different solvents: verification of the concentration of chlorophyll standards by atomic absorption spectroscopy. *Biochimica et Biophysica Acta (BBA)-Bioenergetics,* 975**,** 384-394.

POUSTINI, K. & SIOSEMARDEH, A. 2004. Ion distribution in wheat cultivars in response to salinity stress. *Field Crops Research,* 85**,** 125-133.

PRANTING, M., LOOV, C., BURMAN, R., GORANSSON, U. & ANDERSSON, D. I. 2010. The cyclotide cycloviolacin O2 from Viola odorata has potent bactericidal activity against Gram-negative bacteria. *Journal of Antimicrobial Chemotherapy,* 65**,** 1964-71.

QUAEDVLIEG, W., KEMA, G. H., GROENEWALD, J. Z., VERKLEY, G. J., SEIFBARGHI, S., RAZAVI, M., MIRZADI GOHARI, A., MEHRABI, R. & CROUS, P. W. 2011. Zymoseptoria gen. nov.: a new genus to accommodate Septoria-like species occurring on graminicolous hosts. *Persoonia,* 26**,** 57-69.

QUIJANO, M. R., ZACH, C., MILLER, F. S., LEE, A. R., IMANI, A. S., KUNZLER, M. & FREEMAN, M. F. 2019. Distinct Autocatalytic alpha- N-Methylating Precursors Expand the Borosin RiPP Family of Peptide Natural Products. *Journal of the American Chemical Society,* 141**,** 9637-9644.

RAJPAR, I., KHANIF, Y. M., SOOMRO, F. M. & SUTHAR, J. K. 2005. Effect of NaCl Salinity on the Growth and Yield of Inqlab Wheat (Triticum aestivum L.) Variety. *American Journal of Plant Physiology,* 1**,** 34-40.

RAMM, S., KRAWCZYK, B., MUHLENWEG, A., POCH, A., MOSKER, E. & SUSSMUTH, R. D. 2017. A Self-Sacrificing N-Methyltransferase Is the Precursor of the Fungal Natural Product Omphalotin. *Angewandte Chemie International Edition in English,* 56**,** 9994-9997.

REBETZKE, G. J., ELLIS, M. H., BONNETT, D. G., CONDON, A. G., FALK, D. & RICHARDS, R. A. 2011. The Rht13 dwarfing gene reduces peduncle length and plant height to increase grain number and yield of wheat. *Field Crops Research,* 124**,** 323-331.

REDDING, K., HOLCOMB, C. & FULLER, R. S. 1991. Immunolocalization of Kex2 protease identifies a putative late Golgi compartment in the yeast Saccharomyces cerevisiae. *The Journal of Cell Biology,* 113**,** 527-538.

REN, H., DOMMARAJU, S. R., HUANG, C., CUI, H., PAN, Y., NESIC, M., ZHU, L., SARLAH, D., MITCHELL, D. A. & ZHAO, H. 2023. Genome mining unveils a class of ribosomal peptides with two amino termini. *Nature Communications,* 14**,** 1624.

RICHARDS, T. A., SOANES, D. M., FOSTER, P. G., LEONARD, G., THORNTON, C. R. & TALBOT, N. J. 2009. Phylogenomic analysis demonstrates a pattern of rare and ancient horizontal gene transfer between plants and fungi. *Plant Cell,* 21**,** 1897-911.

ROSEWICH, U. L. & KISTLER, H. C. 2000. Role of horizontal gene transfer in the evolution of fungi. *Annual Review of Phytopathology,* 38**,** 325-363.

RUBIN, G. M. & DING, Y. 2020. Recent advances in the biosynthesis of RiPPs from multicore-containing precursor peptides. *Journal of Industrial Microbiology & Biotechnology,* 47**,** 15.

RUDD, J. J., ANTONIW, J., MARSHALL, R., MOTTERAM, J., FRAAIJE, B. & HAMMOND-KOSACK, K. 2010. Identification and characterisation of Mycosphaerella graminicola secreted or surface-

associated proteins with variable intragenic coding repeats. *Fungal Genetics and Biology,* 47**,** 19-32.

RUDD, J. J., KANYUKA, K., HASSANI-PAK, K., DERBYSHIRE, M., ANDONGABO, A., DEVONSHIRE, J., LYSENKO, A., SAQI, M., DESAI, N. M., POWERS, S. J., HOOPER, J., AMBROSO, L., BHARTI, A., FARMER, A., HAMMOND-KOSACK, K. E., DIETRICH, R. A. & COURBOT, M. 2015. Transcriptome and metabolite profiling of the infection cycle of Zymoseptoria tritici on wheat reveals a biphasic interaction with plant immunity involving differential pathogen chromosomal contributions and a variation on the hemibiotrophic lifestyle definition. *Plant Physiology,* 167**,** 1158-85.

RUDD, J. J., KEON, J. & HAMMOND-KOSACK, K. E. 2008. The wheat mitogen-activated protein kinases TaMPK3 and TaMPK6 are differentially regulated at multiple levels during compatible disease interactions with Mycosphaerella graminicola. *Plant Physiology,* 147**,** 802-15.

RUDD, M. D. & LUSE, D. S. 1996. Amanitin greatly reduces the rate of transcription by RNA polymerase II ternary complexes but fails to inhibit some transcript cleavage modes. *Journal of Biological Chemistry,* 271**,** 21549-21558.

SAARI, E. & WILCOXSON, R. D. 1974. Plant disease situation of high-yielding dwarf wheats in Asia and Africa. *Annual Review of Phytopathology,* 12**,** 49-68.

SAINTENAC, C., LEE, W. S., CAMBON, F., RUDD, J. J., KING, R. C., MARANDE, W., POWERS, S. J., BERGES, H., PHILLIPS, A. L., UAUY, C., HAMMOND-KOSACK, K. E., LANGIN, T. & KANYUKA, K. 2018. Wheat receptor-kinase-like protein Stb6 controls gene-for-gene resistance to fungal pathogen Zymoseptoria tritici. *Nature Genetics,* 50**,** 368-374.

SAIRAM, R. K., RAO, K. V. & SRIVASTAVA, G. C. 2002. Differential response of wheat genotypes to long term salinity stress in relation to oxidative stress, antioxidant activity and osmolyte concentration. *Plant Science,* 163**,** 1037-1046.

SAMAIN, E., ERNENWEIN, C., AUSSENAC, T. & SELIM, S. 2022. Effective and durable systemic wheat-induced resistance by a plant-growth-promoting rhizobacteria consortium of Paenibacillus sp. strain B2 and Arthrobacter spp. strain AA against Zymoseptoria tritici and drought stress. *Physiological and Molecular Plant Pathology,* 119.

SANCHEZ-VALLET, A., MCDONALD, M. C., SOLOMON, P. S. & MCDONALD, B. A. 2015. Is Zymoseptoria tritici a hemibiotroph? *Fungal Genetics and Biology,* 79**,** 29-32.

SANDERSON, F. R. 1972. A Mycosphaerella species as the Ascogenous state of Septoria tritici Rob. and Desm. *New Zealand Journal of Botany,* 10**,** 707-709.

SANDERSON, F. R. & HAMPTON, J. G. 1978. Role of the perfect states in the epidemiology of the common Septoria diseases of wheat. *New Zealand Journal of Agricultural Research,* 21**,** 277-281.

SARDAR, D., PIERCE, E., MCINTOSH, J. A. & SCHMIDT, E. W. 2015. Recognition sequences and substrate evolution in cyanobactin biosynthesis. *ACS Synthetic Biology,* 4**,** 167-76.

SAVARY, S., WILLOCQUET, L., PETHYBRIDGE, S. J., ESKER, P., MCROBERTS, N. & NELSON, A. 2019. The global burden of pathogens and pests on major food crops. *Nature Ecology & Evolution,* 3**,** 430-439.

SCHARF, D. H., HEINEKAMP, T. & BRAKHAGE, A. A. 2014. Human and plant fungal pathogens: the role of secondary metabolites. *PLOS Pathogens,* 10**,** e1003859.

SCHRODER, J. L., ZHANG, H., GIRMA, K., RAUN, W. R., PENN, C. J. & PAYTON, M. E. 2011. Soil Acidification from Long-Term Use of Nitrogen Fertilizers on Winter Wheat. *Soil Science Society of America Journal,* 75**,** 957-964.

SEIFBARGHI, S., RAZAVI, M., AMINIAN, H., ZARE, R. & ETEBARIAN, H.-R. 2009. Studies on the host range of Septoria species on cereals and some wild grasses in Iran. *Phytopathologia Mediterranea,* 48**,** 422-429.

SHAW, M. & ROYLE, D. 1989. Airborne inoculum as a major source of Septoria tritici (Mycosphaerella graminicola) infections in winter wheat crops in the UK. *Plant Pathology,* 38**,** 35-43.

SHEWRY, P. R. & HEY, S. J. 2015. The contribution of wheat to human diet and health. *Food and Energy Security,* 4**,** 178-202.
SHEWRY, P. R., PELLNY, T. K. & LOVEGROVE, A. 2016. Is modern wheat bad for health? *Nature Plants,* 2**,** 16097.
SHIFERAW, B., SMALE, M., BRAUN, H.-J., DUVEILLER, E., REYNOLDS, M. & MURICHO, G. 2013. Crops that feed the world 10. Past successes and future challenges to the role played by wheat in global food security. *Food Security,* 5**,** 291-317.
SIDHU, Y. S., CAIRNS, T. C., CHAUDHARI, Y. K., USHER, J., TALBOT, N. J., STUDHOLME, D. J., CSUKAI, M. & HAYNES, K. 2015. Exploitation of sulfonylurea resistance marker and non-homologous end joining mutants for functional analysis in Zymoseptoria tritici. *Fungal Genetics and Biology,* 79**,** 102-9.
SIEGEL, M. R. & LATCH, G. C. 1991. Expression of antifungal activity in agar culture by isolates of grass endophytes. *Mycologia,* 83**,** 529-537.
SINGH, M. & SAREEN, D. 2014. Novel LanT associated lantibiotic clusters identified by genome database mining. *PLoS One,* 9**,** e91352.
SINGH, N. K., KARISTO, P. & CROLL, D. 2021. Population-level deep sequencing reveals the interplay of clonal and sexual reproduction in the fungal wheat pathogen Zymoseptoria tritici. *Microbial Genomics,* 7.
SMIKA, D. & SHAWCROFT, R. 1980. Preliminary study using a wind tunnel to determine the effect of hot wind on a wheat crop. *Field Crops Research,* 3**,** 129-135.
SOGAHATA, K., OZAKI, T., IGARASHI, Y., NAGANUMA, Y., LIU, C., MINAMI, A. & OIKAWA, H. 2021. Biosynthetic Studies of Phomopsins Unveil Posttranslational Installation of Dehydroamino Acids by UstYa Family Proteins. *Angewandte Chemie International Edition in English,* 60**,** 25729-25734.
SPITELLER, P. 2015. Chemical ecology of fungi. *Natural Product Reports,* 32**,** 971-93.
SPRAGUE, R. 1950. Some leafspot fungi on Western gramineae. V. *Mycologia,* 42**,** 758-771.
SRINIVASACHARY, GOSMAN, N., STEED, A., SIMMONDS, J., LEVERINGTON-WAITE, M., WANG, Y., SNAPE, J. & NICHOLSON, P. 2008. Susceptibility to Fusarium head blight is associated with the Rht-D1b semi-dwarfing allele in wheat. *Theoretical and Applied Genetics,* 116**,** 1145-53.
STAPLEY, J. & MCDONALD, B. A. 2022. Quantitative trait locus mapping of osmotic stress response in the wheat pathogen *Zymoseptoria tritici*. *bioRxiv*.
STEED, G., RAMIREZ, D. C., HANNAH, M. A. & WEBB, A. A. R. 2021. Chronoculture, harnessing the circadian clock to improve crop yield and sustainability. *Science,* 372**,** 1-7.
STEPHENS, C., OLMEZ, F., BLYTH, H., MCDONALD, M., BANSAL, A., TURGAY, E. B., HAHN, F., SAINTENAC, C., NEKRASOV, V., SOLOMON, P., MILGATE, A., FRAAIJE, B., RUDD, J. & KANYUKA, K. 2021. Remarkable recent changes in the genetic diversity of the avirulence gene AvrStb6 in global populations of the wheat pathogen Zymoseptoria tritici. *Molecular Plant Pathology*.
STERLING, M., BAKER, C. J., BERRY, P. M. & WADE, A. 2003. An experimental investigation of the lodging of wheat. *Agricultural and Forest Meteorology,* 119**,** 149-165.
STERNER, O., ETZEL, W., MAYER, A. & ANKE, H. 1997. Omphalotin, A New Cyclic Peptide with Potent Nematicidal Activity fromOmphalotus OleariusII. Isolation and Structure Determination. *Natural Product Letters,* 10**,** 33-38.
STEWART, E. L., CROLL, D., LENDENMANN, M. H., SANCHEZ-VALLET, A., HARTMANN, F. E., PALMA-GUERRERO, J., MA, X. & MCDONALD, B. A. 2018. Quantitative trait locus mapping reveals complex genetic architecture of quantitative virulence in the wheat pathogen Zymoseptoria tritici. *Molecular Plant Pathology,* 19**,** 201-216.
STEWART, E. L., HAGERTY, C. H., MIKABERIDZE, A., MUNDT, C. C., ZHONG, Z. & MCDONALD, B. A. 2016. An Improved Method for Measuring Quantitative Resistance to the Wheat Pathogen Zymoseptoria tritici Using High-Throughput Automated Image Analysis. *Phytopathology,* 106**,** 782-8.

STEWART, E. L. & MCDONALD, B. A. 2014. Measuring quantitative virulence in the wheat pathogen Zymoseptoria tritici using high-throughput automated image analysis. *Phytopathology,* 104**,** 985-92.

STIRPE, F. & FIUME, L. 1967. Studies on the pathogenesis of liver necrosis by α-amanitin. Effect of α-amanitin on ribonucleic acid synthesis and on ribonucleic acid polymerase in mouse liver nuclei. *Biochemical Journal,* 105**,** 779-782.

STOCCO, M. C., MONACO, C. I., ABRAMOFF, C., LAMPUGNANI, G., SALERNO, G., KRIPELZ, N., CORDO, C. A. & CONSOLO, V. F. 2016. Selection and characterization of Argentine isolates of Trichoderma harzianum for effective biocontrol of Septoria leaf blotch of wheat. *World Journal of Microbioloy and Biotechnology,* 32**,** 49.

STUKENBROCK, E. H., QUAEDVLIEG, W., JAVAN-NIKHAH, M., ZALA, M., CROUS, P. W. & MCDONALD, B. A. 2012. Zymoseptoria ardabiliae and Z. pseudotritici, two progenitor species of the septoria tritici leaf blotch fungus Z. tritici (synonym: Mycosphaerella graminicola). *Mycologia,* 104**,** 1397-407.

SUFFERT, F., SACHE, I. & LANNOU, C. 2011. Early stages of septoria tritici blotch epidemics of winter wheat: build-up, overseasoning, and release of primary inoculum. *Plant Pathology,* 60**,** 166-177.

SVANGÅRD, E., GÖRANSSON, U., HOCAOGLU, Z., GULLBO, J., LARSSON, R., CLAESON, P. & BOHLIN, L. 2004. Cytotoxic Cyclotides from Viola t ricolor. *Journal of Natural Products,* 67**,** 144-147.

SYDEMAN, W., GARCÍA-REYES, M., SCHOEMAN, D. S., RYKACZEWSKI, R., THOMPSON, S., BLACK, B. & BOGRAD, S. 2014. Climate change and wind intensification in coastal upwelling ecosystems. *Science,* 345**,** 77-80.

TALAT, N. 2020. Alleviation of soil salinization and the management of saline soils, climate change, and soil interactions. *Climate Change and Soil Interactions.*

TAM, J. P., LU, Y.-A., YANG, J.-L. & CHIU, K.-W. 1999. An unusual structural motif of antimicrobial peptides containing end-to-end macrocycle and cystine-knot disulfides. *Proceedings of the National Academy of Sciences of the United States of America,* 96**,** 8913-8918.

TENLAND, E., KRISHNAN, N., RONNHOLM, A., KALSUM, S., PUTHIA, M., MORGELIN, M., DAVOUDI, M., OTROCKA, M., ALARIDAH, N., GLEGOLA-MADEJSKA, I., STUREGARD, E., SCHMIDTCHEN, A., LERM, M., ROBERTSON, B. D. & GODALY, G. 2018. A novel derivative of the fungal antimicrobial peptide plectasin is active against Mycobacterium tuberculosis. *Tuberculosis (Edinb),* 113**,** 231-238.

TIAN, H., MACKENZIE, C. I., RODRIGUEZ-MORENO, L., VAN DEN BERG, G. C. M., CHEN, H., RUDD, J. J., MESTERS, J. R. & THOMMA, B. 2021. Three LysM effectors of Zymoseptoria tritici collectively disarm chitin-triggered plant immunity. *Molecular Plant Pathology,* 22**,** 683-693.

TILEY, A. M. M. 2016. *Investigating Asexual Sporulation in Zymoseptoria tritici, a Fungal Pathogen of Wheat.* Degree of Doctor of Philosophy (Ph.D), University of Bristol.

TILEY, A. M. M., FOSTER, G. D. & BAILEY, A. M. 2018. Exploring the Genetic Regulation of Asexual Sporulation in Zymoseptoria tritici. *Frontiers in Microbiology,* 9**,** 1859.

TILEY, A. M. M., LAWLESS, C., PILO, P., KARKI, S. J., LU, J., LONG, Z., GIBRIEL, H., BAILEY, A. M. & FEECHAN, A. 2022. The Zymoseptoria tritici white collar-1 gene, ZtWco-1, is required for development and virulence on wheat. *Fungal Genetics and Biology,* 161**,** 103715.

TILEY, A. M. M., WHITE, H. J., FOSTER, G. D. & BAILEY, A. M. 2019. The ZtvelB Gene Is Required for Vegetative Growth and Sporulation in the Wheat Pathogen Zymoseptoria tritici. *Frontiers in Microbiology,* 10**,** 2210.

TISCHLER, Y. K., THIESSEN, E. & HARTUNG, E. 2018. Early optical detection of infection with brown rust in winter wheat by chlorophyll fluorescence excitation spectra. *Computers and Electronics in Agriculture,* 146**,** 77-85.

TORRIANI, S. F., BRUNNER, P. C., MCDONALD, B. A. & SIEROTZKI, H. 2009. QoI resistance emerged independently at least 4 times in European populations of Mycosphaerella graminicola. *Pest Management Science,* 65**,** 155-62.

TORRIANI, S. F., MELICHAR, J. P., MILLS, C., PAIN, N., SIEROTZKI, H. & COURBOT, M. 2015. Zymoseptoria tritici: A major threat to wheat production, integrated approaches to control. *Fungal Genetics and Biology,* 79**,** 8-12.

TSUKUI, T., NAGANO, N., UMEMURA, M., KUMAGAI, T., TERAI, G., MACHIDA, M. & ASAI, K. 2015. Ustiloxins, fungal cyclic peptides, are ribosomally synthesized in Ustilaginoidea virens. *Bioinformatics,* 31**,** 981-5.

UKA, V., CARY, J. W., LEBAR, M. D., PUEL, O., DE SAEGER, S. & DIANA DI MAVUNGU, J. 2020. Chemical repertoire and biosynthetic machinery of the Aspergillus flavus secondary metabolome: A review. *Comprehensive Reviews in Food Science and Food Safety,* 19**,** 2797-2842.

UMEMURA, M. 2020. Peptides derived from Kex2-processed repeat proteins are widely distributed and highly diverse in the Fungi kingdom. *Fungal Biology and Biotechnology,* 7**,** 11.

UMEMURA, M., KOIKE, H., NAGANO, N., ISHII, T., KAWANO, J., YAMANE, N., KOZONE, I., HORIMOTO, K., SHIN-YA, K., ASAI, K., YU, J., BENNETT, J. W. & MACHIDA, M. 2013. MIDDAS-M: motif-independent de novo detection of secondary metabolite gene clusters through the integration of genome sequencing and transcriptome data. *PLoS One,* 8**,** e84028.

UMEMURA, M., KURIIWA, K., DAO, L. V., OKUDA, T. & TERAI, G. 2020. Promoter tools for further development of Aspergillus oryzae as a platform for fungal secondary metabolite production. *Fungal Biology and Biotechnology,* 7**,** 3.

UMEMURA, M., KURIIWA, K. & VIET DAO, L. 2022. Tandem repeats in precursor protein stabilize transcript levels and production levels of the fungal ribosomally synthesized and post-translationally modified peptide ustiloxin B. *Fungal Genetics and Biology,* 160**,** 103691.

UMEMURA, M., NAGANO, N., KOIKE, H., KAWANO, J., ISHII, T., MIYAMURA, Y., KIKUCHI, M., TAMANO, K., YU, J., SHIN-YA, K. & MACHIDA, M. 2014. Characterization of the biosynthetic gene cluster for the ribosomally synthesized cyclic peptide ustiloxin B in Aspergillus flavus. *Fungal Genetics and Biology,* 68**,** 23-30.

VAN DER VELDEN, N. S. 2017. *Biosynthesis, function and targets of ribosomally produced toxins from mushroom forming fungi.* Degree of Doctor of Sciences, ETH Zurich.

VAN DER VELDEN, N. S., KÄLIN, N., HELF, M. J., PIEL, J., FREEMAN, M. F. & KÜNZLER, M. 2017. Autocatalytic backbone N-methylation in a family of ribosomal peptide natural products. *Nature Chemical Biology,* 13**,** 833-835.

VAN EGMOND, H. P. & JONKER, M. A. 2004. Current situation on regulations for mycotoxins. *JSM Mycotoxins,* 2003**,** 1-15.

VAN EGMOND, H. P., SCHOTHORST, R. C. & JONKER, M. A. 2007. Regulations relating to mycotoxins in food: perspectives in a global and European context. *Analytical and Bioanalytical Chemistry,* 389**,** 147-57.

VAN WARMELO, K., MARASAS, W., ADELAAR, T., KELLERMAN, T., VAN RENSBURG, I. & MINNE, J. Experimental evidence that lupinosis of sheep is a mycotoxicosis caused by the fungus Phomopsis leptostromiformis (Kühn) Bubak. Symposium on Mycotoxins in Human Health, 1971. Springer, 185-193.

VANYOLOS, A., DEKANY, M., KOVACS, B., KRAMOS, B., BERDI, P., ZUPKO, I., HOHMANN, J. & BENI, Z. 2016. Gymnopeptides A and B, Cyclic Octadecapeptides from the Mushroom Gymnopus fusipes. *Organic Letters,* 18**,** 2688-91.

VETTER, J. 1998. Toxins of Amanita phalloides. *Toxicon,* 36**,** 13-24.

VIGNOLLE, G. A., MACH, R. L., MACH-AIGNER, A. R. & DERNTL, C. 2020. Novel approach in whole genome mining and transcriptome analysis reveal conserved RiPPs in Trichoderma spp. *BMC Genomics,* 21**,** 258.

VOGT, E. & KUNZLER, M. 2019. Discovery of novel fungal RiPP biosynthetic pathways and their application for the development of peptide therapeutics. *Applied Microbiology and Biotechnology,* 103**,** 5567-5581.

WALTON, J. 2018. *The Cyclic Peptide Toxins of Amanita and Other Poisonous Mushrooms*, Springer.

WALTON, J. D., HALLEN-ADAMS, H. E. & LUO, H. 2010. Ribosomal biosynthesis of the cyclic peptide toxins of Amanita mushrooms. *Biopolymers,* 94**,** 659-64.
WANG, J., LIU, X., ZHANG, X., DU, S., HAN, X., LI, J. Q., XIAO, Y., XU, Z., WU, Q., XU, L. & QIN, Z. 2022. Fungicidal Action of the Triphenylphosphonium-Driven Succinate Dehydrogenase Inhibitors Is Mediated by Reactive Oxygen Species and Suggests an Effective Resistance Management Strategy. *Journal of Agricultural and Food Chemistry,* 70**,** 111-123.
WANG, X., WANG, J., LAI, D., WANG, W., DAI, J., ZHOU, L. & LIU, Y. 2017. Ustiloxin G, a New Cyclopeptide Mycotoxin from Rice False Smut Balls. *Toxins (Basel),* 9.
WELCH, T., BAYON, C., RUDD, J. J., KANYUKA, K. & KETTLES, G. J. 2022. Induction of distinct plant cell death programs by secreted proteins from the wheat pathogen Zymoseptoria tritici. *Scientific Reports,* 12**,** 17880.
WHITE, T. J., BRUNS, T., LEE, S. & TAYLOR, J. 1990. Amplification and direct sequencing of fungal ribosomal RNA genes for phylogenetics. *In:* INNIS, M. A., GELFAND, D. H., SNINSKY, J. J. & WHITE, T. J. (eds.) *PCR protocols: a guide to methods and applications.* San Diego, California, USA: Academic Press, Inc.
WIECZOREK, T. M., BERG, G., SEMAŠKIENĖ, R., MEHL, A., SIEROTZKI, H., STAMMLER, G., JUSTESEN, A. F. & JØRGENSEN, L. N. 2015. Impact of DMI and SDHI fungicides on disease control and CYP51 mutations in populations of Zymoseptoria tritici from Northern Europe. *European Journal of Plant Pathology,* 143**,** 861-871.
WIELAND, T. 1968. Poisonous principles of mushrooms of the genus Amanita. *Science,* 159**,** 946-952.
WIELAND, T. 1977. Interaction of phallotoxins with actin. *Advances in Enzyme Regulation,* 15**,** 285-299.
WIELAND, T. 1983. The toxic peptides from Amanita mushrooms. *International Journal of Peptide and Protein Research,* 22**,** 257-276.
WILLEY, J. M., WILLEMS, A., KODANI, S. & NODWELL, J. R. 2006. Morphogenetic surfactants and their role in the formation of aerial hyphae in Streptomyces coelicolor. *Molecular Microbiology,* 59**,** 731-42.
WILLIAMSON, P. M., HIGHET, A. S., GAMS, W., SIVASITHAMPARAM, K. & COWLING, W. A. 1994. Diaporthe toxica sp. nov., the cause of lupinosis in sheep. *Mycological Research,* 98**,** 1364-1368.
WISECAVER, J. H. & ROKAS, A. 2015. Fungal metabolic gene clusters-caravans traveling across genomes and environments. *Frontiers in Microbiology,* 6**,** 161.
WITTENBERG, A. H., VAN DER LEE, T. A., BEN M'BAREK, S., WARE, S. B., GOODWIN, S. B., KILIAN, A., VISSER, R. G., KEMA, G. H. & SCHOUTEN, H. J. 2009. Meiosis drives extraordinary genome plasticity in the haploid fungal plant pathogen Mycosphaerella graminicola. *PLoS One,* 4**,** e5863.
WOLPERT, T. J. & LORANG, J. M. 2016. Victoria Blight, defense turned upside down. *Physiological and Molecular Plant Pathology,* 95**,** 8-13.
WOLPERT, T. J. & MACKO, V. 1989. Specific binding of victorin to a 100-kDa protein from oats. *Proceedings of the National Academy of Sciences of the United States of America,* 86**,** 4092-4096.
WONG, J. H. & NG, T. B. 2006. CHAPTER 20 - Toxins from Basidiomycete Fungi (Mushroom): Amatoxins, Phallotoxins, and Virotoxins. *In:* KASTIN, A. J. (ed.) *Handbook of Biologically Active Peptides.* Burlington: Academic Press.
XING, M.-Z., ZHANG, X.-Z., SUN, Z.-L. & ZHANG, H.-Y. 2003. Perylenequinones act as broad-spectrum fungicides by generating reactive oxygen species both in the dark and in the light. *Journal of Agricultural and Food Chemistry,* 51**,** 7722-7724.
XU, X.-M., NICHOLSON, P., THOMSETT, M., SIMPSON, D., COOKE, B., DOOHAN, F., BRENNAN, J., MONAGHAN, S., MORETTI, A. & MULE, G. 2008. Relationship between the fungal complex causing Fusarium head blight of wheat and environmental conditions. *Phytopathology,* 98**,** 69-78.

YANG, F., LI, W. & JORGENSEN, H. J. 2013. Transcriptional reprogramming of wheat and the hemibiotrophic pathogen Septoria tritici during two phases of the compatible interaction. *PLoS One,* 8**,** e81606.

YANG, N., OVENDEN, B., BAXTER, B., MCDONALD, M. C., SOLOMON, P. S. & MILGATE, A. 2022. Multi-stage resistance to Zymoseptoria tritici revealed by GWAS in an Australian bread wheat diversity panel. *Frontiers in Plant Science,* 13**,** 990915.

YE, Y., MINAMI, A., IGARASHI, Y., IZUMIKAWA, M., UMEMURA, M., NAGANO, N., MACHIDA, M., KAWAHARA, T., SHIN-YA, K., GOMI, K. & OIKAWA, H. 2016. Unveiling the Biosynthetic Pathway of the Ribosomally Synthesized and Post-translationally Modified Peptide Ustiloxin B in Filamentous Fungi. *Angewandte Chemie International Edition in English,* 55**,** 8072-5.

YE, Y., OZAKI, T., UMEMURA, M., LIU, C., MINAMI, A. & OIKAWA, H. 2019. Heterologous production of asperipin-2a: proposal for sequential oxidative macrocyclization by a fungi-specific DUF3328 oxidase. *Organic & Biomolecular Chemistry,* 17**,** 39-43.

YILMAZ, I., ERMIS, F., AKATA, I. & KAYA, E. 2015. A Case Study: What Doses of Amanita phalloides and Amatoxins Are Lethal to Humans? *Wilderness & Environmental Medicine,* 26**,** 491-6.

YOSHIMI, A., UMEMURA, M., NAGANO, N., KOIKE, H., MACHIDA, M. & ABE, K. 2016. Expression of ustR and the Golgi protease KexB are required for ustiloxin B biosynthesis in Aspergillus oryzae. *AMB Express,* 6**,** 9.

YOSHINAGA, Y., DAUM, C., HE, G. & O'MALLEY, R. 2018. Genome Sequencing. *In:* DE VRIES, R. P., TSANG, A. & GRIGORIEV, I. V. (eds.) *Fungal Genomics: Methods and Protocols.* New York, NY: Springer New York.

YU, X., GUDA, K., WILLIS, J., VEIGL, M., WANG, Z., MARKOWITZ, S., ADAMS, M. D. & SUN, S. 2012. How do alignment programs perform on sequencing data with varying qualities and from repetitive regions? *BioData Mining,* 5**,** 1-12.

YU, Z. & FISCHER, R. 2019. Light sensing and responses in fungi. *Nature Reviews Microbiology,* 17**,** 25-36.

ZAINUDIN, N. A., CONDON, B., DE BRUYNE, L., VAN POUCKE, C., BI, Q., LI, W., HOFTE, M. & TURGEON, B. G. 2015. Virulence, Host-Selective Toxin Production, and Development of Three Cochliobolus Phytopathogens Lacking the Sfp-Type 4'-Phosphopantetheinyl Transferase Ppt1. *Molecular Plant-Microbe Interactions,* 28**,** 1130-41.

ZEITLIN, P. L., BOYLE, M. P., GUGGINO, W. B. & MOLINA, L. 2004. A phase I trial of intranasal Moli1901 for cystic fibrosis. *Chest,* 125**,** 143-149.

ZHAN, J. & MCDONALD, B. A. 2011. Thermal adaptation in the fungal pathogen Mycosphaerella graminicola. *Molecular Ecology,* 20**,** 1689-701.

ZHAN, J., PETTWAY, R. E. & MCDONALD, B. A. 2003. The global genetic structure of the wheat pathogen Mycosphaerella graminicola is characterized by high nuclear diversity, low mitochondrial diversity, regular recombination, and gene flow. *Fungal Genetics and Biology,* 38**,** 286-297.

ZHANG, J., WANG, F., LIU, M., FU, M. & DONG, C. 2022a. Dynamic Genome-Wide Transcription Profiling and Direct Target Genes of CmWC-1 Reveal Hierarchical Light Signal Transduction in Cordyceps militaris. *Journal of Fungi (Basel),* 8.

ZHANG, Q., MEN, X., HUI, C., GE, F. & OUYANG, F. 2022b. Wheat yield losses from pests and pathogens in China. *Agriculture, Ecosystems & Environment,* 326.

ZHONG, Z., MARCEL, T. C., HARTMANN, F. E., MA, X., PLISSONNEAU, C., ZALA, M., DUCASSE, A., CONFAIS, J., COMPAIN, J., LAPALU, N., AMSELEM, J., MCDONALD, B. A., CROLL, D. & PALMA-GUERRERO, J. 2017. A small secreted protein in Zymoseptoria tritici is responsible for avirulence on wheat cultivars carrying the Stb6 resistance gene. *New Phytologist,* 214**,** 619-631.

ZHOU, L., LU, S., SHAN, T., WANG, P., SUN, W., CHEN, Z. & WANG, S. 2012. Chemistry and biology of mycotoxins from rice false smut pathogen. Nova Science Publishers: New York, NY, USA.

ZIEMERT, N., ISHIDA, K., LIAIMER, A., HERTWECK, C. & DITTMANN, E. 2008. Ribosomal synthesis of tricyclic depsipeptides in bloom-forming cyanobacteria. *Angewandte Chemie International Edition in English,* 47**,** 7756-9.

ZIOGAS, B. N. & MALANDRAKIS, A. A. 2015. Sterol Biosynthesis Inhibitors: C14 Demethylation (DMIs). *In:* ISHII, H. & HOLLOMON, D. W. (eds.) *Fungicide Resistance in Plant Pathogens: Principles and a Guide to Practical Management.* Tokyo: Springer Japan.

ZIV, O., SACKS, J. & EYAL, Z. 1981. Inheritance of tolerance to Septoria leaf blotch of wheat. *Phytopathology,* 71**,** 119-123.

ZWIERS, L. H. & DE WAARD, M. A. 2001. Efficient Agrobacterium tumefaciens-mediated gene disruption in the phytopathogen Mycosphaerella graminicola. *Current Genetics* 39**,** 388-93.

9 Appendices

9.1 Professional Internships for PhD Students (PIPS)

In January 2021 to April 2021, I undertook a placement at BBSRC as part of the SWBio PIPS scheme. During this time, I conducted a small research project into the equality, diversity and inclusivity seen within BBSRC-funded PhD studentships (looking at responses to a survey that collected EDI data including socioeconomic background). The findings from this research were fed back to different stakeholders in BBSRC and I made recommendations regarding what measures could be put into place to address any gaps I had identified. My work in this role ultimately led me to take on a position within the University of Bristol that allowed me to go into schools, or invite school classes to the university, to encourage different demographic groups to study at university level with the hope that this may feed into more diverse students conducting doctoral research in the future.

9.2 Supplementary tables and figures

Table 9.1 Primers used in diagnostic PCR to determine successful transformation of *Z. tritici.*

Primer name	Type (Forward/Reverse)	Sequence
P-5'-F	Forward	AATGGCAGGACCTCCAGTATCTTTTCGTGC
ZttxP-R	Reverse	GCACAGGCTATTGGAGGTAACAGAGGAGC
P-3'-R	Reverse	ACTGCAACGGACGTGGAGTGAGGTTCA
Y2-5'-F	Forward	TTGACGCTCGCTGAGTCACTCCCAAATTGC
ZttxY2-R	Reverse	CAATTGCGTACCTTTGTCCAATCACGGC
Y2-3'-R	Reverse	AGTCGGGCTATGAACAAGCGATCCCGAGGC
Q-5'-F	Forward	CACGTCAATGCTATGGAGAGTTTCACGC
ZttxQ-R	Reverse	GCTTCCCATATGTGCAACGTCCAGC
Q-3'-R	Reverse	TGACGATATCGATGTGATCGGGCAGGC
Y3-5'-F	Forward	TTTGAACGACCGGGATGAAAGTCTAGACGC
ZttxY3-R	Reverse	TTGTCGAGTCCAACAAGGCATGGGATGC
Y3-3'-R	Reverse	GCGAGAGAATGCCGACTCACTTTCCCTGC
Y4-5'-F	Forward	GTCGAAGCAATGATTCAGATGGAGACTGC
ZttxY4-R	Reverse	TTCCGGTGCACGAAATGCCGTGACATTGC
Y4-3'-R	Reverse	CTACTGGAACACAAATTCCTGGGACGAGC
S28-5'-F	Forward	TGATGAACACAGTAACGCCGAGGAGC
ZttxS28-R	Reverse	TATGCGATGTACGTCGAGTCGTTGAAGC
S28-3'-R	Reverse	TCGAAGCGCAATCACTGGAACTCTTTGC
T-5'-F	Forward	ACGCTTCAACGACTCGACGTACATCGC
ZttxT-R	Reverse	TGTGATACCCTGGGAGCGATACATGGC
T-3'-R	Reverse	ATATGTGGTGCGGGCAAGATTCGGC
M-5'-F	Forward	CTTGTTTTTCGACGGCTTCTCGAATCGC
ZttxM-R	Reverse	AGTTTGGAAGACGCGAAATCGTACTCGGC
M-3'-R	Reverse	CAACTGAGCTACATGACCAAAACCGACGC
O-5'-F	Forward	TAACAGCAGGAGCGATTCTTCATCTGC
ZttxO-R	Reverse	AGGGATCTGTTCACTCGACATCACAGGC
O-3'-R	Reverse	TGATCCGCAAAGAGTGGCAAGGAAGC
Hyg-R2	Reverse	AACAGCGGGCAGTTCGGTTTCAGGCAGGTC
Hyg-F2	Forward	TAGAAGTACTCGCCGATAGTGGAAACCGAC

Table 9.2 Primers used for generation of knockout construct fragments.

Primer name	Gene for deletion	Gene left flank (LF) or right flank (RF)	Type (Forward/ Reverse)	Primer sequence
LF-P-F	ZttxP	LF	Forward	ACTGAATTAACGCCGAATTAATTCCTAGGCCGTCAGC CCTCGTGACTGCTCTTTCGTT
LF-P-R	ZttxP	LF	Reverse	AAATGCTCCTTCAATATCATCTTCTGTCGAAGGGACTA AGGTACGCGAATTGTACCAAG
RF-P-F	ZttxP	RF	Forward	AGCACTCGTCCGAGGGCAAAGGAATAGGGATCGATG ACGATACGGCTGATGTTCACCCGC
RF-P-R	ZttxP	RF	Reverse	TTACATGCTTAACGTAATTCAACAGAAATTCGGTGGG GGTGGCAATGATATTGTGGCAA
LF-Y1-F	ZttxY1	LF	Forward	ACTGAATTAACGCCGAATTAATTCCTAGGCCTGTCGTT GACACACTGATGAGCGATCCG
LF-Y1-R	ZttxY1	LF	Reverse	AAATGCTCCTTCAATATCATCTTCTGTCGATATTCAAA GACACGCGCGCGGGCCACCTCG
RF-Y1-F	ZttxY1	RF	Forward	AGCACTCGTCCGAGGGCAAAGGAATAGGGATCTCTT GAAAGAACGAGGGCAGGGCAGG
RF-Y1-R	ZttxY1	RF	Reverse	TTACATGCTTAACGTAATTCAACAGAAATTACGTTCCC TTCGTCTGCGATCATGTCG
LF-Y2-F	ZttxY2	LF	Forward	ACTGAATTAACGCCGAATTAATTCCTAGGCTTCCAACT CCTCTCTGTCCACCATGAGC
LF-Y2-R	ZttxY2	LF	Reverse	AAATGCTCCTTCAATATCATCTTCTGTCGAGACCTCGA GAGCAGCAACGTAGCCT
RF-Y2-F	ZttxY2	RF	Forward	AGCACTCGTCCGAGGGCAAAGGAATAGGGATCATGG GTACCCAAGACTATTTTGTAGGTC
RF-Y2-R	ZttxY2	RF	Reverse	TTACATGCTTAACGTAATTCAACAGAAATTAATCGTCC ACTCGCATGATATGACCG
LF-Y3-F	ZttxY3	LF	Forward	ACTGAATTAACGCCGAATTAATTCCTAGGCTCGCAAC GCAAGACGAGACCAT
LF-Y3-R	ZttxY3	LF	Reverse	AAATGCTCCTTCAATATCATCTTCTGTCGACAATTCGG GCCTATTGAACGTCATTCATG
RF-Y3-F	ZttxY3	RF	Forward	AGCACTCGTCCGAGGGCAAAGGAATAGGGATCGTCT GAGCGCTGCCGTAGTTCT
RF-Y3-R	ZttxY3	RF	Reverse	TTACATGCTTAACGTAATTCAACAGAAATTCACGACCA GAAGCTCATCATCTCACAC
LF-Y4-F	ZttxY4	LF	Forward	ACTGAATTAACGCCGAATTAATTCCTAGGCCAGCTCC GTTGCCATTTTTGCTGTTTT
LF-Y4-R	ZttxY4	LF	Reverse	AAATGCTCCTTCAATATCATCTTCTGTCGAAAGGTGAT TCTGTTCCGTATATACCAGATGGTCGAGCG
RF-Y4-F	ZttxY4	RF	Forward	AGCACTCGTCCGAGGGCAAAGGAATAGGGATCGTCT GTACTATCTAAAATTACGGTCGTTGGCTGT

RF-Y4-R	ZttxY4	RF	Reverse	TTACATGCTTAACGTAATTCAACAGAAATTCATCAATGGAGACGATTCGCTGGT
LF-Q-F	ZttxQ	LF	Forward	ACTGAATTAACGCCGAATTAATTCCTAGGCCCTCGCTGATCTCGACCTTCCATAATG
LF-Q-R	ZttxQ	LF	Reverse	AAATGCTCCTTCAATATCATCTTCTGTCGATGACTGTGACAGCGACCTGTGAC
RF-Q-F	ZttxQ	RF	Forward	AGCACTCGTCCGAGGGCAAAGGAATAGGGATCGGAACTTTGCCACGCCAATGCAAA
RF-Q-R	ZttxQ	RF	Reverse	TTACATGCTTAACGTAATTCAACAGAAATTGCCAAAGTGGTCGCCAGACT
LF-S28-F	S28 peptidase	LF	Forward	ACTGAATTAACGCCGAATTAATTCCTAGGCCCGTTCGTTCTCATCGTATTCTTTCA
LF-S28-R	S28 peptidase	LF	Reverse	AAATGCTCCTTCAATATCATCTTCTGTCGAGGTCTTCTGTCTAAATGTGAACTAG
RF-S28-F	S28 peptidase	RF	Forward	AGCACTCGTCCGAGGGCAAAGGAATAGGGATCCAGGCGAAGACCGCAAACGAAAG
RF-S28-R	S28 peptidase	RF	Reverse	TTACATGCTTAACGTAATTCAACAGAAATTCGGCACGGATACGAGGCTTGGCAATGAAT
LF-T-F	ZttxT	LF	Forward	ACTGAATTAACGCCGAATTAATTCCTAGGCGATGTGTGGGTTCATTTGGCCGT
LF-T-R	ZttxT	LF	Reverse	AAATGCTCCTTCAATATCATCTTCTGTCGAACAGTTCTTGGTCTAGGACTGTCCATCG
RF-T-F	ZttxT	RF	Forward	AGCACTCGTCCGAGGGCAAAGGAATAGGGATCACTACACGGTGATCATTACGGCTAGGCT
RF-T-R	ZttxT	RF	Reverse	TTACATGCTTAACGTAATTCAACAGAAATTACGCACATTGGGCTCTTGTGGAT
LF-M-F	ZttxM	LF	Forward	ACTGAATTAACGCCGAATTAATTCCTAGGCAATAGACCAAAGCCCAACCGCCA
LF-M-R	ZttxM	LF	Reverse	AAATGCTCCTTCAATATCATCTTCTGTCGATGTGCCCAGTGGGATTGAGATGC
RF-M-F	ZttxM	RF	Forward	AGCACTCGTCCGAGGGCAAAGGAATAGGGATCCACGTGGGACCTTCGTAGTGATAAGGA
RF-M-R	ZttxM	RF	Reverse	TTACATGCTTAACGTAATTCAACAGAAATTATGCTCATTGATTCCAGCTTGCCACTC
LF-O-F	ZttO	LF	Forward	ACTGAATTAACGCCGAATTAATTCCTAGGCCCGCTCAACCAGTCGGAAAGTG
LF-O-R	ZttO	LF	Reverse	AAATGCTCCTTCAATATCATCTTCTGTCGAAGATGGATCGTTTGTCGGTCGCGT
RF-O-F	ZttO	RF	Forward	AGCACTCGTCCGAGGGCAAAGGAATAGGGATCGGAGCGAGCAACAGTATCGGATCG
RF-O-R	ZttO	RF	Reverse	TTACATGCTTAACGTAATTCAACAGAAATTCGCAAAATCGAACATCGAGGAGTGC

Table 9.3 *Z. tritici* RT-qPCR primers.

Primer	Gene	Type (Forward/Reverse)	Sequence
ZttxP-F	ZttxP	Forward	CGTGCATATCCAAGCCCATCGC
ZttxP-R	ZttxP	Reverse	CCTTGCCCATGACGGCCATCT
ZttxY1-F	ZttxY1	Forward	TGGGTAAAGGCTTCGTGCACATC
ZttxY1-R	ZttxY1	Reverse	CCCTAGCCATTCGAGGGTCGTAT
ZttxY2-F	ZttxY2	Forward	ATTCGGAAATCGCTGTACCCGGA
ZttxY2-R	ZttxY2	Reverse	GGTGACACTGCCAGACTCCCATT
ZttxQ-F	ZttxQ	Forward	CCTTGCAAGTCTATTGCCATCCGC
ZttxQ-R	ZttxQ	Reverse	CACAGTGTTCCCTCAGCGATGC
ZttxY3-F	ZttxY3	Forward	AAGAGCATCCCATGCCTTGTTGGA
ZttxY3-R	ZttxY3	Reverse	GCTCCTCGGCGTTACTGTGTTCA
ZttxY4-F	ZttxY4	Forward	CAGAGAGCAAATTGCCCGCACTC
ZttxY4-R	ZttxY4	Reverse	GCACATCAACTGTTTCCGAAGCGT
S28-F	S28 peptidase	Forward	ACGCATCACGTCCCTGGTACA
S28-R	S28 peptidase	Reverse	CGTCGAACTGCCTTTCTTGACGAA
ZttxT-F	ZttxT	Forward	CTCTTCGTACAGCCCAACGCT
ZttxT-R	ZttxT	Reverse	TCTGTCAGCCCAGGTCATGGT
ZttxM-F	ZttxM	Forward	AGCTCTGTCCTCGACATTGGCTG
ZttxM-R	ZttxM	Reverse	GCACAACGTCGCTGCGTCTATAC
ZttxO-F	ZttxO	Forward	TTGAGTGAGACCAACAGCTTCCG
ZttxO-R	ZttxO	Reverse	GCTGATGAGCTCCGACGTCCAA
ZttxR-F	ZttxR	Forward	GCCATGCCTGAACTGTGTGCA
ZttxR-R	ZttxR	Reverse	GTCTCCTGGAGGGCTTCGACTT
ZttxA-F	ZttxA	Forward	ATACATCAAGCGCCACATGGGC
ZttxA-R	ZttxA	Reverse	TCGCTTGGTCTTGTCGAGGTAGT
Mg Tub F	beta tubulin	Forward	ATCTACCGCGGAAAGGTGTCCA
Mg Tub R2	beta tubulin	Reverse	GGTCGCCGACACGCTTAAAGAG
FWD_HH3	Histone H3	Forward	TCAATGGGAGGCGTAAAGAAACCGC
RVS_HH3	Histone H3	Reverse	AACCACCCCAAGCGCCGCGTATCCG

Table 9.4 Wheat RT-qPCR primers.

Primer name	Type (Forward/Reverse)	Sequence	Source
Ta54227-F	Forward	CAAATACGCCATCAGGGAGAACATC	Paolacci et al. (2009)
Ta54227-R	Reverse	CGCTGCCGAAACCACGAGAC	Paolacci et al. (2009)
TLP-F	Forward	GCCGCAAGCCTACCAACA	Deihimi et al. (2013)
TLP-R	Reverse	CGCGGTGCGACGTATAGAG	Deihimi et al. (2013)
TaNAC69-1F	Forward	ACTACCAGCTGCCTCCCGAAAACC	Baloglu et al. (2012)
TaNAC69-1R	Reverse	GCCGTAGTCATCTACGCGCGCC	Baloglu et al. (2012)
TtNAMB-2F	Forward	AACAGGAGCAGAAATGTCGGCAAC	Baloglu et al. (2012)
TtNAMB-2R	Reverse	GGATGACATGCTGTTGATGGTAGG	Baloglu et al. (2012)

Table 9.5 Primers used for sequencing of RiPP regions cloned into pJET.

Primers include those used for amplifying the product to be cloned into pJET and those used for sequencing reactions.

Primer	Sequence (5'-3')	Source
ZttxA-F1	ATCAAGCGCCACATGGGCATTGTTTGC	This work
ZttxA-R2	TCGTGCGCAGTATGAGATTAAGCGC	This work
pJET1.2-F	CGACTCACTATAGGGAGAGCGGC	Thermo Scientific
pJET1.2-R	AAGAACATCGATTTTCCATGGCAG	Thermo Scientific

Table 9.6 Primers used for ZttxA:GFP fusion construct design.

Primer name	Type (Forward/Reverse)	Sequence
pCAM0380_ZttxAPro_F	Forward	ACTGAATTAACGCCGAATTAATTCCTAGGCTAGAAGCCACAGTAGTGTGTCACTA
ZttxA-R3	Reverse	AGCGCGCTTGGTCTTGTCGACG
ZttxA-ZtGFP-F	Forward	ATCCCCGTCGACAAGACCAAGCGCGCTATGGTCTCCAAGGGCGAGGAGCTCTTCACC
Hyg-ZtGFP-R	Reverse	GCTCCTTCAATATCATCTTCTGTCGATTACTTGTAGAGCTCGTCCATGCC
Hyg-F	Forward	TCGACAGAAGATGATATTGAAGGAGC
Hyg-pCAM-R	Reverse	TACATGCTTAACGTAATTCAACAGAAATTGATCCCTATTCCTTTGCCCTCGGACGAGTGC

Table 9.7 Diagnostic PCR primers for ZttxA:ZtGFP fusion transformants of *Z. tritici.*

Primer name	Type (Forward/Reverse)	Sequence
ZttxA-FR	Forward	AGGACTACCTCGACAAGACCAAGC
ZttxA-ZtGFP-F	Forward	ATCCCCGTCGACAAGACCAAGCGCGCTATGGTCTCCAAGGGCGAGGAGCTCTTCACC
ZtGFP-R	Reverse	TTACTTGTAGAGCTCGTCCATGCC
Hyg-F	Forward	TCGACAGAAGATGATATTGAAGGAGC
Hyg-R2	Reverse	AACAGCGGGCAGTTCGGTTTCAGGCAGGTC
Hyg-R	Reverse	CTATTCCTTTGCCCTCGGACGAGTGCT

Table 9.8 Primers employed in diagnostic PCR of *ZttxA* putative knockouts.

Primer name	Type (Forward/Reverse)	Sequence	Source
LF-5'-F	Forward	ATGGCCGCACGGCAAGCTTCGC	This work
Hyg-R2	Reverse	AACAGCGGGCAGTTCGGTTTCAGGCAGGTC	This work
Hyg-F2	Forward	TAGAAGTACTCGCCGATAGTGGAAACCGAC	This work
3'-R	Reverse	AATTCTACGACACCGCCTCATCGGAGAATT	This work
ZttxA-F1	Forward	ATCAAGCGCCACATGGGCATTGTTTGC	This work
ZttxA-R	Reverse	AGGTAGTCCTCGACCGCCGTGACTGC	This work
ITS1-F	Forward	CTTGGTCATTTAGAGGAAGTAA	Gardes and Bruns (1993)
ITS2	Reverse	GCTGCGTTCTTCATCGATGC	White et al. (1990)

Table 9.9 Analysis of RiPP core subunit repeat number between *Z. tritici* strains studied in Rudd et al. (2010)

An asterisk is used to denote repeat numbers that have been assigned from sequence information; for the IPO323 strain this is based on NCBI genome sequence data (Goodwin et al., 2011), for IPO92006 this was confirmed by sequencing in Rudd et al. (2010). It was determined whether the amplicon size was greater than the IPO323 strain (>), equal to IPO323 (=) or less than IPO323 (<).

Strain	Amplicon size relative to IPO323 (>/=/<)	Estimated core repeat unit number
IPO87019	=	9
IPO88004	>	10
IPO89011	=	9
IPO94269	>	10
IPO92006	>	12*
IPO001	<	8
IPO90012	>	10
IPO323		9*
IPO95052	<	7

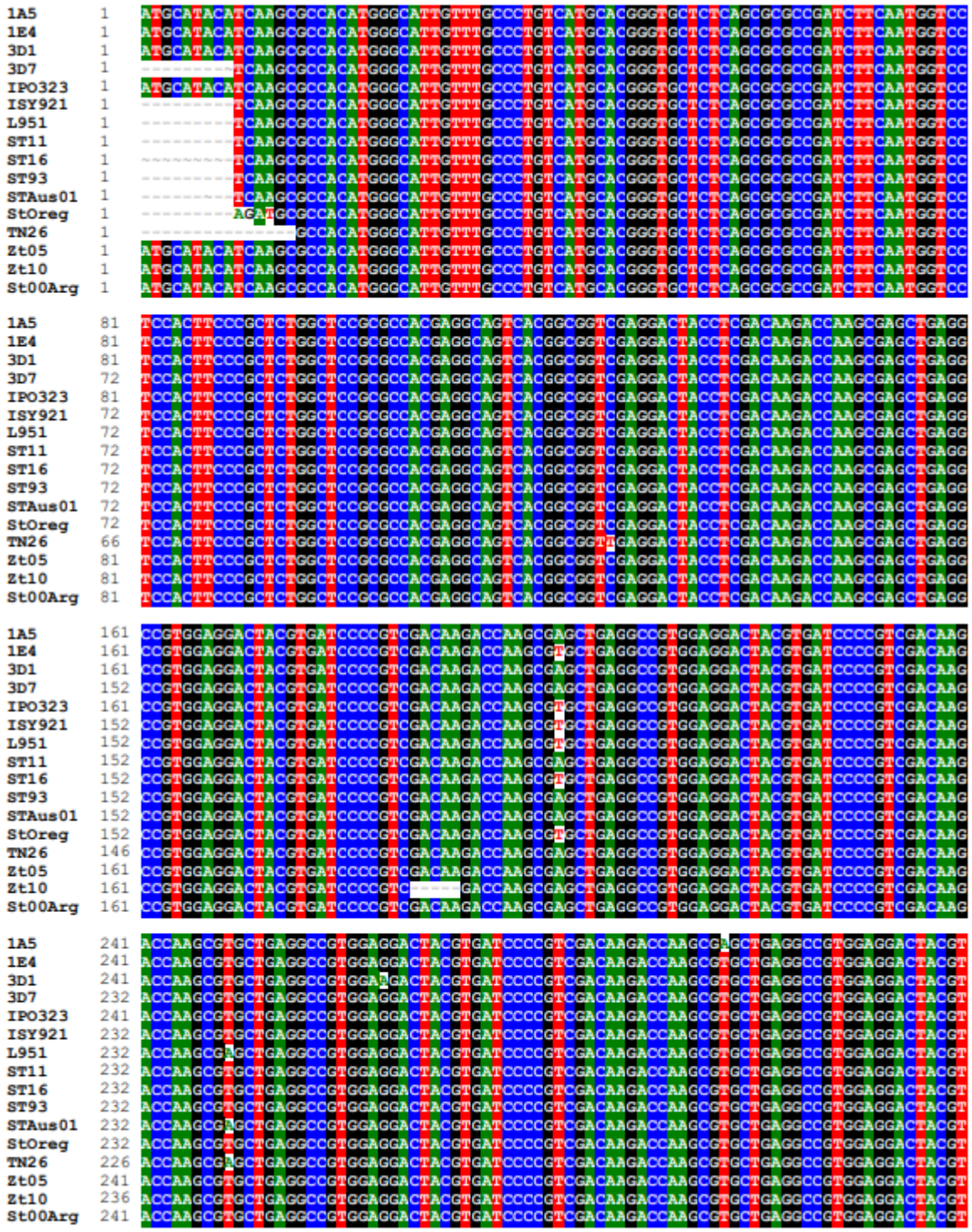

Figure 9.1 continued.

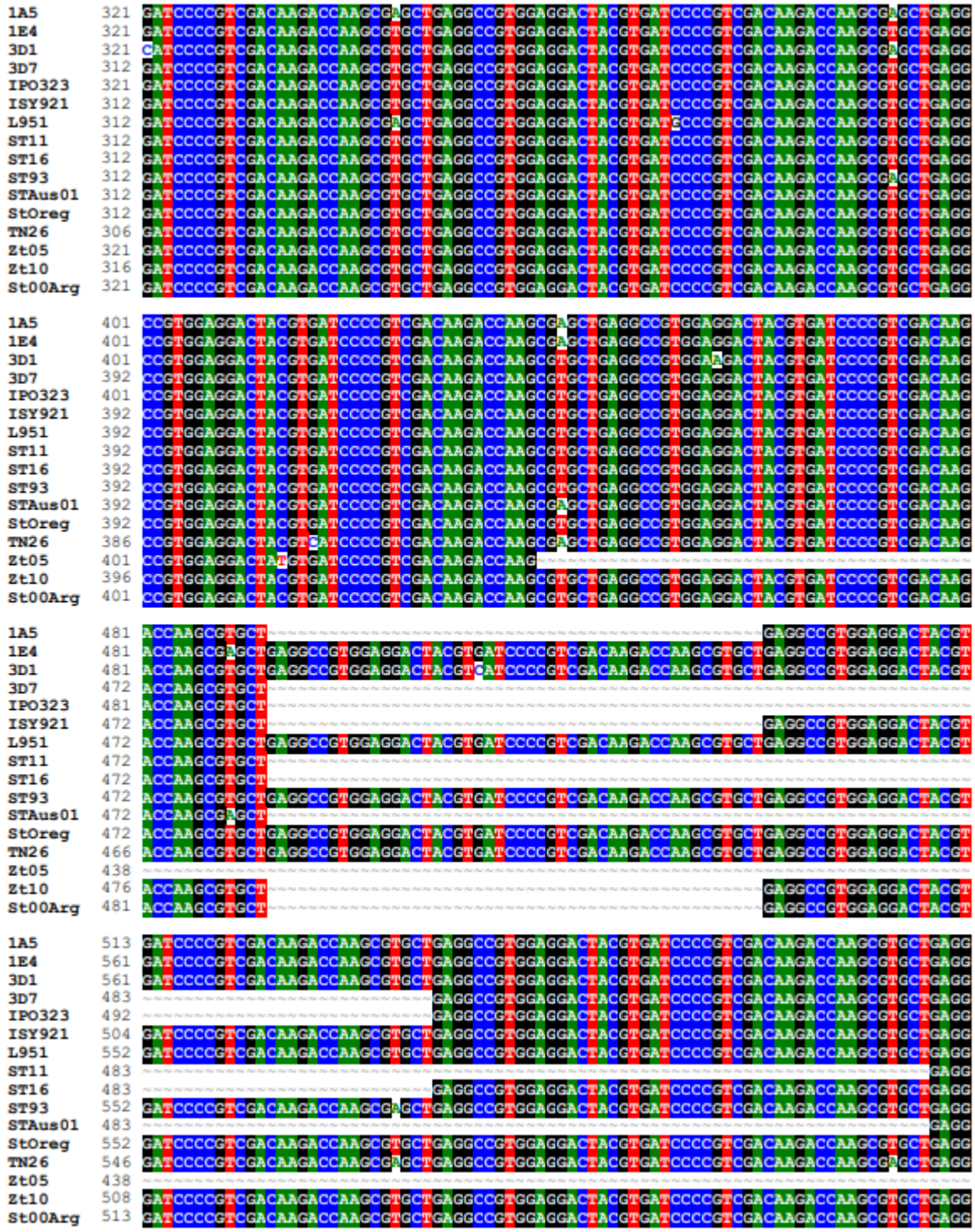

Figure 9.1 continued.

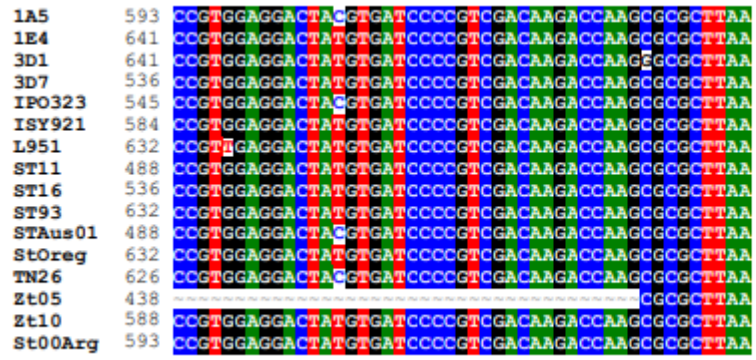

Figure 9.1 Aligned *ZttxA* DNA sequences of the *Zymoseptoria tritici* strains used within this work.

Mutations within the genomic sequences encoding the *ZttxA* gene (intron removed) are seen to be infrequent. These data combined with amino acid sequence alignments determine the few deviations from IPO323 to be synonymous changes mostly. The 5 bp deletion in Zt10 is clearly detectable.

Table 9.10 Putative RiPP producers identified by (Ding et al., 2016) also identified in this work.

The amino acid sequences of previously identified precursor peptides are listed alongside the species from which these peptides had been identified. The number of core repeats in each precursor is noted alongside how many repeat variants there are.

Fungal species	Repeats	Precursor peptide amino acid sequence
Pseudocercospora fijiensis CIRAD86 (EME81786.1)	3 repeats (1 type)	MHKNYAAWLLIALSSGAFGAAIGLAPIIARVDKRAEAVED**YIIPID**KRHG AEAIEKRHGAEAVED**YIIPID**KRHGAEAVDD**YIIPID**
Aspergillus oryzae 3.042 (EIT79501.1)	7 repeats (1 type)	MKLILTLLVSGLCALAAPAAKVSKSYLIQRDGVED**YAIGID**KRNSVED**Y AIGID**KRNSVED**YAIGID**KRNSVED**YAIGID**KRNSVED**YAIGID**KRGGSV ED**YAIGID**KRGGSVED**YAIGID**KRHGGH
Aspergillus oryzae RIB40 (BAE63088.1)	15 repeats (1 type)	MKLILTLLVSGLCALAAPAAKRDGVED**YAIGID**KRNSVED**YAIGID**KRN SVED**YAIGID**KRNSVED**YAIGID**KRNTVED**YAIGID**KRNSVED**YAIGID**K RNTVED**YAIGID**KRNSVED**YAIGID**KRNSVED**YAIGID**KRGGSVED**YAI GID**KRNSVED**YAIGID**KRNSVED**YAIGID**KRGSVED**YAIGID**KKRGTVE D**YAIGID**KRGGSVED**YAIGID**KRHGGH
Neurospora crassa OR74A (EAA30507.1)	10 repeats (4 types)	MKYSSSILIAAFCVSVLAAPAAKRSSVED**YVIEVD**KRSSVEDKRGAVED KRHNSVED**YVIAVD**RRGSVEDKRSSVED**YVISVD**NKRSSVED**YAIGVD** KRGAVED**YVIEVD**KRHNSVED**YAIGVD**KRGAVEDKRGAVEDKRHNSV ED**YAIGVD**KRGAVED**YVIEVD**KRHGGVED**YAIGVD**KRGSVEDKRHNS VED**YVIEVD**KA
Neurospora tetrasperma FGSC 2508 (EGO55879.1)	9 repeats (2 types)	MKYSSSILIAAFCVSVLAAPAAKRSSVED**YVIEVD**KRSSVEDKRSSVED YVISVDNKRSSVED**YAIGVD**KRGAVEDKRSAVED**YVIEVD**KRHNSVED **YAIGVD**KRGSVEDKRSAVED**YVIEVD**KRHNSVED**YAIGVD**KRGSVED KRSAVED**YVIEVD**KRHNSVED**YAIGVD**KRGSVEDKRSAVED**YVIEVD**K A
Sordaria macrospora k-hell (CCC12843.1)	5 repeats (2 types)	MKYSSSVLIAAFCVSVLAAPVAKSNAVED**YVIPID**KRSSVED**YVIPID**KR GSVED**YVIPID**KRSSVED**YVIPID**KRNGAVED**YAIPID**KAQLRRGLCDPD R
Colletotrichum higginsianum IMI 349063 (CCF41414.1)	4 repeats (1 type)	MKAFDIAFVLAFAAGALAMPTQGGHLATTGEAQGGIENSNGNPVED**Y VIPID**KRDEAPVED**YVIPID**KRDEAPVED**YVIPID**KRDEAPVED**YVIPID**K
Aspergillus parasiticus SU-1 (KJK68632.1)	17 repeats (1 type)	MKLMLTLLVSGLCALAAPTAKRDGIED**YAIGID**KRNSVED**YAIGID**KRN SVED**YAIGID**KRNSVED**YAIGID**KRGGSVED**YAIGID**KRGGSVED**YAIGI D**KRGGSVED**YAIGID**KKRNSVED**YAIGID**KRNSVED**YAIGID**KRNSVED **YAIGID**KRNSVED**YAIGID**KRNSVED**YAIGID**KRNSVED**YAIGID**KRNSV ED**YAIGID**KKRNSVED**YAIGID**KRGSVED**YAIGID**KRGGSVE D**YAIGID**KRHGGH

Table 9.11 KEPs identified by Umemura (2020) also identified as dikaritin RiPPs in this work.

The amino acid sequences of the KEPs are shown alongside the species from which these peptides had been identified. The number of core repeats in each precursor is noted alongside how many repeat variants there are.

Species and accession number	**Repeats**	**Sequence**
Aspergillus arachidicola (PIG90226.1)	13 repeats (1 type)	MKLMLTLLVSGLCALAAPAAKRDGIED**YAIGID**KRNSVED**YAIGID**KRNSVED**YAIGID**KRNSVED**YAIGID**KRGGSVED**YAIGID**KRNTVED**YAIGID**KRNSVED**YAIGID**KRNSVEDYAIGIDKLED**YAIGID**KKRSSVED**YAIGID**KRNSVED**YAIGID**KKRNSVED**YAIGID**KRGSVED**YAIGID**KRGGSVED**YAIGID**KRHAGH
Cordyceps fumosorosea ARSEF 2679 (XP_018708364.1)	1 repeat	MKFSATFVLAALTAWSSAAPTPGKTVEDYTIGPGKVKSVEDYTIGPGKQAKSVEDYTIGPGKQVKSVEDYTIGPGQQVKSVEDYTIGPGKQAKSVED**YTIGPR**KRGMSVEDYTIGPSKQAKSVEDYTIGPGKQAKSVEDYTIGPGKQVKSVEDYTIGPGKQAKSVEDYTIGPGKHA
Penicillium freii (KAJ5528728.1)	10 repeats (2 types)	MKLTIISILAPYLSTLVLAAPAFQERAMAERGSIED**YVIGVD**KRDVED**YVIGVD**KRGPVED**YVIGVD**KRDVED**YVIPVD**KRGPVED**YVIGVD**KRDVED**YVIGVD**KRDVED**YVIPVD**KRGPVED**YVIGVD**KRDVED**YVIPVD**KRGPVED**YVIGVD**KRHENHGAV
Penicillium polonicum (OQD60631.1)	15 repeats (2 types)	MKLTIISILAPYLSTLALAAPAFQERAMAKRGVED**YAIGVD**KRGSVED**YAIGVD**KRNVED**YAIGVD**KRGSVED**YAIGVD**KRGSVED**YAIPVD**KRGSVED**YAIGVD**KRGSVED**YAIGVD**KRNVED**YAIGVD**KRGSVED**YAIGVD**KRNVED**YAIPVD**KRGSVED**YAIGVD**KRGSVED**YAIGVD**KRNVED**YAIPVD**KRDVED**YAIGVD**KRNVED**YAIGVD**KRHGNHGAV